



The University of
Nottingham

UNITED KINGDOM • CHINA • MALAYSIA

Buker, Mahmut Sami (2015) Building integrated solar thermal collectors for heating & cooling applications. PhD thesis, University of Nottingham.

Access from the University of Nottingham repository:

<http://eprints.nottingham.ac.uk/29009/1/Thesis%20-%20MSBUKER.pdf>

Copyright and reuse:

The Nottingham ePrints service makes this work by researchers of the University of Nottingham available open access under the following conditions.

This article is made available under the University of Nottingham End User licence and may be reused according to the conditions of the licence. For more details see:
http://eprints.nottingham.ac.uk/end_user_agreement.pdf

A note on versions:

The version presented here may differ from the published version or from the version of record. If you wish to cite this item you are advised to consult the publisher's version. Please see the repository url above for details on accessing the published version and note that access may require a subscription.

For more information, please contact eprints@nottingham.ac.uk

Faculty of Engineering

Department of Architecture and Built Environment

Institute of Sustainable Energy Technology



The University of
Nottingham

BUILDING INTEGRATED SOLAR THERMAL COLLECTORS FOR HEATING & COOLING APPLICATIONS

Mahmut Sami Bker

B Eng, MSc

Thesis submitted to the University of Nottingham for
the degree of Doctor of Philosophy

January 2015

BUILDING INTEGRATED SOLAR THERMAL COLLECTORS FOR HEATING & COOLING APPLICATIONS

Mahmut Sami Bker

B Eng, MSc

ABSTRACT

International Energy Agency Solar Heating & Cooling (IEA SHC) programme states the fact that space/water heating and cooling demand account for over 75% of the energy consumed in single and multi-family homes. Solar energy technology can meet up to 100% of this demand depending on the size of the system, storage capacity, the heat load and the region's climate.

Solar thermal collectors are particular type of heat extracting devices that convert solar radiation into thermal energy through a transport medium or flowing fluid. Although hybrid PV/T or thermal-alone systems offer some advantages to improve the solar heat utilisation, there are a few technical challenges found in these systems in practice that prevented wide-scale applications. These technical drawbacks include being expensive to make and install, inability of switching already-built photovoltaic (PV) systems into PV/T systems, architectural design etc. The aims of this project, therefore, were to investigate roof integrated solar thermal roof collectors that properly blend into surrounding thus avoiding 'add on' appearance and having a dual function (heat absorption and roofing). Another objective was to address the inherent technical pitfalls and practical limitations of conventional solar thermal collectors by bringing unique, inexpensive, maintenance free and easily adaptable solutions. Thus, in this innovative research, unique and simple building integrated solar thermal roof collectors have been developed for heating & cooling applications. The roof systems which mainly based on low cost and structurally unique polyethylene heat exchanger are relatively cost effective, competitive and developed by primarily exploiting components and techniques widely available on the market.

The following objectives have been independently achieved via evaluating three aspects of investigations as following:

- Investigation on the performance of poly heat exchanger underneath PV units
- Investigation on the performance of a Building Integrated PV/T Roof 'Invisible' Collector combined with a liquid desiccant enhanced indirect evaporative cooling system
- Investigation on the build-up and performance test of a novel 'Sandwich' solar thermal roof for heat pump operation

These works have been assessed by means of computer simulation, laboratory and field experimental work and have been demonstrated adequately. The key findings from the study confirm the potential of the examined technology, and elucidate the specific conclusions for the practice of such systems.

The analysis showed that water temperature within the poly heat exchanger loop underneath PV units could reach up to 36°C and the system would achieve up to 20.25% overall thermal efficiency. Techno-economic analysis was carried out by applying the Life Cycle Cost (LCC) method. Evaluations showed that the estimated annual energy savings of the overall system was 10.3 MWh/year and the cost of power generation was found to be £0.0622 per kWh.

The heat exchanger loop was coupled with a liquid desiccant enhanced indirect evaporative cooling unit and experimental results indicated that the proposed system could supply about 3 kW of heating and 5.2 kW of cooling power.

Lastly, the results from test of a novel solar thermal collector for heat pump operation presented that the difference in water temperature could reach up to 18°C while maximum thermal efficiency found to be 26%. Coefficient Performance of the heat

pump (COP_{HP}) and overall system (COP_{SYS}) averages were attained as $COP_{HP}=3.01$ and $COP_{SYS}=2.29$, respectively. An economic analysis pointed a minimum payback period of about 3 years for the system.

Keywords: Solar Energy, Building Integration, PV/T, Solar Thermal Roof Collector, Polyethylene Heat Exchanger, Solar Cooling, Liquid Desiccant Evaporative A/C, Heat Pump

ACKNOWLEDGEMENT

Wear gratitude like a cloak and it will feed every corner of your life. ~ Rumi

I would like to express my sincere and heartfelt gratitude to my supervisor: Prof Saffa Riffat for the tremendous help he provided both technically and academically, it is a privilege to be one of your students. Also, Dr Blaise Mempouo and all the technicians at the department's workshops for the technical help. I also gratefully acknowledged the support of Geo Green Power Ltd for funding the part of work described in this communication.

I wish to thank those the two pillars of my life, without them this entire PhD would not be possible: my mom and dad. They have been backbone for my entire life and I could not have become the person I am today without the will, nurture and support they provided. Thank you so much mom and dad. From a tiny toddler to now a doctorate of engineering. I hope I have made you proud. I also won't forget my two younger brothers for being there for me!

A special thank you to my fiancée. Words cannot describe how lucky I am to have her in my life. She has selflessly given more to me than I ever could have asked for. I love you, and look forward to our lifelong journey.

Lastly, but not least, I would like to thank Allah Almighty for giving me the inspiration, patience, time and strength to achieve all this!

TABLE OF CONTENTS

ABSTRACT	II
ACKNOWLEDGEMENT	V
TABLE OF CONTENTS	VI
LIST OF FIGURES.....	X
LIST OF TABLES	XV
LIST OF ACRONYMS	XVI
NOMENCLATURE	XVIII

1. INTRODUCTION 2

1.1 STATEMENT OF THE PROBLEMS	3
1.2 RESEARCH AIMS AND OBJECTIVES.....	6
1.3 SCOPE OF THE PROJECT	8
1.4 NOVELTY	9
1.5 RESEARCH METHODS AND METHODOLOGY	10
1.6 STRUCTURE OF THE THESIS	11

2. BUILDING INTEGRATED SOLAR THERMAL COLLECTORS..... 15

2.1 INTRODUCTION.....	15
2.2 PHOTOVOLTAIC/THERMAL (PV/T) COLLECTORS	16
2.2.1 PV/T AIR COLLECTORS	17
2.2.2 PV/T WATER COLLECTORS	22
2.2.3 REFRIGERANT BASED PV/T COLLECTORS	27
2.2.4 HEAT PIPE BASED PV/T COLLECTORS	30
2.2.5 CONCENTRATING PV/T COLLECTORS.....	33
2.2.6 HYBRID PV/T TRANSPIRED COLLECTORS	36
2.3 SOLAR THERMAL COLLECTORS	38
2.3.1 SOLAR THERMAL AIR COLLECTORS.....	39
2.3.2 SOLAR THERMAL WATER HEATERS.....	42
2.3.3 ROOF INTEGRATED MINI-PARABOLIC SOLAR COLLECTORS	47
2.3.4 CERAMIC SOLAR COLLECTORS	49
2.3.5 POLYMER SOLAR THERMAL COLLECTORS.....	51
2.3.6 SOLAR LOUVRE COLLECTORS.....	52
2.4 FUTURE POTENTIAL OF BUILDING INTEGRATED SOLAR THERMAL COLLECTORS	55
2.5 IEA TASK 41 SOLAR ENERGY AND ARCHITECTURE	56
2.6 DISCUSSION & CONCLUSIONS.....	57

3 RECENT DEVELOPMENTS IN SOLAR ASSISTED LIQUID DESICCANT EVAPORATIVE COOLING TECHNOLOGY..... 63

3.1 INTRODUCTION.....	63
3.1.1 THERMAL COMFORT.....	64

3.2 LIQUID DESICCANT DEHUMIDIFICATION FOR SOLAR COOLING.....	66
3.3 HYBRID SOLAR LIQUID DESICCANT AND EVAPORATIVE COOLING SYSTEMS .	72
3.3.1 HYBRID SOLAR LIQUID DESICCANT AND DIRECT EVAPORATIVE COOLER.....	75
3.3.2 HYBRID SOLAR LIQUID DESICCANT AND INDIRECT EVAPORATIVE COOLER.....	80
3.4 SOLAR LIQUID DESICCANT REGENERATION METHODS.....	84
3.4.1 SOLAR THERMAL REGENERATION.....	84
3.4.2 PHOTOVOLTAIC ELECTRODIALYSIS (PV-ED) REGENERATION.....	87
3.5 DISCUSSION AND SUMMARY	88
3.5.1 BENEFITS OF LIQUID DESICCANT COOLING.....	91
3.6 CONCLUSIONS.....	94
4 SOLAR ASSISTED HEAT PUMP SYSTEMS FOR LOW TEMPERATURE WATER HEATING APPLICATIONS: A SYSTEMATIC REVIEW	98
4.1 INTRODUCTION.....	98
4.1.1 CLASSIFICATION METHOD	98
4.1.1.1 Systematic visualization scheme of solar assisted heat pump concepts	101
4.2 SOLAR ASSISTED HEAT PUMP SYSTEMS	104
4.2.1 LITERATURE REVIEW FOR SAHP.....	107
4.2.1.1 IEA: SHC Programme Task 44.....	107
4.2.1.2 Comparative studies of SAHP Systems	108
4.2.1.3 Direct Series Systems	113
4.2.1.4 Indirect Series Systems	117
4.3 DESIGN COMPONENTS.....	121
4.3.1 SAHP COMPONENTS AND INVESTIGATED PARAMETERS	121
4.3.1.1 Collector-evaporator	122
4.3.1.2 Compressor.....	123
4.3.1.3 Condenser.....	124
4.3.1.4 Expansion valve and pump	125
4.3.2 TYPES OF REFRIGERANT USED IN SAHP SYSTEMS.....	125
4.4 THERMAL PERFORMANCE CHARACTERISTICS OF SAHP	126
4.4.1 COEFFICIENT OF PERFORMANCE (COP)	127
4.5 DISCUSSION & CONCLUSIONS.....	129
5 PERFORMANCE EVALUATION AND TECHNO-ECONOMIC ANALYSIS OF A NOVEL BUILDING INTEGRATED PV/T ROOF COLLECTOR: AN EXPERIMENTAL VALIDATION	135
5.1 INTRODUCTION.....	135
5.2 INTEGRATION OF UNIQUE POLYETHYLENE HEAT EXCHANGER LOOP UNDERNEATH PV MODULES	139
5.2.1 OPERATING PRINCIPLE	139
5.2.2 PROTOTYPE DESIGN	141
5.2.3 MATHEMATICAL ANALYSES OF THERMAL PERFORMANCE AND EES MODEL SETUP.....	144
5.2.3.1 Thermal Model.....	146
5.2.3.1.1 Energy Efficiency	151
5.2.3.1.2 Exergy Efficiency	151

5.2.3.1.3	Uncertainty Analysis.....	153
5.2.4	TECHNO-ECONOMIC ANALYSIS.....	154
5.3	RESULTS AND DISCUSSION	157
5.3.1.1	Financial Assessment	164
5.4	DISCUSSION & CONCLUSIONS.....	167
6	EXPERIMENTAL INVESTIGATION OF A BUILDING INTEGRATED PV/T ROOF COLLECTOR COMBINED WITH A LIQUID DESICCANT ENHANCED INDIRECT EVAPORATIVE COOLING SYSTEM	171
6.1	INTRODUCTION.....	171
6.2	SYSTEM CONFIGURATION.....	173
6.2.1	EXPERIMENTAL SETUP	174
6.2.1.1	Roof Unit.....	174
6.2.1.1.1	Energy Efficiency	180
6.2.1.2	Liquid Desiccant Dehumidification unit.....	182
6.2.1.3	Indirect Evaporative cooling unit.....	188
6.3	RESULTS AND DISCUSSION	192
6.3.1	ROOF UNIT	192
6.3.2	LIQUID DESICCANT DEHUMIDIFICATION UNIT	196
6.3.3	INDIRECT EVAPORATIVE COOLER	199
6.3.4	COMBINED DEHUMIDIFICATION AND INDIRECT EVAPORATIVE COOLING SYSTEM.....	202
6.4	DISCUSSION & CONCLUSIONS.....	206
7	BUILD-UP AND PERFORMANCE TEST OF A NOVEL SOLAR THERMAL ROOF FOR HEAT PUMP OPERATION.....	209
7.1	INTRODUCTION.....	209
7.1.1	IEA: SHC PROGRAMME TASK 44	211
7.2	DESCRIPTION OF THE “SANDWICH” ROOF UNIT AND ITS COMBINED OPERATION WITH HEAP PUMP	213
7.2.1	PROTOTYPE DESIGN	217
7.3	MATHEMATICAL MODELLING AND EES MODEL SET-UP	220
7.3.1	ENERGY ANALYSIS OF “SANDWICH” ROOF UNIT.....	222
7.3.2	ENERGY ANALYSIS OF HEAT PUMP UNIT.....	225
7.3.3	UNCERTAINTY ANALYSIS.....	226
7.4	RESULTS AND ANALYSIS	228
7.4.1	OUTDOOR TESTING	232
7.4.1.1	Solar Roof	232
7.4.1.2	Heat Pump	234
7.4.2	ECONOMIC STUDIES	237
7.5	DISCUSSION & CONCLUSIONS.....	238
8	DISCUSSION, CONCLUSIONS & RECOMMENDATIONS	243
8.1	GENERAL DISCUSSION	243

8.2 GENERAL CONCLUSIONS	248
8.3 RECOMMENDATIONS	250
8.4 FUTURE WORK	252
REFERENCES.....	253
APPENDIX 1	276
APPENDIX 2.....	338

LIST OF FIGURES

FIGURE 1.2.1 THE RESEARCH MODEL	8
FIGURE 2.2.1. SCHEMATIC OF A TYPICAL BUILDING INTEGRATED PV/T AIR DESIGN (KARAVA ET AL. 2011).....	18
FIGURE 2.2.2 CROSS-SECTIONAL VIEW OF COMMON TYPE PV/T AIR COLLECTORS (CHOW, 2010)	19
FIGURE 2.2.3 SCHEMATIC VIEW OF BIPVT/A (AGRAWAL AND TIWARI, 2010)	21
FIGURE 2.2.4 TYPES OF PV/T WATER COLLECTORS (ZHANG ET AL., 2012)	23
FIGURE 2.2.5 SCHEMATIC DIAGRAM OF A HYBRID SOLAR ROOF PANEL (YIN ET AL., 2013).....	24
FIGURE 2.2.6 CONCEPTUAL AND EXPERIMENTAL VIEW OF THE BIPVT/WATER UNIT (KIM ET AL., 2014).....	25
FIGURE 2.2.7 TYPICAL PV TEMPERATURE-EFFICIENCY CURVE (IBRAHIM, 2011)	26
FIGURE 2.2.8 CROSS-SECTIONAL VIEW OF A REFRIGERANT BASED PV EVAPORATOR ROOF PANEL (ZHAO ET AL., 2011)	28
FIGURE 2.2.9 SCHEMATIC DIAGRAM OF THE PV-SAHP EXPERIMENTAL SET-UP (FU ET AL., 2012)	29
FIGURE 2.2.10 REFRIGERANT BASED PV EVAPORATOR MODULES (JI ET AL., 2008)	30
FIGURE 2.2.11 SCHEMATIC DIAGRAM OF A TYPICAL HEAT PIPE MECHANISM (KUMAR ET AL., 2015)	31
FIGURE 2.2.12 CROSS-SECTIONAL VIEW OF HEAT PIPE PV/T COLLECTOR (ZHANG ET AL., 2013)	32
FIGURE 2.2.13 SCHEMATIC DIAGRAM OF A CONCENTRATING PV/T COLLECTOR (BERNARDO ET AL., 2011) ...	33
FIGURE 2.2.14 ILLUSTRATION OF CPVT MOUNTED ON THE ROOF (AL-ALILI ET AL., 2012)	35
FIGURE 2.2.15 ARCHITECTURAL DESIGN OF THE BUILDING INTEGRATED CPVT SYSTEM (CHEMISANA ET AL., 2013)	35
FIGURE 2.2.16 CONCEPT SCHEMATIC OF FACADE AND ROOF TILE PV/T TRANSPIRED COLLECTORS (ATHIENITIS ET AL., 2011; DELISLE ET AL., 2007)	37
FIGURE 2.2.17 PHOTOGRAPHIC VIEW OF A PV/T CLAY ROOF TILE (BUILDING SERVICES, 2015).....	38
FIGURE 2.2.18 THE VIEW OF A TRANSPIRED SOLAR COLLECTOR (NOTTON ET AL., 2014)	38
FIGURE 2.3.1 SCHEMATIC DIAGRAM OF A ROOF INTEGRATED SOLAR THERMAL AIR COLLECTOR (ALKILANI ET AL., 2011)	39
FIGURE 2.3.2 A SCHEMATIC DIAGRAM OF SOLAR THERMAL AIR COLLECTOR APPLICATION ON A SINGLE FAMILY HOUSE (SOLARVENTI, 2015)	40
FIGURE 2.3.3 AN ILLUSTRATION OF BUILDING INTEGRATED SOLAR THERMAL AIR COLLECTOR SYSTEM IN A COMMERCIAL BUILDING (MUNARI ET AL., 2007).....	42
FIGURE 2.3.4 THE CROSS SECTIONAL VIEW OF A FLAT PLATE SOLAR WATER COLLECTOR AND ITS TYPICAL SOLAR WATER HEATING APPLICATION (JAISANKAR ET AL., 2011)	43
FIGURE 2.3.5 A NATURAL CIRCULATION WATER-IN-GLASS SOLAR WATER HEATER (BUDIARDJO ET AL., 2009)	46
FIGURE 2.3.6 BUILDING INTEGRATION OF ARRAY OF SOLAR THERMAL COLLECTOR ON A GREEN OFFICE BUILDING (BINE, 2015).....	46
FIGURE 2.3.7 THE SCHEMATIC VIEW OF A MICRO-CONCENTRATING SYSTEM AND THE CROSS-SECTION OF THE COLLECTOR (SULTANA ET AL., 2012)	47
FIGURE 2.3.8 A SOLAR MICRO-CONCENTRATOR SYSTEM (SULTANA ET AL., 2010).....	48
FIGURE 2.3.9 AN AWARD WINNING DESIGN OF A BUILDING INTEGRATED COMPOUND PARABOLIC CONCENTRATOR SYSTEM (HYDRO, 2015)	49
FIGURE 2.3.10 AN ALL-CERAMIC SOLAR THERMAL COLLECTOR AND ITS INTERIOR VIEW (YANG ET AL., 2013)	50
FIGURE 2.3.11 SOLAR CERAMIC COLLECTORS AS BALCONY RAILINGS (YANG ET AL., 2013).....	50
FIGURE 2.3.12 THE CROSS-SECTION OF POLYMER ABSORBER (OLIVARES ET AL., 2008)	51
FIGURE 2.3.13 BUILDING INTEGRATED POLYMERIC SOLAR THERMAL COLLECTORS, PASSIVE HOUSE IN RUDSHAGEN, OSLO (IEA-SHC, 2015).....	52
FIGURE 2.3.14 A SCHEMATIC DIAGRAM OF A SOLAR LOUVRE (PALMERO-MARRERO ET AL., 2006)	53
FIGURE 2.3.15 AN APPLICATION OF THE SOLAR LOUVRE SYSTEM ON A BUILDING (CITYTRADE, 2015)	55
FIGURE 3.1.1 ASHRAE 2010 COMFORT CHART (AHMAD ET AL., 2013)	65
FIGURE 3.2.1 SCHEMATIC OF A DESICCANT COOLING AIR CONDITIONING (SALT AIR CONDITIONER)	68
FIGURE 3.2.2 MOISTURE REMOVAL PROCESS BY DESICCANT (MOHAMMAD ET AL., 2013)	68

FIGURE 3.2.3 SCHEMATIC DIAGRAM OF SOLAR AIR PRE-TREATMENT COLLECTOR/REGENERATOR (PENG ET AL., 2009)	70
FIGURE 3.2.4 SCHEMATIC DIAGRAM OF THE SOLAR REGENERATED LIQUID DESICCANT SYSTEM (KATEJANEKARN ET AL., 2009)	71
FIGURE 3.3.1 SCHEMATIC DIAGRAM OF DIRECT AND INDIRECT EVAPORATIVE COOLING CONCEPTS (HVAC, 2015)	73
FIGURE 3.3.2 PSYCHOMETRIC OF DIRECT AND INDIRECT EVAPORATIVE COOLING (DAOU ET AL., 2006).....	74
FIGURE 3.3.3 CONCEPT OF LIQUID DESICCANT BASED EVAPORATIVE COOLING SYSTEM (EVAP, 2015)	74
FIGURE 3.3.4 SCHEMATIC DIAGRAM OF THE SOLAR LDAC SYSTEM (GANDHIDASAN, 1990)	77
FIGURE 3.3.5 SCHEMATIC DIAGRAM OF THE SOLAR LDAC SYSTEM IN QUEENSLAND, AUSTRALIA (ALIZADEH 2008)	78
FIGURE 3.3.6 SCHEMATIC DIAGRAM OF A SOLAR-DRIVEN LIQUID DESICCANT EVAPORATIVE SYSTEM (ABDALLA, 2006)	78
FIGURE 3.3.7 SCHEMATIC OF THE SOLAR ASSISTED LIQUID DESICCANT SYSTEM WITH EVAPORATIVE PAD (LYCHNOS, 2012)	79
FIGURE 3.3.8 SCHEMATIC OF THE LIQUID DESICCANT COOLING SYSTEM (DAS ET AL., 2013).....	82
FIGURE 3.3.9 SCHEMATIC OF THE SYSTEM PROPOSED BY (YIN ET AL., 2009)	82
FIGURE 3.3.10 SCHEMATIC DIAGRAM OF THE SOLAR LIQUID DESICCANT ENHANCED DEW POINT COOLING SYSTEM (KOZUBAL ET AL., 2011).....	83
FIGURE 3.4.1 SCHEMATIC OF A SOLAR THERMAL REGENERATION SYSTEM FOR LDAC (CHENG ET AL., 2013).....	85
FIGURE 3.4.2 A SCHEMATIC OF THE PV-ED REGENERATION SYSTEM (LI ET AL., 2009)	87
FIGURE 3.5.1 SCHEMATIC OF THE PASSIVE & NATURAL AIR-CONDITIONING AND VENTILATION SYSTEM (ENTERIA, 2011)	89
FIGURE 3.5.2 SCHEMATIC OF THERMALLY DRIVEN DESICCANT COOLING CONCEPT (ENTERIA ET AL., 2011) ...	90
FIGURE 4.1.1 INTRODUCTORY SAMPLE OF THE VISUALIZATION SCHEME (RUSCHENBURG ET AL., 2013)	102
FIGURE 4.1.2 SOLAR HEAT PUMP SYSTEM WITH A FLAT-PLATE COLLECTOR AND A DIRECT-EVAPORATION AIR SOURCE HEAT PUMP UNIT ALONG WITH THE CONDENSER IMMERSSED IN A DHW STORAGE. THIS SYSTEM IS EXCLUSIVELY DESIGNED FOR DHW APPLICATIONS (RUSCHENBURG ET AL., 2013).	103
FIGURE 4.1.3 SOLAR HEAT PUMP SYSTEM WITH AN UNGLAZED COLLECTOR AND A HEAT PUMP UNIT ALONG WITH THE CONDENSER IMMERSSED IN A DHW STORAGE. THIS SYSTEM IS EXCLUSIVELY DESIGNED FOR DHW APPLICATIONS (RUSCHENBURG ET AL., 2013).	103
FIGURE 4.1.4 SOLAR HEAT PUMP SYSTEM WITH AN UNSPECIFIED COLLECTOR AND A HEAT PUMP UNIT ALONG WITH THE CONDENSER IMMERSSED IN A COMBINED STORAGE TANK. THIS SYSTEM IS DESIGNED FOR DHW PREPARATION AS WELL AS SPACE HEATING APPLICATIONS (RUSCHENBURG ET AL., 2013).	103
FIGURE 4.2.1 INDIRECT SOLAR DHW SYSTEM (CHU ET AL., 2013)	105
FIGURE 4.2.2 PARALLEL TYPE SAHP (CHU ET AL., 2013).....	106
FIGURE 4.2.3 DIRECT SERIES TYPE SAHP (CHU ET AL., 2013).....	106
FIGURE 4.2.4 INDIRECT SERIES TYPE SAHP (CHU ET AL., 2013).....	107
FIGURE 4.2.5 SERIES TYPE SAHP SPACE-HEATING CONCEPT (CHU ET AL., 2013).....	109
FIGURE 4.2.6 PARALLEL TYPE SAHP SPACE-HEATING CONCEPT (CHU ET AL., 2013)	110
FIGURE 4.2.7 DUAL-SOURCE SAHP SPACE-HEATING CONCEPT (CHU ET AL., 2013)	110
FIGURE 5.2.1 THE INTEGRATION OF UNIQUE POLYETHYLENE HEAT EXCHANGER LOOP UNDERNEATH PV MODULES.....	139
FIGURE 5.2.2 THERMAL ROOF UNIT PIPING	140
FIGURE 5.2.3 THE PROTOTYPE OF THE PROPOSED SYSTEM	144
FIGURE 5.2.4 HEAT TRANSFER PROFILE OF THE ROOF UNIT	145
FIGURE 5.2.5 SCHEMATIC OF THE USE OF POWER PRODUCED BY THE SOLAR ENERGY SYSTEM	156
FIGURE 5.3.1 VARIATION OF TEMPERATURE: (TPV)EFF, TA, AND TW (8 TH JULY-3 RD AUGUST 2013).....	158
FIGURE 5.3.2 VARIATION OF PV MODULE TEMPERATURE - THEORETICAL AND EXPERIMENTAL.....	159
FIGURE 5.3.3 VARIATION OF WATER TEMPERATURE - THEORETICAL AND EXPERIMENTAL.....	159
FIGURE 5.3.4 VARIATION OF AVERAGE WATER TEMPERATURE WITH VARIOUS MASS FLOW RATE (KG/S) AND PRESSURE (BAR).....	160
FIGURE 5.3.5 VARIATION OF AVERAGE WATER TEMPERATURE WITH VARIOUS WIND SPEED IN M/S	161

FIGURE 5.3.6 EFFECT OF FLUID TEMPERATURE ON THE OVERALL THERMAL EFFICIENCY.....	162
FIGURE 5.3.7 EFFECT OF POLY HE ON PV POWER ENERGY EFFICIENCY	163
FIGURE 5.3.8 EFFECT OF POLY HE ON PV EXERGY EFFICIENCY	163
FIGURE 5.3.9 ANNUAL PRESENT VALUE OF THE SYSTEM SAVINGS OVER THE 25-YEARS LIFE CYCLE PERIOD	164
FIGURE 5.3.10 VARIATION OF PB, CUM. SS AND CUM. ECS AS A FUNCTION OF TIME OVER 25-YEAR LIFE CYCLE.....	165
FIGURE 6.2.1 THE SYSTEM CONFIGURATION OF THE COMBINED SYSTEM	173
FIGURE 6.2.2 LIQUID DESICCANT BASED DEHUMIDIFICATION WITH INDIRECT EVAPORATIVE COOLING UNIT....	184
FIGURE 6.2.3 THE DEHUMIDIFIER AND REGENERATION UNIT	186
FIGURE 6.2.4 SCHEMATIC DIAGRAM OF THE INDIRECT EVAPORATIVE COOLER.....	189
FIGURE 6.2.5 EXPERIMENTAL INDIRECT EVAPORATIVE COOLING UNIT.....	191
FIGURE 6.3.1 HOURLY VARIATION OF PV, AMBIENT, WATER TEMPERATURES AND WIND SPEED	193
FIGURE 6.3.2 AVERAGE VARIATION OF PV COVER TEMPERATURE- EXPERIMENTAL AND THEORETICAL	194
FIGURE 6.3.3 EFFECT OF POLY HEAT EXCHANGER ON POWER CONVERSION EFFICIENCY.....	195
FIGURE 6.3.4 USEFUL HEAT GAIN.....	195
FIGURE 6.3.5 AIR TEMPERATURE AND RELATIVE HUMIDITY VARIATION ACROSS THE DEHUMIDIFIER.....	197
FIGURE 6.3.6 AIR TEMPERATURE AND RELATIVE HUMIDITY VARIATION ACROSS THE REGENERATOR	197
FIGURE 6.3.7 LIQUID DESICCANT AND WATER TEMPERATURE VARIATION.....	198
FIGURE 6.3.8 VARIATION IN WET-BULB EFFECTIVENESS OF THE DEHUMIDIFIER	198
FIGURE 6.3.9 (A-B-C-D-E) INDIRECT EVAPORATIVE COOLER PERFORMANCE DATA A) WARM AIR WITH 300M ³ /H B) WARM AIR WITH 600M ³ /H.....	200
FIGURE 6.3.10 INDIRECT EVAPORATIVE COOLER COP AT DIFFERENT FAN SETTINGS.....	201
FIGURE 6.3.11 VARIATION OF AIR TEMPERATURE ACROSS THE COMBINED DEHUMIDIFICATION-COOLING UNIT	203
FIGURE 6.3.12 VARIATION OF RELATIVE HUMIDITY ACROSS THE COMBINED DEHUMIDIFICATION-COOLING UNIT	203
FIGURE 6.3.13 COOLING CAPACITY OF INDIRECT EVAPORATIVE COOLER AND COMBINED UNIT	204
FIGURE 7.2.1 CROSS SECTIONAL VIEW OF THE NOVEL "SANDWICH" THERMAL ROOF COLLECTOR.....	214
FIGURE 7.2.2 SCHEMATIC OF THE COMBINED SYSTEM	216
FIGURE 7.2.3 EXPERIMENTAL DESIGN - NOVEL SOLAR THERMAL ROOF WITH SOLAR SIMULATOR, HEAT PUMP, WATER STORAGE	220
FIGURE 7.3.1 THE HEAT TRANSFER PROFILE OF THE ROOF UNIT	221
FIGURE 7.3.2 P-H CHART OF THE HEAT PUMP REFRIGERATION CYCLE (GLO, 2015)	222
FIGURE 7.4.1 PERFORMANCE OF THE NOVEL ROOF UNDER 400 W/M ² SOLAR INTENSITY AND VARIOUS FLOW RATES.....	229
FIGURE 7.4.2 PERFORMANCE OF THE NOVEL ROOF UNDER 600 W/M ² SOLAR INTENSITY AND VARIOUS FLOW RATES.....	229
FIGURE 7.4.3 PERFORMANCE OF THE NOVEL ROOF UNDER 800 W/M ² SOLAR INTENSITY AND VARIOUS FLOW RATES.....	230
FIGURE 7.4.4 VARIATION OF EFFICIENCY UNDER DIFFERENT SOLAR RADIATION WITH VARIOUS FLOW RATES	231
FIGURE 7.4.5 EFFECT OF COLLECTOR FLUID TEMPERATURE ON THE COLLECTOR EFFICIENCY.....	232
FIGURE 7.4.6 HOURLY VARIATION OF TEMPERATURE T _A , T _S , T _W AND WIND SPEED V _{WIND} (23TH JUNE, 2014)	233
FIGURE 7.4.7 HOURLY VARIATION OF SURFACE TEMPERATURE - THEORETICAL VS EXPERIMENTAL	233
FIGURE 7.4.8 HOURLY VARIATION OF WATER TEMPERATURE - THEORETICAL VS EXPERIMENTAL.....	234
FIGURE 7.4.9 TEST RESULT OBTAINED ON 23TH OF JUNE, 2014	235
FIGURE 7.4.10 TEMPERATURE VARIATION IN ENERGY STORING WITH TIME	236
FIGURE 7.4.11 COEFFICIENT OF PERFORMANCE VARIATION BY TIME	236
FIGURE 7.4.12 VARIATION OF PAYBACK PERIOD AS A FUNCTION OF COLLECTOR AREA FOR VARIOUS INFLATION RATES.....	238
FIGURE 8.4.1 EVAPORATOR PERFORMANCE AT 200 W/M ² , 6 L/MIN AND 2 BAR (WHEN HP IS AT SPACE HEATING MODE)	338

FIGURE 8.4.2 EVAPORATOR PERFORMANCE AT 200 W/M ² , 6 L/MIN AND 2 BAR (WHEN HP IS AT DHW MODE)	338
FIGURE 8.4.3 HP PERFORMANCE AT 200 W/M ² , 6 L/MIN AND 2 BAR (WHEN HP IS AT SPACE HEATING MODE)	339
FIGURE 8.4.4 HP PERFORMANCE AT 200 W/M ² , 6 L/MIN AND 2 BAR (WHEN HP IS AT DHW MODE)	339
FIGURE 8.4.5 EVAPORATOR PERFORMANCE AT 400 W/M ² , 6 L/MIN AND 2 BAR (WHEN HP IS AT SPACE HEATING MODE)	339
FIGURE 8.4.6 EVAPORATOR PERFORMANCE AT 400 W/M ² , 6 L/MIN AND 2 BAR (WHEN HP IS AT DHW MODE)	340
FIGURE 8.4.7 HP PERFORMANCE AT 400 W/M ² , 6 L/MIN AND 2 BAR (WHEN HP IS AT SPACE HEATING MODE)	340
FIGURE 8.4.8 HP PERFORMANCE AT 400 W/M ² , 6 L/MIN AND 2 BAR (WHEN HP IS AT DHW MODE)	340
FIGURE 8.4.9 EVAPORATOR PERFORMANCE AT 600 W/M ² , 6 L/MIN AND 2 BAR (WHEN HP IS AT SPACE HEATING MODE)	341
FIGURE 8.4.10 EVAPORATOR PERFORMANCE AT 600 W/M ² , 6 L/MIN AND 2 BAR (WHEN HP IS AT DHW MODE)	341
FIGURE 8.4.11 HP PERFORMANCE AT 600 W/M ² , 6 L/MIN AND 2 BAR (WHEN HP IS AT SPACE HEATING MODE)	341
FIGURE 8.4.12 HP PERFORMANCE AT 600 W/M ² , 6 L/MIN AND 2 BAR (WHEN HP IS AT DHW MODE)	342
FIGURE 8.4.13 EVAPORATOR PERFORMANCE AT 200 W/M ² , 8 L/MIN AND 2 BAR (WHEN HP IS AT SPACE HEATING MODE)	342
FIGURE 8.4.14 EVAPORATOR PERFORMANCE AT 200 W/M ² , 8 L/MIN AND 2 BAR (WHEN HP IS AT DHW MODE)	343
FIGURE 8.4.15 HP PERFORMANCE AT 200 W/M ² , 8 L/MIN AND 2 BAR (WHEN HP IS AT SPACE HEATING MODE)	343
FIGURE 8.4.16 HP PERFORMANCE AT 200 W/M ² , 8 L/MIN AND 2 BAR (WHEN HP IS AT DHW MODE)	343
FIGURE 8.4.17 EVAPORATOR PERFORMANCE AT 400 W/M ² , 8 L/MIN AND 2 BAR (WHEN HP IS AT SPACE HEATING MODE)	344
FIGURE 8.4.18 EVAPORATOR PERFORMANCE AT 400 W/M ² , 8 L/MIN AND 2 BAR (WHEN HP IS AT DHW MODE)	344
FIGURE 8.4.19 HP PERFORMANCE AT 400 W/M ² , 8 L/MIN AND 2 BAR (WHEN HP IS AT SPACE HEATING MODE)	345
FIGURE 8.4.20 HP PERFORMANCE AT 400 W/M ² , 8 L/MIN AND 2 BAR (WHEN HP IS AT DHW MODE)	345
FIGURE 8.4.21 EVAPORATOR PERFORMANCE AT 600 W/M ² , 8 L/MIN AND 2 BAR (WHEN HP IS AT SPACE HEATING MODE)	346
FIGURE 8.4.22 EVAPORATOR PERFORMANCE AT 600 W/M ² , 8 L/MIN AND 2 BAR (WHEN HP IS AT DHW MODE)	346
FIGURE 8.4.23 HP PERFORMANCE AT 600 W/M ² , 8 L/MIN AND 2 BAR (WHEN HP IS AT SPACE HEATING MODE)	347
FIGURE 8.4.24 HP PERFORMANCE AT 600 W/M ² , 8 L/MIN AND 2 BAR (WHEN HP IS AT DHW MODE)	347
FIGURE 8.4.25 EVAPORATOR PERFORMANCE AT 200 W/M ² , 4 L/MIN AND 2 BAR (WHEN HP IS AT SPACE HEATING MODE)	347
FIGURE 8.4.26 EVAPORATOR PERFORMANCE AT 200 W/M ² , 4 L/MIN AND 2 BAR (WHEN HP IS AT DHW MODE)	348
FIGURE 8.4.27 HP PERFORMANCE AT 200 W/M ² , 4 L/MIN AND 2 BAR (WHEN HP IS AT SPACE HEATING MODE)	348
FIGURE 8.4.28 HP PERFORMANCE AT 200 W/M ² , 4 L/MIN AND 2 BAR (WHEN HP IS AT DHW MODE)	348
FIGURE 8.4.29 EVAPORATOR PERFORMANCE AT 400 W/M ² , 4 L/MIN AND 2 BAR (WHEN HP IS AT SPACE HEATING MODE)	349
FIGURE 8.4.30 EVAPORATOR PERFORMANCE AT 400 W/M ² , 4 L/MIN AND 2 BAR (WHEN HP IS AT DHW MODE)	349
FIGURE 8.4.31 HP PERFORMANCE AT 400 W/M ² , 4 L/MIN AND 2 BAR (WHEN HP IS AT SPACE HEATING MODE)	349
FIGURE 8.4.32 HP PERFORMANCE AT 400 W/M ² , 4 L/MIN AND 2 BAR (WHEN HP IS AT DHW MODE)	350

FIGURE 8.4.33 EVAPORATOR PERFORMANCE AT 600 W/M ² , 4 L/MIN AND 2 BAR (WHEN HP IS AT SPACE HEATING MODE)	350
FIGURE 8.4.34 EVAPORATOR PERFORMANCE AT 600 W/M ² , 4 L/MIN AND 2 BAR (WHEN HP IS AT DHW MODE)	350
FIGURE 8.4.35 HP PERFORMANCE AT 600 W/M ² , 4 L/MIN AND 2 BAR (WHEN HP IS AT SPACE HEATING MODE)	351
FIGURE 8.4.36 HP PERFORMANCE AT 600 W/M ² , 4 L/MIN AND 2 BAR (WHEN HP IS AT DHW MODE).....	351

LIST OF TABLES

TABLE 4.1 SYSTEM CLASSIFICATION TABLE – A SAMPLE OF THE LITERATURE STUDY TO PROVIDE INFORMATION ABOUT SYSTEM CONCEPTS	100
TABLE 4.2 OVERVIEW OF COMPARATIVE STUDIES	112
TABLE 4.3 OVERVIEW OF DIRECT SERIES SYSTEMS.....	116
TABLE 4.4 OVERVIEW OF INDIRECT SERIES SYSTEMS.....	120
TABLE 4.5 OVERVIEW OF SOME SAHP STUDIES WITH THERMAL PERFORMANCE ANALYSES AND EVALUATION METHODS	127
TABLE 5.1 SOLAR OPTICAL PARAMETERS OF PV CELLS AND GLASS COVER.....	142
TABLE 5.2 TECHNICAL PARAMETERS OF THE ROOF UNIT	143
TABLE 5.3 INITIAL DESIGN PARAMETERS	144
TABLE 5.4 SOLAR SYSTEM COMPONENTS AND COSTS.....	155
TABLE 5.5 ECONOMIC PARAMETERS	155
TABLE 5.6 THE ECONOMIC ANALYSIS OF THE PROPOSED SYSTEM (IN £) FOR NOTTINGHAM, UK OVER 25-YEAR LIFE CYCLE.....	166
TABLE 6.1 PERFORMANCE DATA OF THE INDIRECT EVAPORATIVE COOLING UNIT	202
TABLE 6.2 EXPERIMENTAL PERFORMANCE DATA OF THE OVERALL SYSTEM	205
TABLE 7.1 TECHNICAL PARAMETERS	217
TABLE 7.2 INITIAL DESIGN PARAMETERS	220
TABLE 7.3 MEASURED PARAMETERS AND EXPERIMENTAL RESULTS IN AVERAGE	237
TABLE 7.4 ECONOMIC PARAMETERS	238

LIST OF ACRONYMS

A/C	Air Conditioning
ASHRAE	American Society of Heating, Refrigerating and Air Conditioning Engineers
BICPV/T	Building integrated Concentrating Photovoltaic Thermal
BiPVT	Building integrated photovoltaic thermal
BiPVW	Building integrated photovoltaic water heating
BS	British Standard
C/R	Collector/Regenerator
CFD	Computational Fluid Dynamics
COP	Coefficient of Performance
CPC	Compound Parabolic Concentrator
DHW	Domestic Hot Water
DT	Data Taker
DX-SAHP	Direct Expansion Solar assisted Heat Pump
ED	Electrodialysis
EES	Engineering Equation Solver
EIT	Export Tariff
ETR	Effective Tax Rate
FER	Free Energy Ratio
FGM	Functionally graded material
FIT	Feed in Tariff
HCOOK	Potassium Formate
HE	Heat Exchanger
HK	Hong Kong
IEA SHC	International Energy Agency Solar Heating Cooling
IP	Interest Payment
IR	Infrared
ITS	Income Tax Savings
IX-SAHP	Indirect Expansion Solar assisted Heat Pump
LCC	Life Cycle Cost
LDAC	Liquid Desiccant Air Conditioner
NASA	National Aeronautics and Space Agency

NPV	Net Present Value
NREL	National Renewable Energy Laboratory
O&M	Operations and Maintenance
OFGEM	The Office of Gas and Electricity Markets
PCM	Phase Change Material
PT	Property Tax
PV/LHP	Photovoltaic loop Heat Pipe
PV/T	Photovoltaic Thermal
PV-SAHP	Photovoltaic Solar assisted Heat Pump
RH	Relative Humidity
SPF	Seasonal Performance Factor
SS	Solar Savings
STC	Standard Test Conditions
UK	United Kingdom
US	United States
UV	Ultraviolet

NOMENCLATURE

\dot{m}	Mean flow rate
$(T_{PV})_{eff}$	Effective PV module temperature
A_{eff}	Effective area, m ²
C	Specific heat
CUE	Unit cost of produced energy
D_i	Inner diameter of heat exchanger tube, m
D_o	Outer diameter of heat exchanger tube, m
e	Percent deviation
F	Fin efficiency
F'	Flat plate collector efficiency factor
g	Gravitational acceleration, m/s ²
G_r	Grashoff number
h	Heat transfer coefficient, W/m ² K
I	Incident solar radiation, W/m ²
K	Thermal conductivity
L	Cubic root of dwelling volume
M	Mass, kg
m	Variable defined to solve differential equations
N	Life cycle period
Nu	Nusselt number
Q	Energy, W
T	Temperature
$T_{PV/T}$	Operating temperature of PV module
U	Thermal transfer coefficient, W/m ² K
V	Wind speed, m/s
\dot{W}	Compressor power, kW
W	Distance between tubes

Subscripts

<i>a</i>	Ambient air
<i>abs</i>	Absorber surface
<i>air</i>	Air layer
<i>c</i>	Cover layer
<i>c, t</i>	Thermal energy in condenser
<i>cn</i>	Condenser
<i>cool</i>	Cooling
<i>cp, e</i>	Electrical energy in compressor
<i>cs</i>	Collector side
<i>cv</i>	Convective
<i>db</i>	Dry bulb
<i>dp</i>	Dew point
<i>e</i>	Evaporator
<i>é</i>	Electrical
<i>e, t</i>	Thermal energy from evaporator
<i>eq</i>	Equilibrium
<i>ev,cool</i>	Evaporative cooler
<i>f</i>	Fluid
<i>he</i>	Heat exchanger
<i>hein</i>	Inner wall of heat exchanger
<i>hein, w</i>	Inner wall of heat exchanger to water
<i>heo</i>	Outer wall of heat exchanger
<i>heo, hein</i>	Outer wall to inner wall of heat exchanger
<i>HP</i>	Heat pump
<i>In</i>	Inlet
<i>l</i>	Loss
<i>ls</i>	Load side
<i>o</i>	Overall
<i>out</i>	Outlet
<i>p</i>	Pipe
<i>pl</i>	EVA plastic back of a PV module

<i>pv, heo</i>	PV cell layer to outer wall of heat
<i>r</i>	Refrigerant
<i>rd</i>	Radiative
<i>rs</i>	Reference situation
<i>s</i>	Sky
<i>sa</i>	Supply air
<i>SYS</i>	System
<i>t</i>	Thermal
<i>t, net</i>	Net thermal
<i>v</i>	Vapour
<i>w</i>	Water
<i>wb</i>	Wet bulb

Greek letters

α	Absorption
β_p	Temperature coefficient for PV efficiency
β_s	Tilt-angle of PV panels
Δ	Thickness, m
ε	Emissivity
η	Efficiency, %
σ	Stefan-Boltzmann constant
τ	Transmittance
ν	Kinematic viscosity, m ² /s
ρ	Density, kg/m ³
ξ	Packing factor
λ	Thermal conductivity, W/m ² K
Σ	Total



CHAPTER 1 - Introduction

1. INTRODUCTION

Worldwide trends on energy consumption show that primary energy consumption and CO₂ emissions have increased by 49 and 43% throughout the last decades. Energy consumption rates may change from country to country depending on its social, cultural and economic conditions. Developing nations (South America, Middle East, Africa and Southeast Asia) recently have energy consumption rate of 3.2% on average while it is 1.1% for most of the developed nations (US, Japan, Australia and Western Europe), (IEA, 2013). This growing demand for fossil fuels may cause a major disruption and endanger the energy supply chain. The major concerns of depletion in fossil fuel based energy sources, economic and environmental problems associated with the combustion of fossil fuels have led to the critical societal need to transition to renewable energy resources such as solar, wind, and hydropower in recent years (Chaturvedi et al., 2014).

In the EU, energy use in buildings accounts for approximately 40% of total primary energy consumption and is responsible for a similar proportion of total carbon emission. Of the energy used in the building sector, HVAC (heating, ventilation and air conditioning) systems consume approximately 60%, lighting 15% and appliances about 10%. This is supported by the worldwide fact that HVAC and electric lighting are the two main energy consuming applications account for 40-60% and 20-30%, respectively. Improving the efficiency of HVAC and water heating systems employed in the built environment therefore has significant potential to bring about meaningful savings in worldwide energy consumption (IEA, 2013).

In the national level, in 2013, UK's total energy consumption was 205.9 million tons of oil equivalents (mtoe). About 31.7% of this total energy was consumed in domestic applications. Space heating alone accounts for 53% of the energy

consumed in a typical UK household while it is estimated that about 13.7% is for low temperature (<80°C) water heating applications in which energy demand is primarily satisfied through either natural gas or electrical heaters (Department of Energy and Climate Change, 2014). However, use of conventional source of energy based systems leads to increased greenhouse gas emissions into the atmosphere. A typical natural gas water heater releases around 2 tons CO₂ annually. Electric hot water systems are having more harmful effect for about three times the emission of CO₂ for each kWh of electrical energy, compared to natural gas water heaters. The UK Government pledged (December 2006) that by 2016, it will be a requirement for all new homes to be zero-carbon against which all new homes would be rated on a range of various sustainability measures and introduced the Code for Sustainable Homes and the 2008 Climate Change Act sets the target of an 80% reduction in CO₂ emissions from the 1990 level by 2050 (UK Green Building Council, 2008). These requirements stimulate the development of various energy efficient technologies to provide a more energy efficient built environment. Accordingly, in order to accomplish these zero-carbon spaces and HVAC requirements, there is a set of challenges for industry which craves innovation and research towards low carbon technologies worldwide.

1.1 Statement of the problems

Future projections stating the growing gap between energy supply and demand have motivated the development of environmentally benign energy technologies. Among others, solar energy, as a major renewable and eco-friendly energy source with the most prominent characteristic of inexhaustibility, seems to be more promising to offer sustainable solutions towards environmental protection and conservation of conventional energy sources. Thus, solar energy based systems can meet energy

demands to some extent to maintain the balance in the ecosystem. However, public acceptance of solar energy technologies depends heavily on factors such as efficiency, cost-effectiveness, reliability and availability (Shan et al., 2014; Kumar 2011).

Solar thermal collectors are a particular type of heat extracting devices that convert solar radiation into thermal energy through a transport medium or flowing fluid. These collectors, as being a significant part of any solar energy system, absorb the incoming solar radiation, convert it to heat energy and convey through a working fluid such as air, water or refrigerant, for various useful purposes. In general, they are utilized as air drying/heating for agricultural products or heating/air conditioning of buildings (Kumar, 2015).

In addition to being technically and structurally efficient, solar thermal collectors must satisfy the following requirements for architectural integration. These requirements are a generalization of the criterion set by IEA Task 41 Solar Energy and Architecture for aesthetic quality of buildings integrated solar thermal collectors (Wall et al., 2012):

- Integrating naturally
- Architecturally pleasing design
- Good composition of colours and materials
- Size that suits the harmony and combination
- Consistency to the context of the building
- Well composed and innovative design

Building integrated solar thermal collectors may be installed either on the building façade or on the roof causing in each case a different visual impact. Depending on

the type and dimensions, the system may be integrated in such a way that it is invisible, aesthetically appealing or appearing as an architectural concept (Chemisana, 2011).

In addition to building integration matter, solar collectors such as evacuated glass tubes have several drawbacks, which include:

- Susceptibility to damage during transportation, which could lead to large financial losses and material waste;
- Expensive to make and to install;
- Not aesthetically appealing, nor easily integrated into roofs or facades;
- Fragile nature means they could easily be vandalised.

PV cells can be integrated with building facades or roofs, but they are expensive and their electricity conversion efficiency is reduced, if the PV cell temperature is high. Therefore, a practical cooling method is required to enhance the efficiency of PV cells.

For heat pumps, a fundamental factor of great importance for highly efficient operation is the availability of a cheap, reliable heat source for the evaporator. The power quality can be improved by coupling solar energy with heat pump and the combination can represent promising solutions for various domestic applications. That combination of the heat pump and solar energy is a mutual beneficial way of enhancing the coefficient of performance of a heat pump and solar collector efficiency. The heat pump COP can be elevated to the great extent on the temperature of the evaporator. The solar collector loop enables to boost the heat source temperature of the heat pump, thereby improving the annual and seasonal performance (Georgiev, 2008).

Utilization of sunlight for cooling is a long-sought goal. As the demand for cooling is proportional to the solar intensity, thus the time of peak cooling need coincides with the time of maximum resource occurs. Given this relation, it is no doubt that there has been a considerable interest to produce economical solar cooling technologies. Heat-activated systems that mainly driven by heat input from solar thermal energy have been introduced allowing simultaneous production of heat and cooling/refrigeration (Otanicar et al., 2012). Compared to the conventional vapour compression systems, thermally driven air-conditioning technique would be an effective alternative in terms of increasing primary energy savings with less power consumption and therefore less greenhouse gas emissions and hazardous materials and pollutants depleted to the environment (Jradi et al., 2014). Thus, linking solar heat energy for regeneration and a liquid desiccant cooling system can provide sufficient fulfilment of cooling demands for residential and building applications in addition to thermal comfort and indoor air quality.

The main area and aim of the project is, therefore, to address the above limitations by developing a building integrated solar PV/Thermal “invisible” collector and solar thermal roof that properly blends into surroundings thus avoiding ‘add-on’ appearance and providing renewable heat source for solar assisted heating & cooling technologies namely heat pump for water heating and liquid desiccant system for cooling. The integration of unique structured polyethylene heat exchanger loop underneath PV modules to form an ‘invisible’ roof collector, and a solar thermal ‘sandwich’ roof is proposed.

1.2 Research aims and objectives

In order to achieve the above aims, the following have been independently investigated; integration of the novel polyethylene heat exchanger loop underneath

PV modules to combine with Liquid Desiccant Air conditioning system, and integration of the novel polyethylene heat exchanger loop with black aluminum cover to form a “Sandwich” solar roof combining with a heat pump using R718 as a working fluid.

Therefore, the overall objectives of this research are:

- Achieving a roof integrated thermal collector that propitiously blends into its surroundings
- Having a dual function; heat absorption and cooling of PV modules via heat extraction
- Providing free, renewable heat resources/not power source for solar assisted heating and cooling technologies
- To enhance the Coefficient of Performance (COP) of the heat pump via pre-heating of R-718 as a working fluid

The research concept, in this study, is interpreted as consisting of three dimensions that would be carried out: design and development of new solar thermal roof system, its exercise with a heat pump for cold climates and hybrid desiccant cooling system for hot climates (Fig 1). The research area selected in this PhD project covers the analyses of technical, economic and environmental aspects of the new systems. Broadly speaking, these dimensions capture the aspirations for improved utilization of clean energy resources and mitigation of our negative impacts on the environment.

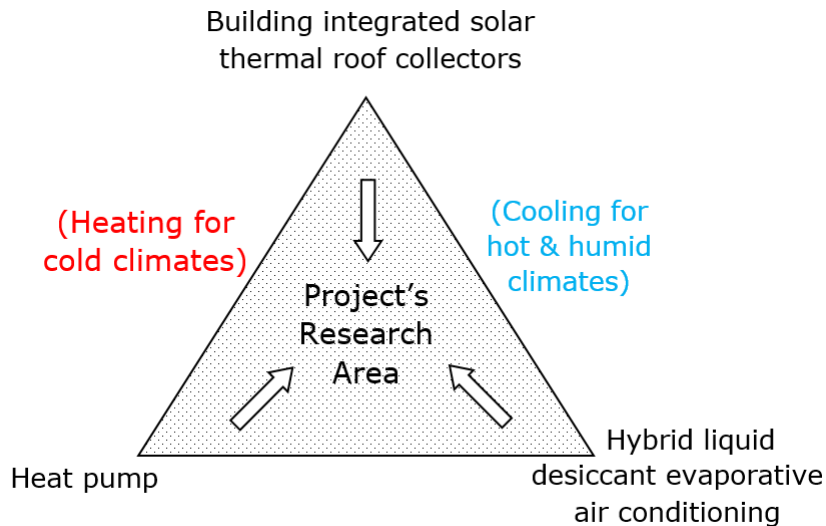


Figure 1.2.1 the research model

The aimed novel outcomes of the project are:

- The use of the polyethylene heat exchanger loop to provide free DHW heating, energy saving and carbon reduction
- The use of the “Sandwich” roof system to provide cost effective solutions for regions that suffer from energy poverty in the residential and commercial areas
- Enabling to couple with different systems for different climates (heating for cold climates and air conditioning for hot & humid climate zones) and to prove that proposed system can operate under various climate conditions
- Using fewer parts, being inexpensive to install in a single house, and requiring minimal maintenance

1.3 Scope of the project

The scope of this project, in order to favorably fulfill the above objectives, is categorized into following distinct stages;

- Literature review of past and present work in order to inspect the recent developments on building integrated PV/T and solar thermal collectors, solar

assisted heat pumps for low temperature water heating applications, and solar assisted liquid desiccant evaporative technology

- Theoretical and experimental performance evaluations on the integration of polyethylene heat exchanger with PV technology, integration of poly heat exchanger based PV/T with liquid desiccant evaporative air conditioning, unique solar thermal roof and its integration with a heat pump for water heating
- Field test of building integrated PV/T for validation during summer season
- Build up and test solar thermal roof collector for a heat pump operation
- Validate theoretical findings with the experimental results
- Discuss the technical, economic and environmental aspects of the new systems

1.4 Novelty

This project has the following novelty aspects:

- The use of polyethylene heat exchanger underneath the solar collectors which can fairly collect the waste heat dissipated by PV modules and forms an 'invisible' collector
- The use of polyethylene heat exchanger with black aluminum cover to form a dual function "Sandwich" roof/solar collector
- The integration of 'sandwich' roof/solar collector with a R718 heat pump
- The combination of solar thermal 'invisible' collector with a hybrid liquid desiccant evaporative air conditioning system

1.5 Research methods and Methodology

The project work, in this thesis, is mainly based on the following stages:

- *Background work and literature review*

Comprehensive literature reviews over building integrated solar thermal collectors, solar assisted heat pumps for low temperature water heating applications, and solar assisted liquid desiccant evaporative technology were performed in order to comprehend the scope of this project and retrieve the relevant data from the previously published studies.

- *Modelling work*

Mathematical modelling has been undertaken through the use of recognised and appropriate software e.g. Engineering Equation Solver (EES) in order to analyse the proposed systems thermodynamically and evaluate the performance in various ways and under different operating conditions.

- *Pilot-scale testing in the laboratory*

Pilot-scale test rigs have been composed for the performance testing of the novel systems. Outdoor testing was also executed to compare the results with the findings obtained in environmental chamber testing.

- *Field testing*

A field trial was carried out on a remote project to detect and monitor the real-time performance characteristics of the proposed system.

1.6 Structure of the thesis

The thesis is divided into eight chapters, following this introductory chapter, the work is presented in the following sections:

Chapter 1: Covers the introductory section to the driving forces of this work. The objectives, scopes and novelty aspects of the project are detailed. Also, the methodology approach to fulfil the objectives is provided in the present chapter.

Chapter 2: Facilitates understanding the questions prevailing in solar thermal collector technology, diagnosing new research directions towards further improvement of the performance, addressing the important issues related to architectural barriers, system design and installation. Also, the review work in this chapter reveals the trend of the technology, particularly the advancement in recent years and the future work required.

Chapter 3: Presents the review work on recent developments in solar assisted liquid desiccant cooling and its various applications combined with evaporative air-conditioning under different climates and advantages the system may offer in terms of energy savings are underscored. A basic description of the principles of hybrid solar liquid desiccant with direct and indirect evaporative cooling is provided. Finally, solar regeneration methods and recent developments for the liquid desiccant air-conditioning system are presented.

Chapter 4: Reviews the past and present work conducted on Solar Assisted Heat Pump (SAHP) systems for low temperature water heating applications. The review approach is based on a visualization scheme to systematically

represent and classify concepts of SAHP systems. Specifically, the key performance data from a number of studies are highlighted and various configurations are compared in order to gain accurate and deep intuitive understandings of SAHP systems. The review faithfully states that having a variety of configurations, parameters and performance criteria may lead to a major inconsistency that increase the degree of complexity to compare and analyse the studies of different systems.

Chapter 5 Describes the experimental set-up of the integration of unique polyethylene heat exchanger loop underneath the PV modules to form PV/T modules without any 'add-on' appearance. This chapter also analyses the design specifications of the component (poly heat exchanger loop, PV solar panels, piping and heat storage) used in the system. A detailed thermal model is described to investigate the thermal performance of the system. Life Cycle Cost (LCC) method based Techno-economic analysis is provided as well.

Chapter 6: Introduces a new concept on solar thermal energy driven liquid desiccant based dew point cooling system that integrates several green technologies; including photovoltaic modules, polyethylene heat exchanger loop and a combined liquid desiccant dehumidification-indirect evaporative air conditioning unit. A pilot scale experimental set-up was developed and tested to investigate the performance of the proposed system and influence of the various parameters such as weather condition, air flow and regeneration temperature.

Chapter 7: Introduces the build-up and performance test of a novel solar thermal roof collector that was developed by primarily exploiting components

and techniques widely available on the market and coupled with a commercial heat pump unit to form an Indirect Expansion Solar assisted Heat Pump (IX-SAHP) water heating system. The analysis based on indoor and outdoor testing predominantly focuses on the solar thermal roof collector. A detailed thermal model was developed to describe the system operation.

Chapter 8: Provides the general discussion and concludes the work based on the theoretical and experimental investigations performed in this project. This section also suggests further works and open doors to the researchers interested in this area.



CHAPTER 2 – General overview of building integrated solar thermal collectors

2. BUILDING INTEGRATED SOLAR THERMAL COLLECTORS

2.1 INTRODUCTION

Future projections stating the growing gap between energy supply and demand have motivated the development of environmentally benign energy technologies. Among others, solar energy, as a major renewable and eco-friendly energy source with the most prominent characteristic of inexhaustibility, seems to be more promising to offer sustainable solutions towards environmental protection and conservation of conventional energy sources. Thus, solar energy based systems can meet energy demands to some extent to maintain the balance in the ecosystem. However, public acceptance of solar energy technologies depends heavily on factors such as efficiency, cost-effectiveness, reliability and availability (Shan et al., 2014; Kumar et al., 2011).

Solar thermal collectors are particular type of heat extracting devices that convert solar radiation into thermal energy through a transport medium or flowing fluid. These collectors, as being a significant part of any solar energy system, absorb the incoming solar radiation, convert it to heat energy and convey through a working fluid such as air, water or refrigerant, for various useful purposes. In general, they are utilized as air drying/heating for agricultural products or heating/air conditioning of buildings (Kumar et al., 2015).

In addition to being technically and structurally efficient, solar thermal collectors must satisfy the following requirements for architectural integration. These requirements are a generalization of the criterion set by IEA Task 41 Solar Energy and Architecture for aesthetic quality of buildings integrated solar thermal collectors (Wall et al., 2012):

- Integrating naturally
- Architecturally pleasing design
- Good composition of colours and materials
- Size that suits the harmony and combination
- Consistency to the context of the building
- Well composed and innovative design

Building integrated solar thermal collectors may be installed either on the building façade or on the roof causing in each case a different visual impact. Depending on the type and dimensions, the system may be integrated in such a way that it is invisible, aesthetically appealing or appearing as an architectural concept (Chemisana, 2011).

A review over all recent developments and applications of building integrated solar thermal collectors is presented in this chapter. In Section 1, introduction regarding the overall solar thermal collectors; Section 2 describes the PV/T concept; Section 3 gives a clear insight into solar thermal collectors; Section 4 investigates the future potential of the building integrated solar thermal collectors; Section 5 discuss the building integration criterion set by IEA SHC Task 41 Solar Energy and Architecture; Section 6 involves the conclusion of this communication.

2.2 PHOTOVOLTAIC/THERMAL (PV/T) COLLECTORS

A photovoltaic/thermal (PV/T) collector is a combination of photovoltaic (PV) and solar thermal components that produce both electricity and heat simultaneously. This dual function of the PVT enables a more effective use of solar energy that results in a higher overall solar conversion. Much of the captured solar energy in a sole PV module elevates the temperature of its cells which results in degradation of module

efficiency. This waste heat needs to be removed to ensure a high electrical output. The PV/T technology recovers part of this extracted heat to utilize for low-and-medium-temperature applications (Zondag et al., 2003).

The merits of PV/T concept comparing to alternative technologies contain eco-friendly, proven long life (20-30 years), noise free and low maintenance. However, several factors restrict the efficiency of the photovoltaic module particularly temperature increase and utilizing only a part of solar spectrum (photon energy threshold is less than $1.11 \mu\text{m}$ for c-Si) for power generation. The band gap of silicon (1.12 eV) limits the total energy collected in solar spectrum even less than $1.11 \mu\text{m}$. So, photons of longer wavelength dissipate their energy as waste heat rather than generating electron-hole pairs. As PV modules are able to convert only 4-17% of the incoming solar radiation into energy depending on the solar cell type and working conditions, cooling PV modules simultaneously by a fluid stream like air or water boost energy yield significantly. Conceptually, re-use of heat energy extracted by the coolant is ideal. Thus, PV/T collectors offer a higher overall efficiency (Chow, 2010).

Various types of PV/T collectors are in use at present based on working fluid and conduit shape such as PV/T air, PV/T water etc. Next section will introduce the types of building integrated PV/T systems briefly.

2.2.1 PV/T air collectors

Substantial research have been conducted on PV/T air collectors regarding design, simulation, building integration, and experimental testing. The air type design, shown in Figure 2.1, can offer a basic and cost-effective solution to PV cooling and also the air can be heated to certain temperatures through forced or natural air flow. In terms of efficiency, the forced flow is superior to the natural flow due to better convective

and conductive heat transfer although energy consumption of fans limits the net electrical power gain.

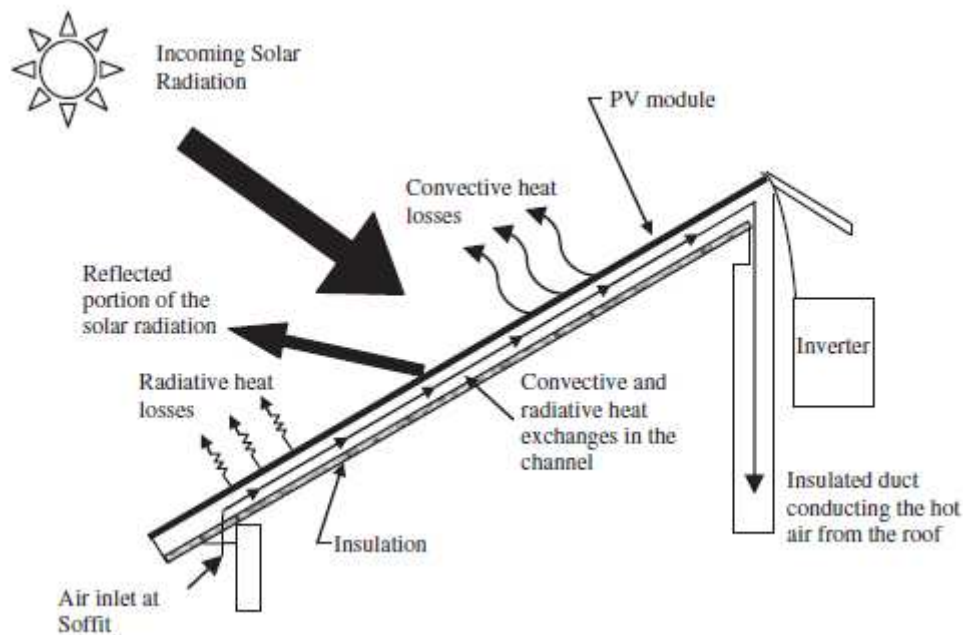


Figure 2.2.1. Schematic of a typical building integrated PV/T air design (Karava et al. 2011)

Hegazy (2000) performed a comparative study using four common designs. The four designs include the configurations of air flow passage above the absorber (I), below the absorber (II), both side of the absorber (III) and double pass (IV) as shown in Figure 2.2. Numerical simulations point out that in terms of electrical and thermal outputs, the configurations II-IV are similar and outperforming the configuration I. Configuration III consumes the least fan power and second lowest is configuration IV.

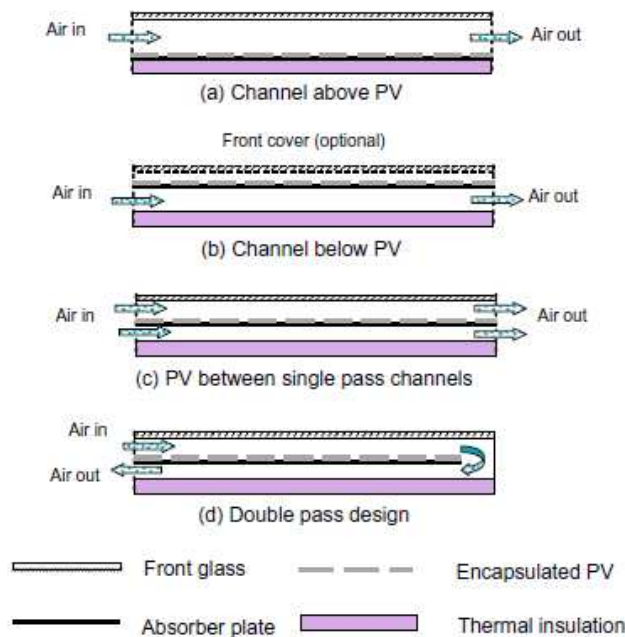


Figure 2.2.2 Cross-sectional view of common type PV/T air collectors (Chow, 2010)

Agrawal et al. (2013) compared the various type PV/T air collectors including glazed, unglazed hybrid PV/T tiles, and conventional hybrid PV/T air collectors. The simulation results revealed that unglazed hybrid PV/T tiles air collector was superior by 27% and 29.3% to the glazed hybrid PV/T tiles air collector and by 61% and 59.8% to the conventional hybrid PV/T air collector with respect to overall annual thermal energy and exergy gain. Annual exergy gain was also upward by 9.6% and 5.38% on the account of unglazed and glazed hybrid PV/T tiles air collectors, respectively in comparison to the conventional PV/T air collector. Dubey et al. (2009) both theoretically and experimentally investigated the performance characteristics of various configurations of glass-to-glass and glass-to-temlar PV/T air collectors at the Indian Institute of Technology. Analytical expressions as a function of climatic and design parameters for electrical efficiency were developed by (Dubey et al., 2009; Solanki et al., 2009). The experimental results showed that glass-to-glass was able to attain higher electrical energy and higher supply air temperature because of transmission of solar radiation falling onto the non-packing area of the glass-to-glass

module through the front cover. Average PV efficiencies annually w/o duct were obtained as 10.4% and 9.75%, respectively. Kamthania et al. (2011) evaluated the performance of a hybrid semi-transparent PV/T double pass façade for space heating applications. The simulations were carried out for the corresponding collector area between 0.15-0.76 m². The annual thermal and electrical energies were found to be 480.81 kWh and 469.87 kWh, respectively. Also, annual net thermal energy produced by the system was calculated as 1729.84 kWh. 5-6°C increase in the room temperature was observed in a typical winter day. Yang et al. (2014) studied a building integrated photovoltaic thermal air system (BiPVT/a) through a series of experiments in a full scale solar simulator. The results of simulations represented that applying two inlets on a BiPV/T air collector enhanced thermal efficiency by 5% and reduced PV temperature by 1.5°C. Also, added vertical glazed solar air collector further improved the thermal efficiency by 8%. The temperature reduction of PV modules was expected to be 5-10°C where the roof length is 5-6 m. Agrawal et al. (2010) investigated the performance of a roof top BiPVT/a system to generate electrical energy and produce thermal energy for space heating. Analysis were carried out for the cold climatic conditions of India by using one-dimensional transient model in order to select the most proper system. The system, as shown in Figure 2.3, comprises six rows each having eight BiPVT/a covering total area of 65 m² capability of producing 7.2 kW_p and also 0.12 kW_p capacity air blower to circulate the air through the duct at a mass flow rate of 1.2 kg/s. Test results displayed that the system is better off connected in series for a constant mass flow rate whereas a better performance was yielded when connected in parallel for a constant velocity of air flow. 53.7% of thermal efficiency along with 16,209 kWh of net electrical energy and 1531 kWh of thermal exergy were attained, respectively. The life cycle analyses

of the proposed system indicate that in terms of energy and exergy performance, mono-crystalline system is more suitable whereas amorphous silicon was found to be more economical. The energy and exergy efficiencies for amorphous silicon BiPVT system were obtained as 33.54% and 7.13%, respectively under the prevailing climatic conditions of New Delhi. The cost of the system was found to be US\$ 0.1009 per kWh which is around the cost of conventional grid power (Agrawal et al., 2010). A hybrid PVT air integrated solar roof system was successfully applied as a first commercial realization at Fiat Research Centre in Italy. The system is capable of generating 20 kWp of power and the hot air produced by the system is utilized for pre-heating in winter and air-conditioning in summer. The results derived from the experiments on 18 May for summer and 15 January for winter showed that electrical and thermal efficiencies varied between 9-10% and 20-40%, respectively (Aste et al., 2008).



Figure 2.2.3 Schematic view of BiPVT/a (Agrawal and Tiwari, 2010)

PV ventilated glazing technology for application in warm climatic conditions can offer substantial energy saving opportunities via reduction in air conditioning load, higher daylight utilization and the renewable based energy generation. The system consists

of outside PV glazing and inside clear glazing. The various combinations of vent openings create different ventilating flow provisions from buoyant-induced to mechanical-driven. Chow et al. (2007) numerically studied different window orientations and its integrated performance on a small office room in Hong Kong. The surface transmission like radiative and convective heat transfer thru the glazing was mainly affected by material characteristics of the inner glass although overall heat transfer was reflecting the impacts of both the outer and inner glass. The experimental results and comparative study between two same-kind glazing configurations with PV glass and absorptive glass were presented (Chow et al., 2009). The associated results manifested that the savings on power consumption for air-conditioning was found to be 26% for single, and 82% for double-vane installation. It was also disclosed that the system can reduce the power consumption considerably in office buildings. The results of the simulation study remarked that the PV glazing system has its own advantages for various climates with different configuration options from naturally ventilated absorptive glazing option to single-pane glazing.

2.2.2 PV/T water collectors

Water based PV/T modules, as shown in Figure 2.4, comprise absorbers in conjunction with a quantity of PV cells that are parallel or series connected and attached to serpentine or series of parallel tubes underneath in which water is forced to flow through. If the water temperature is kept lower, PV cells will be cooled off which leads to enhanced electrical conversion efficiencies while the water temperature will rise as a result of absorbing heat from the PV cell layer. This hot water can be exploited for various purposes including heating, cooling or food drying

etc. In comparison to air based PV/T systems, the water based systems are able to achieve enhanced efficiencies due to higher thermal mass of water, therefore, both thermal and electrical efficiencies would be improved (Zhang et al., 2012). Anderson et al. (2009) theoretically analysed the design of a building integrated photovoltaic thermal water system (BiPVT/w) in Australia. The proposed system was integrated to the standing seam or toughed sheet roof where passageways formed into trough for thermal cooling flow. The steady-state outdoor thermal testing proved the validity of modified Hottel-Whillier model. The results revealed that prime design factors such as fin efficiency, lamination, thermal conductivity and efficiency have notable impacts on the electrical and thermal efficiencies. It was recommended that the replacement of absorption material like copper or aluminium with a cost effective one such as pre-coated steel as the efficiencies were sufficiently maintained. Moreover, the proposed system was suggested to be integrated 'into' (rather than onto) the roof structure, as the rear air space in the attic could make a good insulation as well as any high insulation material.

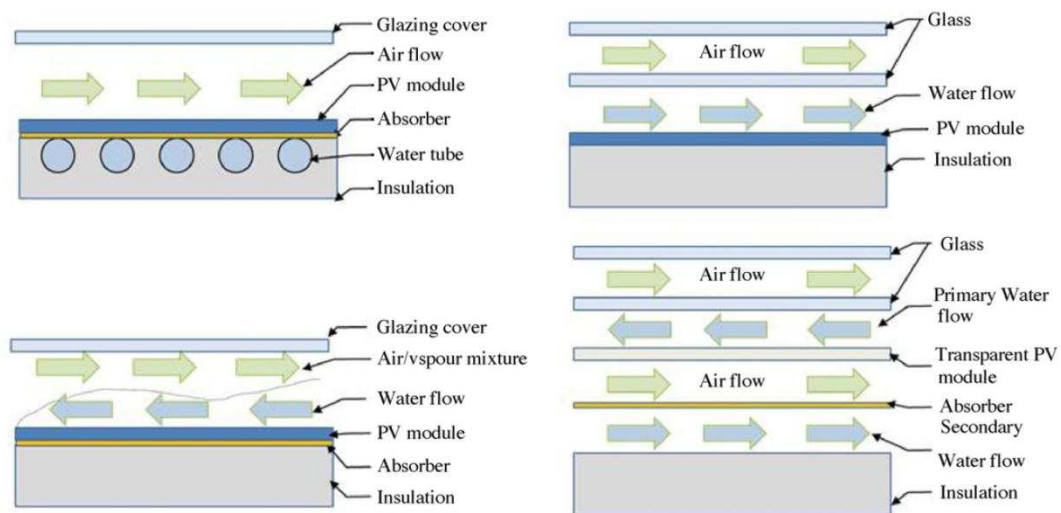


Figure 2.2.4 Types of PV/T water collectors (Zhang et al., 2012)

Yin et al. (2013) designed and examined the performance of a building integrated multifunctional roofing system. In the module, as shown in Figure 2.5, silicon PV

layer is embedded in between a transparent protective layer and a functionally graded material (FGM) which is manufactured from a blend of heat conducting aluminium and insulating high density polyethylene with water channels within the FGM. When the solar energy is captured by PV layer in the form of electricity and heat, the heat is transferred into the FGM. Due to high thermal conductivity of the FGM, the heat, then, is carried away by water flowing through the embedded tubes, so both the control of module's temperature and optimization of PV efficiency is achieved. During the tests, the highest average temperatures for the PV cell were recorded as 50°C and 55°C under the irradianations of 850 W/m² and 1100 W/m², respectively. At these temperatures, PV efficiencies were noted as without water flow 13.1% and 9.9% and with water flow 14.5% and 11.4%, respectively. Also, PV layer temperature was reduced to 32°C and 38°C when water flow introduced. Total energy efficiencies of the hybrid panel was attained as 58.8% and 65.3% for the given solar radiations and PV layer temperatures, respectively.

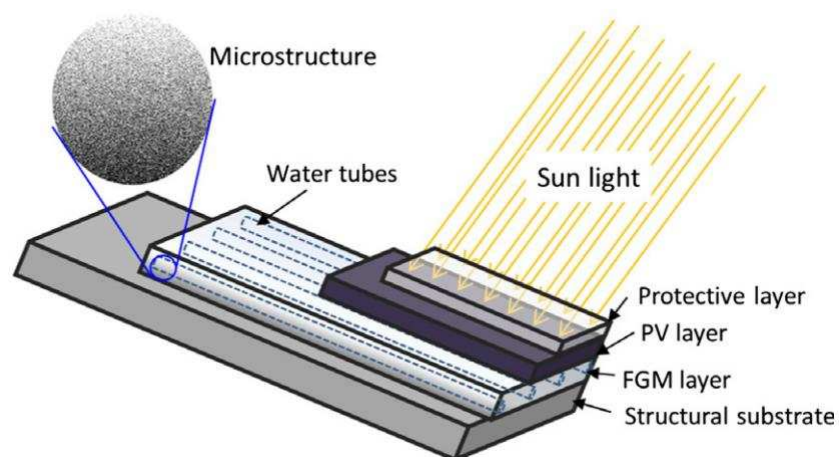


Figure 2.2.5 Schematic diagram of a hybrid solar roof panel (Yin et al., 2013)

Kim et al. (2014) carried out an experimental investigation of a building heating system combined with a PVT/water collector integrated into the roof as the conceptual and experimental view of the collector is illustrated in Figure 2.6.

According to the experimental results, it was revealed that the thermal and electrical efficiency of the proposed system was found to be 30% and 17%, on average. It was also given that the water temperature could reach up to 40°C which could be utilized as a heat source for heating.



Figure 2.2.6 Conceptual and experimental view of the BiPVT/water unit (Kim et al., 2014)

Wei He et al. (2011) performed a comparative study of a photovoltaic thermal system with a monocrystalline silicon PV/T collector, a traditional solar collector and a monocrystalline silicon PV plate. The PV/T collector possessed a thermally insulated 100L capacity water storage tank. It was found that the water temperature in the storage of the PV/T system reached up to 55°C while the water temperature in the storage of the traditional solar thermal system was found to be 63°C under the same conditions. The experimental results also reported that daily thermal efficiency of the PV/T and thermosyphon system was 40% and 75%, respectively while the daily average electrical efficiency was attained as 10% which was slightly less than the PV module. However, primary energy saving efficiency of the PV/T system was much advanced than that of the individual PV and traditional solar collector. Chow et al. (2009) examined the annual performance of a building-integrated photovoltaic/water-heating (BiPVW) system for use in warm climate conditions. A specific BiPVW

system integrated at a vertical wall of a fully air-conditioned building, with flat-box thermal absorber and polycrystalline solar cell type collectors, the year-round average thermal and power conversion efficiencies were attained as 37.5% and 9.39% under typical Hong Kong climatic conditions. The payback period was estimated around 14 years. Major effects changing cell efficiency are cell temperature and solar radiation intensity. Figure 2.2.7 explains the relation between the cell parameters and efficiency. The effect of some of these parameters (such as temperature) can be enhanced or reduced by ways of cooling off PV cells.

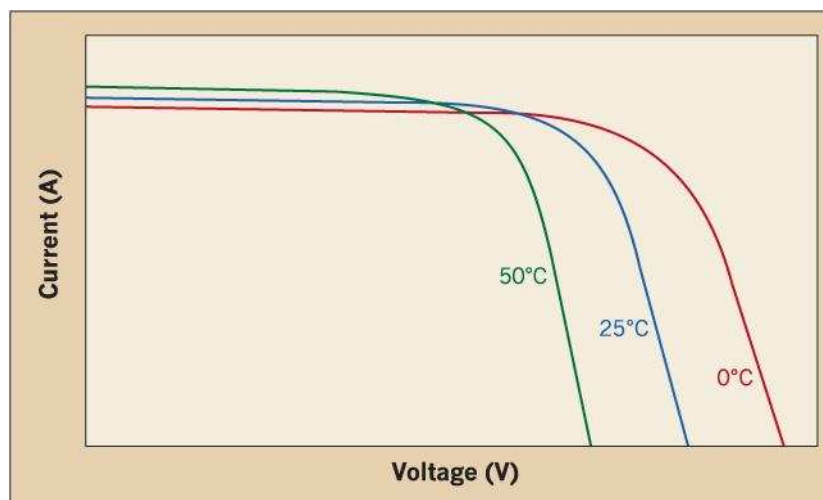


Figure 2.2.7 Typical PV temperature-efficiency curve (PV, 2015)

Corbin et al. (2010) studied computational fluid dynamics (CFD) model of a novel building integrated photovoltaic-thermal (BIPV/T) collector and validated the model experimentally to define the effect of active heat recovery on cell efficiency and effectiveness of the proposed system as a solar water heater. The experimental results presented that the cell efficiency could be improved 5.3%. Additionally, thermal and electrical efficiencies could achieve 34.9% and 19%, in average. Also, a new correlation developed regarding the electrical efficiency to collector inlet water temperature, ambient air temperature and solar radiation would enable to calculate cell efficiency fairly. Mishra et al. (2013) dealt with the analysis of building integrated

PV/T water collectors for two different configurations namely case A (partly covered by PV) and case B (fully covered by PV) and the results were checked against a conventional flat plate collector. The observations showed that case A is favourable in terms of thermal energy while case B is more suitable for power generation. The annual energy gain was estimated to be 4167.3 and 1023.7 and annual net electrical gain was 320.65 and 1377.63 for cases A and B on average. However, overall thermal energy gain was reduced by 9.48% and overall exergy gain was raised around 39.16% from case A to B annually. Buker et al. (2014) studied the integration of unique polyethylene heat exchanger loop underneath PV modules to form a dual function roof element. The experimental values showed that the water temperature could reach up to 40°C with overall thermal efficiency of 20.25%. Also, as a result of techno-economic analysis of the system, annual energy savings was estimated to be 10.3 MWh/year and the cost of power generation was found to be €0.0778 per kWh.

2.2.3 Refrigerant based PV/T collectors

It is a known fact that electricity conversion efficiency of solar cells decreases with any increase in operating temperature. A PV/T system that practices a coolant onto the solar cells can overcome such a drawback by reducing its operating temperature and utilize that thermal energy. The refrigerant used as a working medium at the solar collector draws energy and experiences a phase transition relatively at lower temperatures e.g., 0-20°C. This will result in improved energy conversion efficiency of the solar cells. Also, working medium with thermal energy can be utilized in a Rankine refrigeration device. A direct expansion solar-assisted heat pump system (DXSAHP) is the combination of the Rankine refrigeration device with solar thermal collectors. In such a configuration, the solar collector module operates as an

evaporation section of the heat pump through which the refrigerant absorbs heat energy from solar radiation (Daghigh et al., 2011). The illustration of a refrigerant based novel PV/T collector is provided in Figure 2.7.

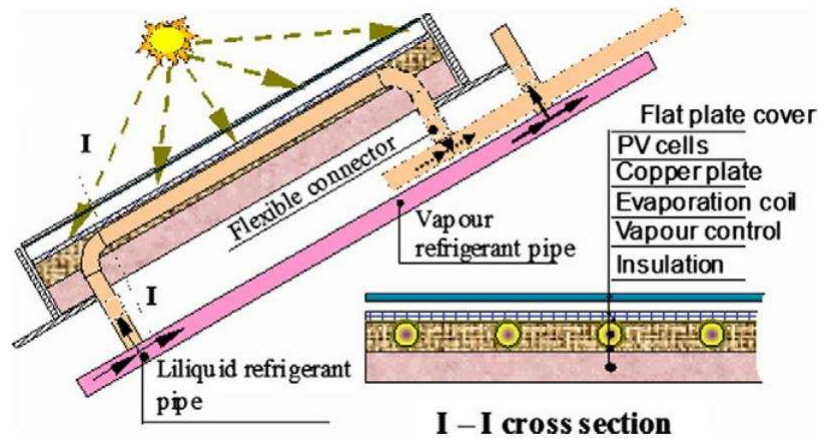


Figure 2.2.8 Cross-sectional view of a refrigerant based PV evaporator roof panel (Zhao et al., 2011)

A novel photovoltaic solar assisted heat pump system (PV-SAHP) using R134a was experimentally studied under the prevailing climatic conditions of Hong Kong (Fu et al., 2012). The proposed system was designed to operate in three different modes, namely, solar assisted heat pump, heat pipe and air source heat pump modes as the schematic diagram of the PV-SAHP experimental set-up shown in Figure 2.8. The results derived from a series of experiments indicate that the system could reach a daily average energy efficiency of 61.1-82.1% if operated in the solar-assisted heat-pump mode. Also, average COP of 4.01 was attained when strong solar radiation was available.

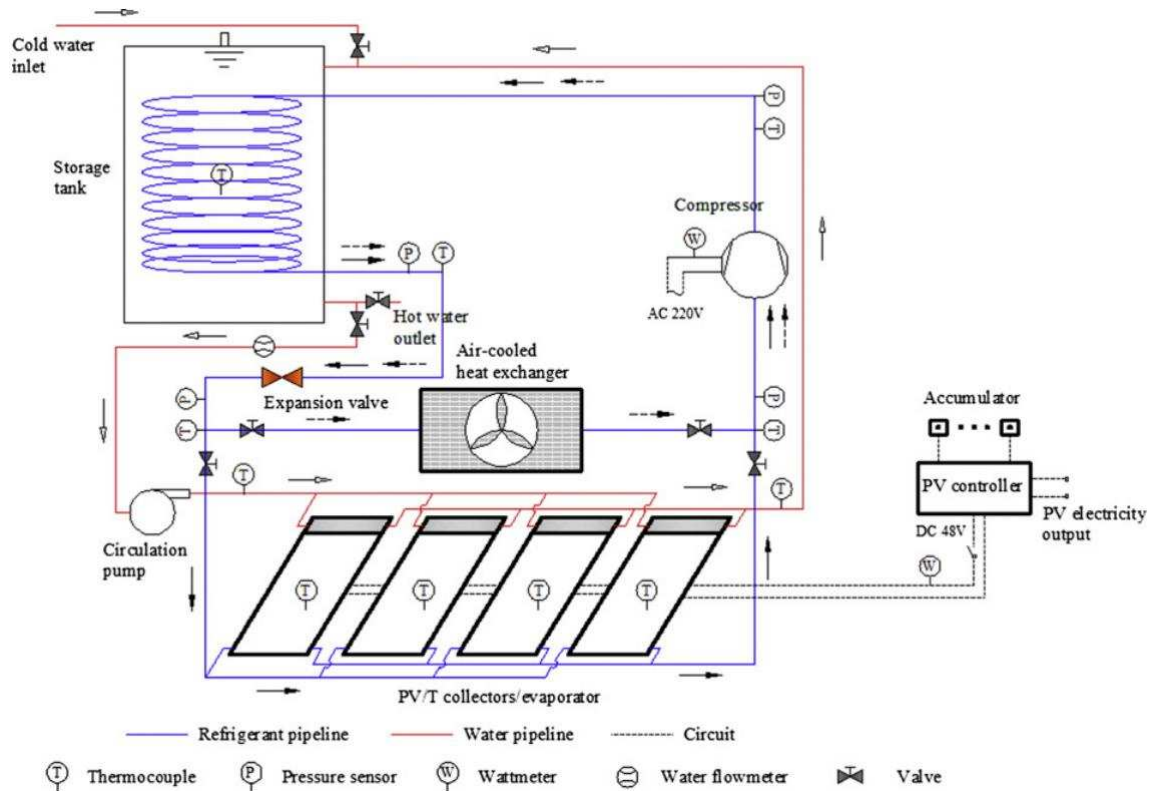


Figure 2.2.9 Schematic diagram of the PV-SAHP experimental set-up (Fu et al., 2012)

Jie et al. (2008) conducted the experimental study of a novel photovoltaic solar assisted heat pump (PV-SAHP) system using R22 as a refrigerant. The performance results of the PV-SAHP system at four different operating modes with distinctive condenser supply water temperatures of 20°C, 30°C, 40°C and 50°C showed that average photovoltaic efficiencies for each condenser inlet temperature given were attained as 10.4, 16.1, 5.4, 8.3 and 13.4% indicating that the PV efficiency was improved. Figure 2.9 demonstrates the PV evaporator modules used for this study. Chen et al. (2011) experimentally analysed a refrigerant based PV/T system as evaporator for heat pump application. Refrigerant R134a was used to cool the PV modules. The results indicate that the electrical performance of PV panel was improved by up to 1.9% based on a reference PV performance of 3.9% in comparison with and without cooling.



Figure 2.2.10 Refrigerant based PV evaporator modules (Ji et al., 2008)

2.2.4 Heat pipe based PV/T collectors

Heat pipes are appraised as efficient heat transfer mechanisms that integrate the principles of both thermal conductivity and phase transition. As illustrated in Figure 2.10, a conventional heat pipe is formed of three sections as evaporation section (evaporator), adiabatic section and condensing section (condenser) and the system provide such an ideal solution for heat removal and transmission. In the structure, there is a photovoltaic layer and a flat plate heat pipe which contains a great number of micro-channel arrays acting as the evaporation section of the heat pipes. The other end of the heat pipe is the condensation part in which heat is released to the flowing refrigerant and that working medium is condensed due to the heat dissipation. The flat plate structure appears to be more efficient as extremely good thermal contact between PV cell layer and heat extraction component is provided. This results in advanced solar conversion efficiency and primitive thermal resistance. Consequently, PV cell performance could be enhanced by 15-30% in comparison to the sole PVs as long as PV cell layer temperature is maintained around 40-50°C.

Overall solar conversion efficiency is noted as around 40% (Quan et al., 2010, Tang et al., 2010).

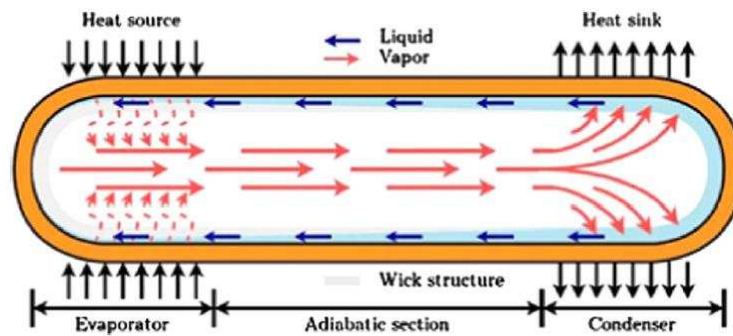


Figure 2.2.11 Schematic diagram of a typical heat pipe mechanism (Kumar et al., 2015)

Nowee et al. (2014) experimentally investigated the performance of a heat pipe on a novel photovoltaic/thermal (PV/T) system. The investigations carried out in both spring and summer showed that the average enhancements attained on electrical power and thermal efficiency were 5.67% and 16.35% for spring and 7.7% and 45.14% for summer, respectively. Also, temperature drop of up to 15°C on the panel surface was achieved. Gang et al. (2012) proposed a novel heat pipe photovoltaic/thermal (PV/T) system using water as a working medium and experimentally discovered its performance patterns under different conditions. The findings from the series of test conducted revealed that heat gain, electrical gain and total PV/T efficiencies increased with increased flow rate. It was stated that the effect of water flow rate on heat gain was much powerful than on electrical gain. Also, any reduction in the tube space of heat pipes would improve the heat and electrical gain, and PV/T efficiencies. Zhang et al. (2013) brought forward a novel solar photovoltaic/loop-heat-pipe (PV/LHP) concept for heat pump operation. Test results of the proposed concept, as shown in Figure 2.11, indicated that under the given testing conditions the electrical, thermal and overall efficiency of the PV/LHP module were around 10%, 40% and 50%, respectively. Also, effects of the operational

parameters such as solar radiation, ambient air temperature, wind velocity, glazing covers and the number of absorbing heat pipes on the performance of the system were investigated individually. Qian et al. (2010) came up with a new concept for building integrated PV/T system utilizing oscillating heat pipe. The concept is intended as the façade-assembled component to convey heat from the concealed PV cell layer. The system mainly includes oscillating heat pipes, risers and headers, finned tube, graphite conductive layer, metal framework, PV laminate module and back insulations. During the operation, the working medium flowing through the metal heat pipes will draw heat from the PV cells and be evaporated into vapour fluid. The vapour, then, is to pass into the finned tube in which it releases heat by condensation to the passing fluid and pour back to the absorber via gravity effect and capillary forces.

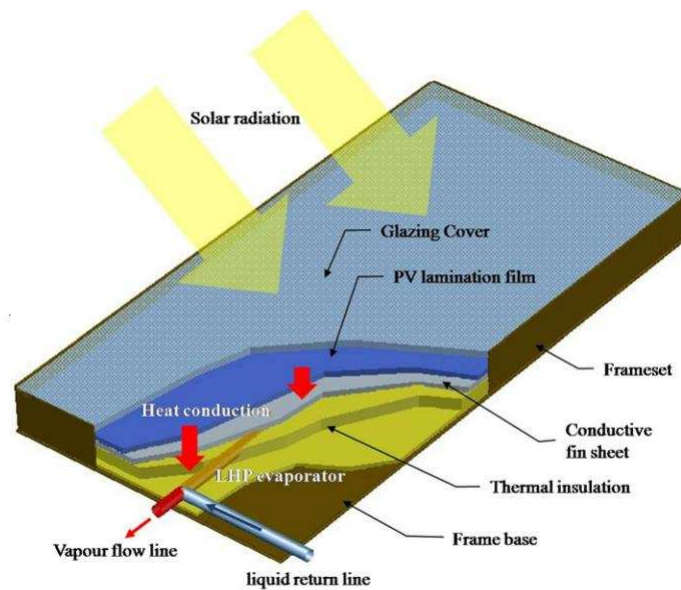


Figure 2.2.12 Cross-sectional view of heat pipe PV/T collector (Zhang et al., 2013)

2.2.5 Concentrating PV/T collectors

Co-generation of electricity and heat in a PV/T system, using the similar structural and concentration components, boosts the overall efficiency of the system. It also provides a better finance for the electricity conversion in comparison to power generation in a conventional PV system, satisfied that the produced heat meets a demand and substitutes thermal energy that would otherwise be purchased or generated in a separate system (Brogren et al., 2002). Currently, the application of concentrating PV/T systems is limited in scale and mainly the systems consist of components in considerable size; solar power towers, parabolic trough concentrators, parabolic dish concentrators and large Fresnel concentrators with two-axis tracking systems. Building integrated concentrating PV/T systems (BICPV/T) can be installed either on the building façade or rooftop. Single axis tracking designs are more suitable for building integration. An illustration of a concentrating PV/T concept consisting of a PV module, thermal absorber, and parabolic reflector, tracking system, glazing and supporting elements is shown in Figure 2.12 (Bernardo et al., 2011).

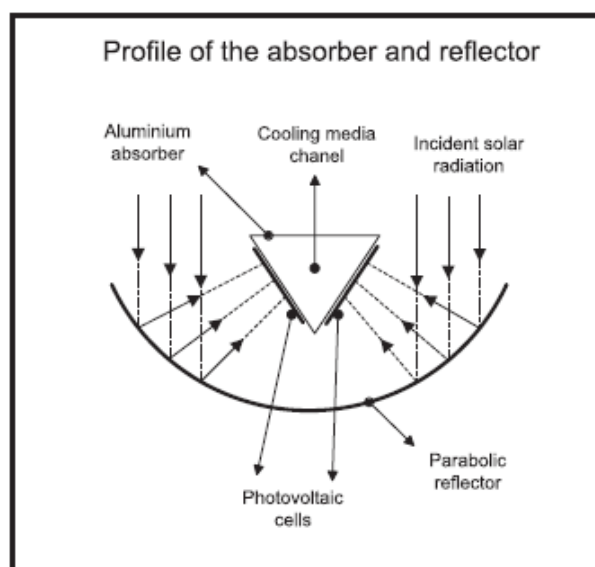


Figure 2.2.13 Schematic diagram of a concentrating PV/T collector (Bernardo et al., 2011)

Kandilli et al. (2013) introduced and experimentally tested a novel concentrating PV combined system (CPVCS) based on the spectral decomposing method. The introduced CPVCS consists of a hot mirror placed in the focal region so that could convey solar energy spectrum beyond the visible region, and reflects the infrared (IR) and ultraviolet (UV). The reflected IR and UV rays by proper optical design are transferred to vacuum tube in which it could be harnessed as useful heat energy. The results of the series of test revealed that the 4.6W of electrical power per solar cells and 141.21W of thermal power in vacuum tubes was produced by CPCVCS. Energy efficiencies of a concentrator, vacuum tube and overall CPVCS were attained as 15.35%, 49.86% and 7.3%, respectively. Al-alili et al. (2012) investigated performance of a CPV/T system along with a conventional vapour compression cooling cycle. The CPV/T system generates electricity and hot water simultaneously and drives a hybrid air conditioner to separate the sensible and latent loads. The results point out that increased water mass flow rate has increasing effect on electrical output due to lower PV cell temperature and decreasing effect on thermal output. Xu et al. (2011) carried out the performance test of a novel low concentrating PV/T integrated with a heat pump system. The PV/T collector along with fixed truncated parabolic concentrators throwing the incident sunlight back onto surface of PV cells without absorbing was employed as the evaporator of the heat pump. The test results show that electrical efficiency of 17.5% was attained which was 1.36 times greater than the conventional system. Also, flux concentrating rate of the fixed parabolic concentrators was noted as 1.6. The CPVT mounted on the roof for this experiment is presented in Figure 2.13 and an example of architectural design of the building integrated CPVT system is illustrated in Figure 2.14.



Figure 2.2.14 Illustration of CPVT mounted on the roof (Al-Alili et al., 2012)



Figure 2.2.15 Architectural design of the building integrated CPVT system (Chemisana et al., 2013)

Parabolic trough concentrators similar to that of high concentration systems are usually installed on flat roofs and ideally hidden from view. In such a system, solar tracking is accomplished via rotating the entire concentrator/receiver on a single axis. Linear Fresnel reflectors present a variety of options depending upon the technology desired: two-axis tracking, sun tracking by moving mirrors or PV receiver. In the configuration the receiver stands still and solar tracking is achieved via rotating the individual mirrors. In this way, total movement is minimised that facilitates the building incorporation of such systems. Linear Fresnel lenses meet the expectations regarding the architectural integration. These systems are able to distinguish the

beam from the diffuse solar radiation which makes them attractive for the control of illumination in the building interior space. What is more, the Fresnel lenses are favoured as they can combine both the concentrating element and optically transparent window or cover in a single unit. Lastly, low concentrating systems are forms of numerous variables of CPV generators, combination of CPCs, planar reflectors, holographic films or fluorescent technologies with various configurations of solar cells. The common characteristic of aforementioned low concentrating systems is that they are static systems. This simplifies the building integration of these systems (Chemisana et al., 2013).

2.2.6 Hybrid PV/T transpired collectors

Solar energy systems mostly have their own restrictions in point of potential fulfilment of demand. So that there is a need to unite more than one system in a single unit in order to maximise the utilisation of resources. Hybrid stands for mixing more than one. There are various solar technologies e.g. photovoltaic (PV), storage, water and air heating that can be integrated into a hybrid transpired collector. Building envelope cladding or outer surface of roof for instance, roof tiles and asphalt shingles (Shukla et al., 2012). PV systems frequently operate in the efficiency range of 6-18% and rest of the energy is dissipated to the environment as waste heat, which adversely affects the efficiency of PV systems. Therefore, BIPV/T systems are designed to utilize both electric and heat generation from PV systems. Various geometries of building integrated hybrid PV/T transpired collectors are reported in the literature. Figure 2.15 shows the schematic of two common hybrid PV/T transpired collectors.

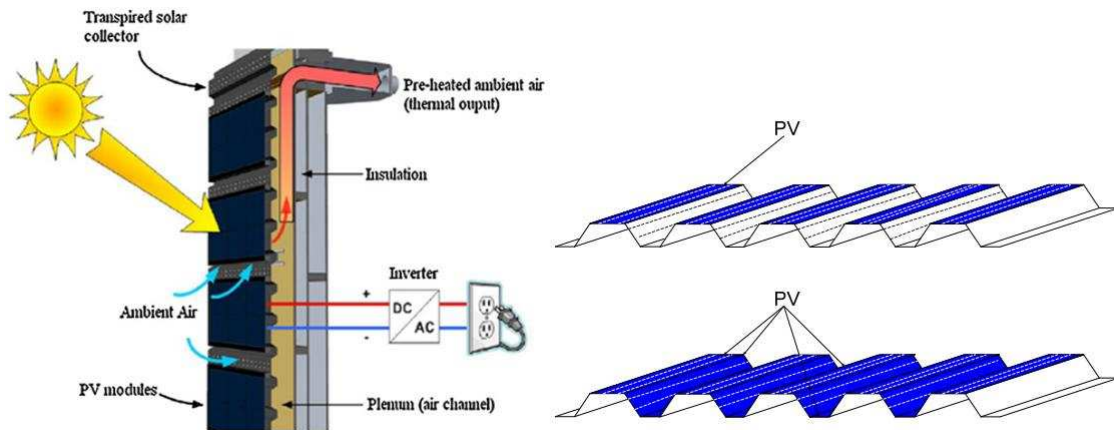


Figure 2.2.16 Concept schematic of facade and roof tile PV/T transpired collectors (Athienitis et al., 2011; Delisle et al., 2007)

The combination of transpired solar collectors with PV cells is a promising concept for buildings that need heat ventilation air in winter season. As non-domestic buildings mostly employ heat recovery ventilators to draw maximum amount of heat from exhaust air, excess heat from BIPV/T system can be exploited for space heating or perhaps hot water. Agrawal et al. (2011) experimentally evaluated the performance of a micro-channel solar cell thermal tile under the climatic condition of Srinagar, India. The evaluations indicate that average values of electrical and thermal efficiency of PV/T tile were attained as 14.7% and 10.8%, respectively. Also, maximum exergy efficiency was realized as 20.28% at 0.000108 kg/s mass flow rate. In another study, Agrawal et al. (2013) tested the performance of unglazed hybrid PV/T tiles with glazed hybrid PV/T tiles. The results show that overall annual thermal energy and exergy gain of the unglazed hybrid PV/T tiles air collector was greater by 27% and 29.3% in comparison to the glazed hybrid PV/T tiles air collector. And also it was observed that the exergy gains of the glazed and unglazed hybrid PV/T tiles air collectors were higher than that of conventional hybrid PV/T air collector by 9.6% and 53.8%. An application of a PV/T roof tile is shown in Figure 2.16. There are great number of architectural integration of solar systems have been achieved

worldwide so it is out of question to make a list of all, however, the author, in the present study, intended to present some of the original concepts. Figure 2.17 presents an example of patented innovative design transpired solar collector.



Figure 2.2.17 Photographic view of a PV/T clay roof tile (Building services, 2015)



Figure 2.2.18 The view of a transpired solar collector (Notton et al., 2014)

2.3 SOLAR THERMAL COLLECTORS

Solar collectors have a history dating back almost 120 years. Yet, benefiting new materials and innovative designs, they keep evolving to more effective systems satisfying the necessities of various applications. With bulk production and ever increasing demand in many markets, the installation cost of this technology continues to fall drastically which is rendering solar thermal technologies

economically viable with a growing market potential. This part gives a brief overview of present day building integrated solar thermal collector technologies.

2.3.1 Solar Thermal air collectors

The solar air collectors are widely applied in many commercial applications such as hot air supply to shopping malls, agricultural barns etc. They are usually low cost, with no freezing and high pressure problems. However, one of the main disadvantages of solar thermal air collectors is their relatively low efficiency due to the low density, volumetric heat capacity and thermal conductivity of air causing to low coefficients of convective heat transfer from solar energy to the air. To address this drawback, air needs to be encapsulated in larger collector areas which puts cost and roof size problem in front (Ucar et al., 2006). A schematic of the working principle of a roof integrated solar thermal air collector is illustrated in Figure 2.18.

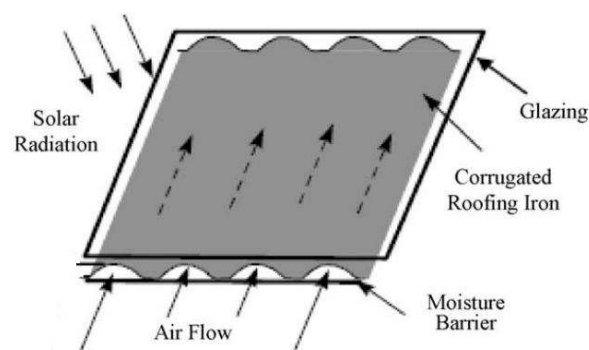


Figure 2.3.1 Schematic diagram of a roof integrated solar thermal air collector (Alkilani et al., 2011)

The solar energy absorbing uppermost layer may have a solar selective coating and internal duct configuration to increase heat transfer ratio from the heated absorber layer to the internal air stream. A flat transpired solar thermal air collector is formed an unglazed, perforated solar absorbing layer. The air stream heated at the layer is pulled through an array of small perforations by a fan. A large proportion of the heated air, that would otherwise compose convective heat loss from the heated surface, is thus loaded into the system. At relatively high flow rates and low supply

temperatures, the solar thermal air collector system can display high solar conversion efficiency (Norton, 2006). A schematic diagram of solar thermal air collector application is shown in Figure 2.19.

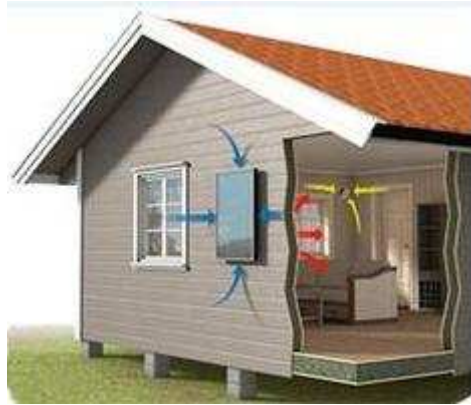


Figure 2.3.2 A schematic diagram of solar thermal air collector application on a single family house
(SolarVenti, 2015)

Karim et al. (2006) conducted a study to investigate the performance of flat plate, finned and v-corrugated air heaters both experimentally and theoretically in an effort to enhance the performance of conventional air heaters. A series of test to find out the performance characteristic were carried out under the climatic conditions of Singapore based on the ASHRAE standards. After the close examinations of the performance of all three collectors, the v-corrugated collector was found to be the most efficient and the flat plate is the least efficient one. The results of the test revealed that the v-corrugated collector was 10-10% and 5-11% more efficient under single and double-pass modes, respectively in comparison to flat plate collectors. Karsli (2007) conducted a comparative performance study of four types of air heating flat plate solar collectors namely a finned collector with an angle of 75° , a finned collector with an angle of 70° , a collector with tubes and a base collector. The results derived from the first and second laws of efficiencies showed that the first law of efficiency for collector-I was varied between 26% and 80%, for collector-II between

26% and 42%, for collector-III between 60% and 70%, and lastly for collector-IV between 26% and 64%. In addition, the second law values were attained varying between 0.27 and 0.64 for all collectors. Lin et al. (2006) performed a parametric study on the thermal performance of innovative cross-corrugated solar air collectors comprising a wavelike absorbing plate and a wavelike bottom plate which is crosswise positioned to constitute the air flow channel. The objective of using the cross-corrugated absorbing plate and bottom plate is to improve the turbulence and the heat transfer rate inside the air flow channel which is vital towards the desired enhancement of efficiencies of solar air collectors. It was concluded that in order to accomplish higher collector efficiency, it is necessary to build up solar air collector having slender configuration alongside the air flow direction, having a small gap between the absorbing and bottom plate, using high absorptivity but very small emissivity selected coatings and preserving higher mass flow rate and keeping inlet fluid temperature to the collector very close to that of the ambient temperature. El-Sebaili et al. (2011) theoretically and experimentally investigated the performance of the double pass-finned plate solar thermal air collectors under prevailing weather conditions of Tanta. The results from the comparative analysis regarding the effect of mass flow rates of air on pressure drop, thermal and thermohydraulic efficiencies of the double pass-finned and v-corrugated plate pointed that the double pass v-corrugated plate solar air heater is 9.3%-11.9% more efficient comparing to the double pass-finned plate solar air heater. El-Sawi et al. (2010) considered the chevron pattern of fold structure manufactured using continuous folding technique for the first time in the application of solar air collectors. The results of the experimental study comparing flat plate collector with chevron pattern absorbers showed that the solar thermal air collector with the chevron pattern absorber was found to be more

efficient, achieving up to 20% improvement in thermal efficiency and an increase of 10°C in supply air temperature. Munari et al. (2007) addressed the architectural integration of solar thermal technologies and referred more than 170 European architects and other building professionals regarding integration criteria and design guidelines. Subsequently, a unique methodology to design futuristic solar thermal collector systems suitable for the building integration is described and a range of design possibilities are shown. In the Case 4, an application of building integrated solar thermal collectors was evaluated from the viewpoint of architecture and building integration as the illustration of case 4 is presented in Figure 2.20.



Figure 2.3.3 An illustration of building integrated solar thermal air collector system in a commercial building (Munari et al., 2007)

2.3.2 Solar thermal water heaters

Solar water heating collectors prove to be an effective concept for conversion of solar energy into thermal energy. The efficiency of solar thermal conversion reaches up to 70% when compared to direct conversion of solar electrical systems which have an efficiency of around 17%. Thus solar water heating collectors play a crucial role in domestic use as well as industrial sector due to its ease of operation. Flat

plate collector is the pivotal component of any solar water heating system. Thermal performance characteristics of a flat plate solar water heater mainly depend on the transmittance, absorption and conduction of solar energy and good conductivity of the working fluid (Jaisankar et al, 2011). The cross sectional view of a flat plate solar water collector and the schematic view of a typical thermosyphon solar water heating system is shown in Figure 2.21.

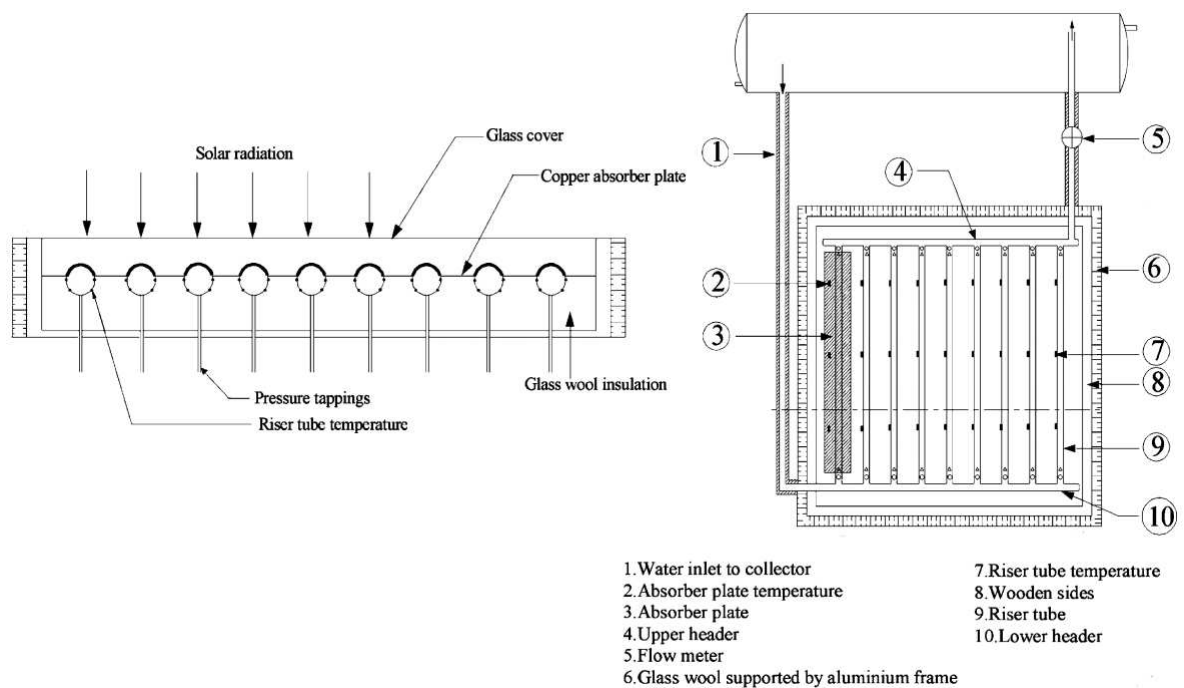


Figure 2.3.4 The cross sectional view of a flat plate solar water collector and its typical solar water heating application (Jaisankar et al., 2011)

Dagdougui et al. (2011) conducted a study investigating the thermal behaviour of a flat plate collector with different configurations under the prevailing weather condition of Tetouan, Morocco. The objective of the study was to inspect the impact of the number and types of covers on the top heat loss and the thermal performance in order to assist decision makers regarding the most cost-effective design as well as the optimal water flow and the optimal collector flat area in order to ensure a good compromise between the collector efficiency and the output water temperature. Jie

et al. (2011) proposed a modified building integrated dual function solar collector which is able to provide passive space heating in cold winter and water heating in warm seasons. Based on the tests conducted under the weather conditions of Hefei, China, the results showed that on typical summer days, the water temperature may reach up to 40°C which is useful for most of hot water applications and also thermal efficiency of the collectors was found to be more than 50% with the solar useful heat gain of water at around 3.4 MJ/m². On typical autumn days, the water temperature could exceed 48°C with the thermal efficiency of 48.4% and corresponding water heat gain of 6.57 MJ/m². It was also concluded that the system operates well in providing hot water in warm season having free of overheating problem. Dharuman et al. (2006) designed, constructed and experimentally tested an integrated solar water based thermal collector. The performance of the unit was tested under various weather conditions. The results indicated that the collector can supply hot water at 45-50°C early in the morning, which is enough for bathing and cleaning in the domestic use. Higher water temperatures were attained during daytime which is utilized for industrial and hospitality use. Also, the system was 30% less expensive as compared to its counterparts due to its simple design features. The overall heat loss coefficient between absorber and ambient was noted in the range of 3 to 5 W/K. Chow et al. (2006) evaluated the potential application of a centralized water-heating system on a high-rise residential building in Hong Kong. In the study, arrays of solar thermal collectors occupying the top south and west facades were proposed for leveraging the domestic hot water system. The results showed that the annual average efficiency of the vertical solar collectors could achieve 38.4% with the solar fraction of 53.4% and payback period of 9.2 years. The payback period could be even shorter if the reduction of the heat transmission through building envelope was

considered. Budihardjo et al. (2009) studies the performance of water-in-glass evacuate tube solar water heaters i.e., optical and heat loss characteristics and compared the results with flat plate solar collectors in a range of locations. It was found that the thermal performance of a typical 30 evacuated tube collector array was lower than a typical 2 panel flat plate array for domestic water heating in Sydney. The water-in-glass evacuated tubular solar water heater is the most widely used form of evacuated tube collector due to higher thermal efficiency as schematic diagram of natural circulation flow in water-in-glass solar water heater is shown in Figure 2.22. Liangdong et al. (2010) investigated the thermal performance of the glass evacuated tube solar collector with U-tube based on the energy balance developed. It was found that the efficiency could increase 10% and outlet fluid temperature 16% if the conductance was to increase from 5 to 40 W/m K. Also, coating temperature would increase 30°C in case thermal resistance of the air was considered. It was concluded that not only heat efficiency but also surface temperature of the absorber coating should be taken into account in order to evaluate the thermal performance of the glass evacuated tube solar collector. Ayompe et al. (2011) conducted a comparative performance study of flat plate and heat pipe evacuated tube collectors for domestic water heating systems under the same weather conditions in Dublin, Ireland. A year round energy performance of both systems was compared and results indicated that a total annual heat energy of 1984 kWh and 2056 kWh were captured by the 4 m² flat plate and evacuated tube collectors under in-plane solar insolation of 1087 kWh m⁻². The annual collector efficiencies were obtained as 46.1% and 60.7% in average whilst the system efficiencies were 37.9% and 50.3%, respectively for flat plate and evacuated tube collectors. Wei et al. (2012) studied the incorporation of glass evacuated-tube heat

pipe solar collectors with thermoelectric module for co-generation. It was theoretically found that water temperature could reach up to 45°C while solar radiation was above 600 W/m². Zhai et al. (2008) demonstrated the application of a building integration of solar thermal collectors on a villa in China. An integrated solar thermal collector was designed and installed on a green office building with the area of 460 m². As hot water demand is not that significant in an office building, the system is mainly for floor heating in winter and air-conditioning in summer. An example of building integrated solar thermal collector is presented in Figure 2.23.

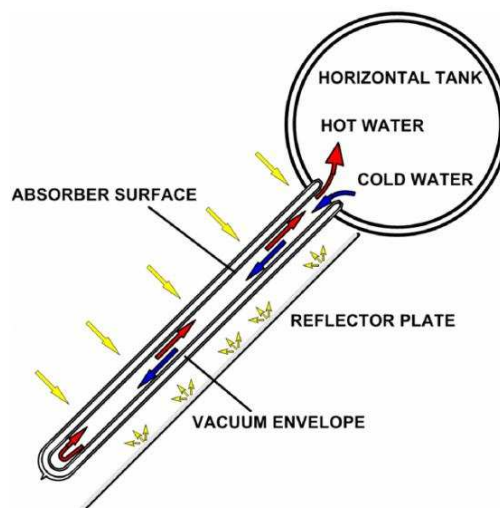


Figure 2.3.5 A Natural circulation water-in-glass solar water heater (Budihardjo et al., 2009)



Figure 2.3.6 Building integration of array of solar thermal collector on a green office building (Bine, 2015)

2.3.3 Roof integrated mini-parabolic solar collectors

Concentrating solar thermal systems offer a promising method for not only large scale solar energy harvesting but also propose huge opportunity to realize rooftop applications for domestic hot water, industrial process heat and solar air conditioning. Sultana et al. (2012) studies a new low-cost micro-concentrator collector designed to operate at temperatures up to 220°C and be seamlessly integrated into the architecture of buildings. The systems employs linear Fresnel reflector optics which concentrate beam radiation to a stationary receiver using with all mirrors connected and active tracking. The design of the system is shown in Figure 2.24.

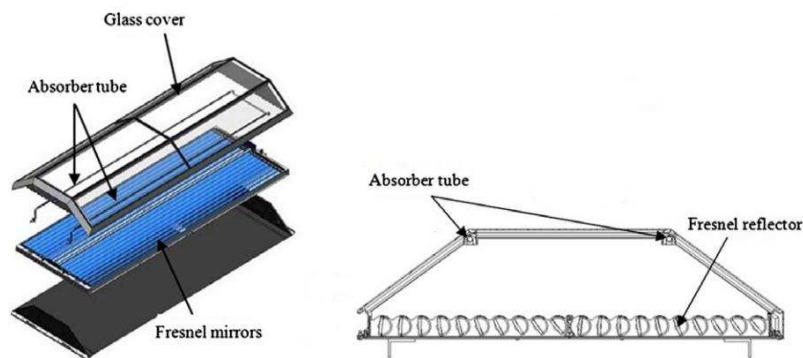


Figure 2.3.7 The schematic view of a micro-concentrating system and the cross-section of the collector (Sultana et al., 2012)

Chemisana et al. (2010) proposed the use of concentrating optical system for building integrated solar applications and presented the study of a stationary wide angle Fresnel lens with a moving compound parabolic concentrator for sun tracking. It was found that the ratio of 12.5 suns is the optimal geometric concentration for Fresnel lens to fulfil both architectural and solar concentration requirements. Petrakis et al. (2009) considered the building integrated mini parabolic thermal collector in the East-West orientation with such a slope that the suns vector impinging normal to the

parabola during the day. The findings from the comparison between theoretical and experimental results pointed out that thermal efficiency increases with the increasing concentration ratio and mass flow rate. An example of solar micro-concentrator unit is presented in Figure 2.28.



Figure 2.3.8 A solar micro-concentrator system (Sultana et al., 2010)

Nkwetta et al. (2012) experimentally tested the thermal performance of an innovative concentrating evacuated tube heat pipe solar collector at a tilt angle of 60° and compared two profiles of concentrated evacuated tube heat pipe solar collectors with single and double-sided absorber under control conditions. These collectors were evaluated as being feasible for building integration for heating demands and the performance characteristic presented thoroughly. Figure 2.26 illustrates the building integration of an award winning compound parabolic concentrator system.



Figure 2.3.9 An award winning design of a building integrated compound parabolic concentrator system (Hydro, 2015)

2.3.4 Ceramic solar collectors

The raw material for this type of collectors is ordinary ceramic material mainly porcelain clay, quartz, feldspar etc. Although most ceramic products are white, all-ceramic solar collectors have a black or fuscous colour coated with V-Ti black ceramic. And the solar absorptance of black ceramic coatings is in the range of 0.93-0.97. This type of collectors is mainly characterized by cost effective, long life cycle, without attenuating in absorptance and well integration in buildings (Yang et al., 2013). Figure 2.27 illustrates an all-ceramic solar collector.



Figure 2.3.10 An all-ceramic solar thermal collector and its interior view (Yang et al., 2013)

The development trend for solar energy systems is building integration. Yang et al. (2013) studied a demonstration of the building integration of ceramic solar collectors in Beijing China as shown in Figure 2.28. In the system, the solar thermal collectors act as not only the heat source of hot water system, but also balcony railings. The ceramic solar collectors with an area of 2.58 m^2 were entrenched on the floor of the balcony. The thermal efficiency of 47.1% was attained. Berto et al. (2007) proposed and described the use of ceramic tiles as part of the range of architectural elements; thereby improving aspects directly related to the quality of life for instance utilization of solar energy as a vital natural source.



Figure 2.3.11 Solar ceramic collectors as balcony railings (Yang et al., 2013)

2.3.5 Polymer solar thermal collectors

The use of solar thermal energy systems in last decade has reached a remarkable edge. Yet, it runs counter to the relatively expensive metal based solar thermal collectors that are still comparatively high priced to buy and install. The continuous research for alternative materials to secure the continuously positive development of solar thermal technologies is called for. The possibility of polymeric material combinations allowing the development of completely new solar thermal collectors should be, therefore, within the consideration. This leads to a significant reduction in cost, and achieves to form efficient and affordable solar thermal energy systems for all climatic and demographic regions. The cross-sectional view of a polymer absorber is shown in Figure 2.29.

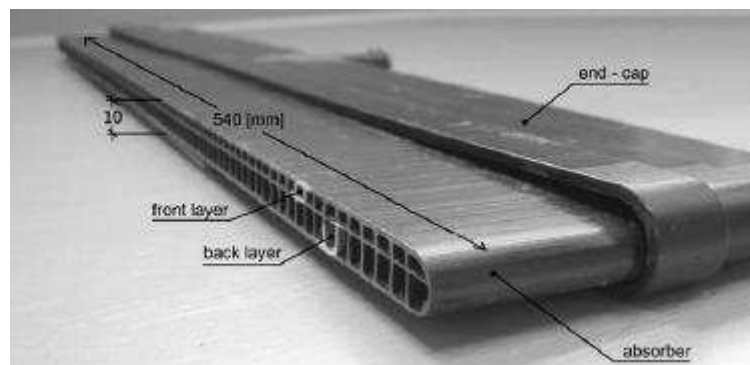


Figure 2.3.12 The cross-section of polymer absorber (Olivares et al., 2008)

The Task 39 of Solar Heating and Cooling Programme of the International Energy Agency (IEA SHC) conducted researches about the application of polymeric solar thermal components and exhibited the most promising components in a showcase in spring 2013 (Koehl et al., 2014). The example of a building integrated polymeric solar thermal collector is shown in Figure 2.30. Cristofari et al. (2002) investigated the thermal performance of a solar flat-plate thermal collector fully made of a copolymer material and examined the influence of various parameters of the

proposed system such as insulation thickness, flow rate and fluid layer thickness. Martinopoulos et al. (2010) developed and experimentally studied the thermal behaviour of a polymer solar collector. Moreover, the proposed novel honeycomb polycarbonate collector was modelled with CFD techniques in order to conduct in-depth analysis of the temperature distribution. Köhl et al. (2012) stated that the implementation of novel polymeric materials in solar-thermal systems has a vast potential as these materials offer significant advantages compared to conventional metal based materials. In addition, there is an international effort to advance polymer based flat plate collectors in order to lower the initial cost. Moreover, overheat protection of the absorber is a-must to prevent overrunning the maximum allowable temperature of the polymer.



Figure 2.3.13 Building integrated polymeric solar thermal collectors, passive house in Rudshagen, Oslo (IEA-SHC, 2015)

2.3.6 Solar louvre collectors

Solar louvre collectors are brand new horizontal overhang louvre modules that incorporate with solar collectors. Apart from blocking a large amount of direct solar radiation, the louvre collectors have several other crucial features including the flexibility to modify suitable systems collecting heat over a temperature range for particular building services application at various climates/zones. Also, considerable

economic advantages would be gained by integrating the solar collectors into a building's structure. Moreover, long-wave radiation emission from conventional louvres would be eliminated as the absorbed heat by the collector would be transferred simultaneously by heat exchange technique in the louvre. Free roof space could be used for installing further collectors (Abu-Zour et al., 2006). Figure 2.31 shows the schematic view of a solar louvre.

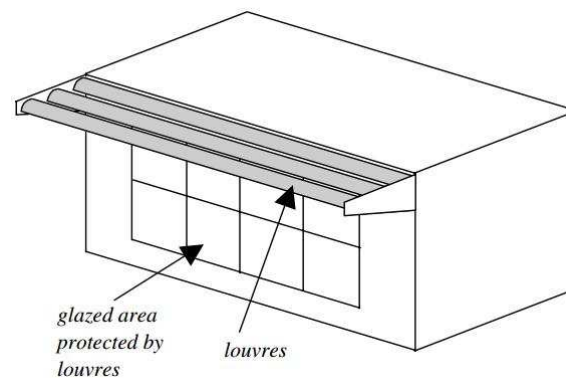


Figure 2.3.14 A schematic diagram of a solar louvre (Palmero-Marrero et al., 2006)

Abu-Zour et al. (2006) evaluated the design of new solar louvre thermal collector, discussed various designs and brought forward a new type of absorber plate based on heat pipe technology. It was stated that in addition to protecting glazed spaces from intense solar light, the collector was able to supply solar thermal energy for building services under a range of climatic conditions. Palmero-Marrero et al. (2006) studied a solar thermal system using building louvre shading devices and concerned the modification of existing louvre designs for shading device integration. Thermal performance of the proposed system obtained for the climatic conditions of Lisbon, Portugal and Tenerife, Spain revealed that the proposed system shows a great potential in terms of economic aspects and renewable energy supply. Oliveira et al. (2007) considered the integration of solar louvre collectors into a cooling system. The performance assessments and results indicated that comfortable indoor thermal

conditions can be ensured. Also, the system may create substantial energy savings as compared to conventional systems. Palmero-Marrero et al. (2010) applied louver devices to a building in east, west and south facades and tested the effect of the system on building energy requirements. It was found that the location, louver inclination angle and window area have substantial impact on the thermal comfort conditions. Moreover, the performance characteristics of the system were assessed under the climatic conditions of cities like Cairo, Lisbon, Madrid and London. Substantial energy savings were notable in cities with high solar radiation and ambient temperatures in summer. However, in cities like London, it may lead to a total annual energy demand higher with the system due to the lower solar heat gain in the heating season. Abu-Zour et al. (2006) evaluated the economic and environmental impact of a novel solar louvre thermal collector. The findings derived from the series of analyses showed that selection of site/climate for application is crucial for payback period and stability of supply. The optimization attempts concerning the design and performance of the louvre collector may reduce the initial cost and therefore shorten the payback period. Also, environmental impact of the solar louvre collector technology is strongly dependent on the performance of the collector. Figure 2.32 illustrates a solar louvre application on a multi-story building.



Figure 2.3.15 An application of the solar louvre system on a building (Citytrade, 2015)

2.4 FUTURE POTENTIAL OF BUILDING INTEGRATED SOLAR THERMAL COLLECTORS

Solar thermal energy has the potential to fulfil the entire heating and cooling demand in the residential sector. A broad range of low-temperature solar thermal collectors and systems, mostly for domestic applications, have been market-available over decades. These products are somewhat credible, generally made to a high technical standard (Fthenakis et al, 2009).

The potential of solar thermal technologies for the heat supply (hot water and space heating) in domestic sector is vast. Passive solar heating combined with energy efficient building construction and applications can reduce the space heating demand up to 30%. On the other hand, active solar systems can decrease the fuel demand for hot water and space heating from 50% to 70% for hot water and 40% to 60% for space heating. The potential of building integrated solar thermal applications will rise greatly if convenient technical solutions like long term storage become

available. Such storage systems could exploit chemical and physical practices to lessen the total storage volume and related costs (Aydin et al., 2015).

Solar assisted cooling is an exceptionally encouraging concept as peak cooling demand coincides with peak solar radiation. With ever-increasing demand for higher thermal comfort in working and living environments, the market for cooling has been regularly escalating in recent years. Today, solar assisted cooling can be counted as most promising for large buildings with central A/C systems. Though, the thriving demand for air-conditioned homes and small offices is creating new sectors for this technology (Faninger, 2010).

Solar thermal systems have the competence to substitute conventional fossil fuels for heating and cooling that more than one third of our energy use is just for heating. Therefore, this technology is a cost effective investment that offer substantial energy savings over years. The solar as a thermal source for solar thermal technologies is adequate and unlimited. It is roughly estimated that about 30% to 40% of the global heat demand could be fulfilled by solar thermal energy and 20% of Europe's heat demand. With the future projections given, the useful solar thermal energy in the long term (2050) will be about 60 EJ to 100 EJ/year globally (Faninger, 2010).

2.5 IEA TASK 41 SOLAR ENERGY AND ARCHITECTURE

In spite of the broad variety of applicable solar energy systems, these technologies are still not recognized as prevailing concepts in building practice. This may have several aspects such as lack of awareness among architects, absence of instruments supporting the design process and shortage in solar technologies that really suits for building integration. In order to refer these issues, EIA conducted a task namely IEA SHC Task 41 "Solar Energy and Architecture" during 2009 to 2012.

The main objective of the project was to bolster the application of solar energy systems in high quality architecture. The major outcome would be a substantial growth in use of building integrated solar energy systems, reduction in use of conventional fossil fuels and greenhouse gas emissions. There were fourteen countries participated in this task and the work was mainly divided into three subtasks: A) integration criteria and guidelines B) tools and methods for architects and C) case studies and communication guidelines (Munari et al., 2013).

2.6 DISCUSSION & CONCLUSIONS

In this chapter, the performance evaluations and applications of building integrated solar thermal collectors were briefly summarized. The various building integration of the solar thermal collectors such as PV/T water, PV/T air, refrigerant based PV/T, heat pipe PV/T, concentrating type PV/T, transpired PV/T, air and water based thermal, mini-parabolic, ceramic, polymer and solar louvre are presented. The concluding remarks are outlined as follows;

Solar thermal systems can satisfactorily fulfil the heat demand of the buildings whilst reducing CO₂ emission substantially. These systems are reliable and work on the noiseless environment. Life span of these systems is around 20-30 years and the maintenance cost is negligible.

In PV/T water collectors, prime design factors such as fin efficiency, lamination, thermal conductivity and efficiency have notable impacts on the electrical and thermal efficiencies.

In PV/T air collectors, in terms of energy and exergy performance, mono-crystalline system is more suitable whereas amorphous silicon was found to be more

economical. Also, the energy and exergy gains of the glazed and unglazed hybrid PV/T tiles air collectors are higher than that of conventional hybrid PV/T air collector. Solar thermal air collectors are relatively low efficiency due to the low density, volumetric heat capacity and thermal conductivity of air causing to low coefficients of convective heat transfer from solar energy to the air (solar thermal air). At relatively high flow rates and low supply temperatures, the solar thermal air collector system can display high solar conversion efficiency. Also, in order to accomplish higher collector efficiency, it is necessary to build up solar air collector having slender configuration alongside the air flow direction, having a small gap between the absorbing and bottom plate, using high absorptivity but very small emissivity selected coatings and preserving higher mass flow rate and keeping inlet fluid temperature to the collector very close to that of the ambient temperature.

In comparison, the thermal efficiency of water based solar thermal collectors is higher than the air based thermal collectors due to the specific heat capacity of water. Flat plate is the most applied configuration while the heat pipe systems come forward as a promising concept although high cost of the heat pipes and effective control of the tubes are the main issues.

For heat pipe PV/T collectors, heat gain, electrical gain and total PV/T efficiencies increase with increased flow rate. The effect of water flow rate on heat gain is much powerful than on electrical gain. Also, any reduction in the tube space of heat pipes would improve the heat and electrical gain, and PV/T efficiencies. The water-in-glass evacuated tubular solar water heater is the most widely used form of evacuated tube collector due to higher thermal efficiency. U-tube configuration of evacuated tube collectors is found to be better in performance. Also, not only heat efficiency but also

surface temperature of the absorber coating should be taken into account in order to evaluate the thermal performance of the glass evacuated tube solar collector

Refrigerant based PV/T collectors could significantly enhance the solar utilization rate and accordingly has the future potential to replace the water or air based systems.

In building integrated concentrating PV/T collectors, increased water mass flow rate has increasing effect on electrical output due to lower PV cell temperature and decreasing effect on thermal output. Also, as parabolic trough low concentrating systems are static systems, this feature simplifies the building integration of these systems. The thermal energy generated by the collectors with concentrators is higher than that by the collectors with no concentrator. Also, thermal efficiency increases with the increasing concentration ratio and mass flow rate. It is proven that absorber plate parameters have significant influence on the thermal efficiency of solar thermal systems.

Glazed solar thermal collectors usually have higher thermal energy output due to the concealed structure of the panels. Also, primary energy saving efficiency of The PV/T system was much advanced than that of the individual PV and traditional solar collector.

The v-corrugated collector was found to be the most efficient among the flat plate, finned and v-corrugated air heaters and the flat plate is the least efficient one.

The recent attempts to break the conventional metal based material dependence and lower the unit price of the solar thermal solar collectors include ceramic collectors, polymer collectors and solar louvres as an example of good building integration. The thermal performance of the new type collectors are sufficient but

needs to be improved. In addition, overheat protection of the absorber is a-must to prevent overrunning the maximum allowable temperature of the polymer.

In solar louvre applications, selection of site/climate for application is crucial for payback period and stability of supply.


The building integrated solar thermal collectors has the potential to become a major source of renewable energy as being efficient, economically viable, environmentally and ecology friendly, but still some drawbacks to deal with including high initial cost, low efficiency for building integrated systems, and unstable system performance due to weather effect.

For aesthetically appealing building architecture, the knowledge such as main technical info, integration possibilities, system sizing and positioning criteria needed to integrate active solar thermal technologies into buildings should be set clear.

According to scenarios, passive solar heating combined with energy efficient building construction and applications can reduce the space heating demand up to 30%. On the other hand, active solar systems can decrease the fuel demand for hot water and space heating from 50% to 70% for hot water and 40% to 60% for space heating. Also, it is estimated that about 30% to 40% of the global heat demand could be fulfilled by solar thermal energy and 20% of Europe's heat demand.

Various solar thermal collectors are presented but their applications are still limited due to product reliability and cost. Therefore, significant research is required mainly in thermal absorber design and fabrication, material and coating choice, energy conversion and effectiveness, cost reduction, performance testing and control of the system. This communication may be accessible for manufacturers, researchers and students working in this field. Chapter 5 investigates a solution to address above drawbacks.

The next chapter reviews different technical arrangements, past work and the recent developments in solar assisted liquid desiccant evaporative cooling technology; many configurations for liquid desiccant dehumidification and evaporative cooling technology and supplementary systems have been reviewed. It also describes and reviews the designs, technologies and systems/sub-systems, which enable the units to operate efficiently.



CHAPTER 3 – Recent developments in solar assisted liquid desiccant evaporative cooling technology

3 RECENT DEVELOPMENTS IN SOLAR ASSISTED LIQUID DESICCANT EVAPORATIVE COOLING TECHNOLOGY

3.1 INTRODUCTION

Conventional cooling technologies employing harmful refrigerants usually need more energy and lead peak loads causing negative effect on the environment. As the energy and environmental issues have to be dealt with globally, developing and promoting environmentally benign sustainable systems emerge as an urgent need. Solar assisted desiccant cooling is one such encouraging system, given the fact that solar energy is abundant renewable source to meet the cooling load requirements. Furthermore, unlike other solar thermal applications such as heating, peak demand for cooling arises when the solar radiation is the most direct and intense.

The idea of a liquid desiccant evaporative cooling system is to combine liquid desiccant dehumidification with an evaporative cooling system to advance the overall system performance and utilize solar energy as a source. In such a hybrid system, the desiccant dehumidification system is motivated to eliminate the latent load, while IEC system is to provide the sensible heat load (Yong et al., 2006). Further, as only low-grade energy is required for the regeneration process of the desiccant dehumidification system, solar energy as a renewable energy source can handle running liquid desiccant air conditioning system (Cheng et al., 2013).

A number of studies can be found in literature investigating the low cost and low regeneration temperature of dilute desiccant solution, and the optimization of the combined liquid desiccant-evaporative cooling system. As the solar energy is a free energy source, the use of low grade solar thermal energy for the regeneration has been investigated extensively both by academia and industry in many applications. Although the initial cost of solar energy technology can be high like most developing

concepts, it can lead to substantial savings in the long run. Moreover, evaporative coolers can act as mass exchange equipment in liquid desiccant systems rather than designing and manufacturing particular mass exchange equipment for such systems (Hamed et al., 2012).

The objective of this study is to present a literature review over the recent theoretical and experimental works on solar assisted liquid desiccant-evaporative air conditioning systems and solar regeneration methods concerning various aspects of this technology.

3.1.1 THERMAL COMFORT

Thermal comfort is vital for climate control systems and beyond. Thermal comfort signifies that in an environment, a person having normal amount of clothes on feel neither cold nor warm. Thermal comfort is crucial for one's well-being. It can only be obtained when air temperature, humidity and air movement are within the "comfort zone" range. According to ASHRAE Standard (ASHRAE, ANSI. Standard 55-2010:"Thermal Environmental Conditions for Human Occupancy"), thermal comfort is defined as that condition of mind which expresses satisfaction in that thermal condition. Also, British standard (British standard BS EN ISO 7730: Modern thermal environments) defines the thermal comfort as that condition of mind which expresses satisfaction with the thermal environment. The factor that influence on the thermal comfort of human beings are categorized as environmental and personal. The environmental factors involve air temperature, humidity, air speed and radiant temperature whilst personal factors are clothing, activity and conditions (Ahmad et al., 2013).

ASHRAE Standard 55-2010 has established an industry consensus standard to define comfort requirements in buildings. The objective of this standard is to set the combinations of indoor thermal environmental and personal factors that render indoor thermal conditions satisfactory for most of the occupants within that location. ASHRAE comfort zone as illustrated on a psychrometric chart in Figure 3.1, features one of the most recognizable standard 55-2010. The comfort chart basically displays the acceptable range of temperature and humidity level for spaces those satisfy the criteria specified in Section 5.2.1.1 of the standard. ASHRAE standard is applicable where the occupants' activity level in metabolic rates between 1.0 and 1.3 met and where the clothing worn that brings between 0.5 and 1.0 clo of thermal insulation. However, the comfort zone can deviate to the right or left in the psychrometric chart depending on the clothing, metabolic rate and radiant temperature (Ahmad et al., 2013).

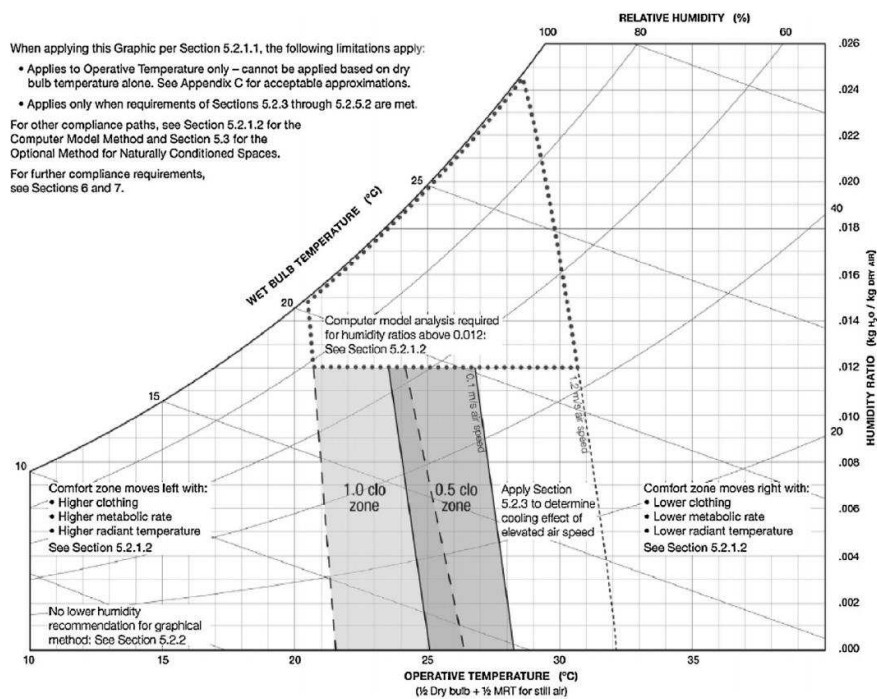


Figure 3.1.1 ASHRAE 2010 Comfort chart (Ahmad et al., 2013)

3.2 LIQUID DESICCANT DEHUMIDIFICATION FOR SOLAR COOLING

A desiccant is a natural or synthetic substance capable of showing a strong attraction for water vapour. It is usually classified as either solid or liquid both commonly used in various applications where low dew point temperature is needed. Each of solid and liquid desiccant substances has their own advantages and shortcomings. To name a few, common solid desiccant materials are polymers, silica, zeolites, alumina, hydratable salts and mixtures etc. while commonly used liquid desiccant materials are lithium chloride (LiCl), calcium chloride (CaCl), lithium bromide (LiBr), tri-ethylene glycol (TEG) and calcium chloride-lithium chloride mixture. The liquid desiccants are expected to possess some crucial properties including low vapour pressure, low viscosity, low regeneration temperature, low crystallization point, high density and being cost effective (Lowenstein, 2008).

A liquid desiccant system has three main components namely the regeneration heat source, dehumidifier and cooling unit. Today, packed bed is the most prevalent technology for these components. However, in order to avoid internal cooling, packed beds must operate with high desiccant flow rates to dehumidify effectively without any internal cooling. The dehumidification process is carried out by spraying the liquid desiccant into the process air to absorb the moisture out of the air then the liquid desiccant falls to a sump and pumped back to the nozzles to be sprayed back to the air again. The solution becomes diluted as a result of absorbing moisture out of the air stream. The concentration of desiccant solution decreases as the water content increases. Liquid desiccant is continuously circulated through the regenerator (Sarbu et al, 2013). So, the desiccant is regenerated to remove the moisture content by using an external heat source. Also, the desiccant solution is heated before contacting the air to adjust the partial pressure higher than that of the

air. Thus, the moisture content of desiccant is transferred to the regeneration air (process 2-3 in Figure 3.3). This regeneration air exits from the regenerator in a hot and humid condition. After the regeneration process, the liquid desiccant solution is more concentrated and free from moisture content and still at high vapour pressure and temperature. Before being sprayed into the process air again to complete the cycle, the liquid desiccant solution is cooled by a chiller or cooling tower to adjust the temperature to the desired level (process 3-1 in Figure 3.3). Then sensible cooling is provided via employing traditional vapour compression and vapour absorption, direct or indirect evaporative coolers (Mohammad et al., 2013). Thermal energy required, at a temperature as low as 40-50 °C, for the regeneration process can be easily obtained employing a flat plate collector (Gommed et al., 2004). In fact, being regenerated at lower temperatures below 80 °C is the one of the favourable features of the liquid desiccant systems than the solid desiccant cooling systems due to the higher moisture mass transfer area. However, carry over to the supply air is one of the main concerns of the liquid desiccant cooling systems. Besides, liquid desiccant substances are usually corrosive and simple handling of the working media is a burden. Thanks to fast advancement in the field, the potential of the liquid desiccant is remarkable (Alizadeh et al., 2002; Enteria et al., 2011). A schematic of a desiccant cooling air conditioning process is illustrated in Figure 3.2.

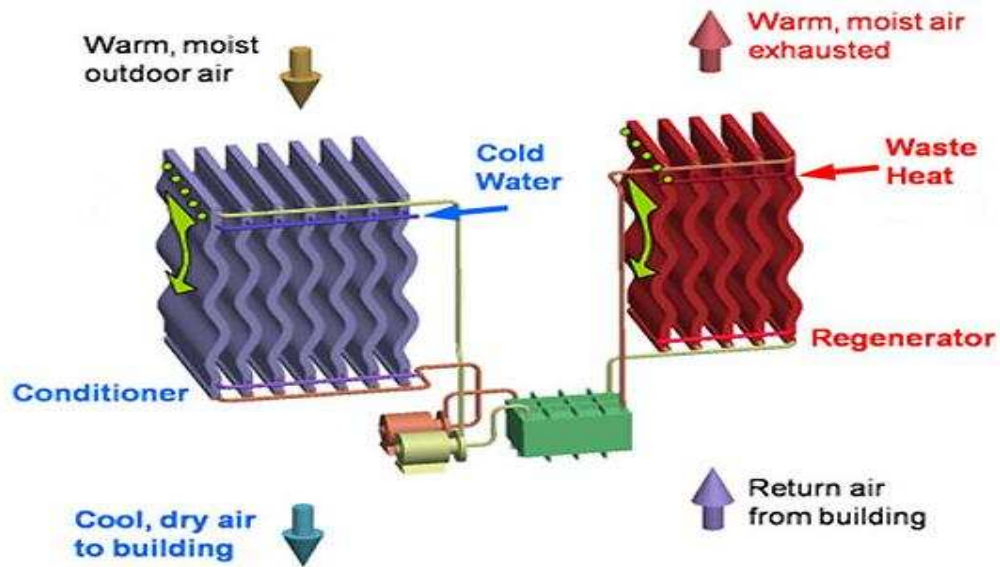


Figure 3.2.1 Schematic of a desiccant cooling air conditioning (Salt Air conditioner)

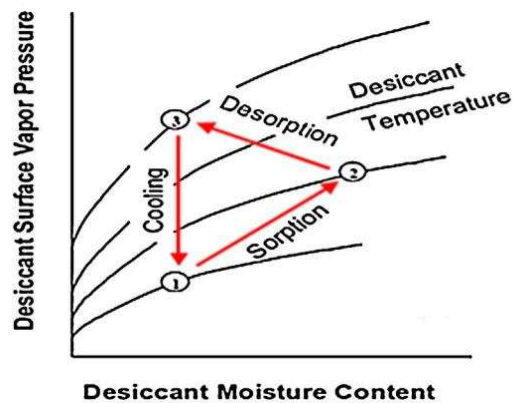


Figure 3.2.2 Moisture removal process by desiccant (Mohammad et al., 2013)

Ever since Lof (1955) explored liquid desiccant solar cooling concept, a number of researchers have conducted studies on liquid desiccant dehumidification systems for solar cooling applications. Enteria et al. (2011) studied solar assisted liquid desiccant air conditioning system. It states that increasing mass flow rate of the desiccant solution caused increase in the performance of both the regenerator and the solar collector. Factors like initial air and solution temperatures, solar radiation as well as the climatic conditions have found to be having effects on the overall performance of

the envisaged system. Henning et al. (2001) conducted an experimental study of a combined solar aided liquid desiccant cooling system with a 20 m² flat-plate solar collector and a 2 m³ hot water storage tank and claimed the primary energy savings up to 50% with a low overall cost. 54 % of collector efficiency, 76% solar fraction between the solar heat and auxiliary heat provided and COP of 0.6 during typical summer conditions were also reported. Not only feasibility study but also comparative study over various systems for different climatic conditions was presented. Yutong and Hongxing (2008) worked on to obtain the best configuration of an open cycle liquid desiccant air-conditioning system. The proposed system employs a counter flow type dehumidifier and solar collectors for the regeneration of dilute desiccant solution. There are two main loops designed in the system: liquid desiccant dehumidification loop and air dehumidification loop along with two solutions tanks for strong and weak solution, respectively. The experimental study was conducted in Hong Kong. It was implied that the higher energy saving was attained when the latent load was higher in the total ventilation load. Total energy saving ranging from 25 to 50% was obtained in comparison to the vapour compression system. Kabeel (2005) investigated the regeneration of the liquid desiccant system thru solar application. It was noted that the enhanced regeneration for forced flow against the natural flow due to the improved mass transfer coefficient. Peng and Zhang (2009) performed numerical and performance analysis of heat and mass transfer process in a novel solar assisted liquid desiccant regeneration system as shown in Figure 3.4. The simulation results indicated that solution outlet concentration increases 70%, regeneration efficiency improves 45.7% and storage capacity extends 44% as effective solution proportion declines from 100% to 62%.

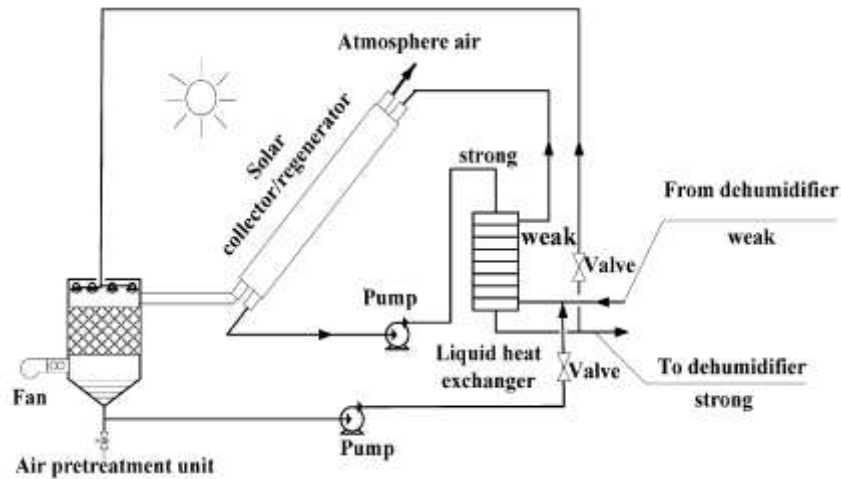


Figure 3.2.3 Schematic diagram of solar air pre-treatment collector/regenerator (Peng et al., 2009)

Katejanekarn et al. (2009) installed and carried out experiments of a solar-regenerated liquid desiccant ventilation pre-conditioning system in Asian Institute of Technology, Thailand. The hot and humid tropical climate of Thailand provided certain advantages in the installation. The proposed system takes full benefit of pure solar energy for the regeneration of liquid desiccant as shown in Figure 3.5. According to experimental results, the system was capable of reducing the temperature by 1.2°C and relative humidity by 11.1%. An important limitation of the system was specified as cooling of air by cold water from the cooling tower. Since the ambient air was humid, the water from the cooling tower could not be removed any further. Audah et al. (2011) proposed and studied the feasibility of a solar powered liquid desiccant system which employs calcium chloride as liquid desiccant solution and parabolic solar concentrators as a heat source for regeneration. The results displayed that an increase from 50.5°C to 52°C was observed in the optimal regeneration temperature with decreasing sink temperatures from 19°C to 16°C. In addition, the liquid desiccant model estimated the amount of water condensation captured from humid air leaving the regenerator as directed through a coil submerged in cold sea water. Gommed and Grossman (2004) examined a solar

powered liquid desiccant air conditioning system applied in an office building in Haifa, Israel. The parametric study proves that ambient air temperature and flow rate affects the heat and mass transfer in the dehumidification process. Factors such as temperature and flow rates of heating and cooling water, flow rate and concentration of the liquid desiccant solution in the dehumidifier and regenerator have impacts on the humidity of supply air.

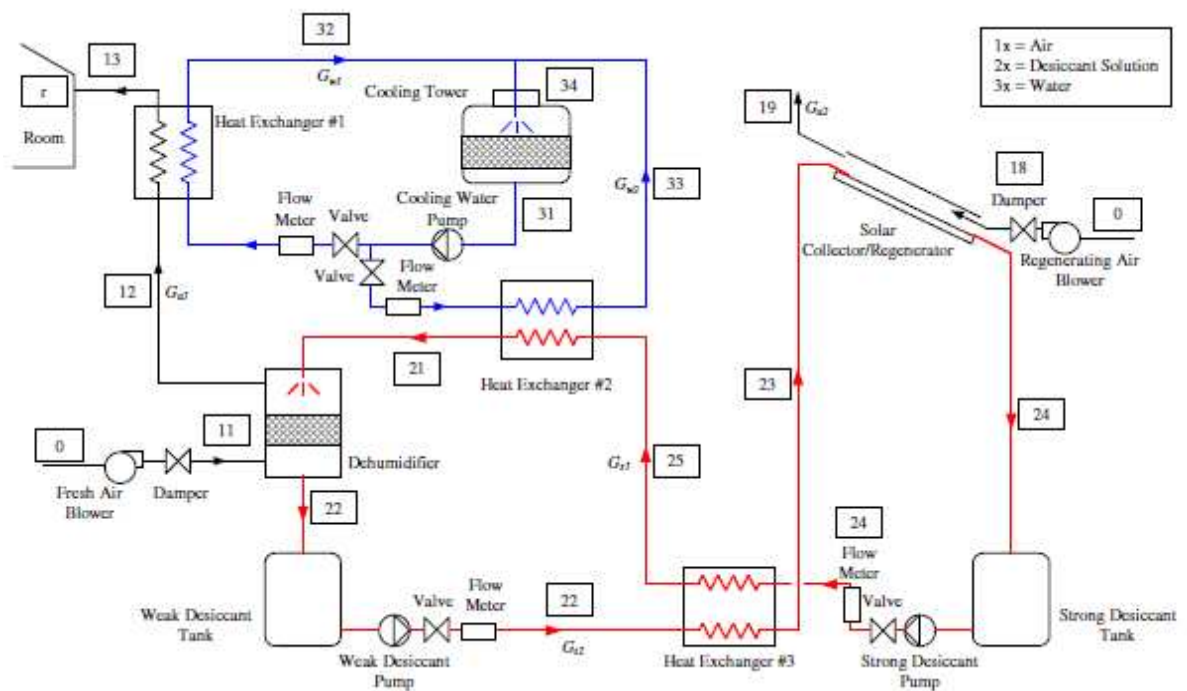


Figure 3.2.4 Schematic diagram of the solar regenerated liquid desiccant system (Katejanekarn et al., 2009)

Aly et al. (2011) conducted a comparative study using Lithium chloride (LiCl) and calcium chloride (CaCl_2) solutions applied as the working desiccant solutions in the investigation. A finite difference method was practiced to simulate the combined heat and mass transfer processes that take place in the liquid desiccant regenerator. By applying the suggested model, the effect of the design parameters namely the regenerator length, desiccant flow rate and concentration, air flow rate on the performance of the system was inspected. The results of experimental tests revealed

that higher vapour pressure difference values were attained with the calcium chloride desiccant than those obtained with the lithium chloride solution. It was also noted that the model successfully estimated the overall performance of the system under various climate conditions. Gao et al. (2013) compared the performance of internally cooled dehumidifiers with adiabatic dehumidifiers by considering the dehumidification effectiveness and moisture removal rate. The findings pointed that internally cooled dehumidifiers can substantially advance the performance in comparison to adiabatic dehumidifiers, particularly if the solution is at a high temperature and/or diluted in the downstream section of the liquid desiccant flow. Optimal solution temperatures were ranged from 20-25 °C for adiabatic dehumidifiers and 25-30 °C for internally cooled types. It was also noted that cooling the water relatively at lower temperatures can lead to higher values for dehumidification effectiveness and moisture removal rate in an internally cooled dehumidifier. She et al. (2014) proposed a new energy efficient liquid desiccant dehumidification and evaporation systems and compared the performance characteristics of the new system with conventional vapour compression refrigeration system. Findings implied that proposed system achieved higher COP than conventional systems and even higher than the reverse Carnot cycle under the same operation conditions. The COPs of the suggested system was 18.8% and 16.3% higher using hot air and ambient air, respectively than conventional vapour compression refrigeration system under varied conditions.

3.3 HYBRID SOLAR LIQUID DESICCANT AND EVAPORATIVE COOLING SYSTEMS

Evaporative cooling is one of the alternatives considered corresponding to mechanical vapour compression for air conditioning applications. In terms of energy

consumption, evaporative coolers use less than a quarter of the electric power than conventional vapour compression systems (Gebrehiwot et al., 2013). These systems are commonly utilized in regions with dry and temperate climates in place of conventional air-conditioning devices due to the lower initial cost and energy consumption. Also, its use has been extended to regions under humid weather conditions by incorporating with a desiccant chamber for air dehumidification before the evaporation process (Worek et al., 2012).

There are two common types of evaporative cooling systems namely direct and indirect evaporative cooling systems [Gandhidasan et al., 1990, Zhao et al., 2008]. The effectiveness in terms of temperature for direct and indirect evaporative cooling systems is 70-95% and 40-60%, respectively. As working principle, a direct evaporative cooling system adds moisture to the process air while an indirect evaporative cooling system provides only sensible cooling to the supply air without adding any moisture. This feature, therefore, makes indirect systems more attractive than direct evaporative cooling systems (Tu et al., 2009). A schematic diagram of direct and indirect evaporative cooling methods is presented in Figure 4.6 and psychometric of direct and indirect cooling is given in Fig 3.7.

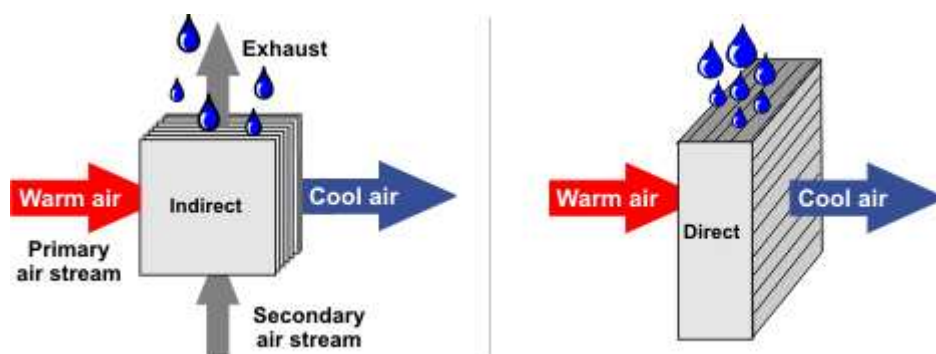


Figure 3.3.1 Schematic diagram of direct and indirect evaporative cooling concepts (HVAC, 2015)

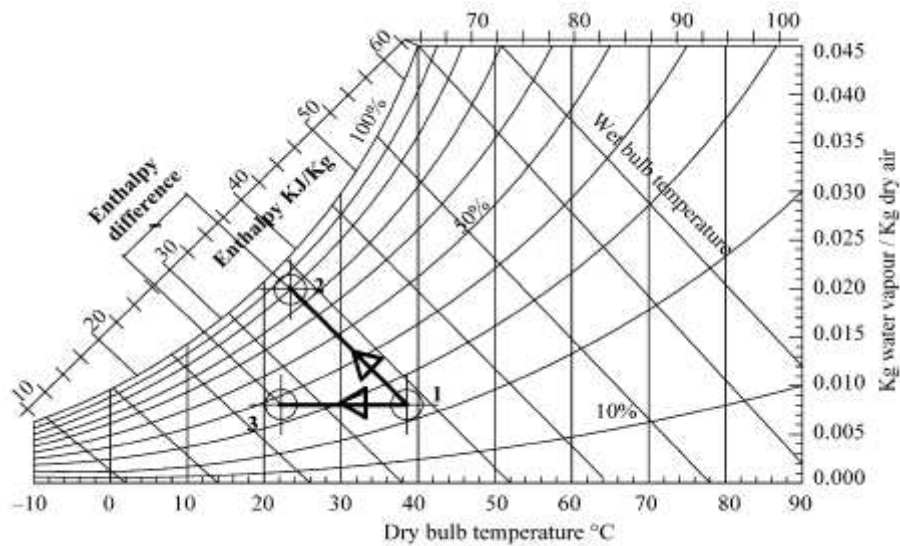


Figure 3.3.2 Psychrometric of direct and indirect evaporative cooling (Daou et al., 2006)

There are various types of designs and applications of the evaporative coolers. Thus, it is widely used incorporation with desiccant cooling systems. However, there are a few solar liquid desiccant studies, in literature, considered evaporative cooling systems as auxiliary cooling units. Such a hybrid desiccant cooling system consists of three subsystems, namely, dehumidifier (liquid desiccant material), regenerator (solar aided), and cooling unit. The liquid desiccant based evaporative cooling concepts is shown in Fig 3.8.

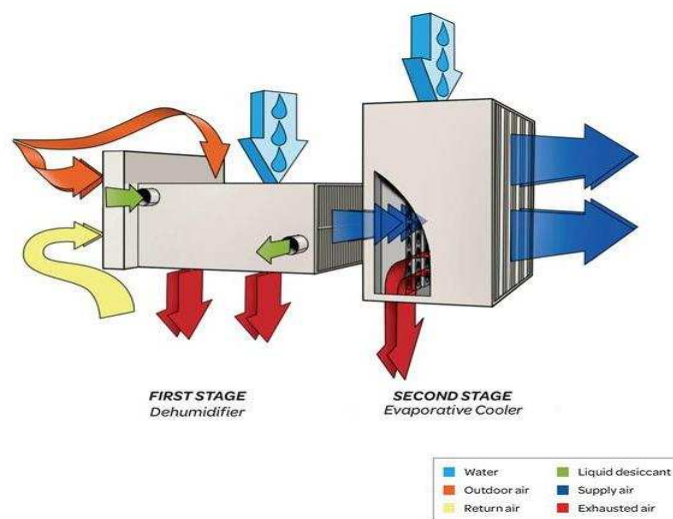


Figure 3.3.3 Concept of liquid desiccant based evaporative cooling system (Evap, 2015)

3.3.1 Hybrid solar liquid desiccant and direct evaporative cooler

Gandhidasan (1990) estimated the total heat removal from the solar liquid desiccant system operating on ventilation mode with respect to known parameters a simplified vapour pressure which is correlated to the effectiveness of the dehumidifier and heat exchanger. The proposed system, as shown in Figure 3.9, in the study operated under atmospheric pressure condition. Calcium chloride, as a liquid desiccant solution, was used for air dehumidification and then the supply air was cooled via the evaporative cooler. Tu, Min et al. (2009) proposed and simulated a novel energy efficient cooling system using lithium chloride (LiCl) solution as liquid desiccant. In the system, 80°C was assumed for regeneration temperature to obtain by flat plate solar collectors. In the process, the air was dehumidified and sensibly cooled by the direct and indirect evaporative coolers. The results of the simulation revealed that desiccant mass flow rate was found to be less than 2.0 [kg/kg] for supply air temperature under 20°C. Krause et al. (2006) conducted a comparative study between solar assisted liquid desiccant air conditioning systems coupled with direct and indirect evaporative coolers. A numerical model was developed in the simulation environment TRNSYS and validated by experimental data for two Australian locations. It was stated that the design of the system had to be adjusted to each climates considering design, location and occupant behaviours of the buildings. Kim et al. (2013) conducted a simulation study using TRNSYS 16 to estimate the impact of the solar liquid desiccant system on direct and indirect evaporative cooler applications in order to be able to suggest an effective integration. Solar thermal side of the system was also quantitatively estimated. The simulation results showed that the energy consumption of the proposed system was 51% less than the conventional counterparts and the contribution of the solar thermal system for regeneration to the

energy saving was notable. Alizadeh (2008) developed and tested a solar liquid-desiccant air conditioner (LDAC) coupled with a direct evaporative cooler in Queensland, Australia as shown in Figure 3.10. The proposed system utilizes high effectiveness cross-flow polymer plate heat exchanger as an absorber and the weak lithium chloride desiccant solution is concentrated using hot water from flat plate solar collectors. In operation, the process air was dehumidified by strong desiccant solution and then the warm and dry air was cooled and humidified through the direct evaporative cooler and the supply air was introduced to the conditioned space. The results of the tests revealed that electrical COP of the system was around 6 with 3.5kW electrical energy consumption and the effectiveness of the conditioner with the desiccant solution was about 82%. A feasibility study was also undertaken and a commercialization strategy for the solar operated LDAC in Queensland has been proposed. Alosaimy and Hamed (2011) theoretically and experimentally investigated the solar water heat coupled with air dehumidifier for regeneration of the desiccant solution which is calcium chloride in his study. An evaporative cooler was also proposed to be coupled for air cooling in arid areas. In order to obtain correlations between inlet parameters and the performance of the system, an artificial neural network was developed and trained. Early results of the experimental study yield that 30-50% of calcium chloride solution was regenerated by solar thermal energy. In addition, predictions upon the overall performance on the basis of the experimental data showed desirable characteristics including the proposed system's wide range application. A feasibility study was also provided. Abdalla et al. (2006) developed and described a solar assisted liquid desiccant direct evaporative air conditioning system as presented in Figure 3.11. Evaluations regarding the performance of the system proved to be promising in humid as well as dry climates and the system was

able to utilize relatively low temperature heat source efficiently. The system was operated only at atmospheric pressure and refrained from pressure sealed units. Experimentally obtained results indicated that the system was able to dehumidify 1.6 kg/s of process air at 30.1°C dry-bulb temperature and 6.6g/kg of humidity ratio which is equivalent to 17°C wet-bulb temperature. A solar powered liquid desiccant air conditioning system for greenhouse food production in hot climates has been proposed in (Lychnos et al., 2012). As shown in Figure 3.12, the system comprised a dehumidifier, solar assisted regenerator and evaporation pad and also magnesium chloride ($MgCl_2$) was used as a desiccant solution. The experimental results revealed that the system was able to lower average daily maximum temperatures in hot season by 5.5-7.5°C and it was concluded that the proposed system was viable and deserve to be tested in a full scale installation at an appropriate location.

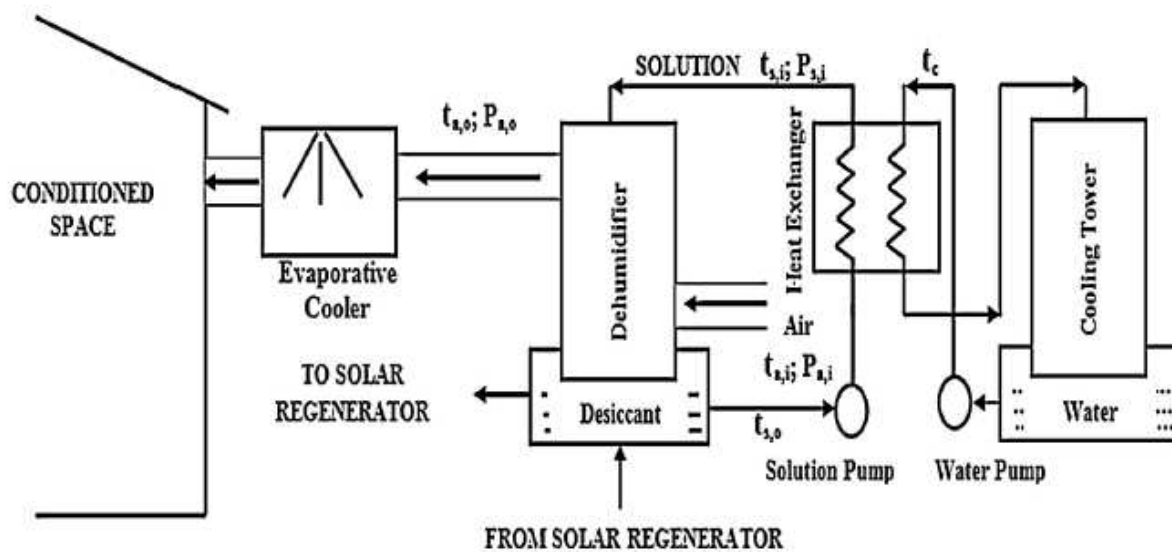


Figure 3.3.4 Schematic diagram of the solar LDAC system (Gandhidasan, 1990)

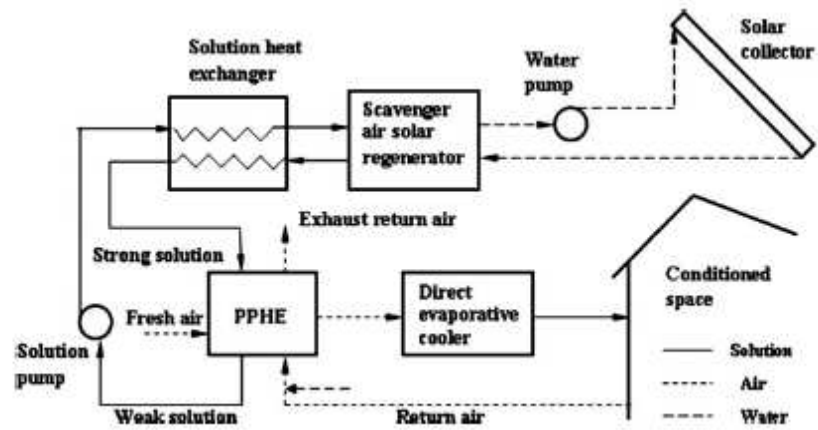


Figure 3.3.5 Schematic diagram of the solar LDAC system in Queensland, Australia (Alizadeh 2008)

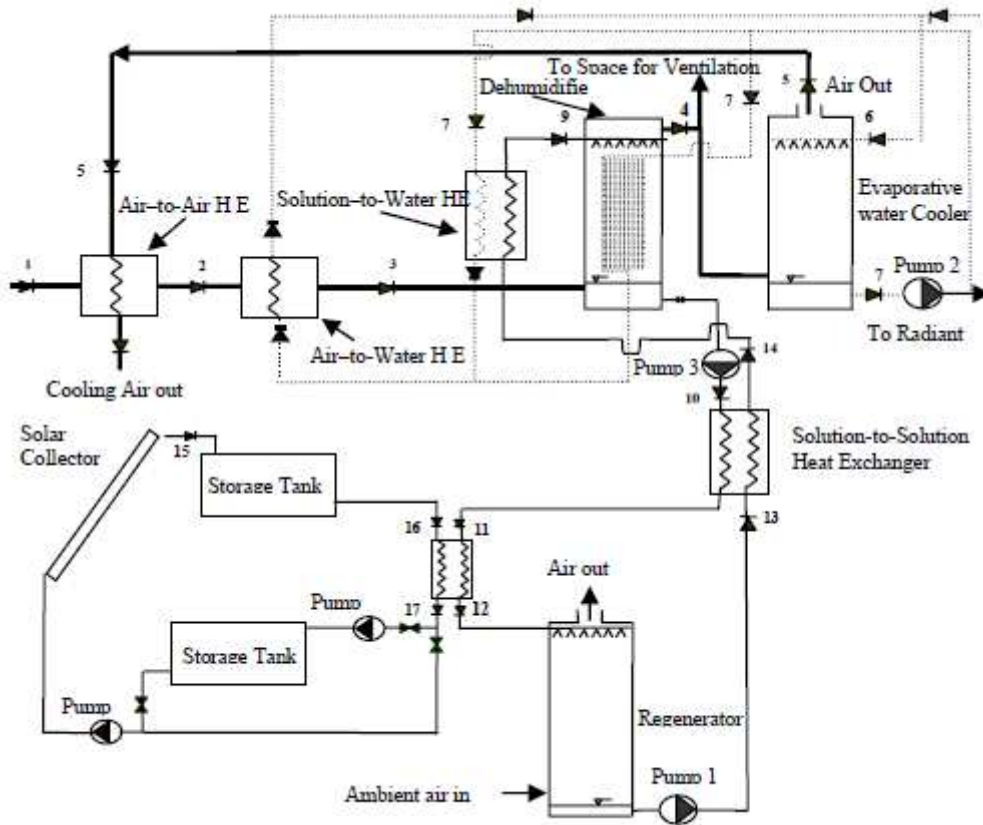


Figure 3.3.6 Schematic diagram of a solar-driven liquid desiccant evaporative system (Abdalla, 2006)

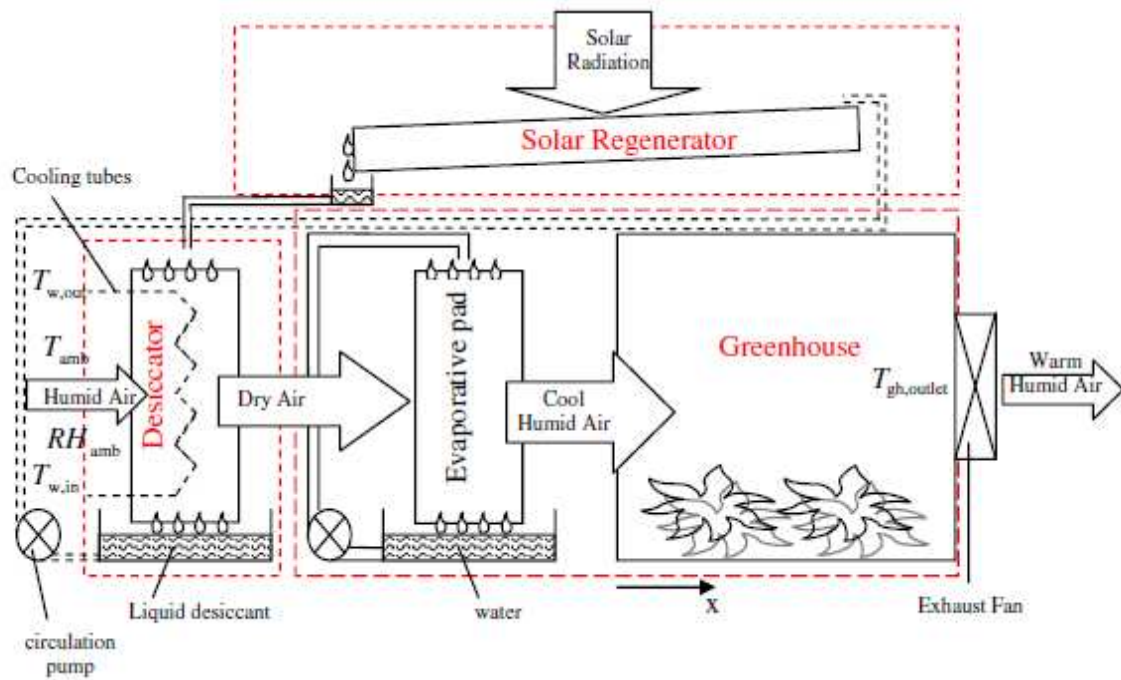


Figure 3.3.7 Schematic of the solar assisted liquid desiccant system with evaporative pad (Lychnos, 2012)

Kim et al. (2014) investigated the annual operating energy performance of a desiccant and evaporative-cooling system and compared the energy saving patterns of the system with a conventional variable air volume system and an existing evaporative-cooling-assisted system. The findings indicated that the proposed system could achieve up to 82% energy savings over the conventional system during the summer, and 54% and 37% during the winter and intermediate season operations, respectively. Basically, the proposed system administered annual energy savings of 68% and 23% in comparison to the conventional and established evaporative-cooling system. It was also suggested that more energy saving could be obtained by incorporating liquid desiccant unit with the water side free cooling and solar thermal system.

3.3.2 Hybrid solar liquid desiccant and indirect evaporative cooler

Krause et al. (2006) carried out a study about the optimisation of a solar liquid desiccant dehumidification system combined with direct/indirect evaporative cooler. A simulation model in TRNSYS environment for two Australian locations was developed and validated using the experimental data. According to the results obtained, a basic conflict between humidification and cooling was noted when direct evaporative cooling system was used. However, in hot and dry climates, the performance of the solar liquid desiccant enhanced direct and indirect evaporative cooling was sufficient to guarantee indoor comfort conditions. Katejanekarn et al. (2008) utilized a heat exchanger to cool the dehumidified air rather than the traditional evaporative coolers to adjust the air dryness. The solar assisted system has two main air loops; one for dehumidification and another for regeneration as well as two liquid loops; liquid desiccant in the dehumidifier and water in the cooling tower. The system was able to decrease the process air temperature and relative humidity by 1.2°C and 11.1%, respectively. Das et al. (2013) presented a study about solar thermal driven liquid desiccant air conditioning system for tropical climates like Delhi. The system consisted of a dehumidifier, regenerator, indirect evaporative cooler, several heat exchanger and solar collectors as shown in Figure 3.13. In order to eliminate the carry-over of desiccant droplets with the process air, an indirect contact heat and mass exchanger as an absorber was employed in the proposed concept. The performance evaluation of the system showed that maximum specific humidity change was achieved as 8g/kg as maximum moisture removal rate of 1.6g/s was attained while the capacity of the system ranged from 2.5 to 5.5 kW and COP was between 0.4 and 0.8, at various ambient conditions. Yin et al. (2009) presented a new ventilation system with radiant cooling and air supplied from liquid

desiccant dehumidification as shown in Figure 3.14. This system was installed in an office in hot and humid climate. Although radiant cooling offered great advantages of improving thermal comfort, there was a high condensation risk if applied with a high latent load. The results showed that the new system could prevent the risk of condensation on the cooling panels and provide a comfortable indoor environment. It was also concluded that the proposed system has great potentials for hot and humid climate conditions. A new concept of a liquid desiccant enhanced evaporative cooling system with the objective of combining the benefits of liquid desiccant and evaporative cooling technologies along with solar thermal utilization was developed in National Renewable Energy Laboratory (NREL) of US Department of Energy (Kozubal et al., 2011). Modelling of the novel system demonstrated that 30-90% less annual combined energy source for the thermal and electrical energy required to run the system was expected and also an additional 50% reduction in energy consumption was anticipated. It was also noted that thermodynamic potential of the proposed system was able to succeed in dealing with many shortcomings of standard refrigeration based expansion cooling systems. An example diagram of a residential installation of the DEVap A/C system is presented in Figure 3.15.

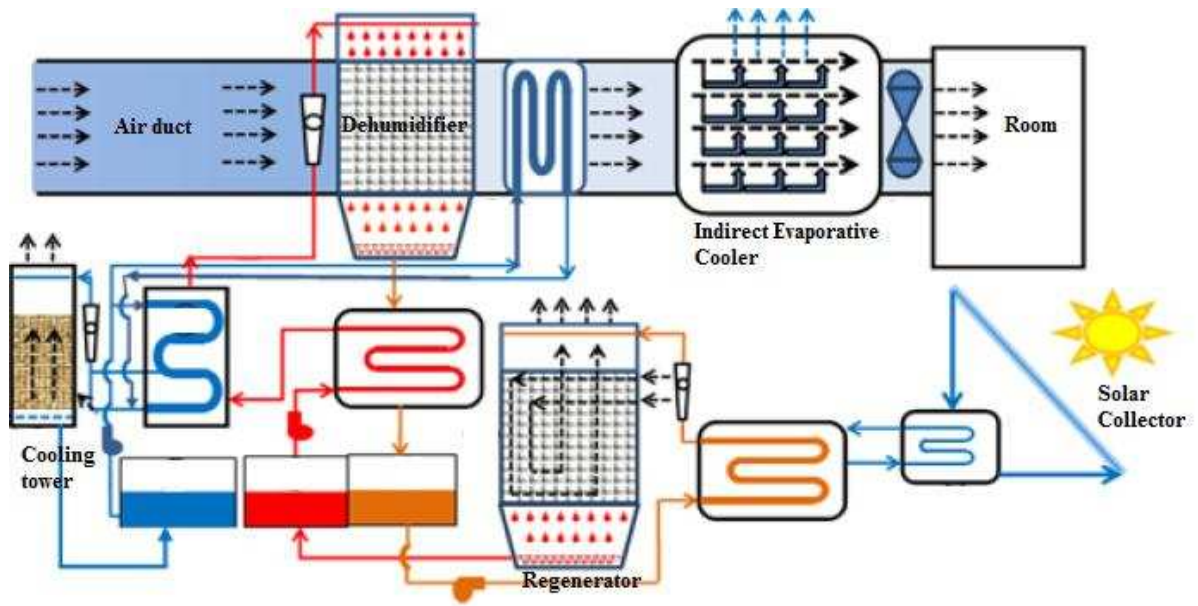


Figure 3.3.8 Schematic of the liquid desiccant cooling system (Das et al., 2013)

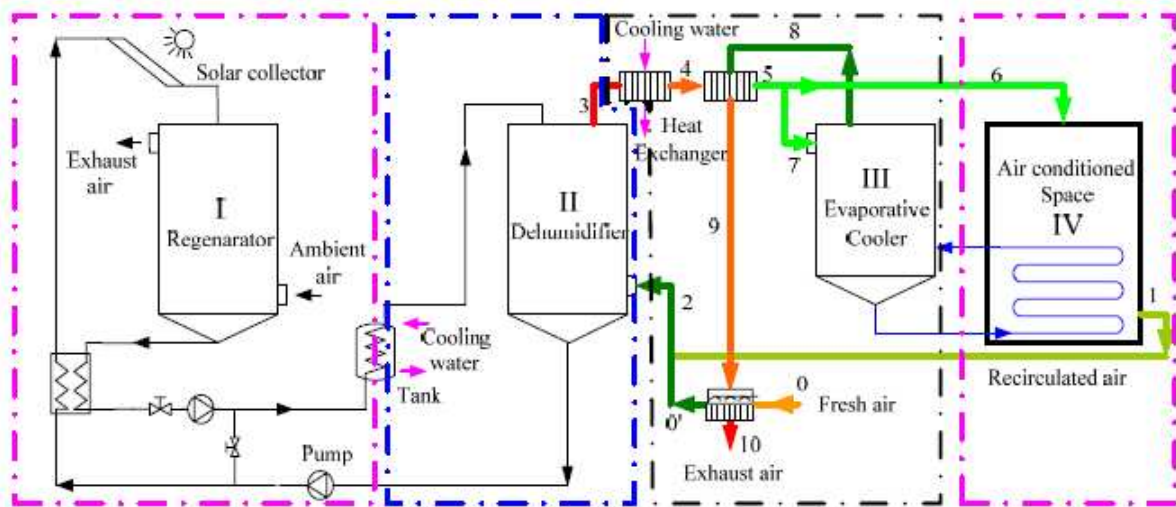


Figure 3.3.9 Schematic of the system proposed by (Yin et al., 2009)

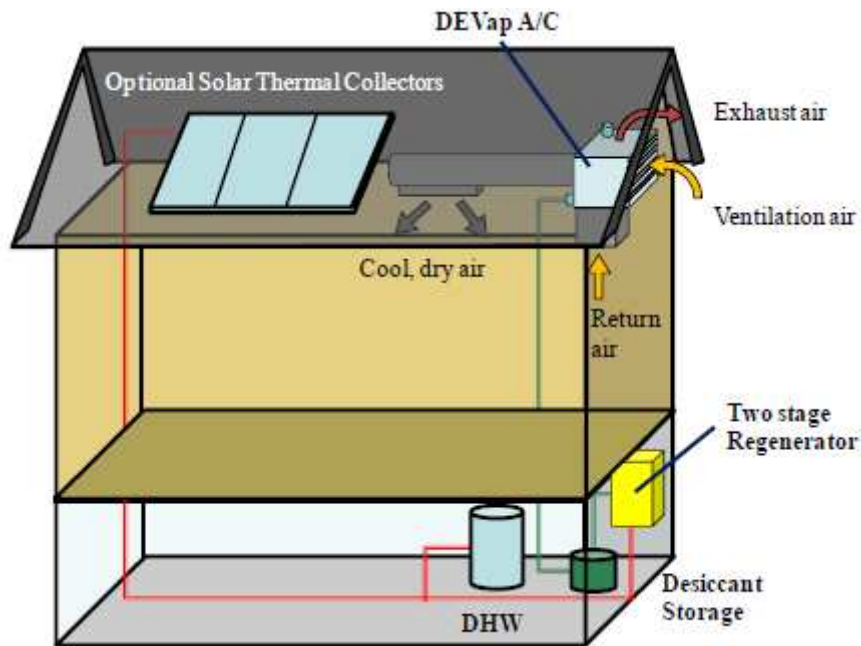


Figure 3.3.10 Schematic diagram of the solar liquid desiccant enhanced dew point cooling system
(Kozubal et al., 2011)

Caliskan et al. (2012) conducted a comparative study on energetic, exergetic and environmental performance assessments of three various novel M-cycle based indirect evaporative coolers. In the study, the analyses were carried out based on efficiency assessment along with environmental impact and sustainability parameters. In the configuration, System I and III draw power from electric grid while System II is a standalone system, produces its own electricity by PV panels. The analysis including energy, exergy and sustainability assessments were performed for six different dead state temperatures ranging from 10°C to 35°C. Lastly, environmental assessments of the systems based on their greenhouse gas (GHG) emissions (gCO_2/kWh) due to the electricity consumption were calculated. Maximum exergy efficiencies and sustainability assessments were attained as 35.13% and 1.5415 for System III, and 34.94% and 1.5372 for System II, respectively. GHG emissions for respective systems I, II and III were obtained as 2119.68 gCO_2/kWh , 153.6 gCO_2/kWh and 3840 gCO_2/kWh , on average. So, it was concluded that

System II powered by PV panels was found to be a better choice towards global warming prevention and sustainable future. Gao et al. (2014) experimentally explored the performance characteristics of an integrated liquid desiccant-indirect evaporative air cooling system utilizing the Maisotesenko cycle and compared the performance patterns in order to investigate the heat and mass transfer performance, effects of air and desiccant inlet parameters as well as working air ratio. The integrated system has two air handling process; namely moisture removal in the dehumidifier and sensible heat removal in the M-cycle indirect evaporative cooler. The results indicated that the variation of dehumidification capacity in the first stage directly influenced the cooling capacity in the second stage if inlet parameters of air or desiccant were increased. It was also found that to enhance the performance in the second stage, the water flow rate to the wick surface had to be five times greater than that of the evaporative water.

3.4 SOLAR LIQUID DESICCANT REGENERATION METHODS

3.4.1 Solar Thermal Regeneration

The use of solar energy to regenerate liquid desiccant has attracted much interest. Currently, solar desiccant regeneration systems are mostly driven by solar thermal energy. Solar electrodialysis regeneration is also being investigated as a means of new solar regeneration method (Cheng et al., 2013).

A common type of solar thermal regeneration system for LDAC is shown in Figure 3.16. Weak desiccant solution flows from the dehumidifier into the solar collector and soaks the heat in there, which causes to increase in the temperature. Then, hot but still dilute desiccant solution is discharged to the regenerator and contacts with the air passing upwards. Water molecules in the desiccant solution get absorbed by the air stream and the dilute solution becomes regenerated. The concentration of the

desiccant solution is adjusted and strong desiccant solution is obtained as a result of this process. The strong solution is introduced to the dehumidifier from the strong solution storage to carry on the dehumidification cycle.

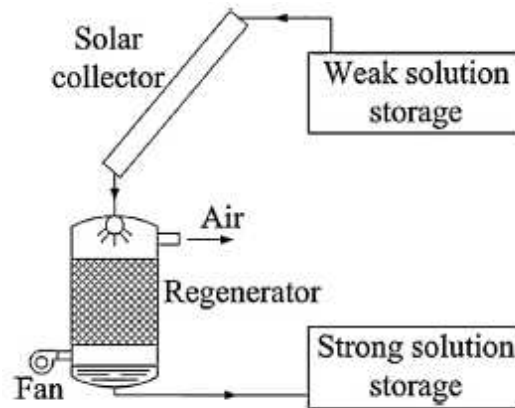


Figure 3.4.1 Schematic of a solar thermal regeneration system for LDAC (Cheng et al., 2013)

Li and Yang (2008) performed investigations on the energy performance of using exhaust air for the regeneration of the dilute desiccant solution and heating the solution beyond the equilibrium value of various lengths of the collector/regenerator(C/R) panels. Findings revealed that the performance was substantially improved and implementing this technique would allow shortening the length of the solar collector/regenerator without degrading the performance considerably. Energy saving in the range of 25-50% compared to a traditional vapour compression system was also reported. Yin and Zhang (2008) proposed a new internally heated regenerator which was expected to achieve a better performance compared to conventional packed regenerators. The results of the experimental test indicated that not only higher regeneration rate was achieved, but also higher energy utilization was monitored. Elsarrag (2008) experimentally tested a novel regeneration system altered from solar tilted still. During the experiments, the effect of the liquid to air flow rate ratio, the desiccant temperature and concentration, and the inlet air

humidity ratio on the evaporation rate were monitored. Peng and Zhang (2008, 2009) proposed a novel solar air pre-treatment collector/regenerator for solar liquid desiccant air conditioning system. This system was designed with the objective of operating in high humidity region. The simulation results unclosed the great potential of the novel solar air pre-treatment collector/regenerator to improve the solution regeneration performance. Xiong et al. (2010) investigated the performance of two kinds of desiccant solution (lithium chloride and calcium bromide) in the two separate dehumidification stages of a two stage solar assisted liquid desiccant dehumidification system. During the operation, air moisture (latent) load is separately pre-dehumidified by low-cost calcium chloride and then dehumidified via stable lithium bromide in a main dehumidifier. It was deduced that the effect of pre-dehumidification on the performance was remarkable in a high humidity ambient.

Although solar regenerators are successful in producing intended outcomes, the corrosion problem related with the liquid desiccant solution on the energy absorbing surface cannot be disregarded. Luo et al. (2012) studied low corrosive ionic liquids as a substitute of common liquid desiccant solutions. The experimental findings demonstrated that [Dmim]OAc and [Emim]BF₄ with inlet mass concentrations of 81.7% and 85.5% could achieve same dehumidification rates as LiCl and LiBr with the mass concentrations of 40.9% and 45.0%, respectively.

Bassuoni (2011) compared the performance of the structured packing dehumidifier/regenerator in a liquid desiccant system with vapour compression system. The performance of the system was assessed using the mass transfer coefficient, moisture removal rate, effectiveness and coefficient of performance (COP). According to economic analysis, the payback period of 11 month was

attained with annual running savings of 31.24% compared with vapour compression system.

3.4.2 Photovoltaic Electrodialysis (PV-ED) Regeneration

Apart from the thermal regeneration technique, a recent solar method for the liquid desiccant regeneration is being studied. Electrodialysis (ED) is a technology based method that ions transport through the selective membranes under the influence of an electrical field (Li et al., 2009; 2011). Cation and anion exchange membranes are alternately set in between a cathode and anode within an electrolyszer. Under the electrical field, the anions and cations inside the electrolyszer cells move towards the anode and cathode. During this process, the anions and cations pass through anion exchange membranes and cation exchange membranes, respectively. This flow causes a rise in the ions concentration in the concentrate compartments and fall into the dilute compartment. By this way, both the concentrated desiccant solution and pure water can be acquired. A schematic diagram of the PV-ED regeneration method is presented in Figure 3.17.

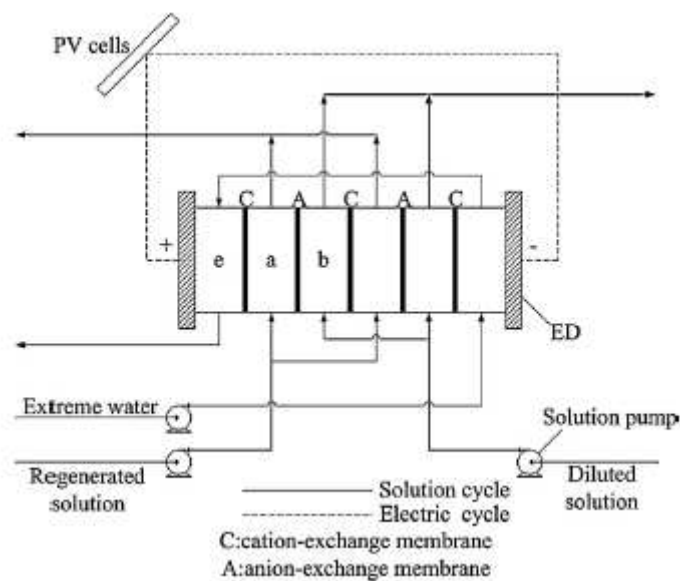


Figure 3.4.2 A schematic of the PV-ED regeneration system (LI et al., 2009)

In a PV-ED regeneration process, the dilute desiccant solution is drained from the dehumidifier to the regenerator. The PV cells driven regenerator is made of ED stacks formed of a mass of cells located in parallel between two electrodes. As shown in a schematic of an ED regenerator (Figure 3.17), the cells a, b and e are the concentrate, dilute and electrode rinse cells, respectively. The weak solution is introduced to the dilute cell and regenerated solution to the concentrate cell. After this process, the dilute solution becomes regenerated which is sent to the dehumidifier unit of the LDAC system (Cheng et al., 2013).

As regards the PV-ED regeneration concept, Li et al. (2009, 2011) investigated this new regeneration method for the liquid desiccant cooling system. In this novel regeneration method, the regenerator was formed as an ED stack, and the required electric power for the regeneration process was provided by the photovoltaic cells. In addition, new double stage photovoltaic/thermal ED regeneration (PV/T-ED) system was introduced in (Li et al., 2009). The results of the performance analysis remarked that double stage system outperformed the single stage one in terms of efficient regeneration of liquid desiccant solution.

3.5 DISCUSSION AND SUMMARY

Domestic energy use is one of the major consumers of conventional energy sources in the form of electric power and also one of the main contributors to the carbon emissions (IEA Key World Energy Statistics, 2013; Birol, World Energy Outlook, 2010). It is a future projection that energy consumption in buildings will permanently be augmented by rise in living standards, industrialization and urbanization. Achieving indoor air quality and thermal comfort via vapour compression air conditioning and ventilation system constitutes a major part of building energy use (Enteria et al., 2011). Passive and natural air conditioning and ventilation can

become a preference in order to lower the domestic energy consumption as some of the natural and passive methods are shown in Figure 3.18. Prevailing wind speed and direction determine the wind-induced natural ventilation practice (Khan et al., 2008). Solar induced ventilation is applicable in dry and cool environments (Khanal et al., 2011). However, direct ventilation of outdoor air to the indoor environment ruins the thermal comfort in hot and humid ambient air conditions. Therefore, desiccant based air dehumidification and air-conditioning can make a major alternative for reduction in air humidity and temperature with the application of renewable energy source like solar energy.

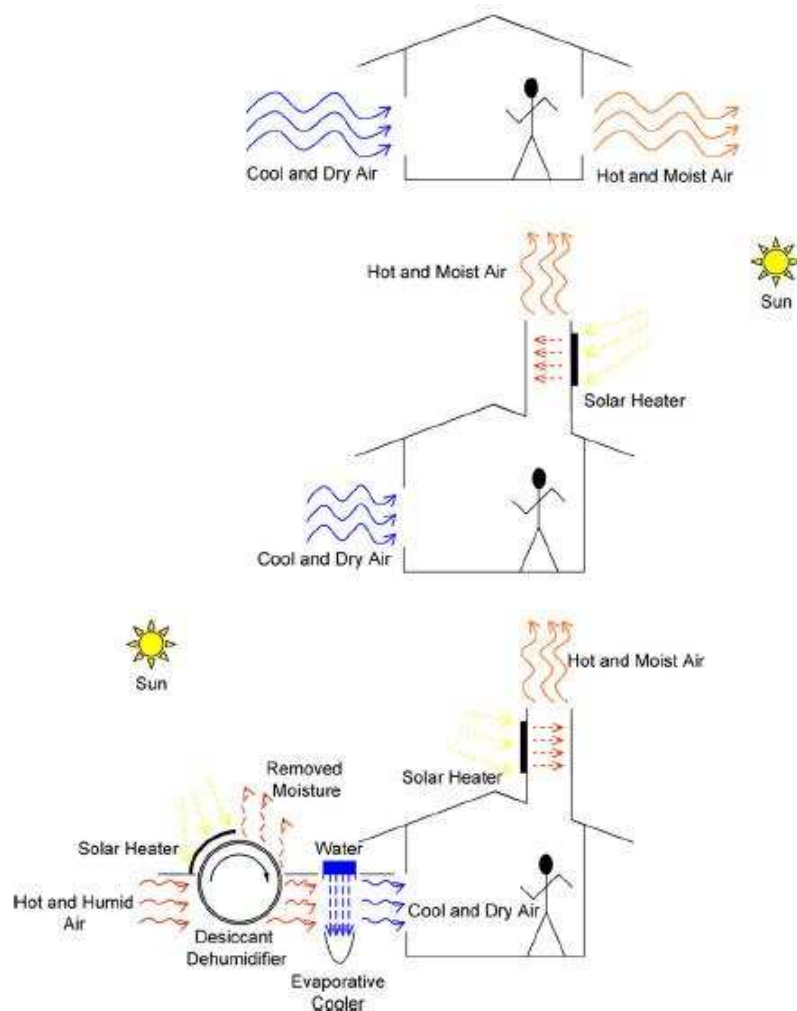


Figure 3.5.1 Schematic of the passive & natural air-conditioning and ventilation system (Enteria, 2011)

The desiccant based dehumidification and cooling technique makes effective use of the ability of desiccant substances extracting the air moisture by sorption. The sorption process (adsorption and absorption) is defined as the intermolecular interaction between sorbent and sorbate molecules. As water vapour concentration is very low in desiccant materials, the moisture content in the airstream is attracted by the desiccant substance due to the pressure difference. Thermal energy is required to regenerate the desiccant substance in order to adjust its concentration by removing the moisture content as the process is shown in Figure 3.19. Temperature of the dehumidified air rises because of the release of the condensation and sorption heat. As the temperature of dry air is still above the thermal comfort threshold, evaporative cooling method is applied by increasing air moisture content slightly or keeping it constant either directly or indirectly in a secondary air stream.

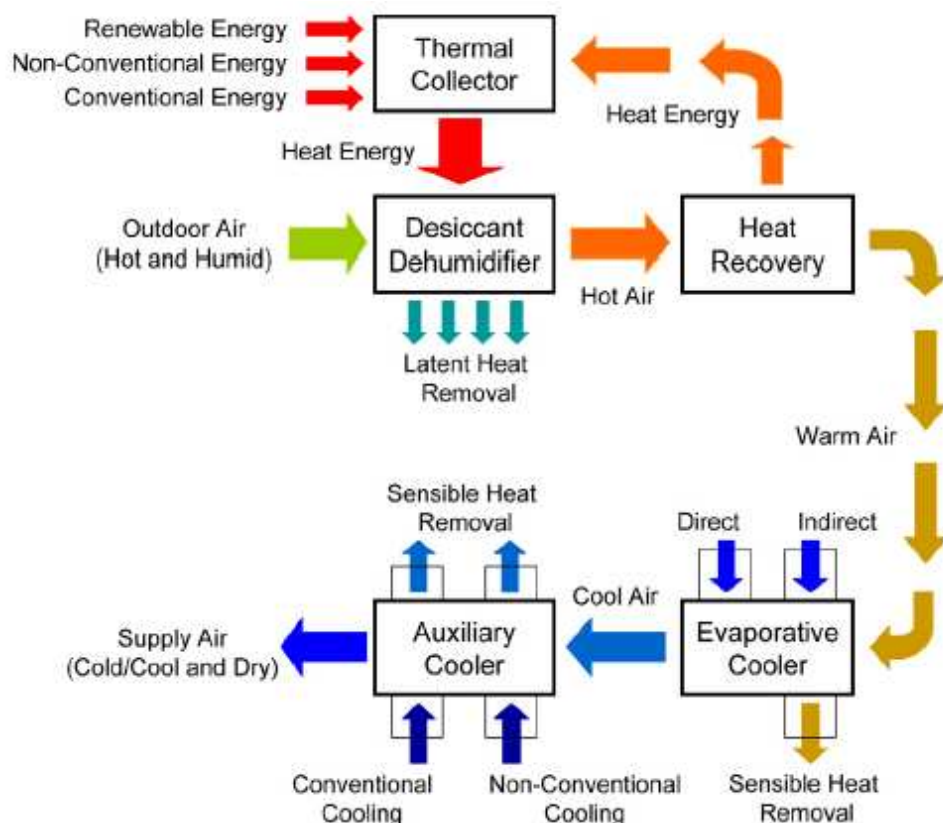


Figure 3.5.2 Schematic of thermally driven desiccant cooling concept (Enteria et al., 2011)

In terms of operational flexibility and ability of absorbing pollutants and bacteria, the liquid desiccants are more attractive than solid desiccants. Moreover, liquid desiccants are usually regenerated at lower temperatures (less than 82°C) and equally create lower airside pressure drops (Gommed and Grossman, 2004). The liquid desiccant cooling system could reach up to 40% of energy saving compared to corresponding conventional vapour compression systems and those savings would be even greater when the thermal energy required for the regeneration is extracted from a renewable source such as solar energy (Mei et al., 2008).

3.5.1 Benefits of Liquid desiccant cooling

Some features of the liquid desiccant conditioners offer extra advantage in air conditioning applications as (ASHRAE Handbook, 2012):

- High moisture removal capacity with low regeneration temperature requirement.
- Liquid desiccant materials are typically very effective antifreeze so the conditioners can continue its operation without frosting or freezing problems. Lithium chloride/water solution, for instance, can cool air to temperature as low as -54°C.
- Liquid desiccant conditioners usually possess high contact efficiency. As a result, air keeps almost the same temperature and humidity ratio from inlet to outlet.
- The cost of energy for regeneration is lower in comparison to air dehumidification by chilling below dew point.
- The latent load is large against the sensible load.
- Higher thermal COP than the solid desiccant systems.

In liquid desiccant systems, regeneration process of the dilute desiccant solution consumes most of the energy. Therefore, thermal energy is required (ASHRAE Handbook, 2012):

- To raise the temperature of the desiccant solution enough to have vapour pressure substantially higher than the ambient air.
- For desorption of moisture content from the airstream.
- To vaporize the moisture content from the dilute desiccant solution to maintain the desiccant solution at the proper concentration.

Also, air fans to move the air for dehumidification and regeneration have their share in total energy consumption. Apart from that, cooling of the dehumidified air is another process that requires energy to sustain the cooling cycle. Therefore, solar thermal/photovoltaic applications can meet the system electric energy requirement (Mittelman et al., 2007).

Solar-driven liquid desiccant evaporative cooling is an innovative method in seeking for environmentally friendly air conditioning system that preserves and improves indoor air quality for inhabitants. Flexibility of these hybrid systems allows operation in different modes suitable for certain climate conditions. Solar assisted liquid desiccant evaporative systems can satisfy higher capacity and better thermal COP ensuring its feasibility and effectiveness. Besides, the main advantage of a hybrid system is the ability of handling air latent and sensible energy contents separately. In such a concept, the performance of the evaporative cooler is substantially improved as it only copes with the air sensible energy content while the liquid desiccant system processes the air latent energy content (Fong et al., 2011). Evaporative cooling, itself, is not an effective method in climates in which the wet bulb

temperature is really high. However, coupling with liquid desiccant cooling can extend their climatic applicability scope. So that its potentials in improving air quality, cost and energy savings as well as environmentally friendly nature attract much interest while depletion of conventional fossil fuel resources and environmental degradation are of global concerns (Wang et al., 2009).

Solar thermal energy is the most widely method for the regeneration of liquid desiccant substances. However, solar thermal (TH) regeneration may not be able to meet the dehumidification demand especially when the air hot and humid. In such a case, a new regeneration method called solar electro dialysis (ED) which requires electrical power from PVs can operate dependably under various climatic conditions. Therefore, solar ED method can be more appropriate solution to regenerate the dilute solution under hot and humid environment. One of the main advantages of solar ED method is that less heat intensity would be introduced to the dehumidification since heat causes harm in dehumidification process and also there would be zero carry-over of desiccant solution droplets with the supply air. Although the solar ED regeneration systems are more energy efficient, the cost of these systems could prevent its wide scale application in the near future (Cheng et al., 2013).

The near future is to be the most decisive for the success and promotion of solar assisted liquid desiccant evaporative cooling systems that rely on the incentives and subsidies introduced by policymakers. Moreover, the efforts undertaken by manufacturer towards low cost systems would be a key factor to public acceptance.

3.6 CONCLUSIONS

In this chapter, the recent works on solar assisted liquid desiccant cooling and its various applications combined with evaporative air-conditioning under different climates are reviewed and advantages the system may offer in terms of energy savings are underscored. Also, a basic description of the principles of hybrid solar liquid desiccant with direct and indirect evaporative cooling is provided. Moreover, solar regeneration methods and recent developments for the liquid desiccant air-conditioning system are presented. The concluding remarks are outlined as follows;

Although the initial cost of solar energy technology can be high like most developing concepts, it can lead to substantial savings in the long run.

As an advantage, evaporative coolers can act as mass exchange equipment in liquid desiccant systems rather than designing and manufacturing particular mass exchange equipment for such systems.

The favourable features of the liquid desiccant systems over the solid desiccant cooling systems can be summarized as low vapour pressure, low viscosity, low regeneration temperature ($<80^{\circ}\text{C}$) due to the higher moisture mass transfer area, low crystallization point, operational flexibility and ability of absorbing pollutants and bacteria, high density and being cost effective. However, carry-over to the supply air is one of the main concerns of the liquid desiccant cooling systems. Besides, liquid desiccant substances are usually corrosive and simple handling of the working media is a burden.

Today, packed bed is the most prevalent technology for a liquid desiccant cooling system. However, in order to avoid internal cooling, packed beds must operate with high desiccant flow rates to dehumidify effectively without any internal cooling.

Internally cooled dehumidifiers can substantially advance the performance in comparison to adiabatic dehumidifiers. Also, effect of pre-dehumidification on the performance is notable in highly humid regions. Furthermore, internally heated regenerators usually achieve a better performance in terms of higher regeneration rate and higher energy utilization as compared to conventional packed regenerators.

Total energy savings rate of the liquid desiccant enhanced evaporative cooling systems is ranged from 25 to 50% in comparison to the vapour compression system. In terms of energy consumption, evaporative coolers use less than a quarter of the electric power than conventional vapour compression systems.


The main advantage of a hybrid system is the ability of handling air latent and sensible energy contents separately. As a working principle, a direct evaporative cooling system adds moisture to the process air while an indirect evaporative cooling system provides only sensible cooling to the supply air without adding any moisture. So this feature makes indirect systems more attractive than direct evaporative cooling systems. All, hybrid solar assisted liquid desiccant indirect evaporative system comes forward as a best option among the similar systems. Chapter 6 investigates the performance of a solar assisted hybrid liquid desiccant indirect evaporative cooling system to address the regeneration process with a unique solar heat extraction component.

Although solar regenerators are successful in producing intended outcomes, the corrosion problem related with the liquid desiccant solution on the energy absorbing surface cannot be disregarded. Apart from the thermal regeneration technique, a new regeneration method for the liquid desiccant cooling system namely photovoltaic electro dialysis (PV-ED) regeneration method has become a new area for researcher.

Although the solar ED regeneration systems are more energy efficient, the cost of these systems could prevent its wide scale application in the near future.

The research on desiccant materials regenerating under lower temperatures would augment extend of the contribution that desiccant cooling can potentially bring towards amelioration of indoor air quality and comfort, energy and cost savings. Moreover, zero water carry-over evaporative coolers using various membranes are required for further investigation to improve the overall performance of indirect evaporative cooling technology. Also, search for the integration and control of different energy conversion systems for various climates and purposes may create synergic efficiency enhancement.

The next chapter reviews the past and present work conducted on the SAHP systems for low temperature water heating applications. Specifically, the key performance data from a number of studies are highlighted and various configurations are compared in order to gain accurate and deep intuitive understandings of SAHP systems.



CHAPTER 4 – Solar assisted heat pump systems for low temperature water heating applications

4 SOLAR ASSISTED HEAT PUMP SYSTEMS FOR LOW TEMPERATURE WATER HEATING APPLICATIONS: A SYSTEMATIC REVIEW

4.1 INTRODUCTION

A solar-assisted heat pump system (SAHP) is a particular technique to reduce or eliminate the primary energy (coal, natural gas, etc.) consumption through substitution of renewable based energy sources to achieve reduced CO₂ emission. The system is able to convert and transport thermal energy from the sun to water or working medium or absorbers. In addition, this system allows transferring heat for storage purposes. Through modification in the system configuration, reduction in the number of system units and cost, and enhancement in efficiencies would be achievable. There has been a growing interest for such hybrid systems with a variety of system configurations for various climate conditions. A number of research studies have been presented in the literature on fundamentals of system design, modelling and optimization of performance characteristics, as well as experimental investigations of pilot scale designs (Omojaro, 2013). The main objective of this study is to present a systematic review of the research and developments on solar assisted heat pump systems. This study is arranged into three main parts:

- Solar assisted heat pumps and low temperature heating applications
- Design components and configurations
- Thermal performance characteristics of SAHP

4.1.1 Classification method

There are different types of system classifications designed in various categories. Solar assisted heat pump systems can be classified by the type of applied components like collector types, flat plate, glazed-unglazed etc. or alternatively type

of refrigerant used in the heat pump cycle. However, the efficiency of such systems immensely depends on environmental conditions, system and component size and load characteristics. Therefore, there wouldn't be any simple classification method to conform the public to an easy communication. Yet, these various specifications, in literature, to compare the SAHP systems are systematically shown by Frank et al. (2010). A comprehensive table that displays research, design and development work and an overview of design approach such as refrigerant type, with or without storage, the location of the storage, can indicate particular know-how about solar heat pump applications. Hence, a methodical display in Table 4.1 was presented from literature including system information and boundary conditions regarding climate.

Table 4.1 System classification table – a sample of the literature study to provide information about system concepts

	Şevik, Seyfi, et al. 2013	Fernández-Seara et al. 2012	Hawliader et al. 2008	Badescu et al. 2003	Cerit et al. 2013	Huang, B. J. et al. 2010	Li et al. 2010	Chow, Tin Tai, et al. 2012	Chen et al. 2012	Panaras et al. 2014	Zhang, Xingxing, et al. 2014	Ji, Jie, et al. 2008
SYSTEM INFORMATION												
1.Solar collector type												
Direct evaporation (uncovered)		X	X									
Flat plate (uncovered)									X			
Flat plate (covered)	X						X	X		X		X
Evacuated tube						X					X	
Solar air collector			X	X								
Roll-bond					X							
2.Solar heat sink												
Domestic hot water	X							X				
Space heating	X	X	X	X	X			X	X		X	X
Heat pump evaporator		X	X	X	X						X	X
Boreholes									X			
Storage (cold side of HP)				X		X	X	X		X		
3.Heat sources for heat pump												
Solar collector (direct evaporation)		X	X	X	X			X				X
Solar collector (heat exchanger)	X					X	X	X	X		X	
Air			X	X						X		
4.Refrigerant (ns-not specified)												
	ns	R134a	R134a	R114	R134a	R22	R22	R22	ns	ns	ns	ns
5.Heat pump sink												
Domestic hot water		X			X		X	X		X	X	X
Space heating	X		X	X		X			X			
6.Storage concept (cold side HP)												
None		X	X		X							
Water	X					X	X	X	X	X	X	X
Seasonal storage				X								
7.Storage concept (load)												
None	X		X			X						
Water		X		X	X		X	X	X	X	X	X
8.Additional heating (backup)												
Electricity (direct)	X	X	X	X	X	X	X	X	X	X	X	X
BOUNDARY CONDITIONS												
9.Climate - Country												
	TR	SP	SIN	US	TR	TWN	CN	HK	HK	GR	UK	CN
10.Application												
Temperature, °C	45	55	40	22	ns	80	36	33	ns	55	45	30
Domestic hot water		X			X		X	X	X	X	X	X
Space heating-water									X			
Space heating-air	X		X	X		X						

4.1.1.1 Systematic visualization scheme of solar assisted heat pump concepts

System classification for various solar assisted heat pump concepts is performed by considering distinctive system configuration features like collector type, heat sink of the system, storage concept etc. Table 4.1 presented in previous section provides a piece of information for a plain classification method. In the energy flow like visualization scheme, only solar assisted heat pump system is illustrated rather than a whole building. As a result of analysing many combined solar and heat pump systems, it is found that solar assisted heat pumps systems comprise five recurring components namely solar collector, heat pump and backup heater, along with storages either cold or load or both side of the heat pump units. Fixed positions for all these components are defined although specifications, like type of the collector, may vary in different configurations.

Assorted colours used in the visualization scheme distinguish the energy flow in the system as final (grey), boundaries (grey background), environmental energy (green), useful energy (red), energy converters (orange) and storages (blue). Yet colouring is an additional feature as it is not essential to comprehend the concept. The final energy (to be purchased such as electricity) is shown at the system boundary on the left-hand side where useful energy (i.e. domestic hot water-DHW) flow is introduced on the right. Environmental energy sources enter the system from the top while any losses would be downwards although no losses leaving the system depicted as being redundant to system characterisation. Lastly, the connection of system components is illustrated to analyse and compare the concepts. Each line style aims at the carrier medium, excluding driving energies mostly without mass i.e. solar radiation.

One should remark that all potential operating modes of one combined solar and heat pump system is presented simultaneously by one flow chart visualization. All components in a solar heat pump concept are depicted as filled; others remain shaded as placeholders for orientation and comparison purposes.

A simple example of a visualization scheme is provided in Figure 4.1 to comprehend the classification method. In Figure 4.2-4.4, widely available combined solar and heat pump configurations are presented through the visualization scheme proposed. The figures offer the possibility to make a comparison among the solar assisted heat pump systems. Additionally, energy flows usually from left-to-right and up-down directions in the arrangement of the visualization scheme, despite a range of combinations may be exceptional.

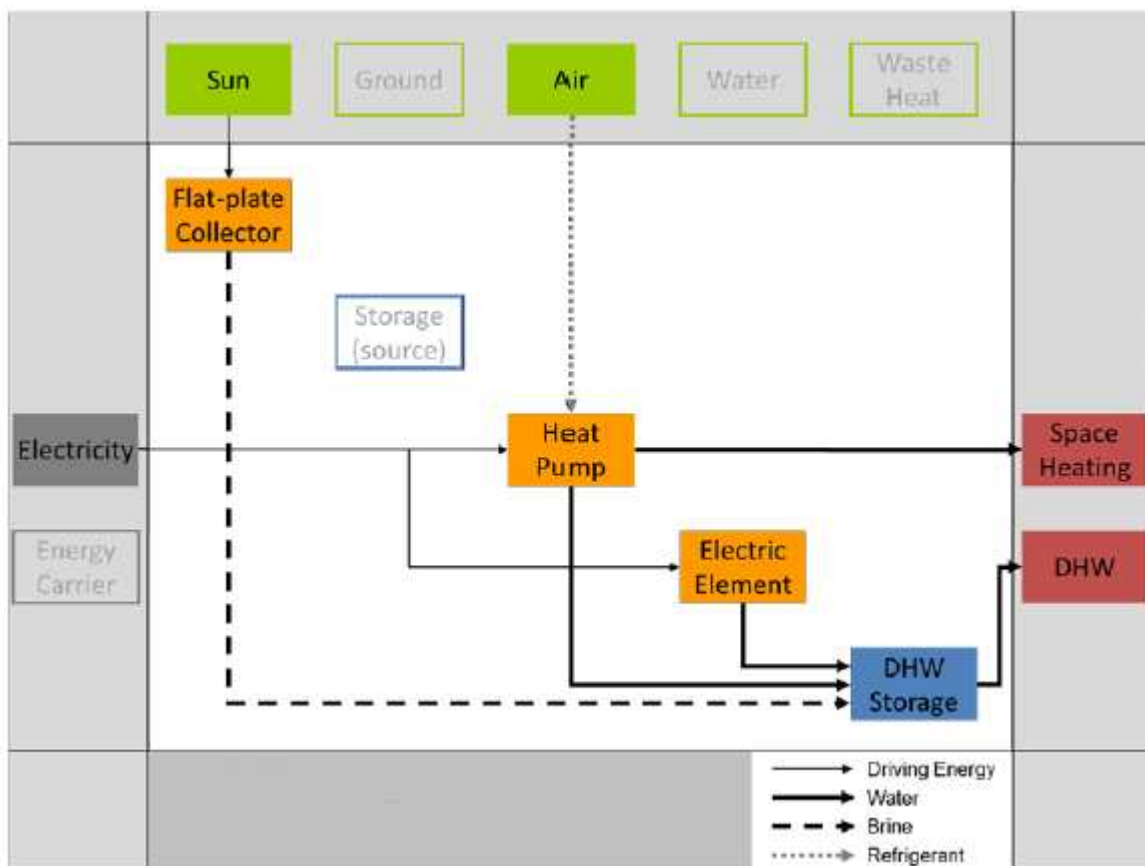


Figure 4.1.1 Introductory sample of the visualization scheme (Ruschenburg et al., 2013)

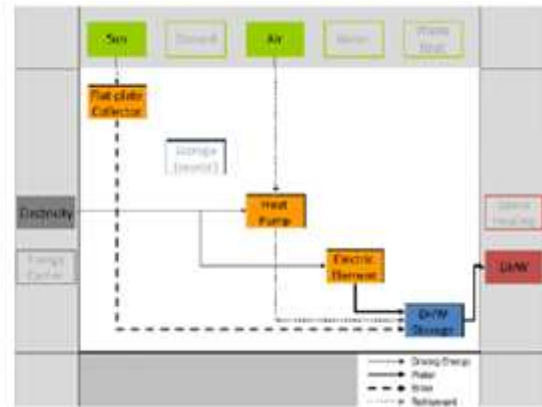
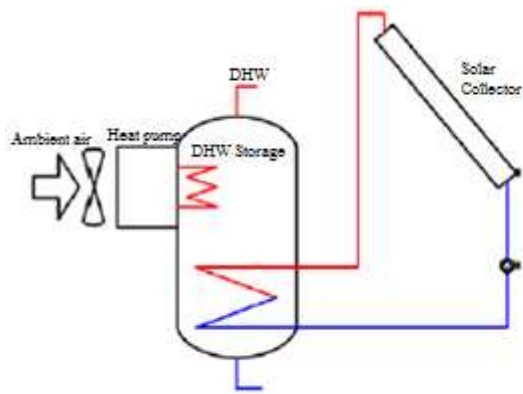


Figure 4.1.2 Solar heat pump system with a flat-plate collector and a direct-evaporation air source heat pump unit along with the condenser immersed in a DHW storage. This system is exclusively designed for DHW applications (Ruschenburg et al., 2013).

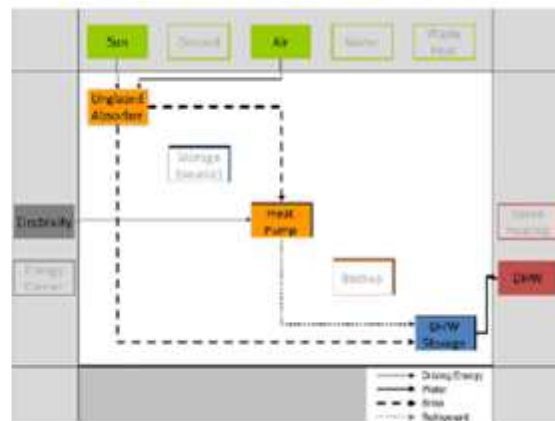
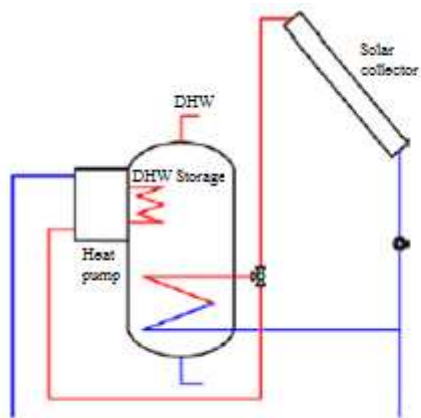


Figure 4.1.3 Solar heat pump system with an unglazed collector and a heat pump unit along with the condenser immersed in a DHW storage. This system is exclusively designed for DHW applications (Ruschenburg et al., 2013).

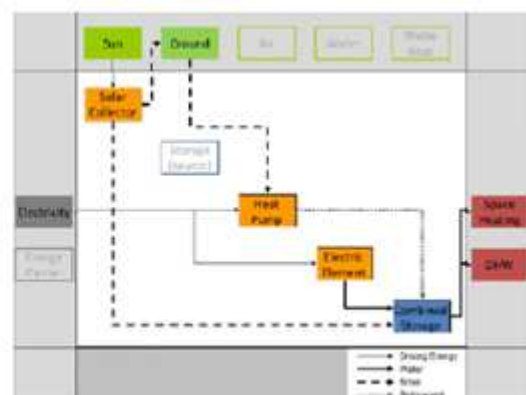
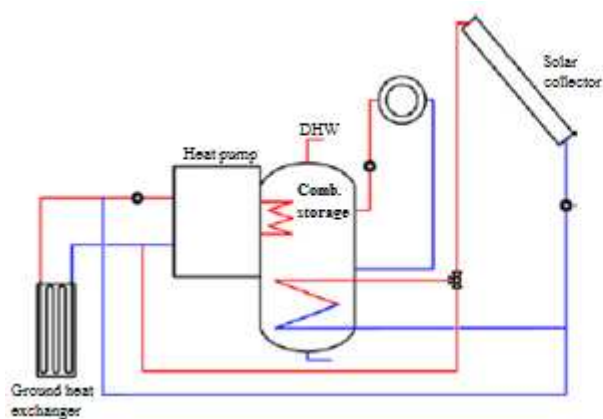


Figure 4.1.4 Solar heat pump system with an unspecified collector and a heat pump unit along with the condenser immersed in a combined storage tank. This system is designed for DHW preparation as well as space heating applications (Ruschenburg et al., 2013).

4.2 SOLAR ASSISTED HEAT PUMP SYSTEMS

The basic principle of solar thermal energy systems is to collect solar energy in the form of heat. A solar collector comprises pipes running behind an absorber and transferring a working fluid. The working fluid absorbs the energy in heat form and carries to thermal energy storage or to a heating/cooling system (Chu et al., 2013) as a schematic of indirect (via heat exchanger) solar DHW system can be found in Figure 4.5. So, the solar energy system captures heat during the periods when solar energy is available. Else, a heat pump is a device that transports heat from a source to other by running a refrigeration cycle. An important thermodynamic fact is that heat flows from warmer to cooler however; a HP reverses the flow direction and pumps the heat to move. A refrigerant, also known as working fluid, in a heat pump cycle is compressed to liquid state then expanded to a vapor state to absorb and remove heat (Hepbasli and Kalinci, 2009). Combined solar thermal energy technologies and heat pump into a SAHP system is a promising application offering great potentials to offset low temperature ($< 80^{\circ}\text{C}$) applications like DHW, space heating etc. A benefit to combine solar thermal and heat pump systems together is to improve the performance of the subsystems, eventually result in enhancing performance of the SAHP system as a whole.

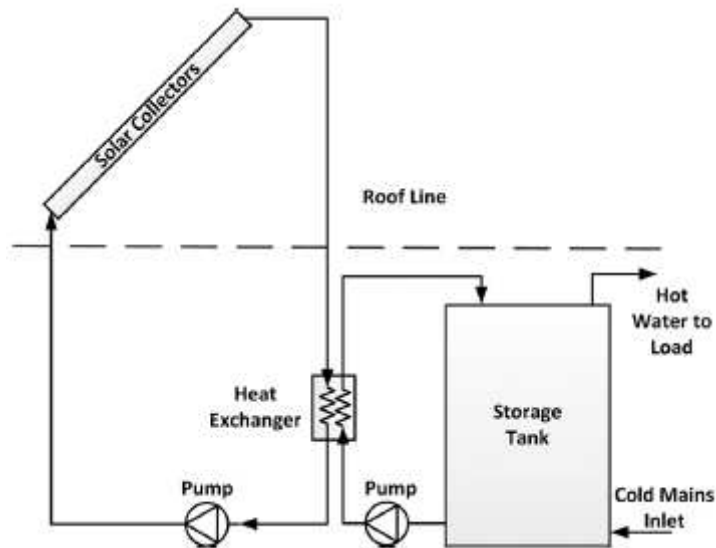


Figure 4.2.1 Indirect solar DWH system (Chu et al., 2013)

The system configurations are characterized by the method the solar thermal and heat pump components interact by Freeman et al. (1979). The solar thermal collector and heat pump units can independently supply useful energy through charging one or more heat storages. This configuration is mostly stated as 'parallel' and in these systems; the collectors would feed the storage and if the energy level is insufficient then an auxiliary heat source such as an air-source heat pump or ground heat exchanger would run in parallel to the collectors to attain the required amount of energy. A schematic of a parallel system is presented in Figure 4.6. The solar thermal collector can act as a heat source of the heat pump unit, either primary or supplementary, and either directly or via buffer storage. This concept is denoted as 'serial'. When coupled in series, the captured heat energy is fed into the evaporator of the heat pump by working fluid. Then, the evaporator receives this energy from the working fluid and temperature of the working fluid is reduced as a result of this cycle. Systems in series could be installed in a direct or indirect configuration. As shown in Figure 4.7, the collector serves as the evaporator in a direct series configuration and this concept is also called direct expansion. The heat transfer

fluids flowing through the collectors would be, also, refrigerant of the heat pump units. In an indirect series concept, a liquid-to-liquid heat pump can be assembled as a closed unit and the heat energy from the solar collectors is conveyed to the refrigerant loop of the heat pump through the evaporator heat exchanger. Figure 4.8 presents a schematic diagram of the indirect series concept.

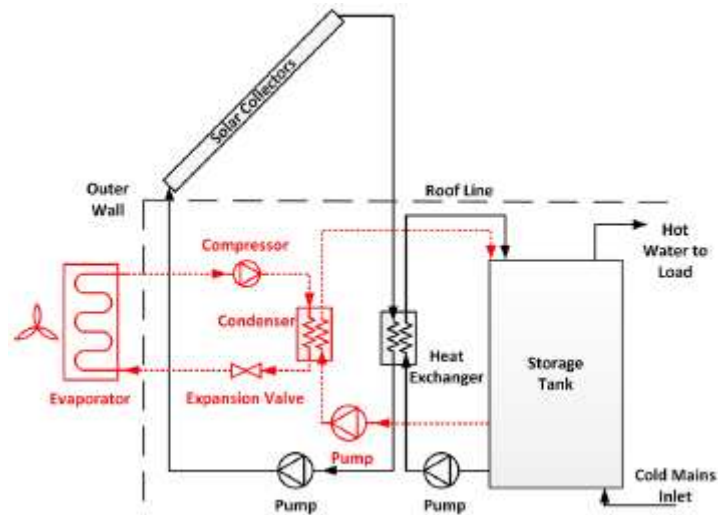


Figure 4.2.2 Parallel type SAHP (Chu et al., 2013)

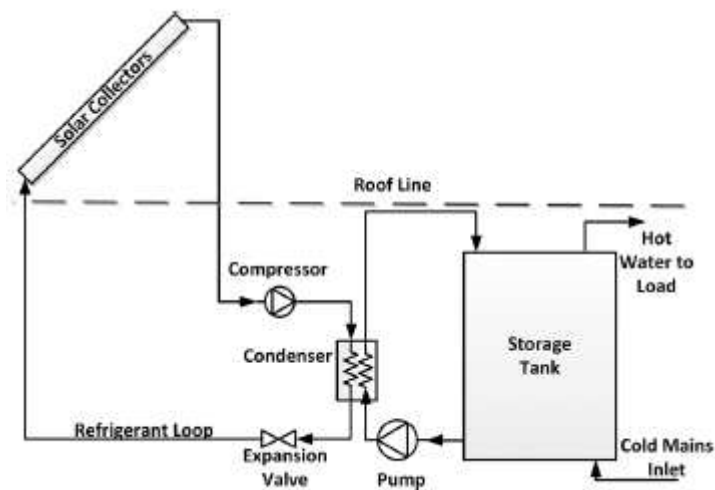


Figure 4.2.3 Direct series type SAHP (Chu et al., 2013)

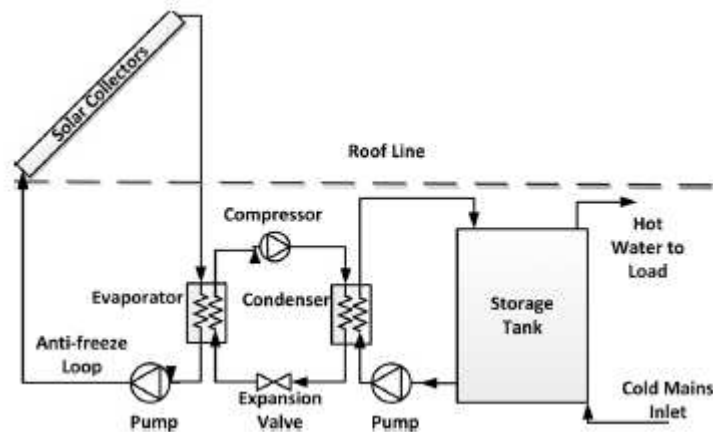


Figure 4.2.4 Indirect series type SAHP (Chu et al., 2013)

4.2.1 Literature review for SAHP

Ever since Sporn et al. (1955) and Jordan et al. (1954) enlightened the SAHP concept, a number of experimental studies have been conducted and published in the literature such as Morgan (1982), Chaturvedi and Mei (1979), MacArthur et al. (1978) and some others have contributed to the development of this technology as well. Since 1970s SAHP systems have experienced considerable developments, as a reaction to the global energy concerns like energy crisis and greenhouse effect. One of the early studies on SAHP systems was carried out by Lior (1977) and the focus of this study was mainly on the reduction of resource energy consumption of vapour compression heat pump by utilizing solar energy. Also, Krakow and Lin (1983) developed a computer model for system simulation of heat pump performance.

4.2.1.1 IEA: SHC Programme Task 44

The objective of International Energy Agency (IEA)'s Solar Heating and Cooling (SHC) programme Task 44 was to optimize combined solar and heat pump systems for single dwelling applications and to provide a common definition for the performance of such systems (Hadorn, 2012). This project was performed along with

the IEA Heat Pump programme denoted as Annex 38. The task mainly focused on small-scale heating and domestic hot water systems, electrically driven heat pumps etc. Task 44 also involved the assessment of solar and heat pump systems under Subtask B that aims to set common definition of performance metrics and assessment criteria as well (D'Antoni and Sparber, 2011).

4.2.1.2 Comparative studies of SAHP Systems

A comparative study investigates the performance characteristics of more than one SAHP system along with various components and configurations. The comparison is carried out considering experimental or simulation results in order to elicit which concept has better performance than another system. Table 4.2 presents an overview of the system configurations and performances from the reviewed literature. A comparative study of SAHP systems for space heating was performed by Kaygusuz et al. (1999). Each of the three configurations was examined theoretically by using the BASIC computer program and performance of the systems was compared. In the first configuration, solar assisted series heat pump system comprising conventional flat-plate water-cooled solar collectors, a heat pump unit with water-to-refrigerant heat exchanger with a phase change material (PCM) filled energy storage tank was used for space heating. In this system, the hot water from the collectors was first fed into the storage, and then was utilized in the heat pump as a heat source. The PCM storage acts as a heat source at night and cloudy days when the solar energy scarcity occurs. A schematic of the series type configuration is shown in Figure 4.9. In the parallel configuration, flat-plate water-cooled solar collectors, water-to-air heat exchanger, an air cooled condenser, and a latent heat energy storage tank were the system components for space heating. This solar assisted parallel heat pump system combined a conventional solar heating system

with a conventional air-to-air heat pump unit. In this system, ambient air was the heat source for the heat pump where solar energy was the heat source of the water-to-air heat exchanger and each contributes to the heating load of the building individually. A schematic of this system is presented in Figure 4.10. Dual source system is the combination of the series and parallel configurations and has two evaporators allowing the heat pump to source energy either from storage tank or ambient air as shown in Figure 4.11. These systems run the same way as the series system unless the storage temperature was above minimum temperature/ambient temperature, otherwise the heat pump would withdraw energy from ambient air. The overall findings of this study show that the dual source heat pump system capitalizes the ideal characteristics of the series and parallel systems and reflect it on the performance for the region where this study was conducted. Also, Free energy ratio (FER) is slightly higher than the series and parallel systems.

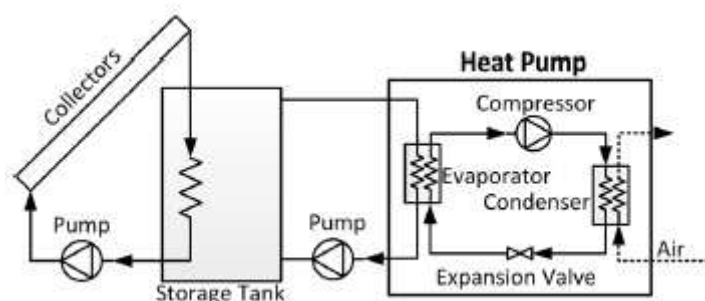


Figure 4.2.5 Series type SAHP space-heating concept (Chu et al., 2013)

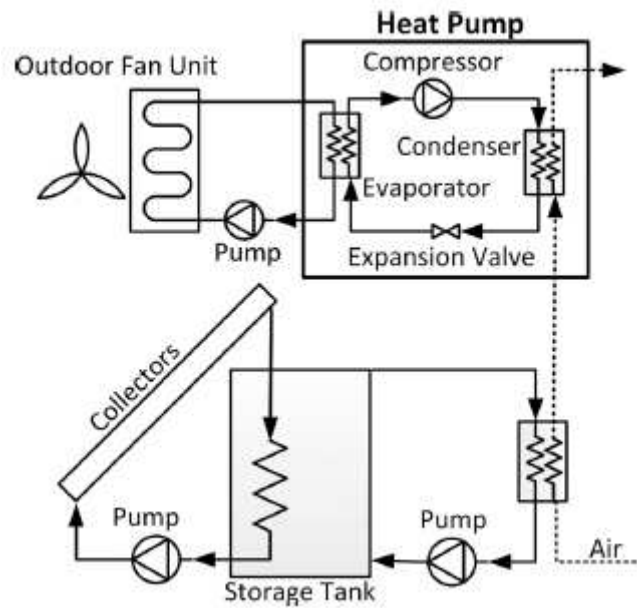


Figure 4.2.6 Parallel type SAHP space-heating concept (Chu et al., 2013)

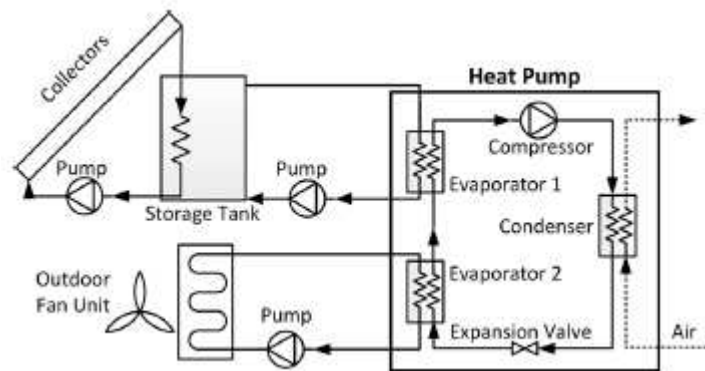


Figure 4.2.7 Dual-source SAHP space-heating concept (Chu et al., 2013)

Bertram et al. (2012) conducted a TRNSYS simulation study as part of IEA, SHC programme Task 44, to compare the performance of the three system configurations including the components of flat plate collector, borehole heat exchangers and a heat pump unit. In the system, the borehole heat exchanger was connected to act as the evaporator of the heat pump and that heat pump made the energy available to DHW and to the underfloor heating system. In the first configuration, the solar collectors charged the boreholes that introduce the energy to the heat pump. In the second configuration, the collectors were connected parallel to the heat pump to load

the DHW storage directly although the heat pump still received energy from the boreholes. In the third configuration, a dual concept which is the combination of first two systems was applied. The boreholes were charged by the collectors when the load from the collectors was not sufficient enough to charge the DHW storage. According to the results, performance of the dual configuration was not any higher than the option two due to the inadequate amount of solar energy conveyed to the hot water tank. Overall findings remark that the system performance was enhanced when solar energy loaded the storage directly rather than charging the borehole heat exchangers (Bertram et al., 2012). In another study, conducted as part of IEA, SHC programme Task 44, Haller et al. (2011) introduced a mathematical relation model by using TRNSYS in order to determine if combined solar collector-evaporator of a dual (solar-air) source heat pump configuration was more advantageous than utilizing solar heat directly. The examined dual configuration in this study can switch its operation between serial and parallel mode. It was shown that indirect utilization of solar heat is more beneficial in terms of system performance factor when the solar radiation is under certain level which depends on solar collector and heat pump characteristics. According to simulation results, using uncovered solar collectors was more advantageous in series mode and also increasing the runtime of the collectors could enhance performance of the series configuration (Haller et al., 2011).

Chandrashekar et al. (1982) conducted a comparative study by using WATSON software in order to analyse six different configurations of SAHP systems including liquid and air based systems for DHW and space heating applications in seven different cities of Canada. The simulations were conducted for the six systems under prevailing climatic conditions of Vancouver and Winnipeg and the results point out that liquid-based systems showed better performance than air-based systems and

became prominent as the best configuration with regards to unit cost of energy for a single family house in Winnipeg. However, the parallel system had come forward with the best performance in terms of energy savings in Vancouver. It was also discovered that the system performances were insensitive to the location where experimental studies took place (Chandrashekar et al., 1982).

Table 4.2 Overview of comparative studies

Authors	SAHP	Yield
Freeman et al. (1979)	<p>Configuration: parallel, series and dual source (liquid based)</p> <p>Collector specifications: flat plate</p> <p>Storage: liquid tank</p> <p>HP sink: DHW and space-heating for floor area of 120 m²</p> <p>Climate region: Madison-Wisconsin-Albuquerque, NM</p>	<p>FER: 0.38-0.8 (collector area of 0-60 m²) in Madison</p> <p>0.38-0.95 (collector area of 0-60 m²) in Albuquerque</p> <p>COP of HP: parallel:2.0, dual source:2.53, series:2.84 in average</p> <p>Solar collector efficiency: Series:50%, dual source:50%, parallel:30% in January (collector area of 10 m²) Series:45%, dual source:45%, parallel:35% in whole year (collector area of 10 m²)</p>
Kaygusuz et al. (1999)	<p>Configuration: parallel, series and dual source (liquid based)</p> <p>HP: hermetic type, 1490 W electrical motor driven</p> <p>Collector specifications: glazed flat plate, 18x1.62 m²</p> <p>Storage: PCM tank</p> <p>HP sink: space-heating for floor area of 75 m²</p> <p>Climate region: Trabzon, Turkey</p>	<p>FER: Series:0.6, parallel:0.75, dual source:0.8</p> <p>SPF: Series:3.3, parallel:3.37, dual source:4.2</p> <p>COP of HP: Series:4.0, parallel:3.0, dual source:3.5</p> <p>Solar collector efficiency: series:0.56-0.64, parallel:0.48-0.54 (average monthly range)</p>
Bertram et al. (2012)	<p>Configuration: three different system</p> <p>Components: flat plate collectors, borehole heat exchangers and a heat pump unit HP: 7.9 kW size</p> <p>Storage: 300 L with solar, 150 L w/o solar</p> <p>HP sink: DHW and space-heating for floor area of 140 m²</p> <p>Climate region: Strasbourg, France</p>	<p>SPF1: 3.85 (collector area of 15 m²)</p> <p>SPF2: 4.95 (collector area of 5 m²)</p> <p>5.21 (collector area of 10 m²)</p> <p>SF: 65% for DWH (collector area of 5 m²) (SF: Solar Fraction)</p>
Haller et al. (2011)	<p>Configuration: parallel, series and dual source</p> <p>HP: 16 kW</p>	<p>This study explores when to change utilizing solar energy in a parallel configuration to</p>

	<p>Collector specifications: covered- uncovered flat plate, 16 m²</p> <p>Storage: 1000 L</p> <p>HP sink: DHW and space-heating, IEA-SHC Task 32 reference system SFH 100 building</p> <p>Climate region: Zurich - Madrid</p>	<p>indirect utilization in a heat pump. The results show that indirect utilization is advantageous when COP rise by 1 while collector efficiency boost 150% in comparison to parallel configuration.</p>
<p>Chandrashekar et al. (1982)</p>	<p>Configuration: liquid based: parallel, series, dual-source, dual storage, air-based: parallel and dual source</p> <p>Collector specifications: flat plate</p> <p>HP sink: DHW and space-heating for floor area of 124 m² of single family house & 10 story multiplex with 100 m² per unit</p> <p>Climate region: Vancouver, Edmonton, Winnipeg, Toronto, Ottawa, Montreal, Fredericton</p>	<p>In this study, the main method in assessing the performance of the systems was the Life Cycle unit cost of energy (LUC) in \$/GJ. It is the ratio of the total cost over the total energy demand throughout the life cycle of the system.</p>

4.2.1.3 Direct Series Systems

Chaturvedi et al. (1998) developed and operated a direct series SAHP containing a bare solar collector which acts as the system evaporator. In the study, the coefficient of performance of the proposed system was monitored for various levels of solar insolation and compressor operation frequency. Test results indicated that the COP of the system was enhanced with the decreasing compressor speed as ambient temperature increases from winter to summer.

Chow, Tin Tai, et al. (2010) developed a mathematical model of a unitary type direct series SAHP water heating system and performed its application in subtropical Hong Kong. The water tank was the condenser of the system. Based on the dynamic simulation model, the system was found to achieve a year-long average COP of 6.46, considerably higher than its conventional counterpart. The system performed better in summer as the instantaneous COP could reach up to 10. Hawlader et al. (2001) experimentally investigated a direct series SAHP water heating system. In the configuration, the tank was installed as the condenser of the system like studied by Chow, Tin Tai, et al. (2010) and the refrigerant of the heat pump circulated through

the coil of the heat storage tank. Also, a mathematical model was introduced in order to analyse the influence of various parameters. Fernández-Seara, José, et al. (2012) experimentally studied the performance of a direct series SAHP system which also used a storage tank as the condenser like Chow, Tin Tai, et al. (2010) and Hawlader et al. (2001). The collectors were tested in an environment chamber under different temperatures varied from 7°C to 22°C while relative humidity was maintained at 55%. The tank was refilled before each test and tests were held until 55°C of water temperature was attained. The test results indicated that as the ambient temperature rises the COP of the heat pump also increases while the time required for heating decreases.

Kuang et al. (2006) presented an experimental study of a multifunctional direct series SAHP system for cooling, DHW and space heating. The collectors acted as an evaporator and water tank as a condenser in direct expansion (DX) configuration in water heating mode. However, space heating mode had slightly different configuration. The collectors served as the evaporator of the heat pump and heat was directly introduced to the space through a radiant floor. As an auxiliary heat supplier, the proposed system also comprised a forced air heat exchanger as the evaporator to assist the system when solar radiation was insufficient. In the cooling application, the collectors, as a condenser, discharged heat out in at night-time. The performance of this system was explored individually for each application. For water heating, 50°C was attained at around an hour in a typical spring day and about 2 hrs required on overcast days. The system was tested 5 days for space heating in February and 2 days for cooling. The experimental results showed that the cold storage efficiency was found to be poor and cold energy stored during the night-time was insufficient to meet the cooling load.

Another study conducted by Axaopoulos et al. (1998) investigated the performance of a direct series solar assisted heat pump along with a conventional thermosyphon solar system. The proposed SAHP system comprised a refrigerant filled bare solar collector as an evaporator, a heat pump unit, and a submerged heat exchanger in water storage tank as condenser. Under Athenian climate condition, COP of above 3.0 was attained and COPs between 4.0 and 5.0 was expected on a larger scale application. The SAHP system achieved to supply hot water at the desired temperature for 24 h period of the day regardless of climate conditions. Furthermore, it was deduced from the experimental results that the performance of SAHP system was more reliant on ambient temperature and wind speed, rather than on solar radiation. Ito et al. (1999) also used a bare flat-plate collector as the evaporator of a HP system in a theoretical and experimental study. The results presented that 25°C of evaporation temperature was attained when the ambient air temperature was 8°C and the COP was monitored as 5.3. As a result of simulations, it was also found that the effect of collector area on COP of SAHPS was minor for the proposed system. Li, Y. W., et al. (2007) and Moreno-Rodríguez, A., et al. (2012) conducted similar studies and obtained same promising results as well.

Xu, Guoying, et al. (2009) developed and numerically studied a new photovoltaic/thermal heat pump system comprising a modified collector/evaporator component which employs multi-port flat extruded aluminum tubes rather than round copper tubes used in conventional collector/evaporator systems. The results demonstrated that the proposed system achieved a 7 and 6% increase in COP and thermal efficiency, respectively. The results also suggested that the new system could heat 150 L water up 50°C year round under both Nanjing and Hong Kong

climate conditions. Table 4.3 presents an overview of the system components and performances from studies themed direct series SAHP systems.

Table 4.3 Overview of direct series systems

Authors	SAHP system components	Performance
Chaturvedi et al. (1998)	HP: 0.00007036 m ³ /s of volumetric displacement Collector type: unglazed flat plate Collector area: 3.48 m ² Load: DHW Climate: Norfolk, Virginia	COP: ranging from 2.5 to 4.0
Chow, Tin Tai, et al. (2010)	HP: 1 kW Collector area: 12 m ² Collector orientation: 25° Energy storage: 2500L Load: DHW Climate: Hong Kong	COP: Max instantaneous: 10 July avg: 7.5 January avg: 5.47 Annual avg: 6.46
Hawlader et al. (2001)	HP: variable speed compressor Collector type: bare flat plate Collector area: 3 m ² Collector orientation: south 10° Energy storage: 250L Load: DHW Climate: Singapore	SF: 0.2 – 0.75 COP: 4.0 – 9.0
Fernández-Seara, José, et al. (2012)	HP: rotary-type hermetic compressor Collector type: bare Collector area: 1.6 m ² Energy storage: 300L Load: DHW	SPF: 2.11 at temperature of 7.8°C, 3.01 at temperature of 21.9°C COP: 2.44 at temperature of 7.8°C, 3.30 at temperature of 21.9°C
Kuang et al. (2006)	HP: rotary type hermetic compressor x3 Collector type: bare flat plate Collector area: 10.5 m ² Collector orientation: south on tilted roof Energy storage: 200L for DHW and 100L for heat storage Load: space-heating, cooling, and DHW Climate: Shanghai, China	SPF: 2.1 – 3.5 for water heating, 2.1 – 2.7 for space heating COP: 2.6 – 3.3 for space heating, 2.9 for cooling during night-time
Axaopoulos et al. (1998)	HP: 350 W hermetic Collector type: bare Collector area: 3x1.4 m ² Collector orientation: south with some inclination Energy storage: 158L for water storage Load: DHW	COP: above 3.0 4.0 – 5.0 expected on a larger scale

Ito et al. (1999)	Climate: Athens HP: 350 W Collector type: bare flat plate Collector area: 3.24 m ² Collector orientation: south 50° Load: DHW	COP: 5.3 at outside temperature of 8°C
Li, Y. W., et al. (2007)	HP: rotary type hermetic compressor 750W Collector type: unglazed flat plate Collector area: 4.20 m ² Collector orientation: south 31.22° Energy storage: 150L for DHW Load: DHW	COP: average of 5.21
Moreno-Rodríguez, A., et al. (2012)	HP: 1.1 kW with R-134a Collector type: bare Collector area: 5.6 m ² Collector orientation: south with some inclination Energy storage: 300L for DHW Load: DHW Climate: Madrid, Spain	COP: min 1.7 at evaporation temperature of -8°C and max 2.9 at evaporation temperature of 18°C
Xu, Guoying, et al. (2009)	HP: with variable speed compressor Collector type: flat plate PV Collector area: 2.25 m ² Collector orientation: Energy storage: 150L Load: DHW, space heating Climate: Nanjing & Hong Kong, China	COP: Annual avg: 4.9 for Nanjing Annual avg: 5.1 for Hong Kong 7% rise in COP 6% rise in thermal efficiency

4.2.1.4 Indirect Series Systems

Wang et al. (2011) developed and experimentally tested a novel indirect series multifunctional system for water heating, space heating and cooling. A dual source system was designed for the space heating mode. There are two evaporators employed, one of which draws energy from the ambient air while other from a storage tank. The storage tank was charged by collectors and the heat pump unit obtained energy from the air. The same storage tank provided energy for space heating and DHW. A liquid-to-air evaporator heat exchanger was employed to cool the indoor air for space cooling mode. In this mode, the heat was transferred to the

storage tank through a condenser heat exchanger as part of the heat pump operation. An electric heater was assembled to simulate solar input for the in-laboratory experimental setup. In the space heating mode, the compressor commenced to run as soon as the water temperature in tank reached 35°C. The experimental results indicated that the efficiency could be enhanced during winter time in a region where the solar radiation was abundant. Bridgeman and Harrison (2008) also experimentally investigated the performance of an indirect series SAHP system in a laboratory environment for DHW. In the experimental setup, the solar heat input was simulated by an electrically heated circulation loop which supplies temperature-controlled fluid to the heat pump evaporator. Tests were performed at various evaporator supply temperatures, ranging from 10 to 30°C. The test results showed that COP values varying between 2.8 and 3.3 depending on the evaporator and condenser temperatures.

Alkhamis and Sherif (1997) conducted a feasibility study of an indirect solar assisted heating/cooling system for an aquatic centre for hot and humid climates. The heating was achieved by hot water obtained via heat exchange with the solar collector working fluid. Two thermal storage tanks were employed for DHW. In another study similar to Alkhamis et al. (1997), the feasibility study of an indirect SAHP system for DHW was modelled in TRNSYS software and compared to conventional and electrical DHW systems by Sterling and Collins (2012). The indirect SAHP, conventional and electrical direct water heating systems were both modelled under the prevailing climatic conditions of Ottawa, Ontario. According to the simulation results, the dual tank indirect SAHP system proved to be the most energy efficient among others. It was also emphasised that the weather, depending on the

geographical location, would have an ultimate impact on the performance and size of the system.

Loose et al. (2011) performed field tests of various combined SAHP systems with different heat sources and presented results, as part of IEA, SHC Programme Task 44. The system employed collectors and geothermal heat pump with borehole heat exchangers to provide DHW and space-heating to a new structure with radiant floor heating system. The collectors fed the storage directly when the sufficient solar radiation was available. Otherwise, low grade energy from the collectors would be used in the heat pump for space heating. In case of reaching energy storage capacity in the tank and the heat pump operation was inactivated; the collectors would feed the borehole heat exchanger. So, the heat pump would draw the stored energy from the boreholes after summer time. This configuration was monitored for three years and the promising results were obtained. The solar regeneration of ground boreholes ensured that the HP system could run with a high rate of seasonal performance factor (SPF) in a long term.

Bakirci and Yuksel (2011) investigated the performance characteristics of an indirect SAHP system for space heating. The collectors directly charged a storage tank which was linked to an evaporator to provide a heat source for the heat pump. The ultimate heat was introduced to the space through a radiator. Zhang et al. (2014) developed and test a novel solar photovoltaic/loop-heat-pipe HP system for space heating or DHW. The solar heat was exchanged through a flat-plate heat exchanger acting as the condenser of the heat pipe loop and the evaporator of the heat pump cycle. The average values of COP for both thermal and PV/T were found to be 5.51 and 8.71 under the prevailing climatic conditions of Shanghai, China. The result proved that proposed system has a potential of achieving enhanced solar thermal

efficiencies around 1.5 – 4 times more than conventional counterparts. In another study, Shilin et al. (2010) proposed and experimentally studied an indirect-expansion SAHP radiant floor space heating system in Beijing, China. The configuration of the system varied as solar alone, solar with water-source heat pump and water source heat pump alone depending on the solar collector’s outlet temperature.

Bai et al. (2012) theoretically analysed an indirect combined hybrid PV/T SAHP system for DHW. The system was modelled with TRNSYS computation environment and year round performance results were simulated under the subtropical climatic conditions of Hong Kong and multiple climates in France. The results proved that COP of 4.1 under the subtropical climate of Hong Kong was attained and also, 67% of high fractional energy saving ratio was accomplished in comparison with a conventional heating system. Table 4.4 presents an overview of the system components and performances from studies themed indirect series SAHP systems.

Table 4.4 Overview of indirect series systems

Authors	SAHP system components	Performance
Wang et al. (2011)	HP: hermetic rotary compressor with the displacement volume of 22.5 m ³ Energy storage: 150L Load: DHW, space heating, and cooling	COP: 4.0 for heating
Bridgeman and Harrison (2008)	HP: 617W Collector type: 3500W electric heater for solar heat input, unglazed solar collectors for simulation Collector orientation: south, 10-80° for simulation Energy storage: 270L for experiment Load: DHW Climate: Toronto, Vancouver, Montreal, Halifax and Winnipeg	COP: 2.8 – 3.3 depending on the evaporator and condenser temperatures
Alkhamis and Sherif (1997)	Collector area: 600-1200m ² (simulation) Energy storage: 11.36m ³ Load: DHW (pool area of 1172m ²) Climate: Miami, Florida	SD (solar displacement): 25%
Sterling and Collins (2012)	HP: Type668 (simulation) Collector type: flat plate Collector area: 4m ²	COP: 2.5 – 5.0

Loose et al. (2011)	Collector orientation: south, 45° Load: DHW Climate: Ottawa, Ontario, Canada HP: 5 kW integrated with 75m borehole heat exchanger Collector area: 11m ² Energy storage: 750L Load: DHW and space heating (140m ² of floor area) Climate: Herford, Germany	SPF: More than 5
Bakirci and Yuksel (2011)	HP: compressor driven by 1491W motor Collector area: 12x1.64 m ² Collector orientation: south, 50° Energy storage: 2000L Load: space heating (175m ² of floor area) Climate: Erzurum, Turkey	SPF: 2.5 - 2.9 COP: 3.3 – 3.8
Zhang et al. (2014)	HP: 0.75 kW Collector type: PV/loop heat pipe Collector area: 0.612m ² Collector orientation: 30° Energy storage: 35L Load: space heating or DHW Climate: Shanghai, China	COP: Thermal: 5.51 PV/T: 8.71 (1.5-4 times more than conventional ones)
Shilin and Fei (2010)	HP: 3 kW electrical heater Collector type: heat pipe vacuum tube Collector area: 17.5m ² Energy storage: 1000L Load: space heating (50m ² of floor area) Climate: Beijing, China	COP: ns
Bai et al. (2012)	HP: 14.61 kW Collector type: PV/T Collector area: 600m ² Collector orientation: south, 23° Energy storage: 60m ³ Load: DHW Climate: Hong Kong, Paris, Lyon, Nice	COP: Mean of 4.9

4.3 DESIGN COMPONENTS

4.3.1 SAHP components and investigated parameters

The long term performance of a SAHP system entirely depends on the size and configuration of the components that must meet the demands for load and the daily radiation at a given location. In this manner, a SAHP system comprises four main components which are collector-evaporator (combined in direct series types),

compressor, thermal expansion valves and the storage-heat exchanging tank. The studies conducted on SAP systems show that collector (also evaporator for direct series type SAHP systems), and the compressor are the components that are mainly effected by the amount of heat obtained from the heat source. Also, compressor and pumps are the power consuming devices in a SAHP system.

4.3.1.1 Collector-evaporator

Glazed and unglazed flat plate solar collectors are the two major collector types mostly used in SAHP system applications that research has focused on. Both of them have been widely used in the research work for SAHP systems as briefly shown in Table 4.5. It is obvious that unglazed flat plate collector is most widely employed and investigated one among the two types. This is mainly owing to encouraging collector efficiencies. Having unglazed collector (also means no cover), heat loss is prevented so that available heat is fully absorbed by the plate and transferred to the low temperature flowing fluid. This key advantage of uncovered flat plate solar collectors has been cited in numerous research studies of SAHP system applications.

Other types of solar collectors including the vacuum tube, photovoltaic/thermal and evacuated tubes modules have also been investigated in tandem with heat pump systems to form SAHP systems. These modules also yielded high temperature difference and found to be worth to assemble at the heat source side of SAPHs. Ji, Jie, et al. (2008) investigated the performance of the photovoltaic modules with heat pump units under prevailing weather conditions of Hefei in Central China and obtained COP of up to 10.4 for the overall PV-SAHP system.

Reduction of heat losses through various designs has largely been practised in determination of system performance. In those practices, certain factors determining the system performance such as size and material of the collectors, pipe size and dimensions, fluid properties, wind velocity, weather conditions and solar radiation etc. have been analysed pertaining to the heat source unit. Among these parameters, the ambient temperature and solar radiation are the most influencing factors but their instability is a major concern (Omojaro and Breitkopf, 2013). Vacuum tube heat pipe collector system was studied by Shilin and Fei (2010) to propose a likely solution of instability and intermittence of solar heating systems. With respect to the analyses, a control scheme and operation suggestion was provided.

4.3.1.2 Compressor

Efficiency and speed are two significant decisive factors for compressor units used in SAHP systems as these factors are related with refrigerant pressure and heating temperature rise. However, considering compressors below their capacities is a real issue if the required output temperature is not delivered or the delivery is too high. This mismatch between compressor speed and instability of the available solar radiation has, in many studies, been found to be highly influential on the performance of the compressor. It is shown in literature reviews that a better compressor performance is achievable by employing variable speed compressors. Kuang and Wang (2006) achieved a COP range between 2.6 and 3.3 in the SAHP configuration using a variable speed compressor. Another study reveals that employing variable frequency compressor in a SAHP system resulted in higher COPs and also getting high solar radiation rate yielded enhanced heat gain in condenser (Chaturvedi et al., 1998).

It is advised that setting the compressor speed at a low rate will not only enhance COP but also extend the life cycle of the compressor. Huang et al. (2010) found that COP decreases from 2.82 to 1.86 with increasing compressor speed. Also, Guoying et al. (2009) results indicated that decreasing compressor speed from 5000 r/min to 1500 r/min resulted in significant improvement in system COP from 5.89 to 7.36 in Nanjing and from 5.59 to 7.09 in Hong Kong. Besides COP, another advantage of setting the compressor at a low speed is the possibility of reducing the compressor energy consumption which will also lead to enhanced COPs.

4.3.1.3 Condenser

For SAHP water heating applications, the condensers mostly function both as heat exchanger and heat storage tank and copper tube piping has been found to be extensively used for refrigerant flow and heat exchange with the cold water in the tank. Hawlader et al. (2001) conducted an investigation on fibre glass made water condensing tank. Condenser performance primarily depends on the reduction of heat loss through radiation so that its design plays a key role towards enhanced performance characteristics. Thus, numerous studies have been concerned with design parameters in relation with other system components. Chow et al. (2010) reported on numerical modelling of a SAHP water heating system that compressor speed can have a strong effect on the condenser heat gain. Moreover, condensing refrigerant properties namely heat transfer coefficient, water and ambient temperature are the factors that should be considered in condenser design and performance. Stratification effect in water tank is also crucial if energy is stored in a water tank for future use. Anderson and Morrison (2007) experimentally indicated that extended area of the condenser in connection with the water tank enhances overall performance of the system.

4.3.1.4 Expansion valve and pump

An expansion valve regulates the pressure and flow rate of the refrigerant in a heat pump cycle. It has various types according to its functions which shown to be highly effective on the performance of compressor and mass flow rate of the working fluid. Besides widely used thermostatic one, electronic type has also been used in SAHP systems (Omojaro et al., 2013). The electronic expansion valve with a controller and a variable speed compressor are recommended to be employed in a SAHP system in order to sustain a high system performance, system reliability and a proper match between solar collector and compressor units (Li et al., 2007).

4.3.2 Types of refrigerant used in SAHP Systems

An effective working fluid for SAHP systems must have a high thermal conductivity, critical temperature and evaporation enthalpy to attain high heat transfer rate and COP. The refrigerant must also possess qualities like very low freezing point, specific volume capacity and viscosity to conform to heat pump operation and reduce power consumption. Ozone layer depletion and climate change are two main refrigerant related concerns that should be considered in their selection criteria. In SAHP systems, there are two types of refrigerants in use namely plain and mixed refrigerants. Especially mixed refrigerants have been considered lately for SAHP systems with the need of environmentally friendly, safe and effective refrigerants. Gorozabel et al. (2005) replaced R12 with R134 and compared the system performance. 2-4% degradation in system performance for collector temperature range of 0-20 °C was reported. Also, a comparison between different refrigerants was conducted and shown that R12 yielded the highest COP followed by R22, R134A, R410A, and R407C/R404A, respectively. Mohanraj et al. (2009) presented a comparison study between R22 and a mixture of R407C for a SAHP system. The

energy performance ratio (EPR) of mixture was found to be 2-5% lower compared to R22. However, total equivalent warming impact of the mixture was reported to be lower compared to R22 under leakage conditions. Although the performance of the mixture type refrigerants was found to be still lower than that of conventional primary refrigerants, promising results show the high potential for mixture over others.

4.4 THERMAL PERFORMANCE CHARACTERISTICS OF SAHP

An in-depth comprehension overview and awareness of the presence of interdependent parameters and their interaction is essential to anticipate the thermal performance in designing stage of any SAHP system. Therefore, from both experimental and theoretical studies conducted to investigate the thermal characteristics of various type SAHP systems, a number of findings have been introduced about thermal performance classifications and the influencing parameters based on the analysis performed. Thermal performance analyses types, in this study, have been categorized as coefficient of performance (COP), energy and exergy analyses. Table 4.5 provides a list of the thermal performance analyses of SAHP systems reviewed, findings and evaluation methods, respectively.

Table 4.5 Overview of some SAHP studies with thermal performance analyses and evaluation methods

Refs.	Study type	Analysis	Result	Performance Evaluation
Bai et al. (2012)	Num.	COP	4.1	Function of climate conditions, collector specifications, and size of heating area
Anderson (2007)	Exp.	COP	6 & 4.5	Function of climate conditions, heat transfer and power to time required for the heating cycle
Hulin et al. (1999)	Num.	COP	3-4 & 8-9	Function of time
Kuang et al. (2003)	Analy.& Exp.	COP	6.4	Function of climate conditions, collector area, storage volume and compressor speed
Cervantes et al. (2002)	Theo. & Exp.	COP	1.7- 2.5	Function of outlet temperature with respect to various solar insolation values
Li et al. (2007)	Exp.	Exergy	10-30%	Function of time for useful heat gain
Moreno et al. (2012)	Theo. & Exp.	COP	1.7 & 2.9	Function of evaporation temperature, heat and compressor power
Keliang et al. (2009)	Experimental	COP	9.5 & 6.3	Function of condensing temperature, PV efficiency, compressor frequency and time
Cervantes et al. (2002)	Theo & Exp.	Exergy	Ns	Function of climate conditions, temperature difference and time
Kara et al. (2008)	Review & Exp.	Exergy	Ns	Function of fuel consumption and heat delivery
Mohanraj et al. (2009)	Theo. &Exp.	Exergy	0.26 %	Efficiency and losses

4.4.1 Coefficient of performance (COP)

Coefficient of the performance (COP) is the fundamental and predominant performance evaluation approach for SAHP Systems. It is defined as the ratio of heating or cooling effect Q_{sys} , to the total work input W_{sys} . This description is valid for any heat pump either stand-alone or combined with refrigeration cycles and is mathematically stated as

$$COP_{sys} = \frac{Q_{sys}}{W_{sys}} \quad (4.1)$$

Eq. 1 can be further expressed for direct series SAHP (DX-SAHP) systems as (Omojaro et al., 2013):

$$\text{COP}_{\text{sys}} = \frac{m_f c_f \Delta T_{h,c}}{(W_{\text{comp}} + W_{\text{pump}} + W_{\text{valve}})_{h,c}} \quad (4.2)$$

Eq 2 shows that heating or cooling effect of the system is a function of the fluid mass flow rate, m , specific heat capacity, c , and the temperature difference, ΔT . The subscripts, h and c , stand for heating or cooling state, respectively. Total work input is also a function of the sum of the work input to system components.

Eq. 6.1 can be also extended for indirect series SAHP systems as (Bakirci and Yuksel, 2011)

$$\text{COP}_{\text{sys}} = \frac{\dot{m}_{\text{con}} c_w (T_{\text{cwo}} - T_{\text{ewi}})}{\dot{W}_{\text{comp}} + \dot{W}_{\Sigma p}} \quad (4.3)$$

Here, the performance of an indirect series SAHP system is likewise a function of mass flow rate, specific heat capacity and the temperature difference across the system. The subscripts, con , w , cwo , ewi , comp and p represent condenser, condenser water outlet, plate heat exchanger water inlet, compressor and circulation pump, respectively. Other versions of expressing COP also exist for various SAHP configurations. Another form of COP evaluation known as seasonal coefficient of performance (SCP) is the time and season of SAHP applications and is obtained by periodical computation of regular COP for a particular season or time frame.

The effectiveness of a SAHP system, COP, entirely bounds up with solar radiation and ambient air temperature. These factors ultimately determine how high the heat generated at the evaporator and the evaporator temperature is considered in evaluation of the entire SAHP system effectiveness. Ito et al. (1999) stated the

significant contribution of the solar radiation to the evaporation temperatures and COP as well. Further, COP and efficiency increase as ambient temperature rises where COP increases and efficiency drops with the increasing solar radiation level (Kong et al., 2011).

4.5 DISCUSSION & CONCLUSIONS

A wide range of SAHP system configurations and systematic description were presented in a unified visualization scheme called “square view”. This approach mainly simplified the steps to describe and classify combined solar thermal and heat pump systems, and visualize such systems systematically. With this approach, a basis was provided also to compare the combined solar thermal and heat pump systems. Thereby, the comparative studies were carried out on parallel, series and dual source systems showing that performance of the various configurations mainly depend on number of elements including resident behaviour, procedure parameters, building features, system components and climatic conditions. However, it was recognized that various performance criteria was applied and this incoherence complicated the possibility of performing a proper comparison among the broad range of system studies. Therefore, a set of standardized performance criteria would facilitate the analysis and comparison of different SAHP systems. In this regard, Task 44 Subtask B intends to achieve a common method for the assessment of these systems and this work is still under progress (Ruschenburg et al., 2013). On entire SAHP systems, energy sources and total energy load should be clarified for the assessment of those systems as these parameters may vary with components employed in the system, building loads and climate. For this reason, parameters like free energy ratio (FER) or seasonal performance factor (SPF) should also be considered on the entire system. Although the individual performance of the

components is also significant, performance evaluations of solar collectors and heat pump do not merely picture the power need to meet the loads.

It was also noted that variety of configurations, types and factors make it challenging to examine a particular system, match with the others and design it for a specific climate. In this study, key system parameters and performance assessment from a number of previous studies were presented. One should beware that a proper comparison of systems should match the similar systems with the same components, bonded to same energy source and total energy loads. Although this method was applied to each comparative study, the conclusions among the studies were subjected to be unlike as energy source and load differed. For this reason, it is not that simple to compare the individual series systems since there must be a common set of methods for a proper comparison.

A number of past and current works, from different researchers, on solar assisted heat pump (SAHP) systems for low temperature water heating applications has been presented with the visualization approach first introduced by Elimar et al. (2010). Also, various studies from International Energy Agency's Task 44 of the Solar Heating and Cooling Programme investigating solar heat pump systems have been provided besides, a wide range of research on SAHP has also been performed at various institutions worldwide.

Reviewed studies indicate that the effect of solar heat energy on the performance of both collector and heat pump individually, and on the entire SAHP system is majorly significant. Then again, the advanced configuration types of SAHP systems were found to be performing better than the conventional basic types with reference to

reported COPs that might draw considerable interest for further investigations. The concluding remarks can be outlined as follows;

Indirect utilization of solar heat is more beneficial in terms of system performance factor when the solar radiation is under certain level which depends on solar collector and heat pump characteristics. Also, using unglazed solar collectors was more advantageous in series mode and also increasing the runtime of the collectors could enhance performance of the series configuration. The system performances were insensitive to the location where experimental studies took place. The weather, depending on the geographical location, would have an ultimate impact on the performance and size of the system. However, the performance of SAHP system is more reliant on ambient temperature and wind speed, rather than on solar radiation. COP of the system was enhanced with the decreasing compressor speed as ambient temperature increases from winter to summer. Moreover, as the ambient temperature rises the COP of the heat pump also increases while the time required for heating decreases.

Glazed and unglazed flat plate solar collectors are the two major collector types mostly used in SAHP system applications. Unglazed flat plate collector is most widely employed and investigated one among others. This is mainly owing to encouraging collector efficiencies. Having unglazed collector (also means no cover), heat loss is prevented so that available heat is fully absorbed by the plate and transferred to the low temperature flowing fluid.

A better compressor performance is achievable by employing variable speed compressors. Employing variable frequency compressor in a SAHP system usually resulted in higher COPs and also getting high solar radiation rate yielded enhanced

heat gain in condenser. It is advised that setting the compressor speed at a low rate will not only enhance COP but also extend the life cycle of the compressor.

Condenser performance primarily depends on the reduction of heat loss through radiation so that its design plays a key role towards enhanced performance characteristics. Moreover, condensing refrigerant properties namely heat transfer coefficient, water and ambient temperature are the factors that should be considered in condenser design and performance. Stratification effect in water tank is also crucial if energy is stored in a water tank for future use. Also, it has been reported that extended area of the condenser in connection with the water tank enhances overall performance of the system.

Expansion valve and pump are found to be highly effective on the performance of compressor and mass flow rate of the working fluid. The electronic expansion valve with a controller and a variable speed compressor are recommended to be employed in a SAHP system in order to sustain a high system performance, system reliability and a proper match between solar collector and compressor units.

Mixed refrigerants have been considered lately for SAHP systems with the need of environmentally friendly, safe and effective refrigerants. Although the performance of the mixture type refrigerants was found to be still lower than that of conventional primary refrigerants, promising results show the high potential for mixture over others.

Wind velocity along with the solar radiation was another major parameter to be considered in exergetic analyses of SAHP systems. As the wind speed increases, heat loss at the solar collectors also increase and this will ultimately result in degradation in exergy difference at the condenser.

Referring to the works of various researchers, a single optimum SAHP system configuration cannot be identified as the configuration may vary with size of the residential area, load and climatic conditions. Likewise, future studies must apply a common standardized assessment method for the performance evaluations of SAHP systems. Overall, the studies imply that combined solar thermal and heat pump technology has the potential of providing an effective alternative for various climatic conditions with adjustable configurations. Chapter 7 investigates a low cost novel solar thermal roof collector coupled with a heat pump unit to address a solution to prevailing drawbacks of current SAHP configurations.

CHAPTER 5 – Performance evaluation and techno-economic analysis of a novel building integrated PV/T roof collector: modelling, theoretical study and experimental validation

5 PERFORMANCE EVALUATION AND TECHNO-ECONOMIC ANALYSIS OF A NOVEL BUILDING INTEGRATED PV/T ROOF COLLECTOR: AN EXPERIMENTAL VALIDATION

5.1 INTRODUCTION

Recently, integrating PV modules into building construction has generally practised with the growing pressure on reducing fossil fuel dependency and CO₂ emission (Schoen, 2001). Building integrated photovoltaic thermal (BIPVT) systems emerge as a ground-breaking technology that combines photovoltaic and thermal systems, supplying both power and thermal energy at the same time (Agrawal et al., 2010). Currently, the power energy efficiency of PV modules for commercial applications is in the range of 12 - 18%, which is a value measured at the Standard Test Conditions (STC) (1.0 kW/m² of solar radiation, 25 °C of ambient temperature, and 1.5 m/s of wind speed), particularly depending on the solar cell type. Greater than 80% of solar radiation falling upon PV cells is either reflected or dumped as waste heat. This results in to increase PV cells operating temperature and degradation of power energy efficiency (Dubey et al., 2009). 1 °C rise in temperature of PV cells will reduce 0.4 – 0.5% of power energy efficiency for crystalline Si based cells and 0.25% for amorphous silicon (a-Si) cells (Zhao et al., 2011). Moreover, the energy payback time (EPBT) for a photovoltaic system (PV) lies between 10 to 15 years depending on the efficiency of PV modules and the price of electricity. If the efficiency can be enhanced then the energy payback time span can be shortened (Tiwari et al., 2006).

In order to increase the power energy conversion efficiency of PV modules, it is most desired to transfer the accumulated heat out of concealed PV surface and exploit properly. The essential technology for this purpose, namely PV/T technology, has been in the market and still making rapid advances (Zhang et al., 2012).

Air cooling, as the most commonly used method for PV cooling, has been extensively studied as an alternative and cost effective solution to building integrated PV (BIPV) systems. Incorporating an air gap between the PV modules and the building fabric (façade or tilted roof) is used for air circulation to cool PV modules, and pre-heated air can provide practical solutions to domestic thermal needs. The air gap in BIPV systems act as a natural draft when no fan is employed and the airflow is driven by heat and wind-induced pressure difference in the gap (Tonui et al., 2007). This practically constitutes PV/T air collectors. A number of experimental and analytical studies have been reported on PV/T air systems. To name a few, considerable amount of study, both theoretical and experimental, on buoyancy driven air movement behind PV panels have been conducted (Corbin et al., 2010), by adjusting three different air flow configurations (Pantic et al., 2010), by integrating semi-transparent PV module into double-pass facade (Kamthania et al., 2011), by evaluating exergy components and exergy efficiency (Sarhaddi et al., 2010), by connecting PV/T air collectors in series (Dubey et al., 2009), and alternatively by using wind-driven ventilator to enhance the performance of PV modules (Valeh-e-Sheyda et al., 2014). The main concern is of the poor heat removal effectiveness of the air based systems due to the low thermal mass of the air. In the case of air temperature is over 20°C; very low PV cooling performance would be expected (Kalogioru et al., 2006).

Water based PV cooling systems have been developed and extensively used in practice to overcome the disadvantages of air systems. For such a module, unique polyethylene heat exchanger is laid down under the PV panels allowing water to flow through tubes and risers. If circulating water temperature were lower than that of PV cell layer, the efficiency of PV would be enhanced through cool-off. Also, the flowing

water would capture heat from PV cells and fluid temperature would rise. The hot water can act as a good heat source for domestic thermal applications and solar assisted heating and cooling technologies. There are numerous researches conducted relating to PV/T water systems including a wide range of theoretical studies, lab experiments and engineering applications. To name a few, the design characteristics of water based PV/T systems and analyses of liquid based PV/T systems were demonstrated (Bergene et al., 1995). Models for water type PV/T systems, such as water heat extraction model (Zondag et al., 2003); results of models (Chow 2003); domestic PV/T systems (Kalogirou et al., 2006), have been presented. Thermosyphonic PV/T solar water heaters were also evaluated with respect to their performance (Agarwal et al., 1994; Garg et al., 1994) by using different refrigerants R-134a, R407C and R410A, respectively (Esen, 2005). Briefly the water based systems offer some advantages as to enhance the power energy performance of the PV modules and improve the solar heat utilization. However, there are a few technical challenges found in these systems in practice that prevented wide-scale applications. These technical drawbacks include being expensive to make and install the PV/T units, and freezing in cold climates may cause corrosion and ductility for combined PV/T panels in aluminium frames (Zhang et al., 2012). Moreover, the inability to switch already installed photovoltaic (PV) systems into PV/T systems could be mentioned as a practical drawback.

Exergy analysis is a primary thermodynamic performance evaluation of energy systems in addressing the impact of energy resource utilization on the environment. It is an effective technique to determine the actual magnitude of wastes and losses for more efficient use of energy resources via applying conservation of mass and energy principles along with the second law of thermodynamics (Akyuz et al., 2012).

There are several costs relating with acquiring, operating, maintaining and disposing of a system. Life Cycle Cost analysis takes into account of discount rates, interest rates, operation and maintenance costs, etc. In LCC method, all relevant present and future costs essential to the system are summed in present value during a given life period. The purpose of LCC is to provide an effective cost estimation tool for a project in selection of alternatives and design that ensures to provide the lowest overall cost consistent with the quality and function. Obstacles to using LCC are poor data availability, erratic economic changes, uncertainties associated with future operating and maintenance costs, discount rate, asset life and inflation (Agrawal et al., 2010).

Objective

The first objective of this study was to achieve a roof integrated thermal collector that propitiously blends into its surroundings thus avoiding 'add-on' appearance and having a dual function (heat absorption and passive cooling of photovoltaic modules via heat extraction) and the second objective was to address the inherent technical pitfalls and practical limitations by bringing an inexpensive, requiring minimum maintenance and easily adaptable solution to the already mounted PV systems as a concealed heat extraction component without disturbing the original structure of PV modules. Although substantial studies have been performed on the PV/T technologies, integration of such a heat exchanger loop, having a unique structure, with PV modules has yet to be considered. The present study will theoretically and experimentally evaluate the thermal performance, perform energy and exergy analysis, and present LCC based cost analysis of the roof unit.

5.2 INTEGRATION OF UNIQUE POLYETHYLENE HEAT EXCHANGER LOOP UNDERNEATH PV MODULES

5.2.1 Operating Principle

The proposed system consists of polyethylene heat exchanger loop underneath PV modules to form a PV/Thermal roof collector. The complete roof structure has several layers, an outer cover; a layer of photovoltaic cells beneath the cover; EVA plastic layer at the back of PV adjacent to the PV cells layer, polyethylene heat exchanger and roof support.

The piping system is placed below the roof truss and joined using flexible coupled connectors with valves to provide a leak free connection. The supply pipe feeds cold water to polyethylene heat exchanger, and the return pipe transports the hot water from the heat exchanger. The PV modules and steel corrugated roof support are well clamped together, and polyethylene heat exchanger is placed in between. Figure 5.1 is the illustration of layers of the proposed system; Figure 5.2 shows the plumbing of the system.

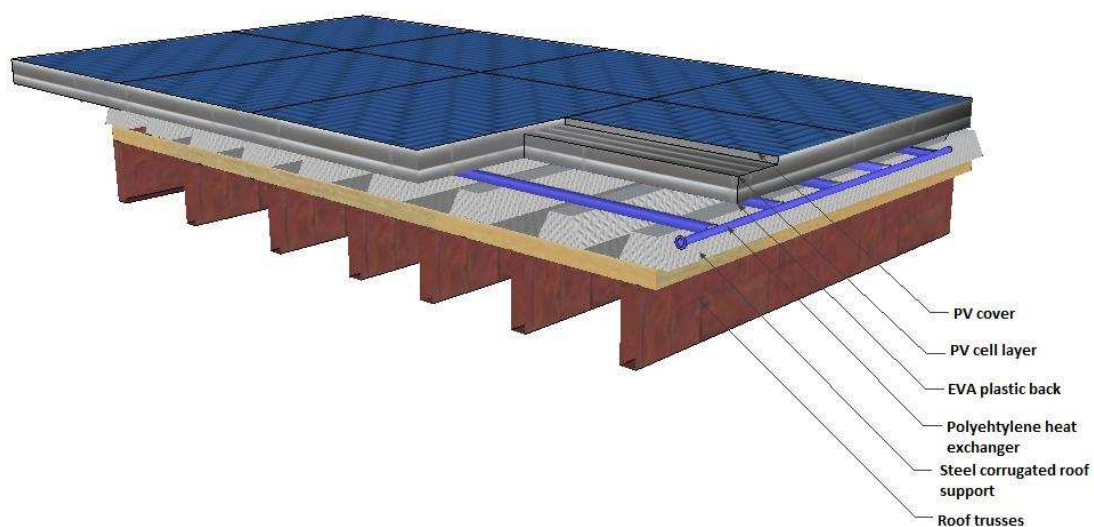


Figure 5.2.1 The integration of unique polyethylene heat exchanger loop underneath PV modules

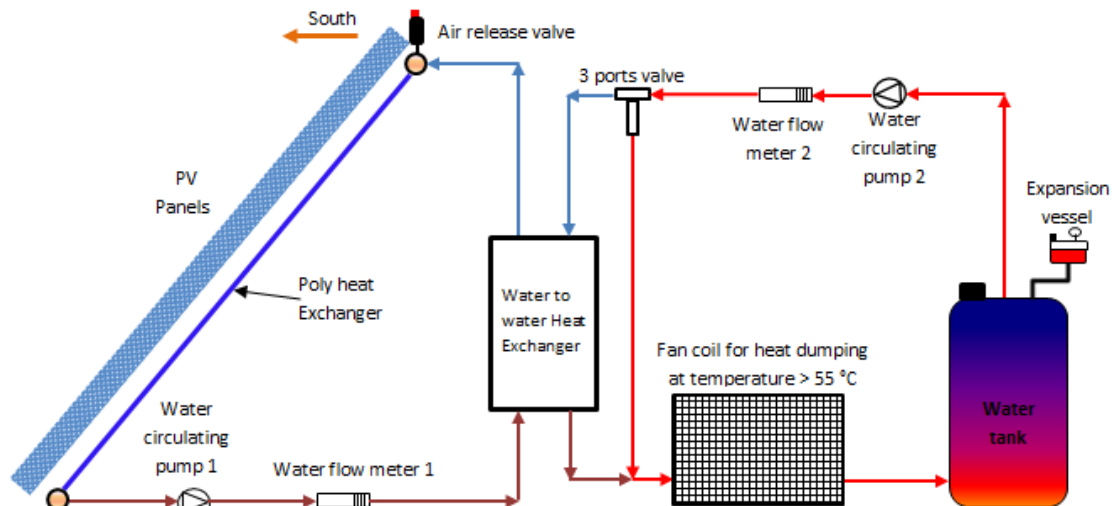


Figure 5.2.2 Thermal roof unit piping

The PV roof modules absorb a greater proportion of solar radiation falling upon the PV cell surface, while dissipating remainder to ambient as waste heat. From the above, a top cover which is transparent and thermally resistant enables to reduce the amount of dissipation and secures that maximum solar radiation reaches the photovoltaic cells. Meanwhile, the temperature of the cell layer, somehow, has to be reduced so as to boost the solar power conversion efficiency of PVs. As a result of the thermodynamics fact that heat flows from ambient to the photovoltaic cells in case of lower temperature of cell surface. Therefore, adjusting water inside the heat exchanger at a lower operation temperature helps to mitigate the cell surface temperature. Although polyethylene heat exchanger is loosely adhered to the rear surface because of the size of the polyethylene heat exchanger, the aluminium frame of the PV modules, and less flexible pipes and risers, relatively lower temperature difference between the cell surface and circulating water is expected. So that the physical structure of the poly heat exchanger prevents the use of thermally conductive adhesives due to uneven contact to the rear of PV modules. Consequently, any decrease in the cell temperature will collaterally increase both power and thermal efficiencies.

The roof unit will convert part of the incoming solar radiation into power energy due to the photogalvanic effect of the silicon cells and remaining heat energy will be conveyed through the circulating water across the heat exchanger. The hot water can be used for heating & cooling, domestic hot water supply, food drying, natural ventilation inside the building and more.

5.2.2 Prototype Design

There are eighty four (84) Sharp NU-R245 (J5) photovoltaic solar panels mounted on the roof which are entirely for power energy without any heating function. The solar cell type is mono-crystalline (156.5 mm²) silicon absorber with the cell efficiency of 14.9%. Anti-reflex coating of the PV modules is to improve the light absorption. The operation range of PV modules is between -40 and +90. The solar optical parameters of the PV module can be found in Table 5.1. The solar PV panels are mounted at a 10° angle oriented to the south to improve the energy capture and the modules are on the solar panel mounting system with horizontal members fixed to steel cladding sheet with anti-condensation backing.

The polyethylene heat exchanger ready loop is made of polyethylene material and the physical structure of the heat exchanger makes it first-of-its-kind. The pipes and fittings used are connected via welding with soldering iron. The flow channels of the working fluid have the internal and external diameters of 2.7 mm and 4.3 mm, respectively and the distance between the flow channels is 10 mm. The technical parameters of the PV modules and heat exchanger can be found in Table 5.2.

In close loop solar roof systems, the circulating pump should overcome the head pressures every time it turns on. Moreover, the pump must be compatible with solar systems in terms of its size, hydraulics, speed stages, maintenance free, high

efficiency and low power consumption. The technical details of the circulation pump can be found in Table 5.2.

Thermocouples (K type) with the maximum deviation of $\pm 1.5^{\circ}\text{C}$ were inserted to investigate the flow rates, inlet-outlet temperature and temperature in the pipes, temperature of PV cell layer. The thermocouples were connected to the data logger, DT500. A Kipp & Zonen pyranometer with $\pm 3\%$ accuracy was mounted on a vertical surface (10° South) to measure the global solar radiation and the related data were recorded on the data logger. Wind speed meter is also installed to find out the heat flow rate through natural convection between the PV cover and the ambient. Direct connection between data logger and PC was provided to store data and transfer it to Excel spreadsheet for examination. All thermocouples were tested for calibration before the testing commenced.

Table 5.1 Solar optical parameters of PV cells and glass cover

PV module type	Absorptance α	Emissivity ε	Thermal Conductivit y (w/m $^{\circ}\text{C}$) K	Thickness δ	Reference efficiency %	Temperature Coefficient ($^{\circ}\text{C}$) β_p
Mono-crystalline Si	0.9	0.96	149	0.02	14.9	0.030
Single glazing		0.9	1		Transmittance τ 0.91	

Table 5.2 Technical parameters of the roof unit

Component	Parameter	Value
PV modules	No. of module	84
	Module dimensions	1652x994x46
	Cell type:	mono-crystalline
	Packing factor	0.91
	Conversion efficiency	14.9%
	Module peak power	245 W
	Estimated power/performance efficiency	K = 80%
	Maximum voltage, V_m	30.5
	Maximum current, I_m	8.04
	Open circuit voltage, V_{oc}	37.5
Short circuit current, I_{sc}	8.73	
Exposed roof area (A_{eff}) and Tilt angle (β_s)	Active total area	140 m ²
	South facing active area of PV arrays with heat exchanger	40 m ²
	Tilt angle	10°
Polyethylene Heat Exchanger	The internal diameters of tubes	
	The external diameters of tubes	$D_i=0.0027$ m
	Distance between tubes	$D_o=0.0043$ m
	Length	$W=0.001$ m
	Height	$L=10$ m
	Max temperature allowed in poly HE	$H=1$ m
	Max pressure allowed in poly HE	60 °C
		1 MPa
Circulating Pump	Model:	WILO
	Max delivery head	6 m
	Max operating pressure	10 bar
	Permissible temperature range	-10 °C to +110 °C
	Mains connection	1~230, 50 Hz
Hot water storage	Dimensions	0.9m * 0.45m
	Capacity	120 l

The tests have been conducted in Wysall, Nottingham, which is geographically located at 52.97° N and 1.10° W. The size of the collector and poly heat exchanger is large enough to be tested so that the performance characteristics can be detected properly. Three rows of poly heat exchanger (1m x 10m each) are placed under the PV modules with the aperture area of 40 m². The prototype is shown in the Figure 5.3, and initial design parameters are given in Table 5.3 below. The system is invisible as the heat exchanger is placed under the PV units. It can also be mentioned as aesthetically pleasing as it doesn't ruin the outer look.



Figure 5.2.3 The prototype of the proposed system

Table 5.3 Initial design parameters

Parameters	Values
Average mass flow rate	0.017 kg/s
C_w	4190 J/kgK
K_c	1.0 W/mK
M_w	45 kg

5.2.3 Mathematical Analyses of Thermal Performance and EES Model Setup

Thermal Energy transfer occurred in the system has two processes, i.e., conversion of solar radiation into thermal energy by PV cell absorbers, and transporting absorbed thermal energy towards polyethylene heat exchangers. These inter-linked processes enable the utilization of waste heat under steady state operation. A computer model was adapted to simulate the thermal performance of the novel system by using EES (Engineering Equation Solver) Software. The adapted version of existing model was first developed by (Zhao et al., 2011) and this model was well-

suitable for the physical structure of the proposed system. For sake of simplicity, the following assumptions have been considered during the model set-up:

- The overall performance of the system is at a quasi-steady state condition
- All surfaces of layers cover uniform temperature
- Temperature gradient around tubes is negligible
- The air layer between PV and heat exchanger is assumed stagnant
- Heat dissipation is considered as one-dimensional
- There is forced flow through heat exchanger tubes
- Edge loss is negligible due to insulation
- Due to advanced thermal resistance features, heat loss through the insulation is negligible

The method and mathematical equations presented in this study, are not necessarily the most accurate available due to considered assumptions; but they are widely applied, easy to use and adequate for most of the design computation. Figure 5.4 illustrates the cross-sectional view of the roof unit's heat transfer profile.

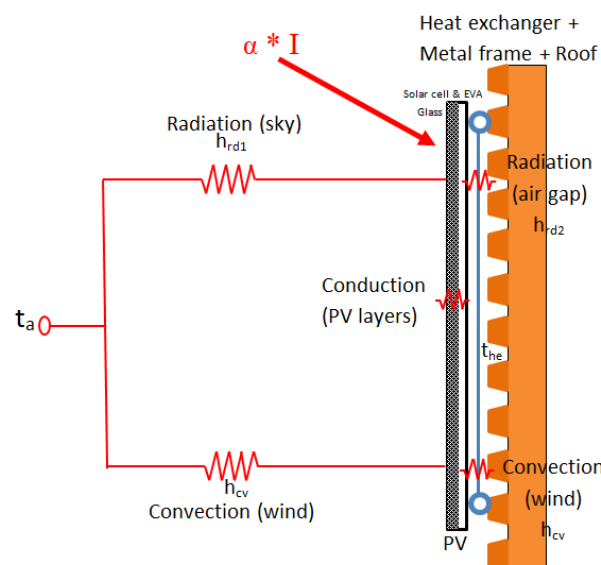


Figure 5.2.4 Heat transfer profile of the Roof unit

5.2.3.1 Thermal Model

The solar energy which is initially absorbed by the PV cells can be expressed as:

$$Q_{\text{abs}} = \tau_c \cdot \alpha_{\text{abs}} \cdot A_{\text{eff}} \cdot I \quad (5.1)$$

This part of incoming energy is converted to power energy by silicon cells, partly carried through the heat exchanger and the rest is dissipated to the ambient due to temperature difference between solar module and atmosphere. So, the loss can be described as follows :

$$Q_l = h_{\text{cv}} \cdot (T_c - T_a) + \varepsilon_c \cdot \sigma \cdot (T_c^4 - T_s^4) + h_{\text{air}} \cdot (T_{\text{pl}} - T_{\text{heo}}) + \varepsilon_{\text{pl}} \cdot \sigma \cdot (T_{\text{pl}}^4 - T_{\text{heo}}^4) \quad (5.2)$$

Combining above equations provides a revised expression of the useful heat energy (Q_t) (Zhao et al., 2011):

$$Q_t = Q_{\text{abs}} - Q_l \quad (5.3)$$

In order to estimate the PV cover temperature (T_c) the method that employs the following empirical relation can be applied as (Chong et al., 2011):

$$T_c = 30 + 0.0175 \cdot (I - 300) + 1.14 \cdot (T_a - 25) \quad (5.4)$$

This relation is applied for standard pc-Si PV modules. In PV/T systems, the relation also accounts for the system operating conditions, such as the effect of heat extraction fluid. The parameter $(T_{\text{PV}})_{\text{eff}}$ is considered to correspond to the PV module temperature in terms of the operating conditions of PV/T systems. Therefore, for the proposed system, $(T_{\text{PV}})_{\text{eff}}$ is calculated by (Chong et al., 2011):

$$(T_{\text{PV}})_{\text{eff}} = T_c + (T_{\text{PV/T}} - T_a) \quad (5.5)$$

The operating temperature of the PV/T system is relevant to the PV module and to the thermal unit temperatures and can be obtained nearly by the mean fluid temperature.

McAdam's convective heat transfer coefficient of the ambient air is widely used in the solar collector theory (Duffie & Beckman, 1980):

$$h_{cv} = 5.7 + 3.8 \cdot V \quad (5.6)$$

The sky temperature can be obtained by Swinbank's equation as a function of the ambient temperature by (Duffie & Beckman, 1980):

$$T_s = 0.037536 \cdot T_a^{1.5} + 0.32 T_a \quad (5.7)$$

Where h_{rd1} and h_{rd2} are the radiation heat transfer through front and back side of the collectors, respectively.

$$h_{rd1} = \varepsilon_c \cdot \sigma \cdot (T_c^4 - T_s^4) \quad (3.8)$$

$$h_{rd2} = \varepsilon_{pl} \cdot \sigma \cdot (T_{pl}^4 - T_{heo}^4) \quad (5.9)$$

Assuming a natural convective air layer in the PV module and heat exchanger, the associated convective heat transfer coefficient, h_{air} , can be expressed as (Zhao et al., 2011):

$$h_{air} = \frac{Nu \cdot K_{air}}{\delta_{air}} \quad (5.10)$$

Where K_{air} is thermal conductivity of air and δ_{air} is thickness of the air layer between PV and heat exchanger. Then Nusselt number can be obtained by (Zhao et al., 2011):

$$Nu = \left[0.06 - 0.017 \cdot \left(\frac{\beta_s}{90} \right) \right] \cdot Gr^{1/3} \quad (5.11)$$

The Grashoff number is given as (Zhao et al., 2011):

$$Gr = \frac{g \cdot (T_{pl} - T_{heo}) \cdot \delta_{air}^3}{V_{air}^2 \cdot T_{air}} \quad (5.12)$$

Instantaneous thermal efficiency of the roof unit is defined as (Zhao et al., 2011):

$$\eta_t = \frac{Q_t}{A_{\text{eff}} \cdot I} \quad (5.13)$$

The heat flows through conduction across the PV cover, cell layer, and EVA plastic layer in the back of the module. After natural convective air layer between PV module and polyethylene heat exchanger, conductive effort, again, takes place between aluminium layer and heat exchanger wall itself and the heat is eventually conveyed to the water. The heat gain of water is as equal as the useful heat energy is (Zhao et al., 2011):

$$Q_t = A_{\text{eff}} \cdot U_t \cdot (T_{\text{abs}} - T_w) \quad (5.14)$$

Where the overall heat transfer coefficient between PV cell and water is given as:

$$U_t = (U_{c,\text{abs}} + U_{\text{abs,pl}} + U_{\text{heo,hein}} + U_{\text{hein,w}})^{-1} \quad (5.15)$$

Heat transfer coefficient ($U_{c,\text{abs}}$) from cover to PV cell layer (absorber) is given as:

$$U_{c,\text{abs}} = \frac{\lambda_c}{\delta_c} \quad (5.16)$$

The average temperature at the absorber (cell layer) then becomes:

$$T_{\text{abs}} = T_c - \frac{Q_t}{A_{\text{eff}} \cdot U_{c,\text{abs}}} \quad (5.17)$$

Heat transfer coefficient ($U_{\text{abs,pl}}$) from PV cell (absorber) to the EVA plastic layer by (Zhao et al., 2011):

$$U_{\text{abs,pl}} = \frac{\lambda_{\text{abs}}}{\delta_{\text{abs}}} \quad (5.18)$$

The temperature at the outer wall of the polyethylene heat exchanger becomes (Zhao et al., 2011):

$$T_{pl} = T_{abs} - \frac{Q_t}{A_{eff} \cdot U_{abs,pl}} \quad (5.19)$$

Heat transfer coefficient ($U_{heo, hein}$) from outer wall to interior wall of heat exchanger is defined as (Zhao et al., 2011):

$$U_{heo,hein} = \frac{2 \cdot \pi \cdot \lambda_{he}}{\ln \left[\frac{D_o}{D_i} \right]} \quad (5.20)$$

The average temperature at the inner wall of polyethylene heat exchanger is given as (Zhao et al., 2011):

$$T_{hein} = T_{heo} - \frac{Q_t}{A_{eff} \cdot U_{heo,hein}} \quad (5.21)$$

Heat transfer coefficient ($U_{hein, r}$) from interior wall of heat exchanger to the water as (Zhao et al., 2011):

$$U_{hein,w} = \frac{Nu_r \cdot \lambda_r}{D_i} \quad (5.22)$$

Where Nusselt number is expressed as (Zhao et al., 2011):

$$Nu_r = 0.023 \cdot Re_r^{0.8} \cdot Pr_r^{0.4} \quad (5.23)$$

In order to compare the theoretical results with the experimental outcomes, the root mean square percent deviation (e) and the coefficient of correlation (r) have been examined by using the following expressions (Tiwari et al., 2006):

$$e = \sqrt{\frac{\sum(e_i)^2}{N}} \quad \text{where } e_i = \left[\frac{X_i - Y_i}{X_i} \right] \times 100 \quad (5.24)$$

$$r = \frac{n(\sum X \times Y) - (\sum X) \times (\sum Y)}{\sqrt{n(\sum X^2) - (\sum X)^2} \times \sqrt{n(\sum Y^2) - (\sum Y)^2}} \quad (5.25)$$

Stating the expressions used by (Duffie & Beckman, 1980)

$$m^2 = \frac{U_t}{K\delta} \quad (5.26)$$

Then, the fin efficiency factor (F) can be found by

$$F = \frac{\tanh m \frac{W - D_o}{2}}{m \frac{W - D_o}{2}} \quad (5.27)$$

The flat plate collector efficiency (F') becomes

$$F' = \frac{1}{\frac{WU_t}{D_o U_{\text{abs,pl}}} + \frac{WU_t}{\frac{K}{\delta}} + \frac{WU_t}{D_o + (W - D_o)F}} \quad (5.28)$$

The flow rate factor (F_R) is given by

$$F_R = \frac{\dot{m}C_f}{A_{\text{eff}}U_t F'} \left[1 - \exp\left(-\frac{A_{\text{eff}}U_t F'}{\dot{m}C_f}\right) \right] \quad (5.29)$$

The mass flow rate (\dot{m}) of water has been assessed as for the measured experimental values of average solar intensity (761.54 W/m²), and outside

temperature (37°C) for the given day. These values are used to evaluate the water temperature and solar cell temperature of the PV modules for validation.

5.2.3.1.1 Energy Efficiency

In order to determine the instantaneous power energy efficiency and power output, some of the widely used energy equations are employed as stated below;

Temperature dependent power energy efficiency of a PV module (η_e) can be stated as follows (Ozgoren et al., 2013):

$$\eta_e = \eta_{rc} (1 - \beta_p (T_c - T_{rc})) \quad (5.30)$$

The rate of instantaneous solar energy available on solar cell and power energy output is (Dubey et al., 2009):

$$Q_e = (\alpha\tau) \cdot \xi \cdot I(t) \cdot A_{eff} \quad (5.31)$$

Packing factor for a PV module is expressed as (Ji et al., 2006):

$$\xi = \frac{A_{cell}}{A_{coll}} \quad (5.32)$$

5.2.3.1.2 Exergy Efficiency

Exergy efficiency of a PV system is determined by considering overall exergy content including internal and external losses which are the exergy destruction rate (EX_{dest}) and heat loss rate (EX_{therm}), respectively. The overall exergy output rate may be found by following equation (Akyuz et al., 2012):

$$EX_{out} = EX_{elec} + EX_{therm} + EX_{dest} \quad (5.33)$$

The power exergy (Ex_{elec}) is calculated by assuming that exergy content received by silicon layer is fully utilized in order to generate the maximum power exergy rate ($V_{oc} \cdot I_{sc}$). This is defined as (Akyuz et al., 2012):

$$Ex_{elec} = V_m \times I_m \quad (5.34)$$

The thermal exergy rate of the system (Ex_{therm}) is analysed thermodynamically due to convective heat loss (Q_{cv}) from the cell surface to the ambient and is expressed by (Akyuz et al., 2012):

$$Ex_{therm} = \left(1 - \frac{T_a}{T_c}\right) \times Q_{cv} \quad (5.35)$$

$$Q_{cv} = h_{cv} \cdot A_{eff} \cdot (T_c - T_a) \quad (5.36)$$

where h_{cv} is calculated by Eqn. 3.6.

One can deduce that the thermal exergy of the PV system is based on the following parameters; convective heat transfer coefficient (h_{cv}), wind speed (V), cell temperature (T_c), ambient temperature (T_a) and the PV area (A_{eff}). Then, the exergy rate of the PV system may be given by (Akyuz et al., 2012):

$$Ex_{pv} = V_m \times I_m - \left[\left(1 - \frac{T_a}{T_c}\right) \cdot (h_{cv} \cdot A_{eff} \cdot (T_c - T_a)) \right] \quad (5.37)$$

The maximum exergy rate that can be drawn out of the solar radiation may be obtained by (Akyuz et al., 2012):

$$Ex_{solar} = \left(1 - \frac{T_a}{T_{sun}}\right) \cdot I \cdot A_{eff} \quad (5.38)$$

where T_{sun} stands for the temperature of the sun which is approximated as a spherical black body with a surface temperature of 5489°C (5762 K). Then, exergy efficiency of the PV system can be calculated by using the previous equations (Akyuz et al., 2012):

$$\ell_{PV} = \frac{V_m \times I_m - \left[\left(1 - \frac{T_a}{T_c} \right) \cdot (h_{cv} \cdot A_{eff} \cdot (T_c - T_a)) \right]}{\left(1 - \frac{T_a}{T_{sun}} \right) \cdot I \cdot A_{eff}} \quad (5.39)$$

5.2.3.1.3 Uncertainty Analysis

The experimental uncertainties were calculated by applying Gauss propagation law. The result R is to be calculated as a function of the independent variables $x_1, x_2, x_3, \dots, x_n$ and $w_1, w_2, w_3, \dots, w_n$ represents the uncertainties in the independent variables. Then, uncertainty R is expressed as (Ozgen et al., 2009):

$$w_R = \left[\left(\frac{\partial R}{\partial x_1} w_1 \right)^2 + \left(\frac{\partial R}{\partial x_2} w_2 \right)^2 + \dots + \left(\frac{\partial R}{\partial x_n} w_n \right)^2 \right]^{1/2} \quad (5.40)$$

The independent parameters measured in the experiments noted here are: solar radiation, temperature of PV panels, temperature of water, ambient temperature and wind velocity. Experiments were carried out by using following instruments: Kipp and Zonen CM11 pyranometer with $\pm 3\%$ accuracy, thermocouples (K-type) with the maximum deviation of $\pm 1.5^\circ\text{C}$, Vortex wind speed sensor with the accuracy of $\pm 4\%$, and the liquid flow indicator with an accuracy of $\pm 2\%$.

It is derived from the Equations (3.1)-(3.3), (3.6), (3.10), and (3.13) that the η_t is the function of several variables, each subject to uncertainty:

$$\eta_t = f(\delta_{air}, T_a, V, I) \quad (5.41)$$

Then, total uncertainty for system efficiency can be written as;

$$w_R = \left[\left(\frac{\partial \eta}{\partial \delta_{air}} w_{\delta_{air}} \right)^2 + \left(\frac{\partial \eta}{\partial T_a} w_{T_a} \right)^2 + \left(\frac{\partial \eta}{\partial V} w_V \right)^2 + \left(\frac{\partial \eta}{\partial I} w_I \right)^2 \right]^{1/2} \quad (5.42)$$

The total uncertainty influencing the efficiency of the proposed system was estimated by Equations. (3.40)-(3.42), respectively. The computations indicate that the total uncertainty in calculating the efficiency is 2.47%.

5.2.4 Techno-economic Analysis

The proposed solar energy system consists of PV module arrays, inverters, polyethylene heat exchanger loop, circulating pumps, water storage and necessary piping for circulation. Based on the solar radiation data of the location (Nottingham: 52.97° N-1.10° W), solar energy generation E_{solar} is estimated by the Eqn. (3.1).

The data gathered is at 0° and 38° on a horizontal surface for over 20 years. Monthly average solar radiation of Nottingham is in the range of 30 – 130 kWh m⁻² (Insolation on Horizontal Surface, NASA Surface meteorology and Solar Energy: Daily Averaged Data, January 2014). Commercial monocrystalline silicon cell PV modules are chosen to convert solar radiation into power energy. Its specifications are listed in Table 5.1 and 5.2. The solar energy generation is approximately 10.3 MWh /year or 28 kWh /day. The power generated by the system is partly (approximately 80%) used by the homeowner for home appliances and agricultural barn at feed-in-tariff rate, and the excess power (20%) is fed into the electricity grid at export tariff rate (Figure 5.5).

The overall system typically costs £16,000 with 10% down payment considered. The remaining capital is financed in 25 years period at 8.2% interest rate. 2.8% average inflation rate is expected in consideration of 25 years payback period according to

the 25 year statistics (UK inflation rate, Trading Economics, January 2014). According to energy prices regulated by OFGEM in the UK, the feed in tariff rate for the systems between 4-10 kW is £0.135 and export in tariff rate for selling excess power to the grid is £0.0464 (Feed-In-Tariffs Scheme (FITs), January 2014). In consideration of the electricity power price trend for renewables, the tariff rate is estimated to rise by 6% annually. Details of the costs, economic parameters and component prices are shown in Tables 5.4 and 5.5.

Table 5.4 Solar system components and costs

Item	Cost
PV modules	£13,440
Inverter	£500
Polyethylene heat exchanger	£300
Water storage	£350
Pump (*2)	£70
Pipe	£40
O&M	£110
Capital cost	£16,000

Table 5.5 Economic parameters

Parameter	Value
Electricity price per kWh	Feed-in-tariff (home use): £0.135 Export tariff (to the grid): £0.0464
Down payment	10%
Inflation rate of electricity price	6%
Inflation rate of council tax	4%
Inflation rate of inverter price	3.5%
Inflation rate (1989 – 2014)	2.8%

Interest rate (1971 – 2014)	8.2%
Income tax rate	20%
UK discount rate	8.75%
Council tax for extra property (% of principal)	2%

The inverter used for the system has standard 5-year manufacturer warranty and is expected to be replaced at the end of each 5-year periods. Its price is estimated to grow by an average of 3.5% annually. The average effective income tax rate is estimated to be 45% throughout the life cycle.

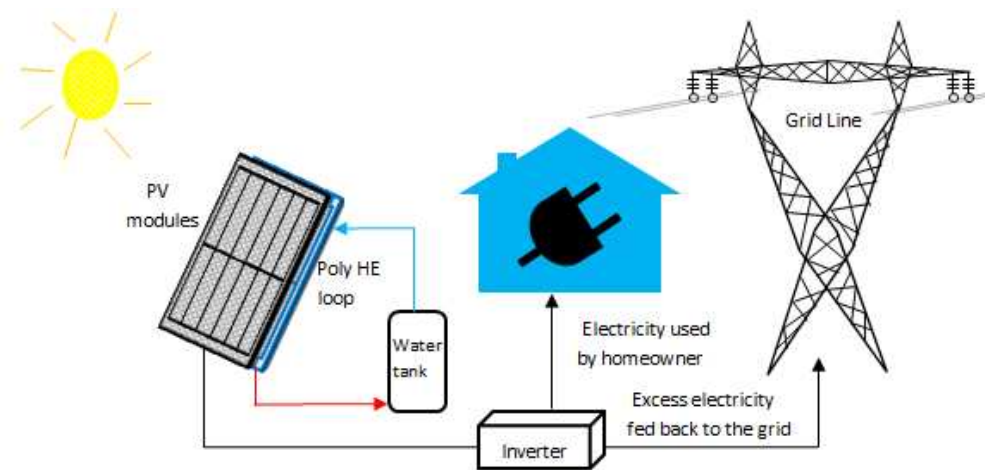


Figure 5.2.5 Schematic of the use of power produced by the solar energy system

For the economic assessment of the proposed system, the Life Cycle Cost (LCC) calculation is used that LCC takes into account the complete range of costs and time equivalent of cash flows.

Solar savings (SS) is the difference between unit cost of the produced energy (CUE) and feed in tariff rate (FIT) and export in tariff of power which is given in kWh by (Chong et al., 2011):

$$SS = (FIT+EIT) - CUE \quad (5.43)$$

Income tax savings of the system can be expressed as (Chong et al., 2011):

$$ITS = ETR \times (IP + PT) \quad (5.44)$$

The present worth factor (PWF) is taken into consideration to assess the economic gain of the system. If annual periodic payments inflate at a rate of i per annum, PWF of the amount is obtained by the equation (Chong et al., 2011):

$$PWF(N, i, d) = \sum_{j=1}^N (1+i)^{j-1} / (1+d)^j \quad (5.45)$$

where N , i and d are the period of the economic assessment, inflation and discount rates, respectively. Then, the present value (PV) of a payment or income at the end of N^{th} period is determined by the following equation (Chong et al., 2011):

$$PV = 1 / (1+d)^N \quad (5.46)$$

Present value (PV) is the expression of the return value of future payments or incomes to present value on a given period. Then, the net present value (NPV) is obtained by the sum of all present values of the individual cash flows.

5.3 RESULTS AND DISCUSSION

Various heat transfer coefficients of the system and design parameters applied in this study are presented in Tables 5.1 and 5.2. The wind speed is observed over the course of tests in order to find out the heat flow rate through natural convection between the PV cover and the ambient. The average data of solar radiation (I), outside temperature and wind speed belonging to the test days (8th July-3rd August 2013 between hours 8am and 5pm) are given. The design parameters and climate data in Tables 5.1-5.3 have been manipulated to assess the water and cell temperatures in Figures 5.6 and 5.7. The root mean square percent deviation and correlation coefficient have also been evaluated and presented in the same figures which are obtained by Equations. 24 and 25, respectively.

Figure 5.6 demonstrates the variations of effective PV module temperature $(T_{PV})_{\text{eff}}$, and water temperature T_w with the ambient temperature, T_a throughout the test

period. It can be clearly observed that the PV module temperature is higher than the water temperature as expected. The increase in water temperature reaches up to 16°C throughout the testing. Considering the changes in temperature tendencies and rise in water temperature, there is a fair agreement with the results obtained by (Tiwari et al., 2006).

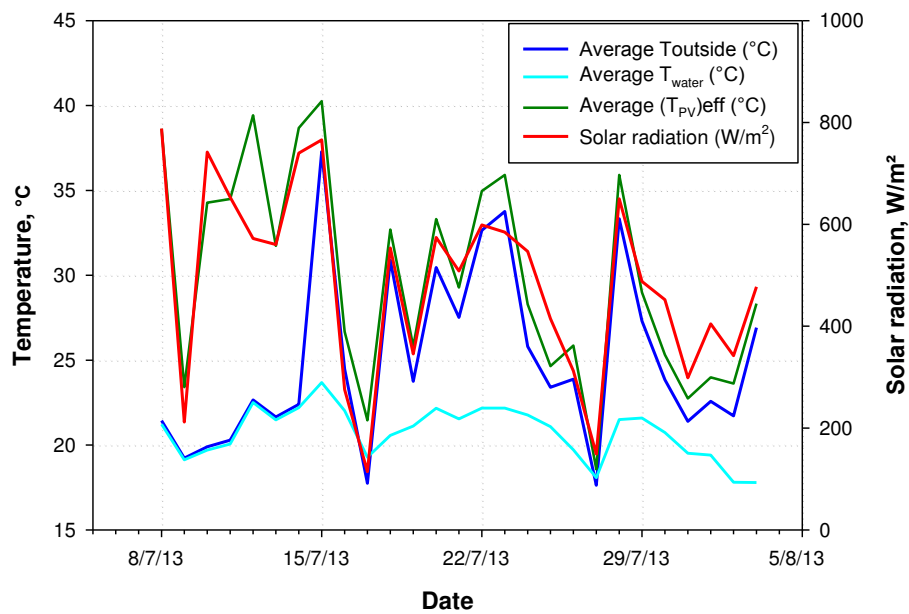


Figure 5.3.1 variation of temperature: $(T_{PV})_{eff}$, T_a , and T_w (8th July-3rd August 2013)

Figure 5.7 compares the theoretical and experimental average values of effective PV module temperature $(T_{PV})_{eff}$. The theoretical values considering the effects of polyethylene heat exchanger indicate that $(T_{PV})_{eff}$ (THE) are in accordance with the experimental values, $(T_{PV})_{eff}$ (EXP). The correlation coefficient and root mean square are attained as 0.94% and 5.1%, respectively.

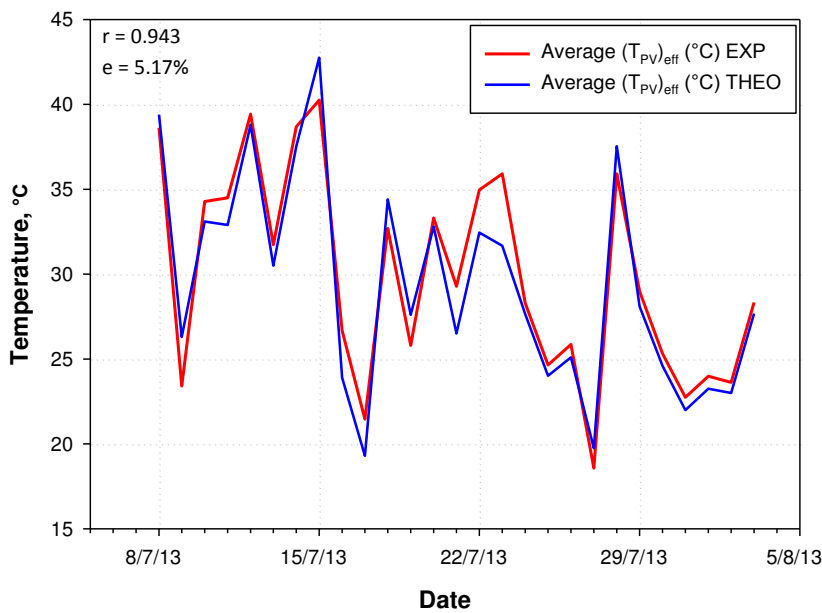


Figure 5.3.2 variation of PV module temperature - theoretical and experimental

Figure 5.8 displays the variations of experimental and theoretical values of the water temperature in the system throughout the test period. Despite higher theoretical water temperature, the correlation coefficient and root mean square percent deviation are attained as 0.96% and 7.66% respectively. These values clearly support the validity of the model adapted in the current study.

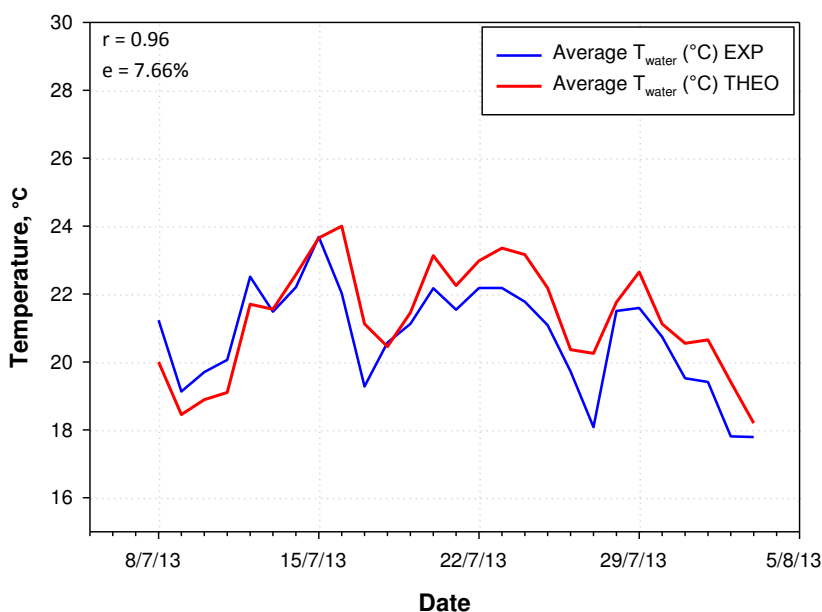


Figure 5.3.3 variation of water temperature - theoretical and experimental

Figure 5.9 exhibits the effects of mass flow rate and water pressure together on the hourly variation of water temperature. The graph illustrates that water mass flow rate and pressure has a minuscule effect on the hourly variation of water temperature over the range of pressure and flow rate considered.

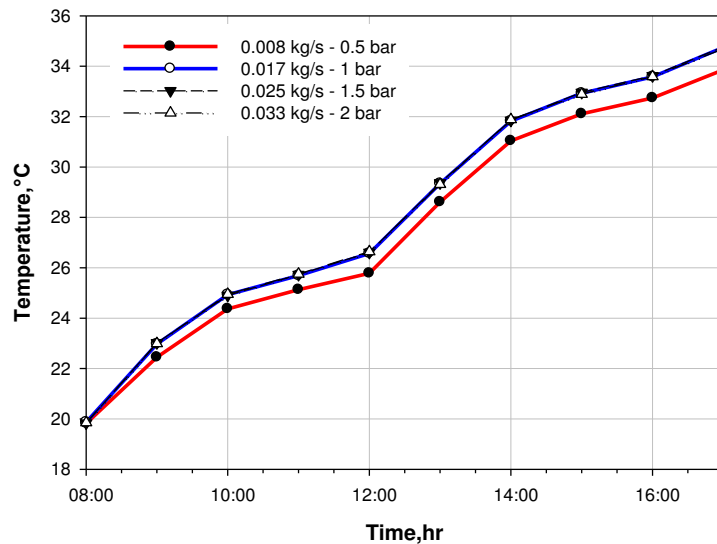


Figure 5.3.4 variation of average water temperature with various mass flow rate (kg/s) and pressure (bar)

Figure 5.10 shows the impacts of various wind speeds recorded on hourly variation of the water temperature. One can conclude that the water temperature evidently drops with the increasing wind speed blowing over PV modules. This is because the increasing heat losses from panel surfaces through the glass cover.

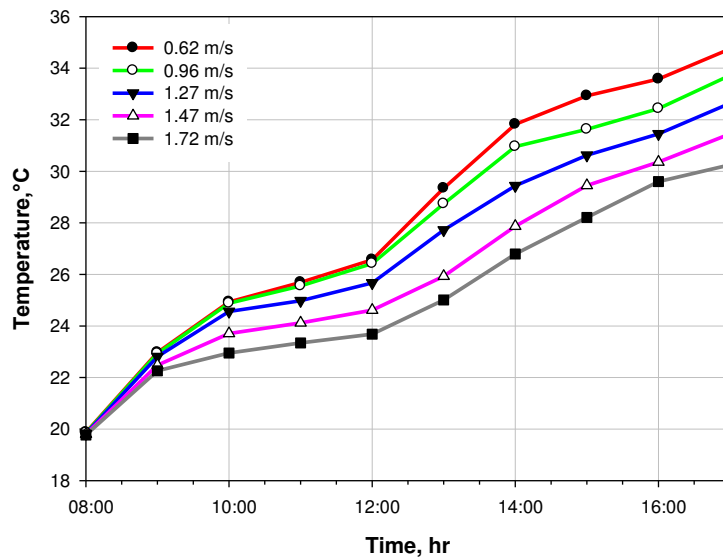


Figure 5.3.5 variation of average water temperature with various wind speed in m/s

Figure 5.11 presents the collector efficiency as a function of the ratio of the difference between the working fluid inlet and ambient air temperatures to the solar insolation incident on the collector surface. The thermal efficiency varies adversely with increasing $(T_w - T_a)/I$ ratio. The momentarily changing climate conditions could have various impacts over the thermal efficiency of the system as follows: lower ambient temperature may lead to higher heat dissipation to the environment, thus causing to lower thermal efficiencies. Higher solar insolation leads to enhanced heat transfer from PVs to the heat exchanger and this will consequently tend to greater efficiencies. Moreover, higher inlet temperatures of the water results in lower efficiencies due to reduced heat transfer across the poly heat exchanger. Confined frame of PV modules also enables to prevent higher heat dissipation to the ambient, so that PV modules could be mentioned as a good heat source to the water flowing through polyethylene tubes and risers. The emissivity is also lower and relatively higher thermal conductivity should also be noted.

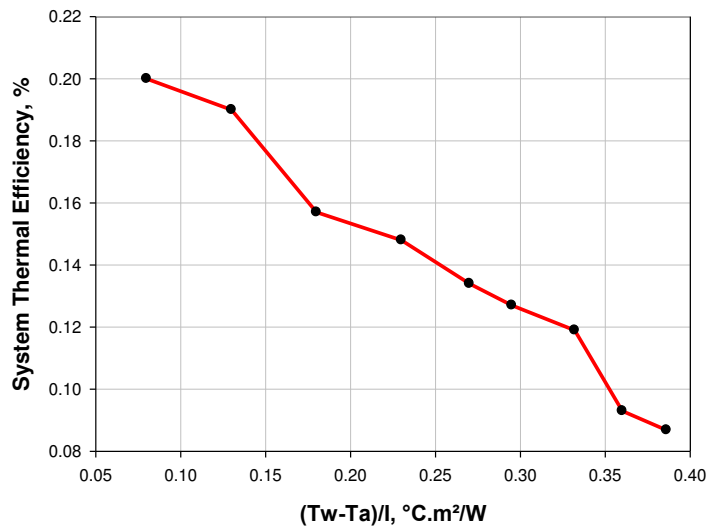


Figure 5.3.6 Effect of fluid temperature on the overall thermal efficiency

Figure 5.12 illustrates the degree of influence of Polyethylene heat exchanger on η_{pv} . For with Poly HE conditions, the increase of cell efficiency through cooling off would lead to an increase of η_{pv} . On the contrary, higher cell temperature would lead to a decrease of η_{pv} . Nevertheless, it has been found that for both cases examined in this study, η_{pv} is always better in the with Poly HE condition than in the without Poly HE condition. This implies that from the viewpoint of the first law of thermodynamics, the “with Poly HE” condition would be a better choice for PV systems to maximizing the overall energy output.

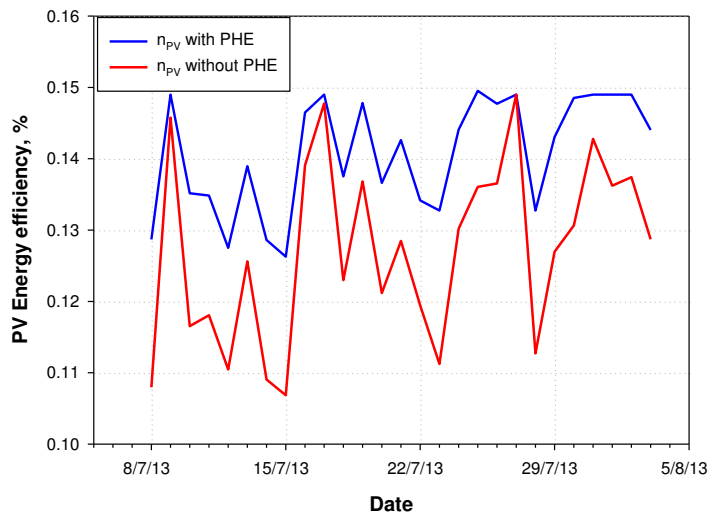


Figure 5.3.7 Effect of poly HE on PV power energy efficiency

Figure 5.13 indicates the findings from exergy efficiency analysis of the proposed system. Enhanced PV cell efficiency will benefit exergy efficiency (ϵ_{PV}) so it is apparently a favourable case from the photovoltaic viewpoint. On the whole, ϵ_{PV} is enhanced with the enhanced cell efficiency in this case. ϵ_{PV} of the 'with Poly HE' exceeds the 'without Poly HE' condition. Similarly, one can conclude that the favourable case outweighs the PV-only case.

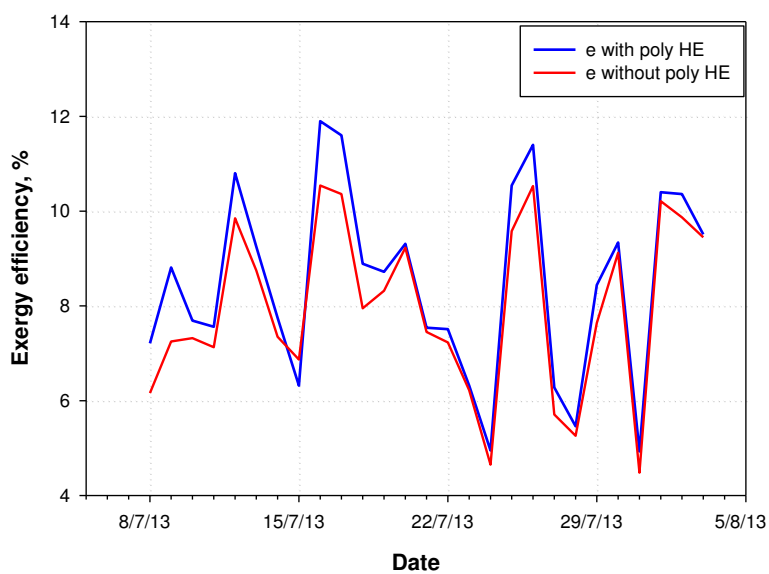


Figure 5.3.8 Effect of poly HE on PV exergy efficiency

5.3.1.1 Financial Assessment

The NPV (Net Present Value) of the system is £15719.5 at the market discount rate of 8.75% over a 25-year period. The sum of the annual present values is the NPV of the gains from the system. The financial calculations are shown in Table 5.6. The economic analysis indicates that cash flow turns positive at year 3 for the first time. However, it becomes negative again due to the converter replacement on years 6 and 11. After the year 11, the cash flow stays positive permanently until the end of the life cycle (Figure 5.14).

Payback time can be expressed in several different ways. The remarking points deducted from Table 5.6 and Figure 5.15 are as follows; the cumulative energy cost savings (£17767.2) surpass the primary capital in year 11. In the following year, the cumulative solar system savings become positive. The cumulative solar system savings (£5122.9) surpass the remaining principal balance (£4698.9) by the end of year 18.

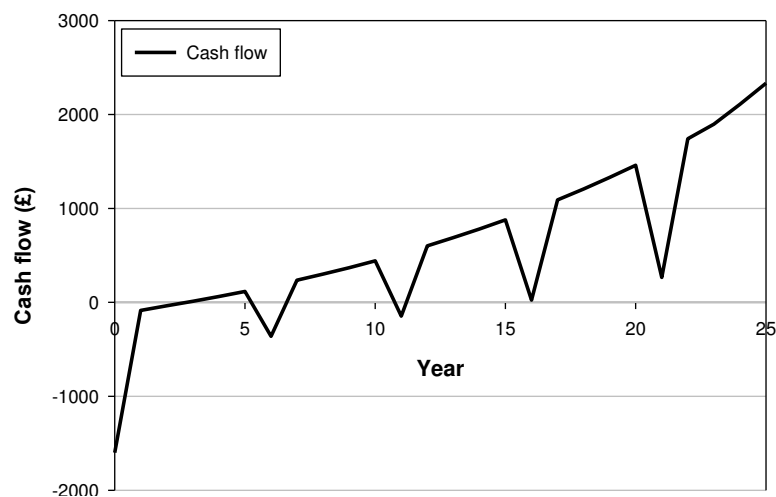


Figure 5.3.9 Annual Present Value of the system savings over the 25-years life cycle period

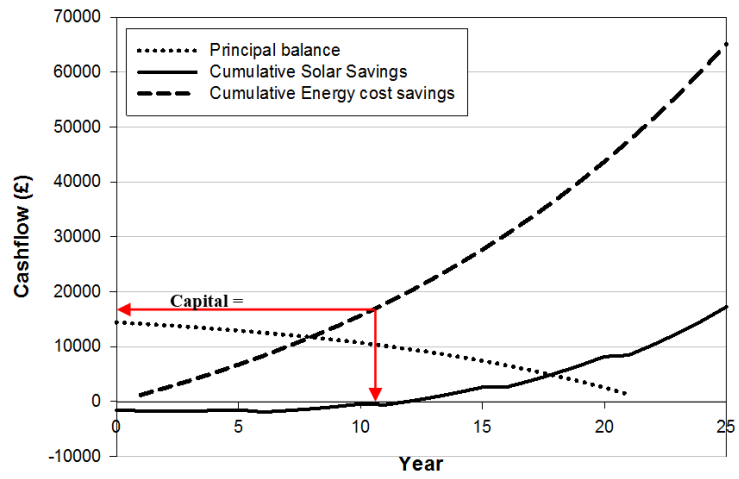


Figure 5.3.10 Variation of PB, Cum. SS and Cum. ECS as a function of time over 25-year life cycle

Table 5.6 the economic analysis of the proposed system (in £) for Nottingham, UK over 25-year life cycle

year	Energy generation (kWh/year)	Cost of energy (£)	Mortgage payment	Interest in year	Principal payment	Principal balance	Inverter replacement	Extra O&M Cost	Council tax for extra Property	Income tax savings	SS (solar savings)	Present Value of Solar savings	Cum. Solar Sys. Savings	Cum. Energy cost savings
0	10300					14,400					(1600)	(1600)	(1600)	
1	10300	1186.7	(1434.84)	1180.8	254.1	14145.9	-	(200)	(320)	675.4	(92.8)	(85.3)	(1692.8)	1186.7
2	10300	1257.9	(1434.84)	1159.9	274.9	13871.1	-	(202)	(332.8)	671.8	(39.9)	(36.8)	(1732.7)	2444.6
3	10300	1333.4	(1434.84)	1137.4	297.4	13573.7	-	(207.7)	(346.1)	667.6	12.4	11.4	(1720.4)	3778.1
4	10300	1413.4	(1434.84)	1113.1	321.8	13251.9	-	(213.5)	(359.9)	662.9	67.9	62.5	(1652.4)	5191.5
5	10300	1498.21	(1434.84)	1086.7	348.2	12903.7	-	(219.5)	(374.4)	657.5	127.0	116.8	(1525.4)	6689.7
6	10300	1588.1	(1434.84)	1058.1	376.8	12526.9	(581.7)	(225.6)	(389.3)	651.4	(391.9)	(360.4)	(1917.3)	8277.8
7	10300	1683.4	(1434.84)	1027.2	407.7	12119.3	-	(231.9)	(404.9)	644.5	256.2	235.6	(1661.1)	9961.1
8	10300	1784.4	(1434.84)	993.8	441.1	11678.3	-	(238.4)	(421.1)	636.7	326.8	300.5	(1334.4)	11,745.5
9	10300	1891.5	(1434.84)	957.6	477.2	11201.1	-	(245.1)	(437.9)	628.0	401.6	369.3	(932.8)	13,636.9
10	10300	2004.9	(1434.84)	918.5	516.4	10684.7	-	(251.9)	(455.5)	618.3	480.9	442.3	(451.8)	15,641.9
11	10300	2125.3	(1434.84)	876.2	558.7	10126.0	(724.3)	(258.9)	(473.7)	607.4	(159.2)	(146.4)	(610.9)	17,767.2
12	10300	2252.8	(1434.84)	830.3	604.5	9521.5	-	(266.3)	(492.6)	595.3	654.4	601.7	43.4	20,019.9
13	10300	2387.9	(1434.84)	780.8	654.1	8867.4	-	(273.7)	(512.3)	581.9	748.9	688.7	792.3	22,407.8
14	10300	2531.2	(1434.84)	727.2	707.7	8159.7	-	(281.4)	(532.8)	567	849.2	780.8	1641.5	24,939
15	10300	2683.1	(1434.84)	669.1	765.8	7393.9	-	(289.3)	(554.1)	550.5	955.3	878.4	2596.8	27,622.1
16	10300	2844.1	(1434.84)	606.3	828.5	6565.4	(1041.2)	(297.3)	(576.3)	532.2	26.5	24.4	2623.3	30,466.1
17	10300	3014.7	(1434.84)	538.4	896.5	5668.9	-	(305.7)	(599.4)	511.9	1186.8	1091.3	3810.1	33,480.8
18	10300	3195.6	(1434.84)	464.9	969.9	4698.9	-	(314.2)	(623.3)	489.7	1312.9	1207.2	5122.9	36,676.4
19	10300	3387.3	(1434.84)	385.3	1049.5	3649.4	-	(323.1)	(648.3)	465.1	1449.3	1329.9	6569.2	40,063.7
20	10300	3590.5	(1434.84)	299.3	1135.6	2513.9	-	(332.1)	(674.2)	438.1	1587.5	1459.8	8156.7	43,654.2
21	10300	3806	(1434.84)	206.2	1228.7	1285.2	(1448.5)	(341.4)	(701.2)	408.3	288.4	265.2	8445.1	47,460.2
22	10300	4034.3	(1434.84)	105.4	1329.5	(44.3)	-	(350.9)	(729.2)	375.6	1894.9	1742.5	10,340.1	51,494.5
23	10300	4276.4	(1434.84)	(3.6)	1438.5	(1482.8)	-	(360.8)	(758.4)	341.3	2063.7	1897.7	12,403.7	55,770.9
24	10300	4532.9	(1434.84)	(121.6)	1556.4	(3039.2)	-	(370.9)	(788.7)	354.9	2293.5	2108.9	14,697.2	60,303.9
25	10300	4805	(1434.84)	(249.2)	1684.1	(4723.3)	-	(381.3)	(820.3)	369.1	2537.7	2333.6	17,234.9	65,108.8
												15,719.5		

5.4 DISCUSSION & CONCLUSIONS

This chapter of the communication presents the integration of first-of-its-kind polyethylene heat exchanger with PV modules along with the performance test results, energy and exergy evaluation and techno-economic analysis of the roof integrated unit under Nottingham's climate conditions. The numerical models are validated by experimental results collected between 8th of July and 3rd of August 2013. The impacts of climate conditions and operating parameters on the system performance were investigated. An LCC based techno-economic analysis was carried out. The remarking points could be outlined as below;

The validation of an adapted version of a prevalently available thermal model for the building Integrated PV/T Roof Collector was carried out by comparing the predicted results with the experimental data. The comparative results indicate that the theoretical model makes a good compliance with the experimental results obtained.

Overall results show that the flowing water generates passive cooling effect and removes waste heat from the PV modules. As given in the results and discussion part, water temperature can increase up to 16°C depending significantly on outside parameters, mostly affected by ambient temperature and global solar radiation.

The PV modules can yield better power energy performance due to achieved collector cooling. Hence the increased performance of the PV/T system will contribute to mitigate the energy supply of buildings and eventually reduce CO₂ emission towards a sustainable environment. Other than the performance, removing waste heat away from

the PV collectors can enhance the life cycle of modules since high operating temperatures may shorten the life-span.

Based on numerical models validated by experimental data, the energy and exergy efficiency of the system 'with poly heat exchanger' was found always better. This case was examined within the scope of study for five operating parameters, namely, cell efficiency, packing factor, solar radiation, ambient temperature and natural convective heat transfer due to the wind velocity. Hence if a system is designed targeting at acquiring thermal energy and more power energy output in quantity, the polyethylene heat exchanger can be a good choice.

The LCC based economic analysis proves that purchase, operation and maintenance are covered in the lifetime of the system. The annual energy savings is 10.3 MW and the Net Present Value (NPV) was calculated as £15,719.5 for the 25-year life span of this project.

As a conclusion, the increase of PV cell efficiency and acquiring thermal energy could be perceived as favourable factors for utilizing poly heat exchanger. Hence, it is feasible and desirable to apply the integration of polyethylene heat exchanger with PV modules to supply hot water for multi-purpose use. The experimental results reveal that substantial amount of energy savings can be achieved by taking advantage of solar waste heat via installing polyethylene heat exchanger on the rear-side of the PV modules.

Polyethylene heat exchanger with the unique structure can act as an efficient and cost-effective heat extraction component for domestic water heating, solar assisted heating-

cooling technologies and solar dryers etc. Therefore, the next chapter investigates the performance the new roof unit coupled with solar thermal energy driven liquid desiccant based dew point cooling system that integrates several green technologies; including photovoltaic modules, polyethylene heat exchanger loop and a combined liquid desiccant dehumidification-indirect evaporative air conditioning unit.

CHAPTER 6 – Experimental investigation of the building integrated PV/T roof collector combined with a liquid desiccant enhanced indirect evaporative cooling system

6 EXPERIMENTAL INVESTIGATION OF A BUILDING INTEGRATED PV/T ROOF COLLECTOR COMBINED WITH A LIQUID DESICCANT ENHANCED INDIRECT EVAPORATIVE COOLING SYSTEM

6.1 INTRODUCTION

Utilization of sunlight for cooling is a long-sought goal. As the demand for cooling is proportional to the solar intensity, thus the time of peak cooling need coincides with the time of maximum resource occurs. Given this relation, it is no doubt that there has been a considerable interest to produce cost effective solar cooling technologies. Heat-activated systems that mainly driven by heat input from solar thermal energy have been introduced allowing simultaneous production of heat and cooling/refrigeration (Otanicar et al., 2012). Compared to the conventional vapour compression systems, thermally driven air-conditioning technique would be an effective alternative in terms of increasing primary energy savings with less power consumption and therefore less greenhouse gas emissions and hazardous materials and pollutants depleted to the environment (Jradi et al., 2014).

A number of experimental investigations have been introduced in the literature for solar cooling systems. Huang et al. (2011) conducted an experimental study of solar heat driven ejector cooling system for cooling load of 3.5 kW and cooling time of 10 h within two locations; Taipei and Tainan, respectively. Bermejo et al. (2010) investigated a hybrid solar/gas cooling plant composed of a double effect LiBr + water absorption chiller with cooling capacity of 174 kW, a linear concentrating Fresnel collector and direct-fired natural gas burner. Another experimental study was performed by Ge et al. (2010) employing a two-stage solar driven rotary desiccant cooling system with newly developed silica gel-haloid composite desiccant to achieve reducing regeneration

temperature and high energy performance. A solar electric-vapor compression refrigeration system was tested by Bilgili, M (2011). Eicker et al. (2011) developed and tested a new photovoltaic-thermal (PVT) system to produce both power and cooling energy for night radiative cooling of buildings.

In addition, several studies have investigated the solar assisted liquid desiccant cooling systems. To name a few, Katejanekarn et al. (2009) presented an experimental study of a solar-regenerated liquid desiccant ventilation pre-conditioning system in hot and humid climate of Thailand. They reported 1.2°C temperature drop and 11.1 % relative humidity reduction of the delivered air. Li et al. (2010) experimentally studied an open cycle solar desiccant dehumidification air-conditioning system in Hong-Kong and a payback period around 7 years was reported. In another study (Bourdoukan et al., 2009), the authors experimentally investigated a desiccant air handling unit powered by vacuum tube solar collectors in a moderately humid climate with regeneration solely by solar energy and the electrical consumption based performance indicator was found to be 4.5. Few researchers have studied the solar enhanced liquid desiccant air conditioning (Bongs et al., 2012; Abdel-Salam et al., 2014; Luo et al., 2012; Zeidan et al., 2011), indicating that solar assisted liquid desiccant cooling systems have a large potential especially in hot and humid areas but additional research and development is still needed to prove their potential.

Combining solar power and a liquid desiccant cooling system can provide cooling demands for residential and building applications in addition to thermal comfort and indoor air quality. Although substantial studies have been performed on the investigation of the regenerators of liquid desiccant cooling systems from solar thermal

applications, regeneration heat capture by such a unique heat exchanger loop with PV modules has yet to be considered. In this study, the performance of the liquid desiccant cooling system with polyethylene heat exchanger loop unit driven regenerator unit is experimentally investigated. The proposed system comprises polyethylene roof loop, a desiccant cooling system with a liquid desiccant-based dehumidification unit and an indirect evaporative cooling unit to dehumidify and cool the supply air. An experimental unit was set up and the system elements were examined experimentally. The system arrangement is described and experimental data is reported.

6.2 SYSTEM CONFIGURATION

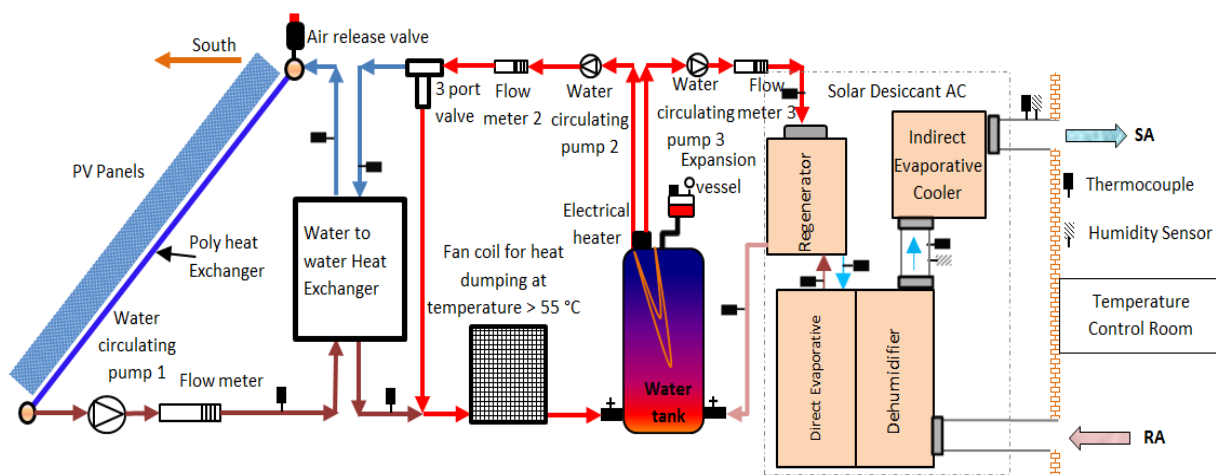


Figure 6.2.1 The system configuration of the combined system

The overall configuration of the combined system is presented in Figure 6.1. The operation of the system is divided into three main processes; roof, dehumidification and cooling. A polyethylene heat exchanger is employed to capture heat from solar PV system to supply regeneration heat to regenerate the dilute desiccant solution. Regeneration temperature is decisive in configuration of many solar driven desiccant air conditioning systems and at around 60-70°C to the desiccant regenerator as shown

Figure 6.1. The desiccant cooling unit utilized in this system can provide thermal comfort and good indoor air quality through the desiccant dehumidification. An indirect evaporative cooling unit is also integrated with the liquid desiccant dehumidification unit to supply supplementary cooling effect to fulfil the cooling demands. The proposed system can operate in both dry and humid regions as employing an integrated liquid desiccant-dew point evaporative cooling unit. In humid environmental conditions, ambient air is dehumidified through the liquid desiccant dehumidification process and then introduced to the dew-point cooling system for cooling effect. However, ambient air can be plainly supplied to the indirect evaporative cooler without any need of a dehumidification process. Next section is about built-up of the experimental system and description of the sub-units.

6.2.1 Experimental setup

6.2.1.1 Roof Unit

Building integrated photovoltaic thermal (BIPVT) systems, inherently, have potential to appear as a major source of renewable energy on the roof top of a building to generate electrical energy and produce thermal energy required for thermal applications (Agrawal et al., 2010). This hybrid technology combines PV and solar thermal components into a single module to boost the solar conversion efficiency and achieve economical use of space. However, as PV/T is a newly emerged technology, various technical challenges relevant to PV/T found in practice e.g., current technical status, difficulties and problems that prevented wide-scale applications of these systems (Zhang et al., 2012). Moreover, inability of converting already-built photovoltaic (PV) systems into PV/T systems could be also mentioned as a practical drawback. Therefore, polyethylene heat exchanger as

a concealed heat extraction component without damaging original configuration of PV modules represent an effective solution to fulfil aforementioned pitfalls and practical limitations of the existing systems. Moreover, polyethylene heat exchanger propitiously blends into its surroundings free from any ‘add-on’ appearances and has a dual function as absorbing heat and passively cooling of photovoltaic modules via extracting waste heat from solar panels.

Employing 84 Sharp NU-R245 (J5) PV modules in the system, incoming solar energy initially absorbed by the PV cells can be expressed as:

$$Q_{\text{abs}} = \tau_c \cdot \alpha_{\text{abs}} \cdot A_{\text{eff}} \cdot I \quad (6.1)$$

The part of incoming solar energy is used to generate power energy by silicon cells, partly carried through the heat exchanger and the rest is dissipated to the ambient due to temperature difference between solar module and atmosphere. So, the loss can be expressed:

$$Q_l = h_{\text{cv}} \cdot (T_c - T_a) + \varepsilon_c \cdot \sigma \cdot (T_c^4 - T_s^4) + h_{\text{air}} \cdot (T_{\text{pl}} - T_{\text{heo}}) + \varepsilon_{\text{pl}} \cdot \sigma \cdot (T_{\text{pl}}^4 - T_{\text{heo}}^4) \quad (6.2)$$

Combination above equations can provide a revised expression of the useful heat energy (Q_t):

$$Q_t = Q_{\text{abs}} - Q_l \quad (6.3)$$

Following empirical relation can estimate the PV cover temperature (T_c):

$$T_c = 30 + 0.0175 \cdot (I - 300) + 1.14 \cdot (T_a - 25) \quad (6.4)$$

This relation is not only applied for standard pc-Si PV modules but in PV/T systems, the relation also accounts for the system operating conditions, such as the effect of heat extraction fluid. Therefore, the parameter ($T_{\text{PV}}\text{eff}$) is considered to correspond to the PV

module temperature in terms of operating conditions of PV/T systems. Thus, for the proposed system, $(T_{PV})_{eff}$ is given by:

$$(T_{PV})_{eff} = T_c + (T_{PV/T} - T_a) \quad (6.5)$$

McAdam's widely used convective heat transfer coefficient of the ambient air in solar collector theory:

$$h_{cv} = 5.7 + 3.8 \cdot V \quad (6.6)$$

The sky temperature as a function of the ambient temperature can be obtained by Swinbank's equation:

$$T_s = 0.037536 \cdot T_a^{1.5} + 0.32 T_a \quad (6.7)$$

Where h_{rd1} and h_{rd2} are the radiation heat transfer through front and rear side of the collectors, respectively and given by:

$$h_{rd1} = \varepsilon_c \cdot \sigma \cdot (T_c^4 - T_s^4) \quad (6.8)$$

$$h_{rd2} = \varepsilon_{pl} \cdot \sigma \cdot (T_{pl}^4 - T_{heo}^4) \quad (6.9)$$

The associated convective heat transfer coefficient, h_{air} , assuming a natural convective stagnant air layer between the PV module and heat exchanger can be expressed as:

$$h_{air} = \frac{Nu \cdot K_{air}}{\delta_{air}} \quad (6.10)$$

Where thermal conductivity of air is K_{air} and thickness of the air layer between PV and heat exchanger is δ_{air} , respectively. Then Nusselt number can be given by:

$$Nu = \left[0.06 - 0.017 \cdot \left(\frac{\beta_s}{90} \right) \right] \cdot Gr^{1/3} \quad (6.11)$$

Then, Grashoff number is given by:

$$Gr = \frac{g \cdot (T_{pl} - T_{heo}) \cdot \delta_{air}^3}{V_{air}^2 \cdot T_{air}} \quad (6.12)$$

In addition, instantaneous thermal efficiency of the roof unit is given by:

$$\eta_t = \frac{Q_t}{A_{eff} \cdot I} \quad (6.13)$$

Conductive heat flow takes place across the PV cover, cell layer, and EVA plastic layer on the panel rear. Under natural convective air layer between PV module and polyethylene heat exchanger, conductive effort, again, takes place between aluminum layer and heat exchanger wall and then, heat is eventually introduced to the water. The heat gain of water is as equal as the useful heat energy itself and is given by:

$$Q_t = A_{eff} \cdot U_t \cdot (T_{abs} - T_w) \quad (6.14)$$

Overall heat transfer coefficient between PV cell and water can be expressed as:

$$U_t = (U_{c,abs} + U_{abs,pl} + U_{heo,hein} + U_{hein,w})^{-1} \quad (6.15)$$

Heat transfer coefficient ($U_{c,abs}$) from cover to PV cell layer (absorber) can be expressed as:

$$U_{c,abs} = \frac{\lambda_c}{\delta_c} \quad (6.16)$$

Then, average temperature at the absorber (cell layer) becomes:

$$T_{abs} = T_c - \frac{Q_t}{A_{eff} \cdot U_{c,abs}} \quad (6.17)$$

Heat transfer coefficient ($U_{\text{abs,pl}}$) from PV cell (absorber) to the EVA plastic layer is given by:

$$U_{\text{abs,pl}} = \frac{\lambda_{\text{abs}}}{\delta_{\text{abs}}} \quad (6.18)$$

The temperature at the outer wall of the polyethylene heat exchanger is given by:

$$T_{\text{pl}} = T_{\text{abs}} - \frac{Q_t}{A_{\text{eff}} \cdot U_{\text{abs,pl}}} \quad (6.19)$$

Heat transfer coefficient ($U_{\text{heo, hein}}$) from outer wall to interior wall of heat exchanger is given by:

$$U_{\text{heo,hein}} = \frac{2 \cdot \pi \cdot \lambda_{\text{he}}}{\ln \left[\frac{D_o}{D_i} \right]} \quad (6.20)$$

The average temperature at the inner wall of polyethylene heat exchanger is given by:

$$T_{\text{hein}} = T_{\text{heo}} - \frac{Q_t}{A_{\text{eff}} \cdot U_{\text{heo,hein}}} \quad (6.21)$$

Heat transfer coefficient ($U_{\text{hein, r}}$) from interior wall of heat exchanger to the water is given by:

$$U_{\text{hein,w}} = \frac{\text{Nu}_r \cdot \lambda_r}{D_i} \quad (6.22)$$

Where Nusselt number is given by:

$$\text{Nu}_r = 0.023 \cdot \text{Re}_r^{0.8} \cdot \text{Pr}_r^{0.4} \quad (6.23)$$

The root mean square percent deviation (e) and the coefficient of correlation (r) is computed in order to match the theoretical results with the experimental outcomes by using the following expressions:

$$e = \sqrt{\frac{\sum(e_i)^2}{N}} \text{ where } e_i = \left[\frac{X_i - Y_i}{X_i} \right] \times 100 \quad (6.24)$$

$$r = \frac{n(\sum X \times Y) - (\sum X) \times (\sum Y)}{\sqrt{n(\sum X^2) - (\sum X)^2} \times \sqrt{n(\sum Y^2) - (\sum Y)^2}} \quad (6.25)$$

Stating the expressions by:

$$m^2 = \frac{U_t}{K\delta} \quad (6.26)$$

Then, the fin efficiency factor (F) can be given as:

$$F = \frac{\tanh m \frac{W - D_o}{2}}{m \frac{W - D_o}{2}} \quad (6.27)$$

The flat plate collector efficiency (F') then becomes:

$$F' = \frac{1}{\frac{WU_t}{D_o U_{\text{abs,pl}}} + \frac{WU_t}{\frac{K}{\delta}} + \frac{WU_t}{D_o + (W - D_o)F}} \quad (6.28)$$

The flow rate factor (F_R) is given as:

$$F_R = \frac{\dot{m}C_f}{A_{\text{eff}}U_t F'} \left[1 - \exp\left(-\frac{A_{\text{eff}}U_t F'}{\dot{m}C_f}\right) \right] \quad (6.29)$$

The mass flow rate (\dot{m}) of water is calculated for the measured experimental values of average solar intensity, and outside temperature for the given test period. Given values

are used to evaluate the water temperature and solar cell temperature of the PV modules for validation.

6.2.1.1.1 Energy Efficiency

In order to determine the instantaneous power energy efficiency and power output, some of the widely used energy equations are employed as below;

Temperature dependent power energy efficiency of a PV module (η_e) can be given as:

$$\eta_e = \eta_{rc} (1 - \beta_p (T_c - T_{rc})) \quad (6.30)$$

The rate of instantaneous solar energy available on solar cell and power energy output is given by:

$$Q_e = (\alpha\tau) \cdot \xi \cdot I(t) \cdot A_{eff} \quad (6.31)$$

Packing factor for a PV module is stated as:

$$\xi = \frac{A_{cell}}{A_{coll}} \quad (6.32)$$

The overall configuration of the solar assisted liquid desiccant cooling system is presented in Figure 6.1 with various system components. The system has three main loops; polyethylene heat exchanger loop, dehumidification loop and cooling loop. The proposed roof system consists of polyethylene heat exchanger loop underneath PV modules to form a PV/Thermal roof collector. The complete roof structure has several layers, an outer cover; a layer of photovoltaic cells beneath the cover; EVA plastic layer at the back of PV adjacent to the PV cells layer, polyethylene heat exchanger and roof support. There are eighty four (84) Sharp NU-R245 (J5) photovoltaic solar panels mounted on the roof which are entirely for power generation without any thermal

function. The solar panels will convert part of the incoming solar radiation into power energy due to the photogalvanic effect of the silicon cells and remaining heat energy will be conveyed through the circulating water across the heat exchanger. The hot water can be used for heating & cooling, domestic hot water supply, food drying, natural ventilation inside the building and more. Part of the heat required to drive regeneration unit of the desiccant dehumidification system is expected to be obtained from waste heat dissipated by solar panels.

The PV solar collectors absorb a greater proportion of incoming solar radiation on the PV cell surface, while dissipating remainder to ambient as waste heat. From top to bottom, a transparent and thermally resistant outer cover enables to reduce dissipation and secures that maximum solar radiation reaches the photovoltaic cells. Meanwhile, the temperature of the cell layer needs to be lowered so as to facilitate the solar power conversion efficiency of PV panels. Heat flows from ambient to the photovoltaic cells in case of lower temperature of cell surface. Thus, adjusting circulating water temperature at a lower range helps to reduce the cell surface temperature to some extent. Although first-of-its-kind polyethylene heat exchanger, due to its physical structure, is loosely adhered to the rear surface because of the aluminium frame of the PV modules, less flexible pipes and risers, relatively low temperature difference between the cell surface and circulating water is expected. Furthermore, the physical structure of the poly heat exchanger prevents the use of thermally conductive adhesives due to uneven contact to the rear of PV modules. Consequently, any decrease in the cell temperature will collaterally enhance both power and thermal efficiencies. Solar optical parameters of the PV modules are presented in Table 5.1 in Chapter 5.

The piping system is placed below the roof truss and joint by flexible coupled connectors with valves to provide a leak free connection as previously shown in Figure 5.3 in Chapter 5. The pipes and fittings are engaged tightly via welding with soldering iron. The supply pipe feeds cold water into the polyethylene heat exchanger whilst the return pipe transports the hot water from the heat exchanger. The PV modules and steel corrugated roof support are well clamped together, and polyethylene heat exchanger is located in between. Technical parameters of the PV solar collectors and polyethylene heat exchanger are previously shown in Table 5.2 in Chapter 5.

Circulating pumps should cope with head pressures every time it turns on, in close loop solar roof systems. Also, the pumps must be compatible with solar applications in point of size, hydraulics, speed stages, efficiency and power consumption. The details of the circulation pumps are previously presented in Table 5.2 in Chapter 5.

Thermocouples (K type) with a maximum deviation of $\pm 1.5^{\circ}\text{C}$ and 1.6s of response time were inserted for various temperature measurements. A Kipp & Zonen pyranometer with the sensitivity of $4.47 \times 10^{-4} \text{ V/Wm}^{-2}$ and response time of 1.66s were integrated on a vertical surface (10° South) to measure the global solar radiation. Wind speed meter was also utilized to find out the heat flow rate through natural convection between the PV cover and ambient and connected along with all other measuring devices to a Datalogger DT500 data logger.

6.2.1.2 Liquid Desiccant Dehumidification unit

Recently, substantial amount of research has mainly focused on desiccant substances and their practical applications, particularly on dehumidification and cooling practices (Lowenstein et al., 2006; Daou et al., 2006; Fumo and Goswami, 2002; Bassuoni,

2011). The desiccants are either natural or synthetic materials having the ability of absorbing or adsorbing moisture through water vapour pressure difference between the ambient air and the desiccant surface. They could be solid, either polymer sorbent or porous material as silica gel and zeolite, liquid solution as lithium bromide solution and lithium chloride with water, etc..., (Daou et al., 2006). In terms of energy consumption, desiccant air conditioning systems consume less than a quarter of energy comparing to its counterparts; conventional vapour-compression systems (Lowenstein, 2008). Liquid desiccant dehumidification systems require lower regeneration and have advanced utilization flexibility and low pressure drop on air side (Oliveira et al., 2000). However, as a major drawback of conventional liquid desiccant systems, liquid desiccant particles on the absorbers could be carried along by the process air flow over an extended surface or packing material. This corrosive solution could eventually have a disturbing effect on the indoor air quality and comfort of the residents. Corrosion and carry-over of liquid desiccant can be diminished by employing an effective direct contact core with a semi-permeable micro-porous membrane for direct-liquid contact (Isetti et al., 1997). In this study, a new, basic and low cost heat and mass exchanger core is utilized for liquid desiccant dehumidification. This selectively permeable multiple porous membranes are employed to reduce the carry-over of liquid desiccant particles and increase heat and mass exchange efficiency. Figure 6.3 shows the overall liquid desiccant air conditioning system consisting of a dehumidifier, regenerator and indirect evaporative cooling units.

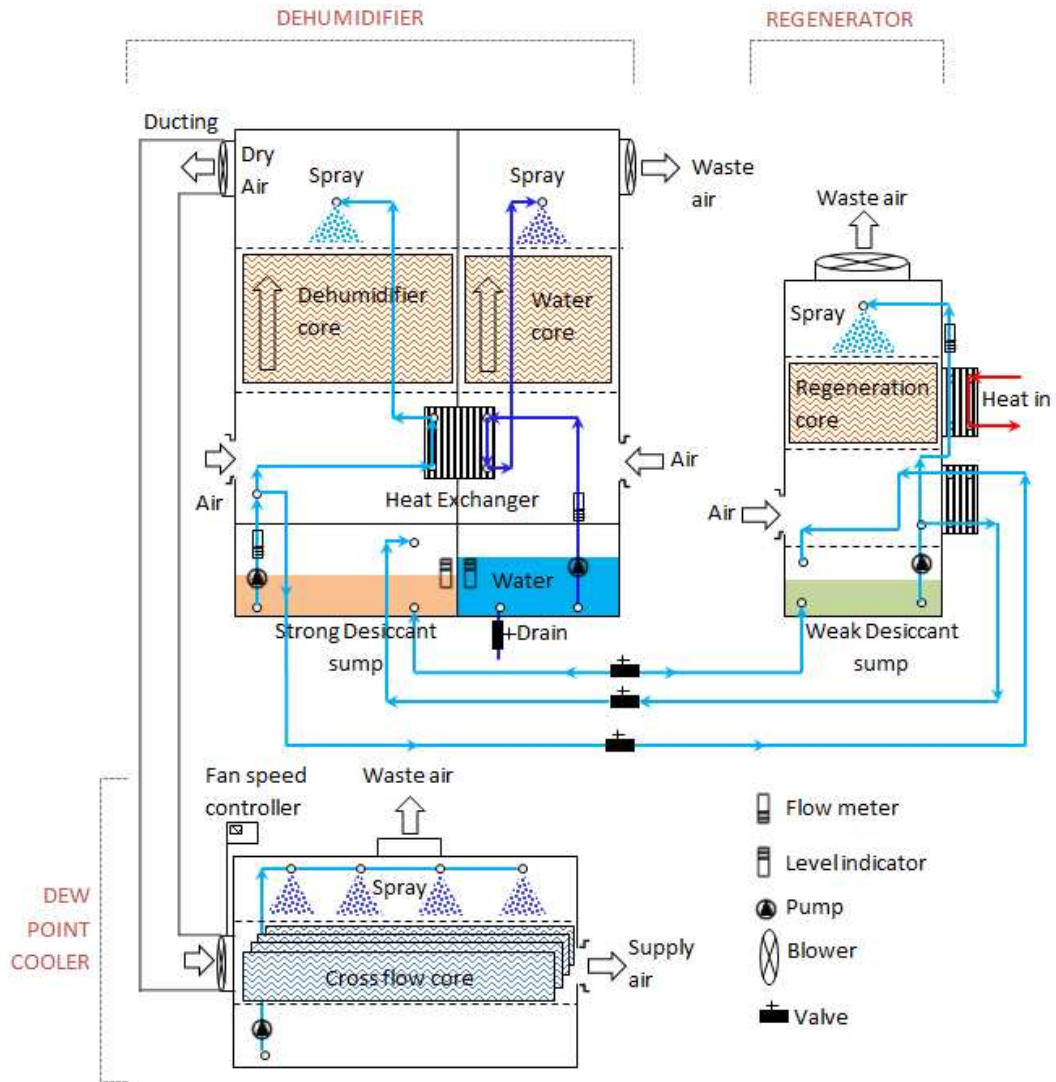


Figure 6.2.2 Liquid desiccant based dehumidification with indirect evaporative cooling unit

The liquid desiccant, in the dehumidifier unit, is sprinkled evenly along the porous membrane of the desiccant core over the humid air flowing upwards whilst the heat and mass exchange between the humid air stream and desiccant solution takes place within the membrane. Moisture from the process air condenses, permeates into the desiccant side and is fully absorbed into the strong desiccant solution. As a result of water absorption, the moisture content of the desiccant solution increases and the strong solution becomes diluted. Also, there is a water core with porous foam membrane in the

dehumidification unit. Water from the sump at the bottom of the unit, as shown in Figure 6.2, is sprayed down over the fresh air streaming upwards that causes water evaporation in the air channel and humidifies the process air. A plate heat exchanger is assembled between the desiccant and water core to allow heat transfer between desiccant and water flows and pre-cool the desiccant solution in the dehumidification process. In addition, a regeneration core with porous foam sheets, similar to the desiccant core, is integrated to the regenerator unit wherein the impure desiccant solution is heated by retrieved solar heat and air flow removes moisture to form a strong desiccant solution. Then, the regenerated desiccant solution is sent back to the desiccant core for better dehumidification performance. In this experimental study, environmentally friendly, relatively less corrosive, lower cost, lower density and viscosity potassium formate (HCOOK) solution was utilized as a liquid desiccant (Riffat et al., 1998).

The performance evaluation of the liquid desiccant air-conditioning system is based on two main parameters, the enthalpy and humidity effectiveness. The humidity, also called moisture, effectiveness is the ratio of actual change in air humidity to the maximum change capacity and can be computed both for the regenerator and dehumidifier units by:

$$\mathcal{E}_w = \frac{W_{a,in} - W_{a,out}}{W_{a,in} - W_{eq}} \quad (6.33)$$

W_{eq} represents the condition for when air humidity ratio at the interfacial area in equilibrium with the liquid desiccant solution, in $\text{kg}_{\text{H}_2\text{O}}/\text{kg}_{\text{air}}$. This moisture content is the

minimum level for ideal air dehumidification and is calculated based on partial vapour pressure of the desiccant solution, P_V by:

$$w_{eq} = 0.62197 \frac{P_V}{1.013 \times 10^5 - P_V} \quad (6.34)$$

Similarly, the enthalpy effectiveness is the ratio of actual enthalpy change in air to the maximum change capacity in ideal conditions and can be calculated both for the dehumidifier and regenerator. Then, it is given by:

$$\varepsilon_h = \frac{h_{a,in} - h_{a,out}}{h_{a,in} - h_{eq}} \quad (6.35)$$

where h_{eq} , J/kg, refers to equilibrium state of air enthalpy with the liquid desiccant solution and can be calculated in terms of air humidity ratio with air temperature equal to the liquid desiccant solution.



Figure 6.2.3 The dehumidifier and regeneration unit

The liquid desiccant dehumidification units utilized in the experimental setup is shown in Figure 6.3. The dehumidifier unit with the outer dimensions of 90x50x130cm has a desiccant core inside the dehumidification part with the dimensions of 50x50x50cm and

water core having with dimension of 35x50x50cm inside the adjacent water cooling part. In addition to the dehumidifier, a regenerator unit is employed with the given dimensions of 30x30x85cm along with a counter flow regeneration core with 30x30x30cm dimensions. There are mainly three pipe connections between the dehumidifier and regeneration units. For those connections, one is for strong desiccant flow to the dehumidifier; another is for weak desiccant flow to the regenerator and the last one for balance of desiccant solution level between two units. Pre-heated hot water from the roof part is first collected in hot water storage and the temperature is detected there if the temperature level is satisfactory for regenerating the weak desiccant solution which is usually at around 60 to 70 °C. It should be noted that the heat source for the desiccant regenerator is of decisive among other units to run the complete desiccant system. If the temperature level is not in desired level, then, an auxiliary three phase water heater submerged in the water tank connected to the solar PV panels heats the water until the desired range of regeneration temperature. For the heat input to regenerate the weak potassium formate (HCOOK) as desiccant solution, a plate heat exchanger is employed in the regeneration unit. 25 litres of desiccant solution having the mass concentration of 75% were stored in the liquid desiccant system. In order to circulate the potassium formate between the dehumidifier and regenerator units, two centrifugal magnetically coupled circulation pumps were integrated enabling secure and leakage free operation. Overall control over the performance of the system covering pumps and fans is handled by a digital controller. HMT130 humidity and temperature transmitters were used for data recording regarding air temperature and humidity at the both inlet and outlet of the dehumidifier and regenerator units. The HMT130 probes used for this experimental

study have operation temperature range of -40 to 80°C with $\pm 0.2^\circ\text{C}$ accuracy and relative humidity range of 0-100% with $\pm 1.5\%$ accuracy and output signal range of 0-10V. Also, liquid desiccant and water temperatures in the system were measured by using thermocouples (K-type) with a maximum deviation of $\pm 1.5^\circ\text{C}$.

6.2.1.3 Indirect Evaporative cooling unit

Evaporative cooling can be an efficient and environmentally attractive alternative to mechanical vapor compression for air conditioning to maintain thermal comfort especially in hot/dry regions. These systems generally consume only a quarter of the electric power that conventional vapor compression systems require. Hence, such systems will save substantial amount of electric power and, therefore, contribute to minimizing greenhouse gas emissions (Riangvilaikul and Kumar, 2010). In addition to the greenhouse gas emission savings, thermally driven desiccant enhanced evaporative cooling systems can potentially lower the peak electricity demand and associated electricity infrastructure expenses (Goldsworthy and White, 2011). Indirect evaporative cooling systems, also called dew point evaporative cooling, use the latent heat of water evaporation as a natural driving resource and usually show high performance as their coefficient of performance (COP) is reported between the ranges of 8-20 (Zhan et al., 2011). Evaporative cooling systems are generally separated into two main techniques as direct and indirect systems. Indirect evaporative systems separate process air from water so does not allow direct contact between air and water, dissimilar to the direct evaporative cooling systems. So, the supply air is cooled sensibly without a significant increase in the moisture content (Qiu et al., 2013). This feature makes IEC systems even more attractive to meet comforting indoor air quality demands. Thus, reducing air

temperature below the wet bulb temperature, or also called sub-wet bulb temperature cooling, has been the main topic of many studies to develop a new and innovative evaporative cooling techniques (Caliskan et al., 2012; Bruno, 2011; Chen et al., 2010). In this regard, indirect evaporative cooling systems, or dew point coolers, aim to reduce air temperature under the wet bulb temperature versus inlet air dew point temperature by using modified heat and mass exchanger configurations, techniques and designs.

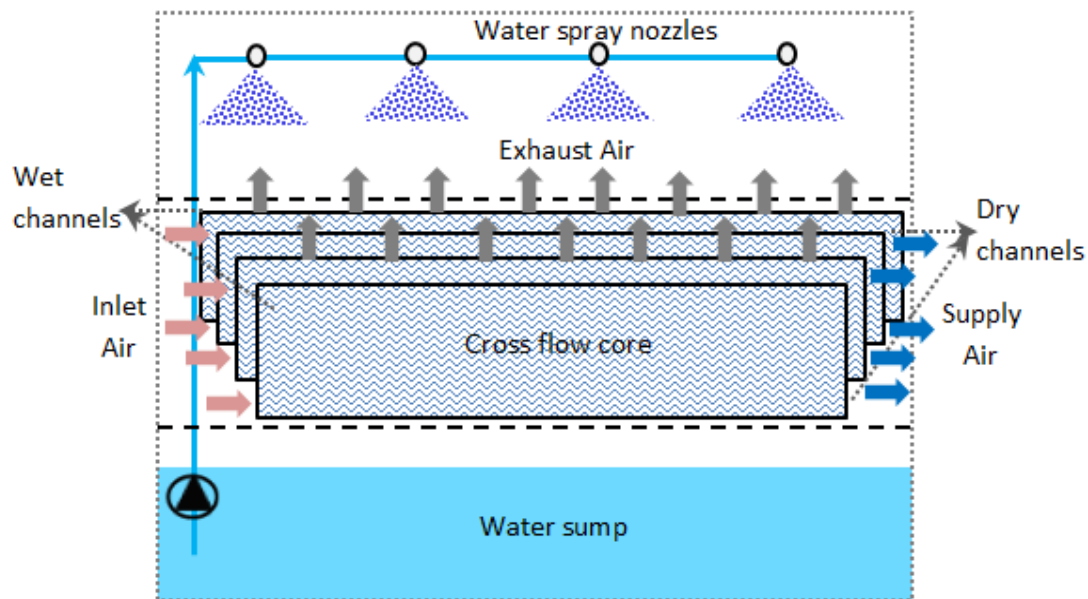


Figure 6.2.4 Schematic diagram of the indirect evaporative cooler

The cross-sectional view of the indirect evaporative cooling system proposed is depicted in Figure 6.4. The unit consists of cross-flow core with fibre sheets stacked together and separated by channel guides located on one side of the each sheet to form adjacent wet and dry channels. Each sheet is coated with polyethylene material to prevent water penetration from the wet channels. Also, the wet channel surfaces are plated with fibrous coating material with superior water absorption ability and large capillary forces to draw off water from the water film surface to allow saturation. The

perforated heat exchanger sheets have orderly deployed numerous holes alongside the flow paths of dry air at the process air flow area. As shown in Figure 6.4, the shape of the heat and mass exchanger disperses air from the dry channels to the wet channels through perforations to create air flows perpendicular to the primary air flow. As a result of heat and moisture exchange, the warmer and highly saturated air is evacuated to the atmosphere. The pre-cooling process of the process air can create a major temperature difference between the wet and dry channels so that heat absorption capacity and cooling effectiveness of the system increase substantially.

The entire cooling capacity of the indirect evaporative cooling unit can be obtained by:

$$Q_{\text{cool}} = \dot{m}_{\text{sa}} (h_{\text{in}} - h_{\text{sa}}) \quad (6.36)$$

As widely known, the indirect evaporative cooler coefficient of performance is the ratio of the overall cooling capacity to the electric power consumed during the operation. In dew point cooler case, there are two equipment that consume the overall electric power, water circulation pump to run the water from water tank to the distribution nozzles and air supply fan. Then, COP of the system is given by:

$$\text{COP}_{\text{ev.cooler}} = \frac{Q_{\text{cool}}}{\dot{W}_{\text{elec,cooler}}} \quad (6.37)$$

The indirect evaporative cooler unit effectiveness can be evaluated by two important parameters, dew point effectiveness and wet bulb effectiveness and are given by:

$$\varepsilon_{\text{dp}} = \frac{T_{\text{in,db}} - T_{\text{sa,db}}}{T_{\text{in,db}} - T_{\text{in,dp}}} \quad (6.38)$$

$$\varepsilon_{\text{wb}} = \frac{T_{\text{in,db}} - T_{\text{sa,db}}}{T_{\text{in,db}} - T_{\text{in,wb}}} \quad (6.39)$$



Figure 6.2.5 Experimental indirect evaporative cooling unit

The indirect evaporative cooler unit, used in this study, with the dimensions of 125x85x75cm is shown in Figure 6.5. The core of the cooler is a cross flow heat and mass exchanger with dry and wet channels. A submerged water circulation pump is integrated in the water sump at the bottom of the unit for water circulation between the collection tank and nozzles at the top of the heat and mass exchanger sprinkling water equally all over the wet channels of the core, shown in Figure 6.5. The sprayed water is distributed alongside the vertical wet channel surfaces and collected in the water tank then again pumped through the distribution pipes to the nozzles. Two HMT130 humidity and temperature probes which have direct link to the Datataker DT500 data logger were connected to measure air temperature both at the inlet and outlet of the indirect evaporative cooling unit.

Overall coefficient of performance of the combination of liquid desiccant dehumidification unit and indirect evaporative cooler is determined by the ratio of whole

cooling capacity supplied over the thermal heat input at the regenerator to regenerate the dilute desiccant solution. In addition, electrical coefficient of performance of the entire unit is determined as the ratio of overall cooling capacity delivered by the dehumidifier and dew point cooler over the total electric power consumption of the system including fans, pumps, electrical heater etc. Both thermal and electrical COP of the system is given by the following equations:

$$\text{COP}_{\text{Therm,Dehum-Cooler}} = \frac{Q_{\text{cool,overall}}}{\dot{W}_{\text{elec,cooler}}} \quad (6.40)$$

$$\text{COP}_{\text{Elec,Dehum-Cooler}} = \frac{Q_{\text{cool,overall}}}{\dot{W}_{\text{elec,total}}} \quad (6.41)$$

6.3 RESULTS AND DISCUSSION

6.3.1 Roof unit

Various heat transfer coefficients and solar optical parameters regarding the roof part of the proposed system are given in Tables 5.1 and 5.2. The wind speed was observed over the course of test to detect the heat flow rate through natural convection between the PV panels and ambient air. Also, average solar radiation data and outside air temperature were recorded throughout the test. The climate data along with the design parameters provided in Tables 5.1 and 5.2 were evaluated to estimate the water and PV cell temperatures in Figures 6.6 and 6.7. The root mean square percent deviations and correlation coefficients were also calculated and shown in Figures 6.6 and 6.7 in order to compare the theoretical results with the experimental outcomes. During test sessions, no working fluid leakage was observed both in the roof and cooling units.

Figure 6.6 presents the variations of effective PV module temperature $(T_{PV})_{eff}$, and water temperature T_w with the ambient temperature, T_a . It is shown that the PV module temperature throughout the operation remains higher than the water temperature as expected. The increase in water temperature circulating through the heat exchanger reaches up to 16°C throughout the testing. Considering the changes in temperature tendencies and rise in water temperature, there is a fair agreement with the results obtained by (Tiwari et al., 2006).

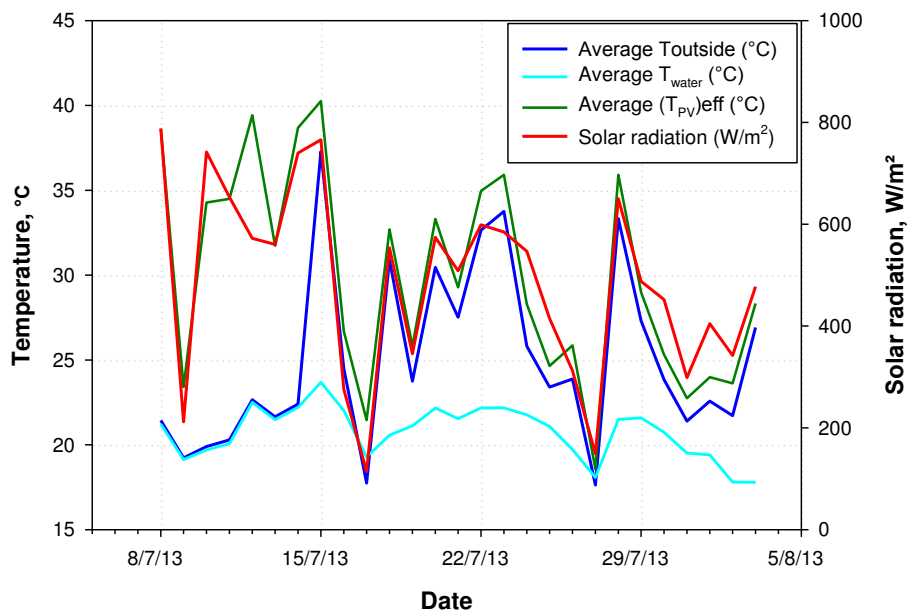


Figure 6.3.1 Hourly variation of PV, ambient, water temperatures and wind speed

Figure 6.7 compares the theoretical and experimental values of effective PV module temperature $(T_{PV})_{eff}$, attained as a result of simulation and experimental testing. The theoretical values considering the effects of polyethylene heat exchanger indicate that $(T_{PV})_{eff}$ (THE) are in accordance with the experimental values, $(T_{PV})_{eff}$ (EXP). The correlation coefficient and root mean square values are obtained as 0.943% and 5.17%, respectively. Figure 6.7 also compares the hourly variations of experimental and

theoretical values of the water temperature in the system. Despite higher theoretical water temperature values, the correlation coefficient and root mean square percent deviation rates are attained as 0.96% and 7.66% respectively. These values clearly support the validity of the model utilized in the present study.

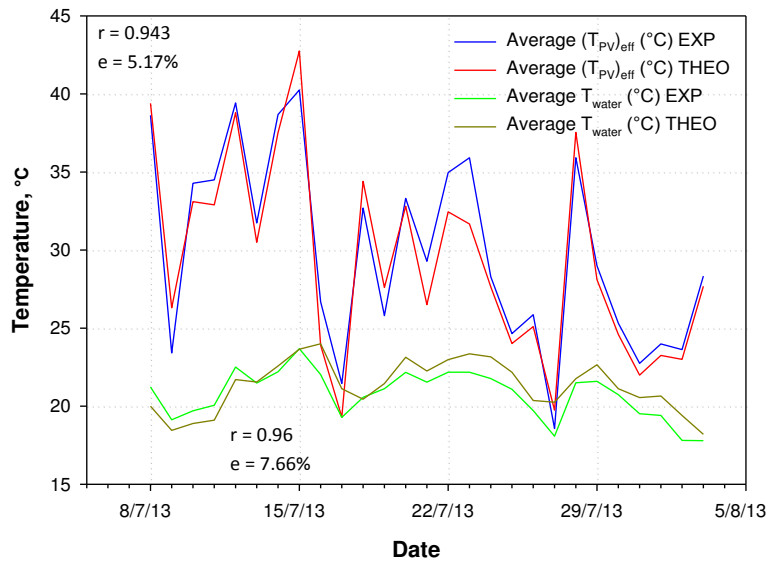


Figure 6.3.2 Average variation of PV cover temperature- experimental and theoretical

Figure 6.8 illustrates the degree of polyethylene heat exchanger influence over the electric power conversion efficiency of the PV modules. For with Poly HE case, the increase of cell efficiency as a result of passive cooling via water circulation would lead to an increase on power conversion efficiency. On the other hand, higher cell temperature would cause a substantial decrease on the cell efficiency. Nevertheless, it was found that for both cases, the cell efficiency is always better off with Poly HE case than without case. This implies that the “with Poly HE” case would be a better choice for PV systems to enhance the overall energy output of PV panels.

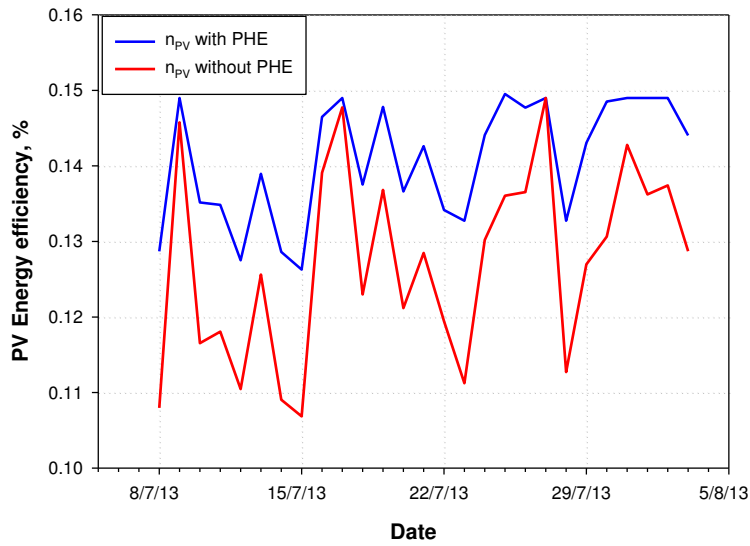


Figure 6.3.3 Effect of poly heat exchanger on power conversion efficiency

Figure 6.9 shows the variation of useful heat gain through circulating water with a mass flow rate of 0.0493 kg/s. The useful heat generated by the polyethylene heat exchanger roof unit ranges between 9.4 kW and 12.5 kW for the given test period.

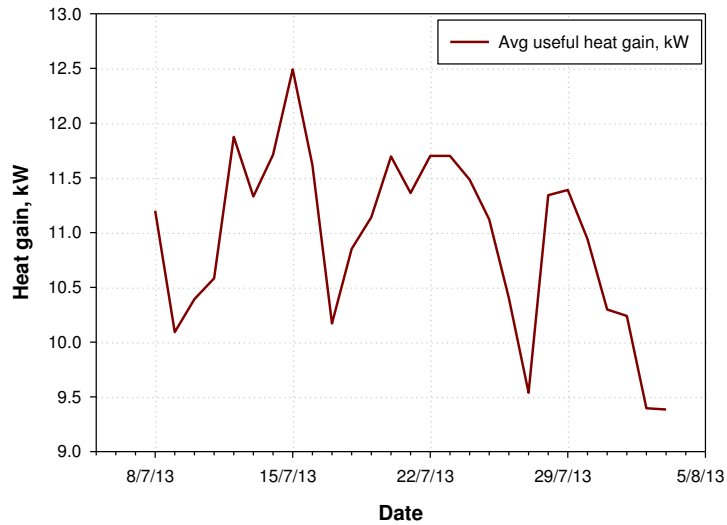


Figure 6.3.4 Useful heat gain

6.3.2 Liquid desiccant dehumidification unit

The liquid desiccant dehumidification system shown in Figure 6.3 was experimentally tested to examine the system performance under the given climate conditions. A temperature control room was constructed to control inlet air temperature and humidity. 20 l potassium formate HCOOK solution with a concentration of 75% and flow rate of 3 l/min was employed and the inlet air mass flow rate was about 0.06 kg/s at around 30°C where the relative humidity of the air was between 70-85%. The reduction in the relative humidity (RH) was directly proportional to the increase in relative humidity of the inlet air. The average relative humidity at the outlet of the dehumidifier was about 61.8%.

Figure 6.10 shows the performance of the dehumidifier unit under the climate conditions provided. The reduction in the relative humidity (RH) was directly proportional to the increase in relative humidity of the inlet air. The average relative humidity at the outlet of the dehumidifier was about 60.5%. Also, Figure 6.11 demonstrates the performance of the regenerator unit and the regeneration water inlet flow rate was 0.074 kg/s. As can be seen in Figure 6.11, the average increase in the air temperature blowing across the regenerator is around 6°C while the maximum change in the relative humidity is noted as 21%. Furthermore, Figure 6.12 displays the temperature variations of regeneration water, cooling water and liquid desiccant solution during the operation. The average temperature of the water supplied to regenerate the dilute potassium formate (HCOOK) desiccant solution was around 57.7°C where the temperature of regenerated and cooled desiccant solution driven to the dehumidifier core and cooling water were 21.73°C and 12.41°C, respectively. It should be stressed that the wet-bulb effectiveness is the main parameter to evaluate the performance of the dehumidification core. Figure

6.13 presents the dehumidifier wet-bulb effectiveness accordingly. Based on the experimental results, the maximum wet-bulb effectiveness was found to be at around 55%.

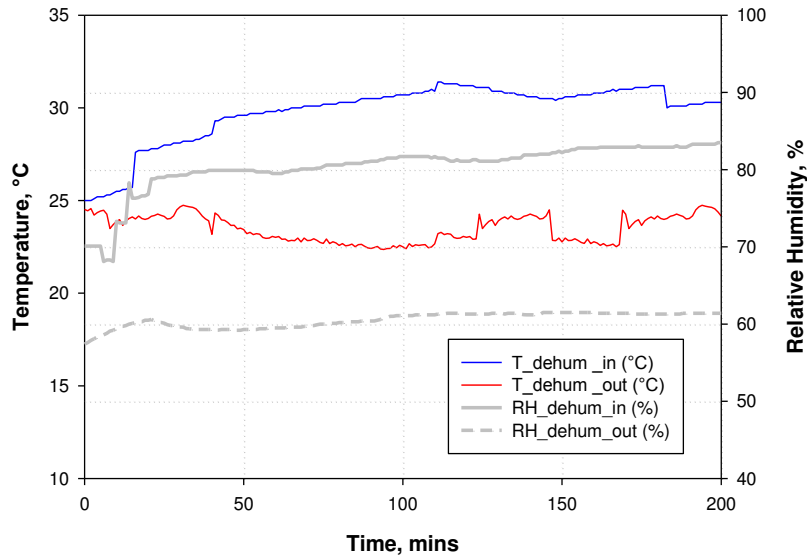


Figure 6.3.5 Air temperature and relative humidity variation across the dehumidifier

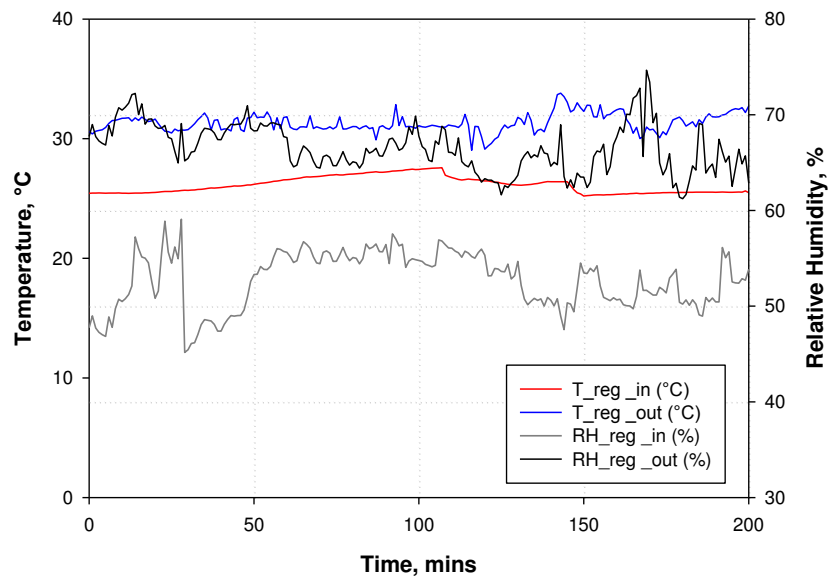


Figure 6.3.6 Air temperature and relative humidity variation across the regenerator

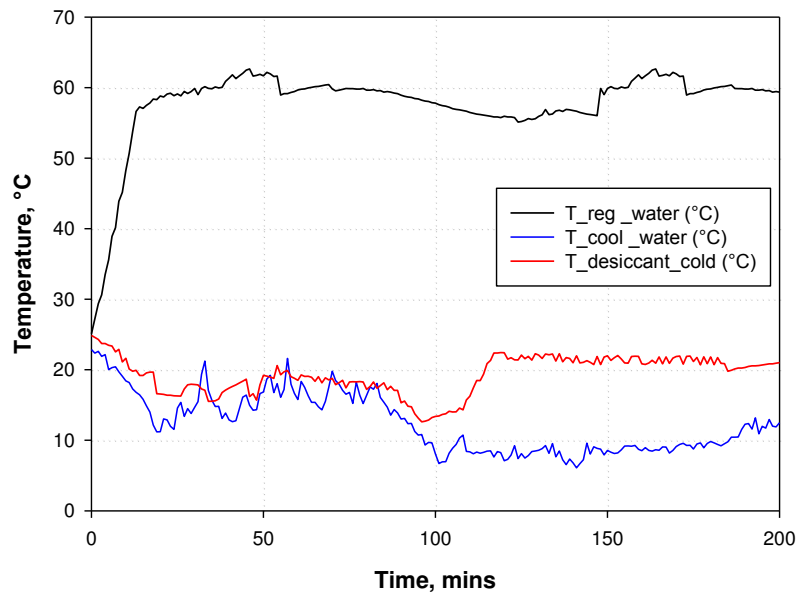


Figure 6.3.7 Liquid desiccant and water temperature variation

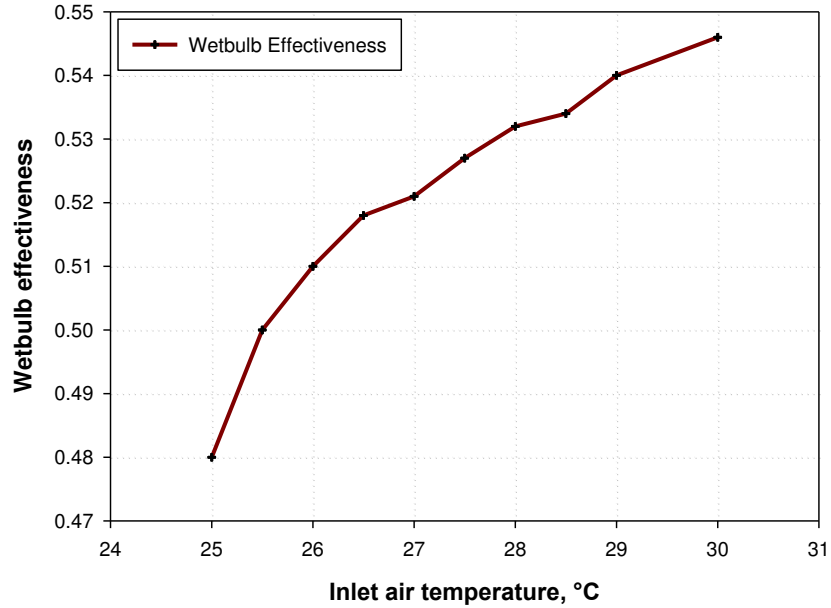


Figure 6.3.8 Variation in wet-bulb effectiveness of the dehumidifier

6.3.3 Indirect Evaporative Cooler

The indirect evaporative cooler unit, as shown in Figure 6.5, employed in the experiment was tested under the given environmental conditions (air temperature: 30 °C, RH: 80%). Figure 14(a-b-c-d-e) shows the cooler performance at five different blower settings 300, 600, 900, 1200, and 1500 m³/h, respectively. A FX-060 digital blower controller is set to maintain inlet air speed with the given flow range. A 2 kW fan heater and 10 l capacity humidifier were employed to keep the control room temperature at around 30 °C and RH of 80%, respectively. The water supplied to the cooler was about 15 °C. Figure 6.14(a) shows the variation of air temperature across the cooler at the lowest fan speed of 300m³/h. The inlet air temperature varies between 29.0 °C and 31.23 °C and the supply air temperature is 14.3 °C-17.6 °C with the temperature difference of 14 °C is recorded across the cooler. At the fan speed of 600m³/h, the maximum exhaust air temperature is recorded as 13.9 °C as presented in Figure 6.14(b). The minimum and maximum supply air temperature attained across the cooler is 15.5 °C and 22.69 °C, respectively. Also, Figure 6.14(e) shows the temperature variations across the cooler at the maximum blower setting of 1500m³/h. the maximum supply air reaches to 23.2 °C with a maximum temperature decrease of 8.9 °C during the cooling operation.

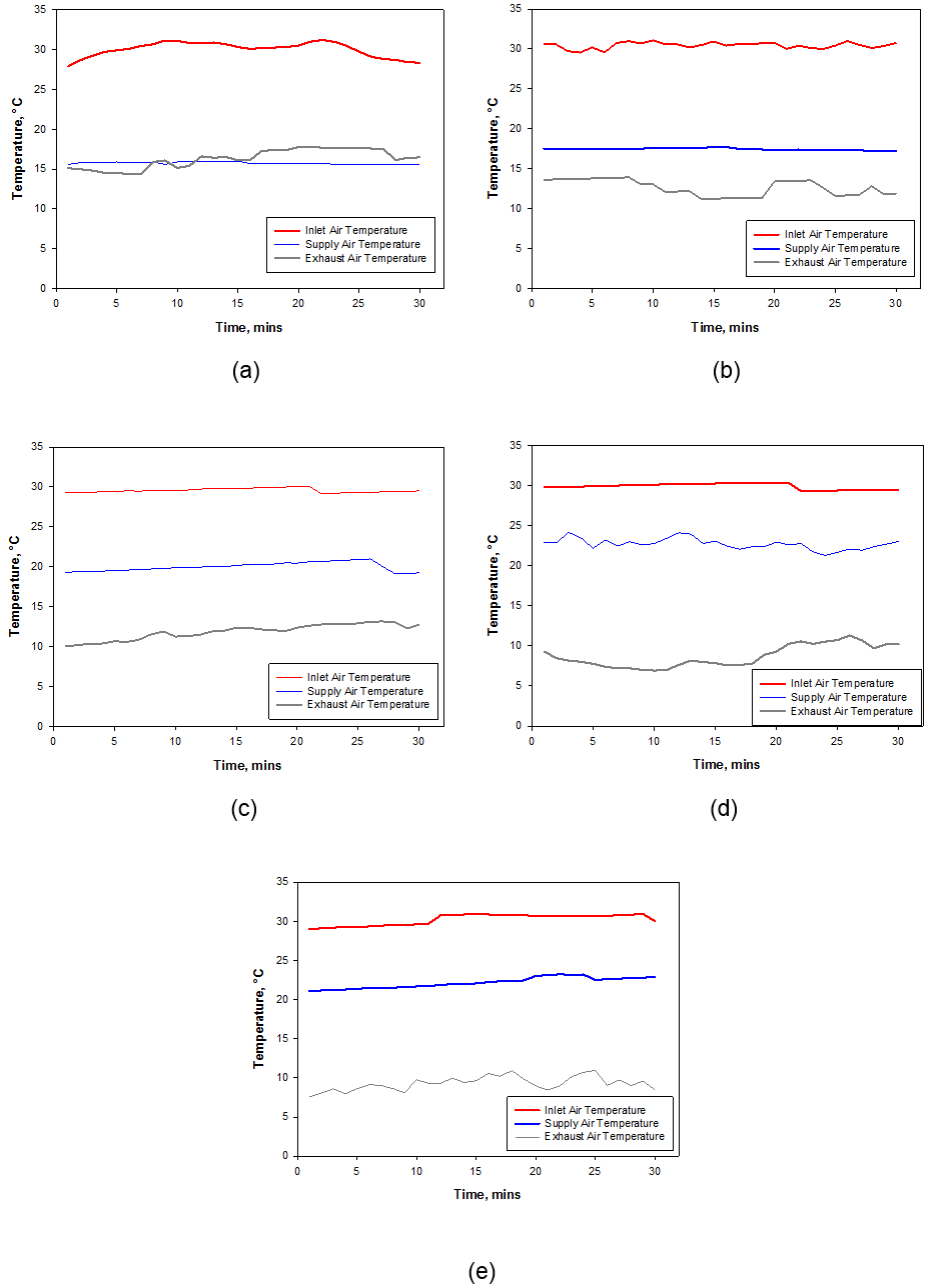


Figure 6.3.9 (a-b-c-d-e) Indirect evaporative cooler performance data a) warm air with 300m³/h b) warm air with 600m³/h

In addition, Figure 6.15 presents the cooler COP calculated using the experimental data recorded in accordance with each fan speed setting. The COP is calculated as the ratio of cooling capacity delivered over the electrical power consumption of each fan and pump employed in the unit. It is illustrated that COP of the unit and inlet air flow rate

vary in inverse proportion to one another. The maximum COP of 12.1 is noted at the minimum blowing rate of 300m³/h and the minimum COP of 6.3 at 1500m³/h.

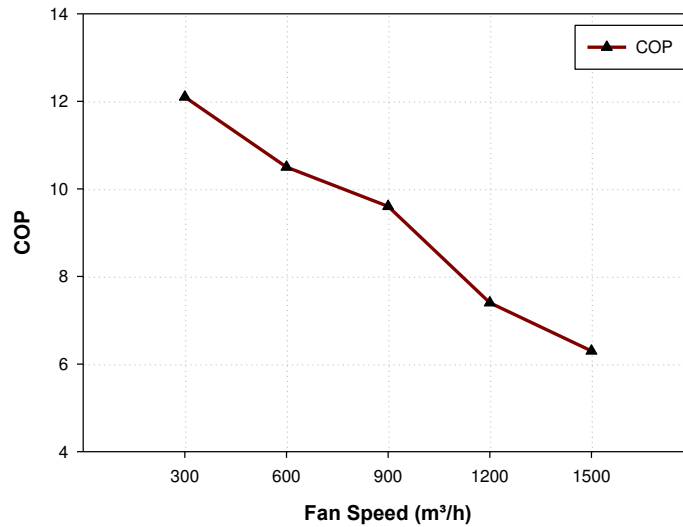


Figure 6.3.10 Indirect evaporative cooler COP at different fan settings

Table 6.1 shows the average performance data obtained during the test session. The measured supply air volumetric rate at five different blowers setting extend between 63.5 l/s to 202.3 l/s as the minimum and maximum flow rates, respectively. One can deduct from the summary data that the air temperature decrease across the cooler is inversely proportional to the blower speed. However, the cooling capacity shows an increasing trend from 1032 W at 300m³/h to 1229 W at 1500m³/h as the air flow rate increases. Moreover, the wet-bulb effectiveness and dew point effectiveness of the cooler at five different fan speeds are presented as wet-bulb effectiveness ranges between 0.96 and 0.67 and dew point effectiveness is from 0.61 to 0.40, respectively. So the effectiveness of the cooling system decreases as the fan speed increases.

Table 6.1 Performance data of the indirect evaporative cooling unit

Fan setting (m³/h)	300	600	900	1200	1500
Volumetric flow rate of supply air (l/s)	63.5	108.3	143.4	171.6	202.3
Inlet air temperature (°C)	30.03	30.44	29.57	29.88	30.24
Inlet air enthalpy (kJ/kg)	64.76	66.02	63.37	64.30	65.40
Supply air Temperature (°C)	15.75	17.45	19.99	22.69	22.17
Supply air relative humidity (%)	78.24	76.55	75.69	72.99	72.5
Temperature difference across the cooler(°C)	14.28	13	9.58	7.19	7.07
Exhaust air temperature (°C)	16.31	12.6	11.9	8.7	9.3
Cooling capacity (W)	1032	1117.5	1173.3	1211.84	1229.82
COP _{cooler}	12.1	10.5	9.6	7.4	6.3
Wet bulb effectiveness	0.96	0.91	0.73	0.68	0.67
Dew point effectiveness	0.61	0.56	0.44	0.42	0.40

6.3.4 Combined Dehumidification and Indirect Evaporative Cooling

System

Overall dehumidification and cooling performance of the system was investigated by combining the liquid desiccant dehumidification unit with the indirect evaporative cooler. Hot and humid air introduced from the temperature and humidity control room is first dehumidified by the liquid desiccant based dehumidifier, and the processed air is, then, delivered to the indirect evaporative cooling unit, also called dew point cooler, to further cooling and adjusting the air quality. HMT130 humidity and temperature probes were used for data recording regarding air temperature and humidity at the both inlet and outlet of the dehumidifier and evaporative cooling units. Figure 6.16 introduces the air temperature variation across the dehumidifier and indirect evaporative cooler. The temperature of the air inlet to the dehumidifier is ranged from 27.5°C to 34.5°C and the average temperature drop across the dehumidifier and cooler units is around 4.5°C and 7.5°C, respectively. Also, average air temperature at the outlet of the cooler is about 19.45°C. One can conclude that substantial ratio of temperature drop (nearly 2:3) takes place across the cooler.

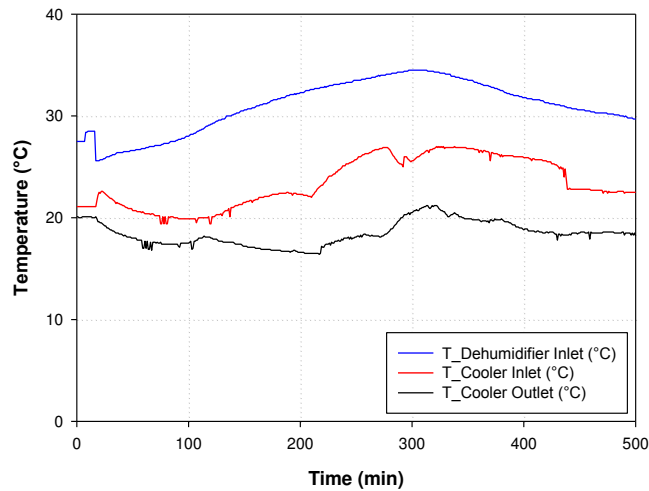


Figure 6.3.11 Variation of air temperature across the combined dehumidification-cooling unit

Moreover, Figure 6.17 presents the change in relative humidity across the dehumidifier and cooler. The process air has the mass flow rate of 0.099 kg/s and liquid desiccant flow rate is around 3 l/min. According to the experimental data, the range of air relative humidity at the dehumidifier inlet was between 78.1% and 83.5% and average drop in relative humidity across the unit was found to be 25.7%. At inlet and outlet of the cooler, the average relative humidity ratios were noted as 55.78% and 60.44%, respectively.

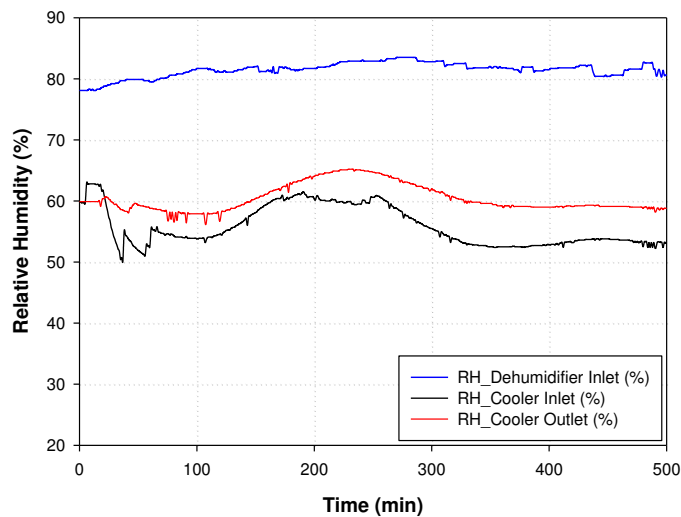


Figure 6.3.12 Variation of relative humidity across the combined dehumidification-cooling unit

Figure 6.18 illustrates the comparison and variation of cooling capacities both for only cooler and combined dehumidification-cooler unit. The maximum cooling capacities delivered by only cooler and the combined unit were 881 W and 6673 W, respectively. The experimental data proves that the main contribution to the overall cooling capacity belongs to the liquid desiccant based dehumidification unit during the operation of the combined dehumidification-cooling system.

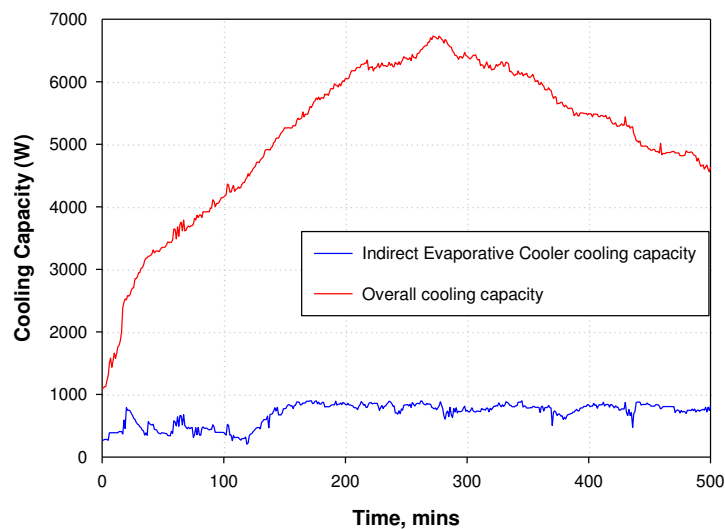


Figure 6.3.13 Cooling capacity of indirect evaporative cooler and combined unit

Table 6.2 summarizes the overall performance data of the building integrated PV/T roof collector combined with a liquid desiccant enhanced indirect evaporative cooling system. Utilizing the renewable energy based-solar thermal source, the roof unit with an average water temperature of 30.25°C and mass flow rate of 6 l/min from the roof unit, supplies the part of the regeneration heat input around 3kW required to adjust the concentration of the dilute liquid desiccant solution. The remaining heat input required for the regeneration is calculated to be 4 kW where the total heat input needed in the regenerator is estimated to be 7 kW for the average regeneration temperature of 60°C-

65°C. In addition, the air temperature decreases from 30.99°C to 26.45°C at the dehumidifier unit and further to 19.45°C at the indirect evaporative cooler. As for the relative humidity variation, it is reduced from 80.39% to 55.78% across the dehumidifier where supply air relative humidity drops to 60.44% through dew point cooling. The cooling capacity of the cooler is about 881 W where the overall cooling capacity is found to be 6673 W for the liquid desiccant enhanced indirect evaporative cooling system. Also, thermal and electrical COPs of the combined cooling system are estimated to be 0.73 and 6.75, respectively. A Gauss propagation based uncertainty analysis was performed to estimate the uncertainty in calculation of the parameters. The maximum uncertainties influencing the efficiency of the proposed system were estimated to be 2.47% for the roof unit, 3.75% for the cooling part, respectively.

Table 6.2 Experimental performance data of the overall system

Parameter	Value	Parameter	Value
Poly HE roof unit water supply temperature (°C)	30.25	Dehumidifier inlet air temperature (°C)	30.99
Poly HE roof unit water mass flow rate (kg/s)	0.074	Dehumidifier inlet air relative humidity (%)	80.39
Poly HE useful heat gain (W)	2982.7	Ind. Evp. Cooler inlet air temperature (°C)	26.45
PV efficiency with Poly HE (%)	12.4	Ind. Evp. Cooler inlet air relative humidity (%)	55.78
PV efficiency w/o Poly HE (%)	11.2	Ind. Evp. Cooler outlet air temperature (°C)	19.45
Regenerating water temperature (°C)	57	Ind. Evp. Cooler outlet air relative humidity (%)	60.44
Regenerating heat input (W)	5845	Ind. Evp. Cooler cooling capacity (W)	780
Regenerating water mass flow rate (kg/s)	0.074	Overall cooling capacity (W)	5135
Liquid desiccant flow rate (kg/s)	0.037	Combined dehumidifier-cooler thermal COP	0.73
Dehumidifier inlet air mass flow rate (kg/s)	0.099	Combined dehumidifier-cooler electrical COP	6.75


6.4 DISCUSSION & CONCLUSIONS

In this chapter, the integration of innovative building integrated solar thermal collector with a pilot scale combined cooling system was introduced and experimentally investigated. A low cost polyethylene heat exchanger loop unit underneath the PV modules was built and tested utilizing solar energy as a heat source and employing water as an environmentally friendly working fluid. Also, a liquid desiccant enhanced indirect evaporative cooling system was developed and tested experimentally including a liquid desiccant based dehumidifier and a dew point evaporative cooler with a cross-flow core. The environmentally friendly, less corrosive, lower cost, lower density and viscosity potassium formate (HCOOK) solution was used as a liquid desiccant also considering its thermodynamic and physical benefits comparing to its conventional counter-parts. Heat input to regenerate the dilute desiccant solution was partly harnessed from the roof loop and the remaining heat demand was met by employing a water immersion heater with rod thermostat. The combined experimental prototype was operated under the given operational conditions to estimate the ability of such a combined small scale system for building applications. The concluding remarks are outlined as follows;

Based on the experimental data recorded, water temperature difference could reach up to 15°C subject to outside parameters, most affected by air temperature and global solar radiation. Thus, experimental findings prove that polyethylene heat exchanger loop can function efficiently as a heat extraction component for solar assisted heating and cooling systems. Overall power efficiency data show that PV modules can improve power energy performance by 10.7 % due to achieved collector cooling as the cold

water flow forms passive cooling effect and partially removes the waste heat from PV modules. Hence improved performance of the photovoltaic systems help to mitigate the energy supply issues and contribute to the CO₂ reduction towards a sustainable environment. Else, waste heat removal away from the PV panels is likely to enhance life cycle of the solar collectors since high operating temperatures may shorten the life-span. The validation of the thermal model for the roof part was performed by comparing the experimental results with the estimated data. The comparison shows that theoretical model makes a fair agreement with the experimental results obtained. In addition, the proposed roof loop is capable of providing about 3 kW heating power where cooling capacity of the overall system was found to be 5.2 Kw. The electrical and thermal COP of the combined dehumidification-cooling system was calculated as 0.73 and 6.75, respectively. With the satisfactory experimental results obtained, one can conclude that the proposed system could meet the cooling needs and improve indoor air quality for occupants.

Similarly, the next chapter investigates the performance of the novel solar thermal roof coupled with a heat pump unit for heating application. Yet, the analysis based on indoor and outdoor testing predominantly focuses on the solar thermal roof collector.



CHAPTER 7 – Build-up and performance test of a novel solar thermal roof for heat pump operation

7 BUILD-UP AND PERFORMANCE TEST OF A NOVEL SOLAR THERMAL ROOF FOR HEAT PUMP OPERATION

7.1 INTRODUCTION

For heat pumps, a fundamental factor of great importance for highly efficient operation is the availability of a cheap, reliable heat source for the evaporator. The power quality can be improved by coupling solar energy with heat pump and the combination can represent interesting solutions for various domestic applications. The evaporator-collector employed in such a system can absorb both solar thermal and ambient energy (Georgiev, 2008). Series of experiments were conducted with R 22 and 744 to identify proper refrigerant (Choi et al., 2014). Solar assisted heat pump systems (SAHP) to produce hot water have been widely investigated in both theoretical and experimental studies. To name a few, considerable amount of study, both theoretical and experimental, on the exergetic performance evaluation of heat pumps systems with various heat sources (Pons, 2012) like ground heat, solar heat and heat recovery (Beccali et al., 2012), heat pump system having PV/T evaporator (Keliang et al., 2009), solar assisted heat pump with an energy storage (Karacavus and Can, 2008), on a direct-expansion solar-assisted heat pump water heating system (Kuang et al., 2003), and heat pump systems for district heating (Zhen et al., 2007). The measurements have been undertaken to discover the building space heating capabilities of the solar assisted heat pump systems (Yang et al., 2011, Bakirci and Yuksel, 2011). Experimental performance analysis of a solar assisted ground-source heat pump for green house heating (Choi et al., 2014) and the development and performance analysis of absorption heat pump system driven by solar energy (Sozen et al., 2002) have been analysed.

Solar assisted heat pump applications and performance assessments for agricultural and marine products drying have been reviewed and concepts have been introduced (Daghighi et al., 2010). Combination of the heat pump and solar energy is a mutual beneficial way of enhancing the coefficient of performance of a heat pump and solar collector efficiency. The heat pump COP can be elevated to the great extent on the temperature of the evaporator. The solar collector loop enables to boost the heat source temperature of the heat pump, thereby improving the annual and seasonal performance of the heat pump. COP value about 6.38 experimentally obtained in a SAHP domestic heating system with an evacuated tubular collector (Caglar and Yamali, 2012). The COP value was attained as 9 in a SAHP water heating system using unglazed flat-plate collectors (Georgiev, 2008). The average COP of heat pump system for agricultural drying was found to be 7 in tropics (Choi et al., 2014). Zhang et al. (2014) developed and test a novel solar photovoltaic/loop-heat-pipe HP system for space heating or DHW. The solar heat was exchanged through a flat-plate heat exchanger acting as the condenser of the heat pipe loop and the evaporator of the heat pump cycle. The average values of COP for both thermal and PV/T were found to be 5.51 and 8.71 under the prevailing climatic conditions of Shanghai, China. The result proved that proposed system has a potential of achieving enhanced solar thermal efficiencies around 1.5 – 4 times more than conventional counterparts. In another study, Shilin et al. (2010) proposed and experimentally studied an indirect-expansion SAHP radiant floor space heating system in Beijing, China. The configuration of the system varied as solar alone, solar with water-source heat pump and water source heat pump alone depending on the solar collector's outlet temperature.

7.1.1 IEA: SHC Programme Task 44

The objective of International Energy Agency (IEA)'s Solar Heating and Cooling (SHC) programme Task 44 was to optimize combined solar and heat pump systems for single house applications and to provide a common definition for the performance of such systems (Hadorn, 2012). This project was performed along with the IEA Heat Pump programme denoted as Annex 38. The task mainly focused on small-scale heating and domestic hot water systems, electrically driven heat pumps etc. Task 44 also involved the assessment of solar and heat pump systems under Subtask B that aims to set common definition of performance metrics and assessment criteria as well (D'Antoni and Sparber, 2011). Loose et al. (2011) performed field tests of various combined SAHP systems with different heat sources and presented results, as part of IEA, SHC Programme Task 44. The system employed collectors and geothermal heat pump with borehole heat exchangers to provide DHW and space-heating to a new structure with radiant floor heating system. The collectors fed the storage directly when the sufficient solar radiation was available. Otherwise, low grade energy from the collectors would be used in the heat pump for space heating. In case of reaching energy storage capacity in the tank and the heat pump operation was inactivated; the collectors would feed the borehole heat exchanger. So, the heat pump would draw the stored energy from the boreholes after summer time. This configuration was monitored for three years and the promising results were obtained. The solar regeneration of ground boreholes ensured that the HP system could run with a high rate of seasonal performance factor (SPF) in a long term. In another study, conducted as part of IEA, SHC programme Task 44, Haller and Frank (2011) introduced a mathematical relation model by using TRNSYS in order

to determine if combined solar collector-evaporator of a dual (solar-air) source heat pump configuration was more advantageous than utilizing solar heat directly. The examined dual configuration in this study can switch its operation between serial and parallel mode. It was shown that indirect utilization of solar heat more beneficial in terms of system performance factor when the solar radiation is under certain level which depends on solar collector and heat pump characteristics. According to simulation results, using uncovered solar collectors was more advantageous in series mode and also increasing the runtime of the collectors could enhance performance of the series configuration.

Objective

The objective of this study is to achieve a roof integrated thermal “Sandwich” solar thermal roof collector that properly blends into surrounding thus avoiding ‘add on’ appearance and having a dual function (heat absorption and roofing). Even though a low cost ‘Sandwich’ roof may produce lower fluid temperatures than water based glazed collectors, it is able to absorb and emit heat from the ambient via convection, and solar radiation. Another objective is to address the inherent technical pitfalls and practical limitations of conventional solar thermal collectors by bringing an inexpensive, maintenance free and easily adaptable solution. Although substantial studies have been performed on the combination of solar PV modules with heat pumps, integration of such a novel roof construction with heat pump has yet to be considered. The present study will both theoretically and experimentally evaluate the thermal performance of the “Sandwich” roof unit with heat pump.

7.2 DESCRIPTION OF THE “SANDWICH” ROOF UNIT AND ITS COMBINED OPERATION WITH HEAP PUMP

The combination of solar thermal roof collector and heat pump system consists of a Thermal “Sandwich” Roof collector that acts as both roof and heat source for the heat pump. The roof module contains several layers, namely the outer surface is a black painted aluminium solar radiation absorber, polyethylene heat exchanger loop tightly screwed to the black aluminium surface for enhanced heat transfer and injected insulation foam back layer against heat loss. Furthermore, thermally conducting adhesion was used to improve the heat transfer between the aluminium cover and poly heat exchanger pipes. By this means, all layers are integrated into the same module to form a “Sandwich” Thermal Roof collector.

In the roofing structure, steel frames form a roof truss which weighs and fits the modules to build up a well-integrated roof. As for the plumbing of the system, supply and return pipes are placed underneath the roof truss and joined using flexible coupled connectors with valves to provide a leak free connection. In doing so, the supply pipe feeds cold water/glycol mixture to polyethylene heat exchanger, and the return pipe transports the hot water/glycol mixture from heat exchanger. To some extent, the sandwich module and roof support are well fixed together with the screws to form a properly functional solar thermal roof. Figure 7.1 is the illustration of layers of “Sandwich” Thermal Roof Collector.

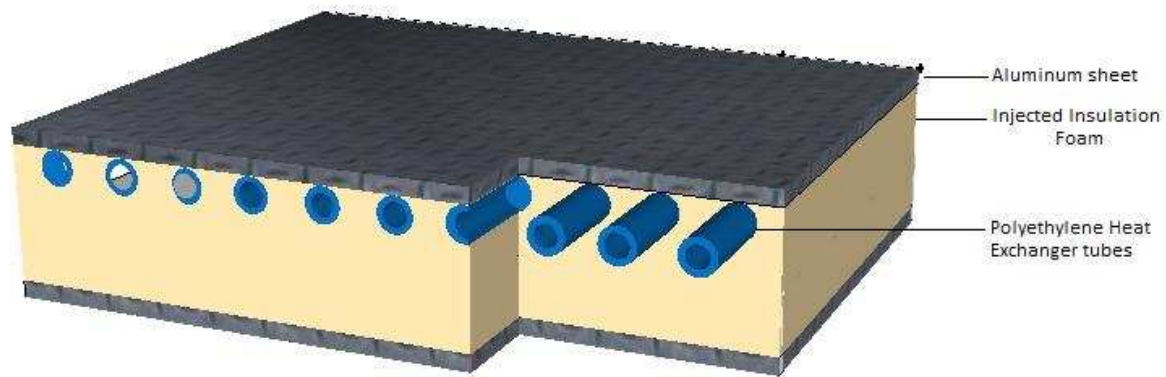


Figure 7.2.1 Cross sectional view of the Novel "Sandwich" Thermal Roof Collector

In operation, the “Sandwich” module receives a substantial amount of solar insolation falling upon the black coated solar absorbing surface as a means of thermal energy, while dispersing remainder to the surrounding. The black painted aluminium top cover enhances the solar heat absorption. As the second law of thermodynamics states that when an object is at a different temperature from its surroundings, heat flows so that the body and surroundings reach the same temperature, at which they are in thermal equilibrium. Such a spontaneous heat transfer occurs from high temperature to low temperature. Thus, setting the surface at a lower temperature than the surrounding by circulating cold water/glycol mixture will cause that heat flow, thermodynamically, moves towards roof collector. The absorbed heat, then, will be conveyed through the circulating water/glycol mixture across the heat exchanger. Consequently, enhanced solar thermal efficiency would be expected. Moreover, fixing the tubes and risers of polyethylene heat exchanger tightly to the black aluminium surface by means of screws would potentially lead to having relatively low temperature difference between the module surface and heat carrying fluid. The hot water obtained out of this operation can be utilized for space

heating & cooling, domestic hot water supply, food drying, assisting natural ventilation inside a building and/or other services.

The system also comprises 3 kW thermal output commercially available heat pump package designed for space heating (through underfloor or radiator) and domestic hot water for buildings. The Indirect Solar-assisted HP system includes a solar thermal collector, evaporator, compressor, condenser, and an expansion valve. In operation, the “Sandwich” structure roof unit supplies free, low grade solar thermal energy to the heat pump evaporator. The solar heat is exchanged through a coil heat exchanger acting as the condenser of the collector loop. Within the secondary sealed side of the evaporator heat exchanger, there is heat transfer fluid, also called refrigerant. When the water/anti-freeze mixture enters the evaporator, the solar thermal energy absorbed by the novel roof is transferred into the refrigerant which begins to boil and becomes a gas. The refrigerant physically does not mix with the water/anti-freeze mixture. They are separated by sandwich like heat exchanger which enables the heat transfer. The gas is then introduced to the compressor in which the refrigerant gas pressure is increases which rises gas temperature as well. The high temperature refrigerant gas then moves along a second heat exchanger, also called the condenser, which has same characteristics as set of heat transfer plates. The condenser supplies water hot enough to serve the space heating system or domestic hot water needs. After transferring its heat, the refrigerant gas becomes a liquid again. This refrigerant in liquid state passes across an expansion valve at the end of the cycle to reduce its pressure and temperature, ready to begin another cycle all over again. The schematic diagram of the solar assisted heat pump system, using environmentally friendly R134a refrigerant

which has practically the same behaviour as other refrigerants in terms of temperature variation and compressor frequency, is given in Figure 7.2 below. The technical parameters of the system components can be found in Table 7.1. In order to maintain the heat pump operation under the climatic conditions where temperatures below freezing point, the antifreeze concentration within the novel roof arrays is kept 20% for the protection level of -10°C . The concentration level can be detected with a refractometer.

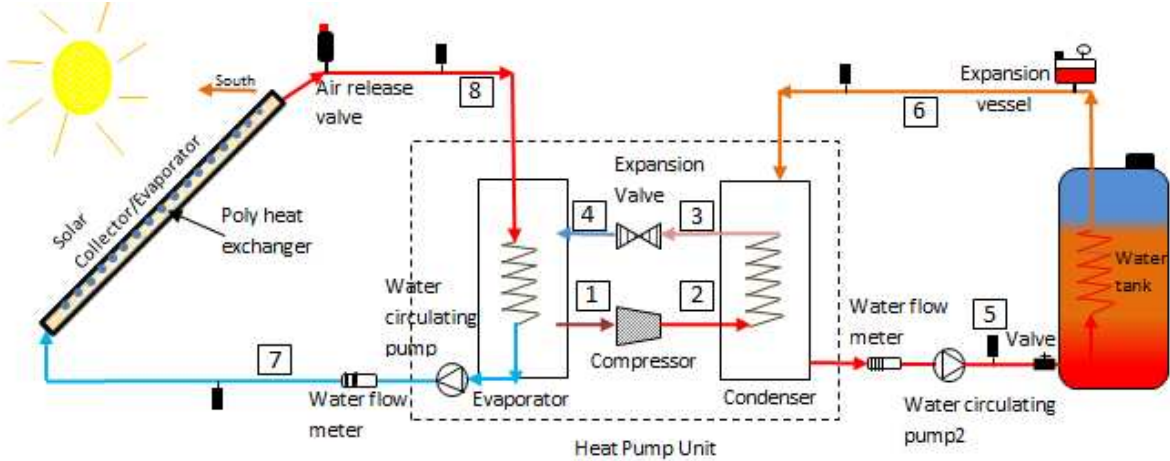


Figure 7.2.2 Schematic of the combined system

Table 7.1 Technical parameters

Component	Parameter	Value
Sandwich Roof	Exposed roof area (A_{eff})	1.92 m ²
	Dimensions (H x W x D)	1.6 m x 1.2 m x 0.02 m
Aluminium	Thickness	5 mm
	Thermal conductivity	450 W/m.K at 25 °C
Polyethylene Heat Exchanger	The internal diameters of tubes	$D_i=0.0027$ m
	The external diameters of tubes	$D_o=0.0043$ m
	Distance between tubes	$W=0.001$ m
	Max temperature allowed in poly HE	60 °C
	Max pressure allowed in poly HE	1 MPa
2 part Polyurethane Liquid Foam	Expanding size	25 times of its original volume
	Time to begin reaction when mixed	20-25 seconds
	Time to reach max size	150 seconds
	Optimum working temperature	20 °C
Heat Pump	Nominal Thermal Output	3 kW
	Process Medium (Refrigerant)	R-134a
	Max inlet Temperature	15 °C
	Min outlet Temperature	-5 °C
	Max flow Temperature	65 °C
	Compressor type	Reciprocal
	Dimensions (H x W x D)	0.53 x 0.475 x 0.37 m
	Dry weight	50 kg
Circulating Pump	Max delivery head	6 m
	Max operating pressure	10 bar
	Permissible temperature range	-10 °C to +110 °C
	Mains connection	1~230, 50 Hz
Hot water storage	Capacity	55 litres
	Max working head	10 m
	Standing heat loss	1.5 kW/h per 24 hrs
Solar Simulator	Tilt angle	15 °
	Max lighting	400 W

7.2.1 Prototype Design

A prototype of the combination of solar thermal roof and heat pump system was assembled and tested both in the laboratories of Institute of Sustainable Energy Technology at the University of Nottingham and outdoor under the prevailing climatic conditions of Nottingham, UK which is geographically located at 52.57°N and 1.09°W.

The key innovation in the proposed system is the utilization of the solar thermal energy as a renewable source with relatively efficient and low cost components by a thermodynamically effective design. The size of the “Sandwich” collector is large enough to be tested so that the performance characteristics can be detected properly. Initial design parameters are given in Table 7.2 below. Figure 7.4 shows the schematic diagram of the roof system.

As absorber, 5 mm thick aluminium cover was coated with high temperature silicone spray in order to enhance solar thermal absorption and avoid moisture condensation and freezing on the collector. As heat extraction component, polyethylene heat exchanger loop was tightly fixed to the black aluminium surface via screws to have a good touch to the absorber for enhanced heat transfer. As roof finishing, insulation foam was injected as back layer against heat loss.

The heat exchanger loop is made of polyethylene thermoplastic substance and its physical structure makes it first-of-its-kind. The pipes and fittings were incorporated via welding with soldering iron. The flow channels have 2.7 mm of internal and 4.3 mm of external diameters and the distance between the flow channels is 10 mm. Technical parameters of the heat exchanger can be found in Table 7.1.

The heat pump unit was connected to a 55 l storage tank with a circulation pump and a flow meter regulator to modulate the mass flow rate of hot water. The storage tank was thoroughly insulated with foam insulation material in order to reduce the heat losses. The water inside the storage tank was heated by employing a helical copper tubular heat exchanger. An expansion vessel was also installed in between the heat pump and storage tank coupling to reduce the likely damages due to excessive increase in

pressure, and also the fluid pressure in the solar thermal roof unit is monitored by a pressure gauge, as shown in Figure 7.2.

The circulating pumps employed in close loop solar roof systems must overcome the head pressures. Also, the pump should be compatible with solar applications in terms of its size, speed, efficiency, and hydraulics and power consumption. Technical details of the circulation pump are provided in Table 7.1.

An array of 30 halogen floodlights was employed in order to simulate the artificial solar sunlight. The solar sunlight simulator was evenly fixed on an aluminium frame installed above and in parallel to the “Sandwich” roof, as illustrated in Figure 7.2. The array was formed as three sub arrays and was connected to the grid through a 3-phase transformer, which allows the level of the radiation flux to be gradually regulated. The maximum electrical power to be consumed by each floodlight is 400 W. A Kipp & Zonen pyranometer with sensitivity of $17.99 \times 10^{-6} \text{ V/W/m}^2$ was mounted on the vertical surface to measure the radiation flux on the surface of the novel roof. An anemometer was also installed for outdoor test. Thermocouples (K type) with a maximum deviation of $\pm 1.5^\circ\text{C}$ were inserted to investigate the temperature variation across system. All related data was recorded on the data logger, DT500 and direct connection between data logger and PC was provided to store data and export on Excel spreadsheet.



Figure 7.2.3 Experimental Design - Novel Solar Thermal roof with Solar Simulator, Heat Pump, Water Storage

Table 7.2 Initial design parameters

Parameters	Values
Average mass flow rates tested (evaporator & load)	0.05, 0.074, 0.1, 0.12 kg/s
Pressure	2 bar
C_w	4190 J/kgK
K_{al}	450 W/m.K
K_{HE}	0.5 W/m.K

7.3 MATHEMATICAL MODELLING AND EES MODEL SET-UP

Energy transfer arose within the proposed system has two major processes including conversion of solar radiation into thermal energy by “Sandwich” roof unit and upgrading the evaporation heat into higher grade energy through the heat pump. These two processes are interconnected and eventually reach a balance under the steady state operation. A numerical model which is well suited to the physical structure of the proposed system was adapted to simulate the thermal performance of the novel system

by using EES (Engineering Equation Solver) Software. Several assumptions have been considered during the first and second law analyses of the system as follows:

- The overall performance of the system is at a quasi-steady state condition with negligible potential and kinetic energy effects and there is no chemical reactions taken for all processes.
- All surfaces of layers cover uniform temperature and temperature gradient around tubes is negligible.
- There is forced flow through heat exchanger tubes and the pressure drop is negligible due to the short length of pipelines.
- Due to advanced thermal resistance features, heat loss through the insulation and edge is negligible

The method and mathematical equations presented in this study are not necessarily the most accurate available; but, they are widely applied, easy to use and adequate for most of the design computation. Heat transfer profile of the roof unit and P-h chart of the refrigeration cycle are shown in Figure 7.4 and 7.5, respectively.

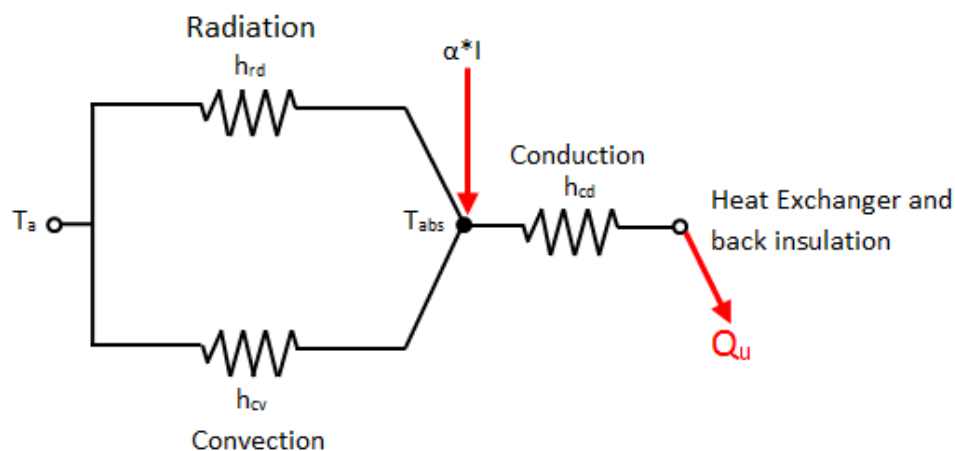


Figure 7.3.1 The heat transfer profile of the roof unit

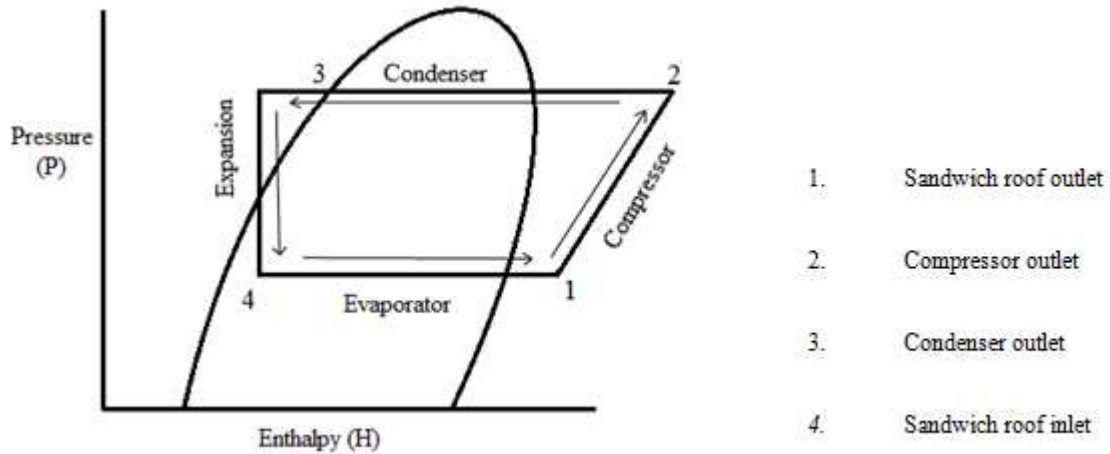


Figure 7.3.2 P-H chart of the heat pump refrigeration cycle (GLO, 2015)

7.3.1 Energy Analysis of “Sandwich” Roof Unit

Initially incoming Solar Energy is defined as (Buker et al., 2014);

$$Q_{\text{abs}} = \alpha_{\text{abs}} \cdot A_{\text{eff}} \cdot I \quad (7.1)$$

Heat loss is mainly through the top due to the good back insulation features of “Sandwich” Roof unit. So the heat loss can be expressed as;

$$Q_l = h_c \cdot (T_{\text{abs}} - T_a) + \varepsilon_{\text{abs}} \cdot \sigma \cdot (T_{\text{abs}}^4 - T_{\text{sky}}^4) \quad (7.2)$$

Combining above equations provides a revised expression of the useful heat energy (Q_t):

$$Q_t = Q_{\text{abs}} - Q_l \quad (7.3)$$

The natural convection heat transfer coefficient (h_c) from roof to the ambient is taken into account for wind velocities lower than or equal to 6 m/s (V) by (Sharples and Charlesworth, 1998);

$$h_c = 6.5 + 3.3 \cdot V \quad (7.4)$$

The sky temperature can be obtained by Swinbank's equation as a function of the ambient temperature by (Buker et al., 2014);

$$T_{\text{sky}} = 0.037536 \cdot T_a^{1.5} + 0.32 T_a \quad (7.5)$$

Radiation heat transfer through the front is defined as;

$$h_{\text{rd}} = \varepsilon_c \cdot \sigma \cdot (T_{\text{abs}}^4 - T_{\text{sky}}^4) \quad (7.6)$$

The heat flow goes through conduction across the absorber (black aluminum), the walls of heat exchanger tubes and is eventually conveyed to the flowing water/glycol mixture.

The heat gain of the water/glycol mixture is as equal as the useful heat energy as;

$$Q_t = A_{\text{eff}} \cdot U_t \cdot (T_{\text{abs}} - T_w) \quad (7.7)$$

Overall thermal resistance between absorber and refrigerant is;

$$U_t = (U_{\text{abs,heo}} + U_{\text{heo,hein}} + U_{\text{hein,w}})^{-1} \quad (7.8)$$

Heat transfer coefficient ($U_{\text{abs, heo}}$) from absorber aluminum layer to outer wall of heat exchanger is by;

$$U_{\text{abs,heo}} = \frac{\lambda_{\text{abs}}}{\delta_{\text{abs}}} \quad (7.9)$$

The temperature at the outer wall of the polyethylene heat exchanger becomes:

$$T_{\text{heo}} = T_{\text{abs}} - \frac{Q_t}{A_{\text{eff}} \cdot U_{\text{abs,heo}}} \quad (7.10)$$

Heat transfer coefficient ($U_{\text{heo, hein}}$) from outer wall to interior wall of heat exchanger is defined as;

$$U_{\text{heo,hein}} = \frac{2 \cdot \pi \cdot \lambda_{\text{he}}}{\ln \left[\frac{D_o}{D_i} \right]} \quad (7.11)$$

The average temperature at the inner wall of polyethylene heat exchanger is given as;

$$T_{\text{hein}} = T_{\text{heo}} - \frac{Q_t}{A_{\text{eff}} \cdot U_{\text{heo,hein}}} \quad (7.12)$$

Heat transfer coefficient ($U_{\text{hein,r}}$) from interior wall of heat exchanger to water;

$$U_{\text{hein,r}} = \frac{\text{Nu}_r \cdot \lambda_r}{D_i} \quad (7.13)$$

Where Nusselt number is expressed as (Buker et al., 2014);

$$\text{Nu}_r = 0.023 \cdot \text{Re}_r^{0.8} \cdot \text{Pr}_r^{0.4} \quad (7.14)$$

The Reynolds number for flows in pipe or tube is generally defined as;

$$\text{Re}_r = \frac{\dot{Q} \cdot D_{\text{he}}}{V_r \cdot A_p} \quad (7.15)$$

In order to compare the theoretical results with the experimental outcomes, the root mean square percent deviation (e) and the coefficient of correlation (r) have been examined by using the following expressions;

$$e = \sqrt{\frac{\sum(e_i)^2}{N}} \quad \text{where } e_i = \left[\frac{X_i - Y_i}{X_i} \right] \times 100 \quad (7.16)$$

$$r = \frac{n(\sum X \times Y) - (\sum X) \times (\sum Y)}{\sqrt{n(\sum X^2) - (\sum X)^2} \times \sqrt{n(\sum Y^2) - (\sum Y)^2}} \quad (7.17)$$

Stating the expressions used by

$$m^2 = \frac{U_t}{K\delta} \quad (7.18)$$

Then, the fin efficiency factor (F) can be found by

$$F = \frac{\tanh m \frac{W - D_o}{2}}{m \frac{W - D_o}{2}} \quad (7.19)$$

The flat plate collector efficiency (F') becomes

$$F' = \frac{1}{\frac{WU_t}{D_o U_{\text{abs, pl}}} + \frac{WU_t}{\frac{K}{\delta}} + \frac{WU_t}{D_o + (W - D_o)F}} \quad (7.20)$$

The flow rate factor (F_R) is given by

$$F_R = \frac{\dot{m}C_f}{A_{\text{eff}}U_t F'} \left[1 - \exp\left(-\frac{A_{\text{eff}}U_t F'}{\dot{m}C_f}\right) \right] \quad (7.21)$$

Energy efficiency is usually defined as the ratio of total energy output to the total energy input as

$$\eta = \frac{\dot{E}_{\text{out}}}{\dot{E}_{\text{in}}} \quad (7.22)$$

7.3.2 Energy Analysis of Heat Pump Unit

The water from the Novel solar thermal roof circulates through the evaporator in the heat pump. There it releases heat to liquid refrigerant passing separately across the evaporator, allowing the environmentally friendly refrigerant R-134a to vaporise. The water then returns to the solar thermal collector to capture heat again in a continuous cycle. The preheated refrigerant vapour goes through the compressor, where it is compressed to high pressure and upgraded to a much higher temperature. High temperature vapour, then, passes through the condenser where it is surrounded by water from the heating system and releases heat to the water circulating via channels. Consequently, vapour becomes saturated liquid with a same pressure. The temperature and pressure of the refrigerant is further reduced by flowing through the expansion device, from where it turns back to the evaporator to repeat the cycle.

The heat received by the evaporator (Q_e) is given by the following equation (Li and Yang, 2010):

$$Q_e = m_r \cdot (H_1 - H_4) \quad (7.23)$$

The heat introduced to the condenser (Q_c) is given by (Li and Yang, 2010):

$$Q_c = m_r \cdot (H_1 - H_4) \quad (7.24)$$

The electrical power required to drive the compressor ($Q_{cp,e}$) is given by (Li and Yang, 2010):

$$Q_{c,e} = m_r \cdot (H_2 - H_1) \quad (7.25)$$

Coefficient of performance of the heat pump (COP_{HP}) is given by (Karacavus and Can, 2008):

$$COP_{HP} = \frac{Q_c}{W_{cp}} \quad (7.26)$$

Coefficient performance of the overall system (COP_{SYS}) is the ratio of condenser load to the total power consumption of the compressor and other two circulation pumps and it is given by (Karacavus and Can, 2008):

$$COP_{SYS} = \frac{Q_c}{W_{cp} + W_{cs} + W_{ls}} \quad (7.27)$$

7.3.3 Uncertainty Analysis

The experimental uncertainties were determined by applying Gauss propagation law. The result R is calculated as a function of the independent variables $x_1, x_2, x_3, \dots, x_n$ and $w_1, w_2, w_3, \dots, w_n$ represents the uncertainties in the independent variables.

Then, uncertainty R is expressed as (Buker et al., 2014):

$$w_R = \left[\left(\frac{\partial R}{\partial x_1} w_1 \right)^2 + \left(\frac{\partial R}{\partial x_2} w_2 \right)^2 + \dots + \left(\frac{\partial R}{\partial x_n} w_n \right)^2 \right]^{1/2} \quad (7.28)$$

The independent parameters measured in the experiments are: solar radiation, temperature of solar thermal roof, temperature of outlet water, ambient temperature, flow rates and power consumption of the heat pump. Experiments were conducted by using following instruments: a Kipp and Zonen CM11 pyranometer with $\pm 3\%$ accuracy, Thermocouples (K type) with the maximum deviation of $\pm 1.5^\circ\text{C}$, liquid flow indicators with the accuracy of $\pm 2\%$ and a watt meter with $\pm 2\%$ accuracy.

It is obtained from the equations (1), (2), (3), (6), (10), and (13) that the η_t is the function of several variables, each subject to uncertainty:

$$\eta_t = f(T_w, T_{abs}, T_a, \dot{m}, I, \dot{W}_{\Sigma p}) \quad (7.29)$$

Where subscripts T_w , T_{abs} , T_a , \dot{m} , I and \dot{W} stand for temperature of outlet water, temperature of collector surface, ambient temperature, mass flow rate, solar radiation and power consumed by compressor, respectively.

Total uncertainty for overall system efficiency can be expressed as;

$$w_R = \left[\left(\frac{\partial \eta}{\partial T_w} w_{T_w} \right)^2 + \left(\frac{\partial \eta}{\partial T_{abs}} w_{T_{abs}} \right)^2 + \left(\frac{\partial \eta}{\partial T_a} w_{T_a} \right)^2 + \left(\frac{\partial \eta}{\partial \dot{m}} w_{\dot{m}} \right)^2 + \left(\frac{\partial \eta}{\partial I} w_I \right)^2 + \left(\frac{\partial \eta}{\partial \dot{W}_{\Sigma p}} w_{\dot{W}} \right)^2 \right]^{1/2} \quad (7.30)$$

Total uncertainty rate affecting the efficiency of the proposed system was computed by using Eqs. 7.28-7.30. The estimation implies that total uncertainty in calculation of the efficiency is found to be 4.08%.

7.4 RESULTS AND ANALYSIS

The theoretical analysis and experimental investigation were performed to evaluate the performance of the solar sandwich roof along with a heat pump unit. In analysis, the effects of the various operating parameters including thermal and overall efficiencies on the performance of the envisaged system were also investigated. The developed mathematical model to describe the system operation was programmed by using Engineering Equation Solver software (EES, 2013). In this software, energy and mass balance equations and the boundary conditions are solved simultaneously. In order to validate the mathematical model, the theoretical and experimental results were compared and shown that there is rather a good compliance between them. From the experimental data, the temperature of the water outlet from the innovative solar thermal collector, the mean values of the COP of the heat pump and of the overall system and efficiency ratios were deduced and presented in Table 7.3.

The novel solar thermal roof unit presented in Figure 7.1 was experimentally investigated to test the system performance under various solar intensities employing the solar simulator to control the incoming solar radiation. The reason that Figures 7.6 and 7.8 provided is to demonstrate the collector performance under increasing solar intensity and the effect of flow rate on the temperature of flowing water/glycol mixture. Figure 7.6 represents the performance of the “Sandwich” thermal collector under 400 W/m² and 0.025-0.074 kg/s water flow rates. The surface temperature ranges between 20.5 and 32.3°C with a flowing water temperature in the range of 10.6 and 16.2°C and a maximum temperature increase of 5.6°C. One should note that maximum temperature

increase is achieved while flow rate is 0.025 kg/s and the least is noted as the flow rate is 0.074 kg/s.

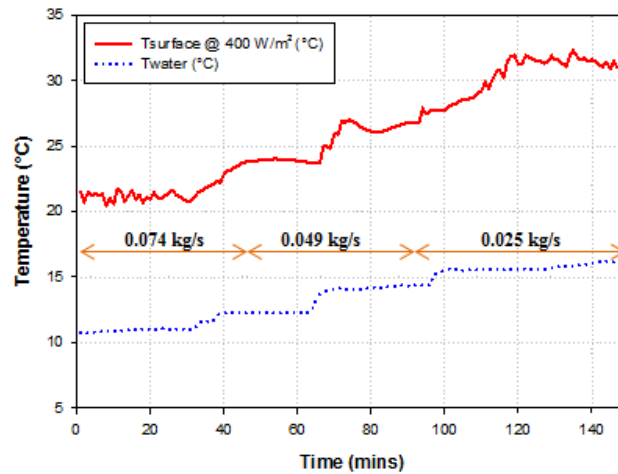


Figure 7.4.1 Performance of the novel roof under 400 W/m² solar intensity and various flow rates

Figure 7.7 represents the performance of the “Novel” roof under 600 W/ m² and water flow rates of 0.025-0.074 kg/s. The surface temperature reaches up to 52.4°C and the maximum surface temperature increase is 19.3°C. Heat carrying water flowing through the polyethylene heat exchanger has the temperature range of 17.6 and 26.2°C as maximum temperature increase is 13°C while the water flow rate is 0.025 kg/s.

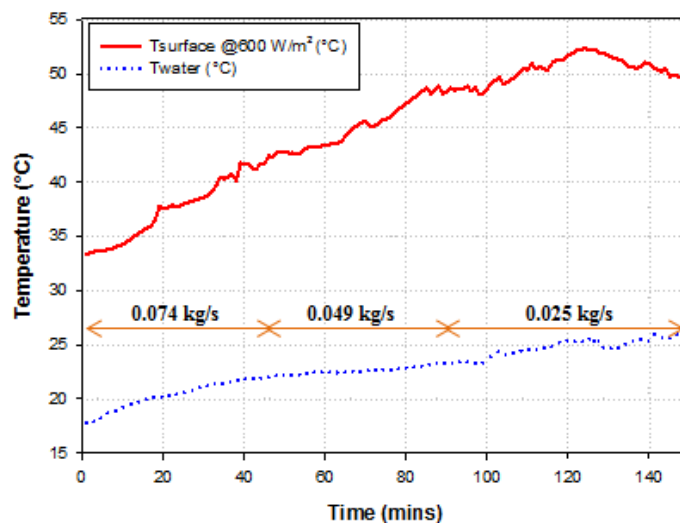


Figure 7.4.2 Performance of the novel roof under 600 W/m² solar intensity and various flow rates

Figure 7.8 presents the associated performance findings of the proposed solar thermal roof under 800 W/m² solar insolation and 6,4, and 0.025 kg/s water flow rates, respectively. The surface temperature ranges between 55.5°C and 66.5°C with a flowing water temperature in the range of 27.67°C and 35.02°C and a maximum temperature increase is of 20°C.

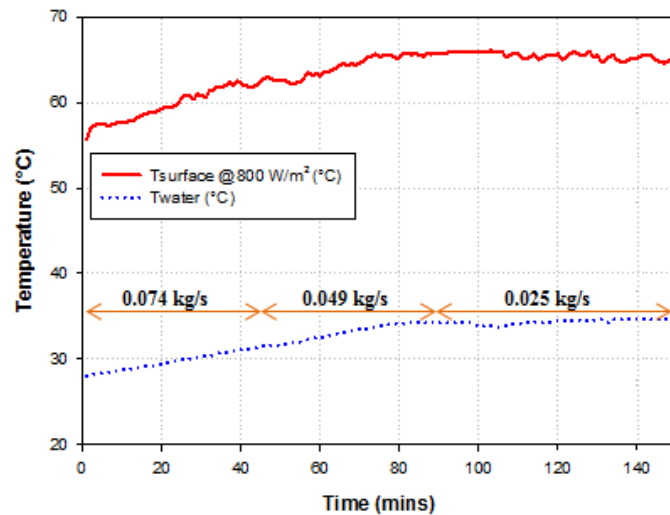


Figure 7.4.3 Performance of the novel roof under 800 W/m² solar intensity and various flow rates

Figure 7.9 presents the efficiency change of the “Novel” solar thermal collector under various solar radiation and water flow rates. It can be seen from the graph that although higher flow rate has the greater efficiency ratios for low solar insolation settings, slower flow rate such as 0.025 kg/s has the superior efficiency ratios for the higher solar radiation levels. As incoming solar radiation to the roof system increases, the efficiency level also increases with the slower flow rates.

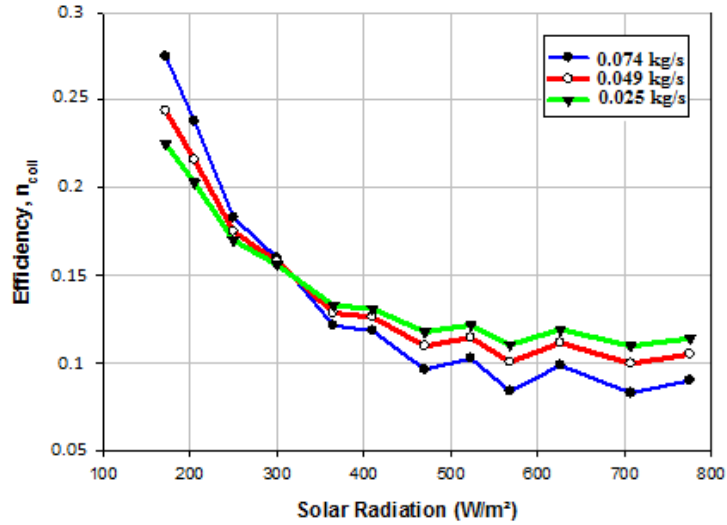


Figure 7.4.4 Variation of efficiency under different solar radiation with various flow rates

Figure 7.10 presents the collector efficiency as a function of the flowing fluid, air temperature and solar radiation on the surface. The thermal efficiency is inversely proportional to the increasing $(T_w - T_a)/I$ ratio. Any momentarily change in climatic conditions could have various impacts over the thermal efficiency of the roof unit as follows; when the air temperature is relatively low, this may lead to more heat dissipation from hot surface to the ambient, thus causing to lower thermal efficiencies. Higher solar radiation contributes to enhanced heat transfer from black aluminium surface towards the polyethylene heat exchanger layer and this will eventually conduce to greater thermal efficiencies of the Novel roof. Also, high temperature of flowing water through the heat exchanger results in low efficiencies due to reduced heat transfer across the poly heat exchanger and confined structure of the “sandwich” roof prevents high heat dissipation towards environment.

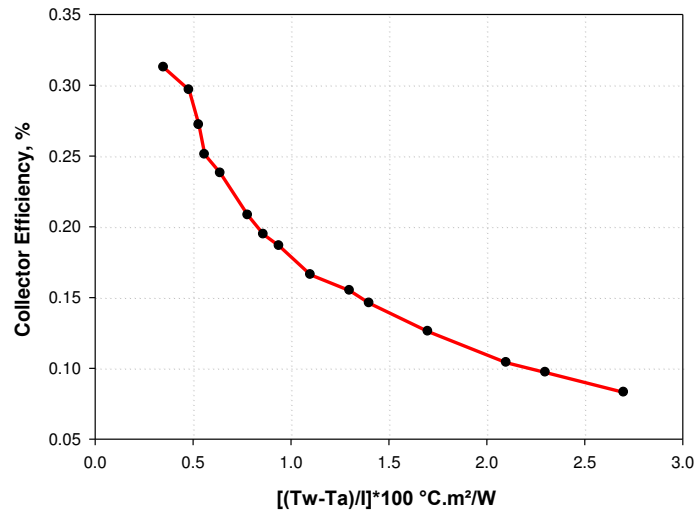


Figure 7.4.5 Effect of collector fluid temperature on the collector efficiency

7.4.1 Outdoor Testing

7.4.1.1 Solar Roof

Figure 7.11 presents the environmental conditions on 23rd of June, 2014 that outdoor test has been performed, outer surface and water temperatures varying depending on the external conditions. The wind speed is measured over the course of the external test to find out the heat flow rate through natural convection between the blackened aluminium surface and the surroundings. Average solar radiation (I), ambient air temperature (T_a), and wind speed on 23rd of June are measured as 701.3 W/m², 27.3°C, and 1.09 m/s, respectively. It is clearly shown in Figure 7.11 that the surface temperature is expectedly higher than the circulating water temperature. Around 9 °C increase in water temperature is noted while the surface temperature is in the range between 22.6°C and 44.6°C. One may conclude that conceiving the changes in temperature tendencies and increase in both surface and water temperature, there seems to be a fair agreement with the results obtained.

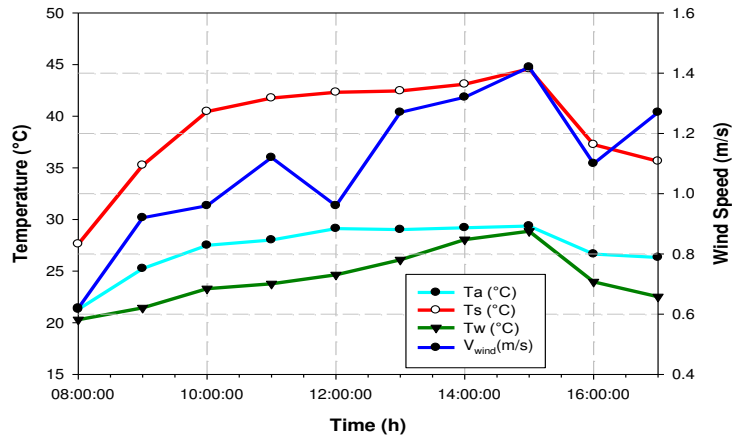


Figure 7.4.6 Hourly variation of temperature Ta, Ts, Tw and wind speed Vwind (23th June, 2014)

The design parameters in Tables 7.1 and 7.2 and climatic data have been utilized to assess the water and surface temperatures in Figures 7.11-7.13. The root mean square percent deviation and correlation coefficient obtained by Eqs. 7.16 and 7.17 have also presented in the same figures. Figure 7.12 presents the comparison between experimental and theoretical values of the surface temperature. The results indicate that predicted and experimental results are in a good agreement as the correlation coefficient and root mean square values are attained as 0.88 and 4.55%, respectively.

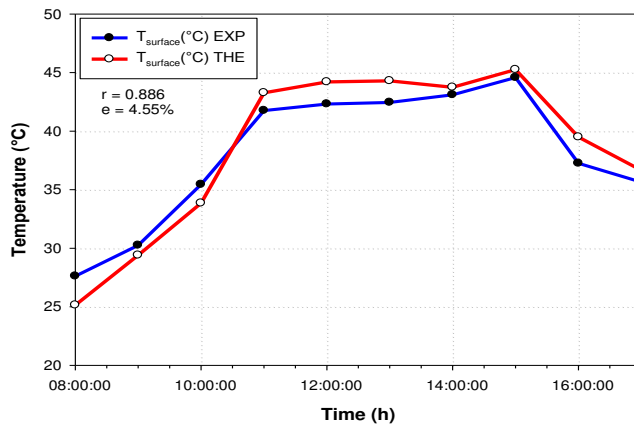


Figure 7.4.7 Hourly variation of surface temperature - theoretical vs experimental

Figure 7.13 presents the comparison between the theoretical and experimental results regarding the water temperature increase as a result of circulating within the heat exchanger being heat extraction component of the novel roof. Data gathered from the analysis show that the results obtained from the numerical investigation are in good compliance with the results of the experimental study. The correlation coefficient and root mean square values for water temperature comparison are attained as 0.92 and 3.03%. So, the estimated and experimental results for surface and water temperatures were found to be closely correlated.

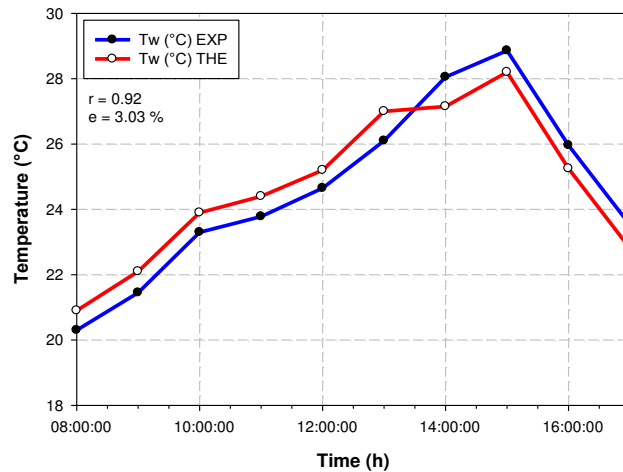


Figure 7.4.8 Hourly variation of water temperature - theoretical vs experimental

7.4.1.2 Heat Pump

Figure 7.14 presents the experimental data plotted during outdoor testing regarding the COP, power consumption of the heat pump, and heat gain in condenser changing with respect to time. The water temperature at the condenser set constant at 35°C for space heating purpose. From results, the energy gain at the condenser is in the range of 1.9 kW to 3.43 kW while the COP is fluctuated between 2.4 to 3.1. Meanwhile, the energy consumption is noted average of 0.7 kW in the test day.

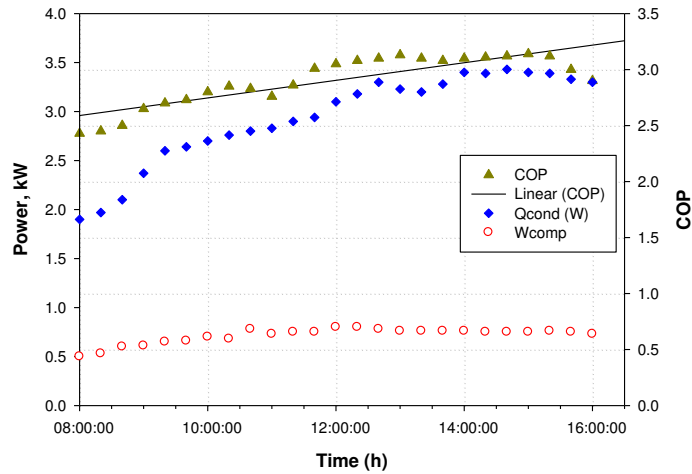


Figure 7.4.9 Test result obtained on 23th of June, 2014

Figure 7.15 presents the temperature variation in the water storage tank versus time of the day. The temperature difference observed between the top and bottom of the storage tank is up to 4 °C. However, the temperature deviation tends to decrease gradually. Figure 7.16 presents the COP of the heat pump versus COP of the overall system in the test day. The COP of the heat pumps is found to be higher than that of the overall system COP. The heat pump COP ranges between 2.4 and 3.1 while system COP is from 1.7 to 2.5, respectively. Daily average values of the measurements taken from 8am to 5pm are provided in Table 7.3.

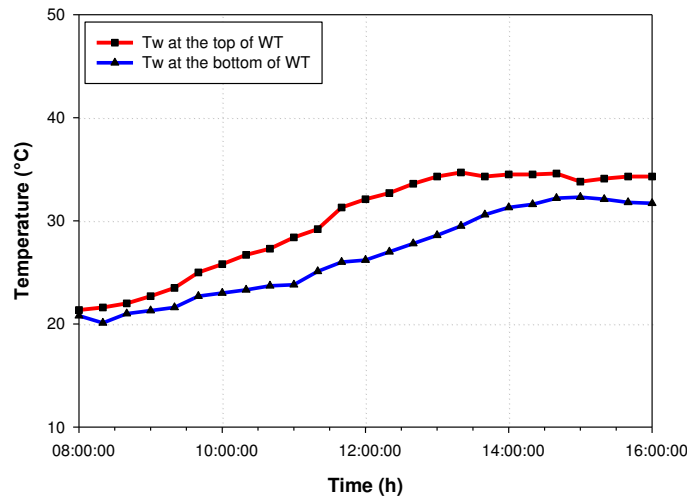


Figure 7.4.10 Temperature variation in energy storing with time

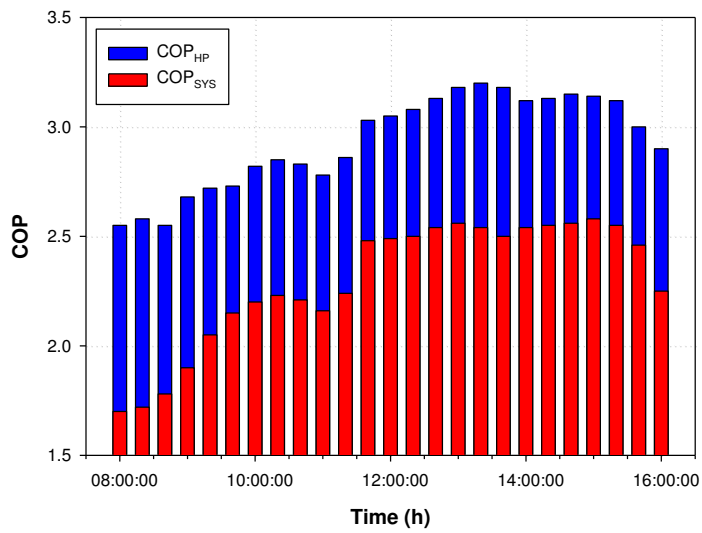


Figure 7.4.11 Coefficient of Performance variation by time

Table 7.3 Measured parameters and experimental results in average

Parameter	Value	Unit
Solar Radiation	701.3	W/m ²
Condensing Temperature (space heating only mode)	35	°C
Evaporating Temperature	8	°C
Temperature of potable water	12	°C
Temperature of water in energy storage tank	29.87	°C
Water-glycol flow rate in solar collector	0.074	kg/s
Water flow rate in load side	0.074	kg/s
Refrigerant flow rate in heat pump	0.106	kg/s
Average outdoor air temperature	27	°C
Power input to the heat pump	0.8	kW
Power input to the refrigerant water pump	0.125	kW
Useful heat received from the solar thermal collector	2.9	kW
Instantaneous collector efficiency	0.209	-
Heating COP of the heat pump	2.904	-
Heating COP of the overall pump	2.29	-

7.4.2 Economic studies

Economic parameters for the proposed system are provided in Table 7.4. In addition, Figure 7.17 illustrates the variation of payback period with increasing collector area. One can deduct from the graph that payback period falls drastically with the increase of collector area. This trend may be expressed by the fact that the increase in fuel savings, with increasing collector area, rises more rapidly compared to the cost of the system. Furthermore, payback period attains minimum value and then increases with the increase in collector area due to rise in collector area dependent cost. In the economic

analysis, the least payback period at around 3 years was achieved corresponding to a collector area of about 5 m².

Table 7.4 Economic parameters

Fuel escalation rate	6%
Discount rate	8.75%
General inflation rate	2.8%
Interest rate	8.2%
Fuel cost	\$0.05509/MJ
Life cycle	20 years
Down payment	10%

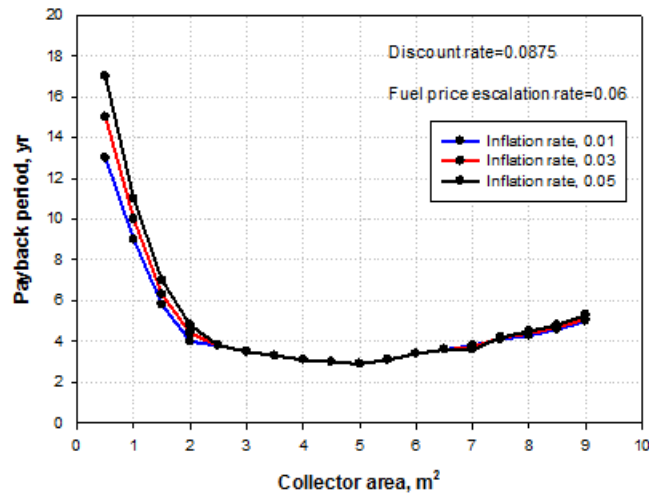


Figure 7.4.12 variation of payback period as a function of collector area for various inflation rates

7.5 DISCUSSION & CONCLUSIONS

A Novel solar thermal roof collector coupled with a heat pump unit was investigated by simulation and experimental methods. The performance test results and energy evaluation analysis were presented. The developed numerical models were validated by

the experimental findings collected on outdoor testing. Also, the impacts of environmental conditions and operating parameters were examined by setting the system for space heating mode. The concluding remarks are outlined as followings;

The selection of the heat pump unit was mainly because of its good compliance with the operating conditions, economic viability, its ability of handling varying evaporating temperatures adequately and environmental impacts, etc. Although initial costs of the heat pump systems are usually high, their low operating, maintenance and life cycle costs and long life cycle expectancy attract considerable interest as a potential alternative to the most conventional systems.

The validation of the developed thermal model was carried out by comparing the theoretical results with the actual findings during experiments. As the comparison indicates, thermal model developed for this prototype has a good agreement with the experimental results obtained.

Overall results prove that the flowing water through tubes and risers of the heat exchanger layer can successfully convey the solar thermal energy and have a cooling effect on the roof surface. The initial tests conducted at the laboratory environment show that the solar roof collector yields the maximum of 32.3°C surface temperature and 17.6°C water outlet temperature at 400 W/m² solar radiation, 52.4°C surface temperature and 25°C water outlet temperature at 600 W/m² solar radiation and lastly 66.5°C surface temperature and 32°C water outlet temperature at 800 W/m² solar radiation, respectively. Although the flow rate of 0.025 kg/s seems nominal at first instance, capturing heat slowly from the surface causes to happen overheating of the surface. This, however, may result in exceeding the maximum temperature threshold for

the heat exchanger and may be harmful to the risers and pipes. To minimize this conflicting trend, the tests were initiated with the water flow rate of 0.074 kg/s for cooler surface then flow rates were gradually reduced until 0.025 kg/s throughout the test season. Hence, the optimum flow rate was assumed as 0.049 kg/s for outdoor test of the system. As for the outdoor performance test, the temperature of water could increase up to 30°C. Thus, temperature increase of the water circulating through the innovative roof module could reach up to 10°C when the liquid within the system is around at around 20°C. The efficiency of the solar thermal collector varies between 0.24 and 0.11, respectively. Experimentally obtained results present that the proposed solar thermal collector can act as an efficient heat extraction component for solar source heat pump systems.

The COPs of the heat pump and overall system are calculated in terms of experimental data obtained from the outdoor test. Overall COP values of the system increase with the ambient air temperature and solar radiation and reach a maximum at 3.2 at an average of 2.98 over the course of testing for space heating mode. The maximum heat transfer rate experimentally attained in the condenser is 3.43 kW. This indirect SAHP system can assure long-term operation under various climatic conditions and relatively low operation costs during wintertime. From the economic analysis of the system, a minimum payback period of around 3 years was achieved. However, its advantages need to be further proven by more experimental and theoretical studies in the future.

Although a number of studies have been conducted on the combination of solar collectors with heat pumps, integration of such a novel roof construction, which was not known before in literature, with heat pump has not been considered yet. The

performance investigation of the system reveals that substantial amount of energy can be saved by utilizing solar thermal energy when implementing such a novel system. This new system may also provide a simple yet effective alternative for regions suffering from energy scarcity in the residential and commercial areas. Solar assisted heat pump systems also provide enormous environmental benefits as they don't exhaust natural resources, and mostly do not allow any kind of air emissions or waste products. Therefore, these systems may also contribute to mitigation of the environmental pollution and provide a remedial action especially in the areas where air emissions arise in dangerous levels (Lazzarin et al., 2007).



CHAPTER 8 – Discussion, Conclusions & Recommendations

8 DISCUSSION, CONCLUSIONS & RECOMMENDATIONS

8.1 GENERAL DISCUSSION

The UK Government pledged that it will be a requirement for all new homes to be zero-carbon by 2016 and introduced the Code for Sustainable Homes and the 2008 Climate Change Act sets the target of an 80% reduction in CO₂ emissions from the 1990 level by 2050 (UK Green Building Council, 2008). These requirements stimulate the development of various energy efficient technologies to provide a more energy efficient built environment. These requirements also point out that zero-carbon homes are to have either low or zero-carbon on-site power generation technologies, low or zero-carbon space and water heating technologies (Energy Saving Trust, 2010). Thus, in order to accomplish these zero-carbon spaces and HVAC requirements, there is a set of challenges for industry which craves innovation and research. However, in March 2015 Code for Sustainable Homes was scrapped by the UK Government.

Among the solutions, the utilization of solar energy is, without a doubt, one of the most encouraging ecological avenues. In a solar thermal system, the solar thermal energy can be exploited via heating working fluid circulating through a heat collector. These collectors, as being a significant part of any solar energy system, absorb the incoming solar radiation, convert it to heat energy and convey through a working fluid such as air, water or refrigerant, for various useful purposes such as heating and air conditioning of buildings. Building integrated solar thermal collectors may be installed either on the building façade or on the roof causing in each case a different visual impact. Depending on the type and dimensions, the system may be integrated in such a way that it is invisible, aesthetically appealing or appearing as an architectural concept.

A photovoltaic/thermal (PV/T) collector is a combination of photovoltaic (PV) and solar thermal components that produce both electricity and heat simultaneously. This dual function of the PVT enables a more effective use of solar energy that results in a higher overall solar conversion. Much of the captured solar energy in a sole PV module elevates the temperature of its cells which results in degradation of module efficiency. This waste heat needs to be removed to ensure a high electrical output. The PV/T technology recovers part of this extracted heat to utilize for low-and-medium-temperature applications. The merits of PV/T concept comparing to alternative technologies contain eco-friendly, proven long life (20-30 years), noise free and low maintenance. However, several factors restrict the efficiency of the photovoltaic module particularly temperature increase and utilizing only a part of solar spectrum (photon energy threshold is less than 1.11 μm for c-Si) for power generation. Currently, the power energy efficiency of PV modules for commercial applications is in the range of 12 - 18%, which is a value measured at the Standard Test Conditions (STC) (1.0 kW/m² of solar radiation, 25 °C of ambient temperature, and 1.5 m/s of wind speed), particularly depending on the solar cell type. Greater than 80% of solar radiation falling upon PV cells is either reflected or dumped as waste heat. This results in to increase PV cells operating temperature and degradation of power energy efficiency. 1°C rise in temperature of PV cells will reduce 0.4 – 0.5% of power energy efficiency for crystalline Si based cells and 0.25% for amorphous silicon (a-Si) cells. Moreover, the energy payback time (EPBT) for a photovoltaic system (PV) lies between 10 to 15 years depending on the efficiency of PV modules and the price of electricity. If the efficiency can be enhanced then the energy payback time span can be shortened. In order to

increase the power energy conversion efficiency of PV modules, it is most desired to transfer the accumulated heat out of concealed PV surface and exploit properly. The essential technology for this purpose, namely PV/T technology, has been in the market and still making rapid advances.

In Chapter III of this communication, it has been demonstrated that PV modules may be integrated with inexpensive, minimum maintenance requiring and easily adaptable polyethylene heat exchanger loop as a concealed heat extraction component without disturbing the original structure of PV modules in order to provide cooling of PV modules that would lead eventually enhanced electrical efficiency and renewable heat source for heating and cooling applications. As a result, the flowing water through the tubes and risers of poly heat exchanger generates cooling effect and removes waste heat from the PV modules as well.

Cooling by solar energy is one of the key solutions to the global energy and environmental degradation issues. Solar liquid desiccant based on evaporative cooling is proposed as an eco-friendly alternative to the conventional vapour compression systems due to its huge untapped energy savings potential. The idea of a liquid desiccant evaporative cooling system is to combine liquid desiccant dehumidification with an evaporative cooling system to advance the overall system performance and utilize solar energy as a source. In such a hybrid system, the desiccant dehumidification system is motivated to eliminate the latent load, while Indirect Evaporative Cooling (IEC) system is to provide the sensible heat load. Further, as only low-grade energy is required for the regeneration process of the desiccant dehumidification system, solar energy as a renewable energy source can handle the operation of liquid desiccant air

conditioning system. In terms of operational flexibility and ability of absorbing pollutants and bacteria, the liquid desiccants are more attractive than solid desiccants. Moreover, liquid desiccants are usually regenerated at lower temperatures (less than 82°C) and equally create lower airside pressure drops. The liquid desiccant cooling system could reach up to 40% of energy saving compared to corresponding conventional vapour compression systems and those savings would be even greater when the thermal energy required for the regeneration is extracted from a renewable source such as solar energy. Therefore, solar-driven liquid desiccant evaporative cooling is an innovative method in seeking for environmentally friendly air conditioning system that preserves and improves indoor air quality for inhabitants. Flexibility of these hybrid systems allows operation in different modes suitable for certain climate conditions. Solar assisted liquid desiccant evaporative systems can satisfy higher capacity and better thermal Coefficient of Performance (COP) ensuring its feasibility and effectiveness. As an example, in Chapter V, the integration of polyethylene heat exchanger loop underneath the PV modules with a hybrid liquid desiccant indirect evaporative cooling system has been experimentally analysed. The roof module provides the heat energy required to regenerate the weak desiccant solution and dew point cooling system provides the air conditioning through the dehumidification of humid air and indirect evaporative cooling.

In 2013, UK's total energy consumption was 205.9 million tonnes of oil equivalent (mtoe). About 31.7% of this total energy was consumed in domestic applications. Space heating alone accounts for 53% of the energy consumed in a typical UK household while it is estimated that about 13.7% is for low temperature (<80°C) water heating applications in which energy demand is primarily satisfied through either natural gas or

electrical heaters. However, use of conventional source of energy based systems leads to increased greenhouse gas emissions into the atmosphere. A typical natural gas water heater releases around 2 tons CO₂ annually. Electric hot water systems are having more harmful effect for about three times the emission of CO₂ for each kWh of electrical energy, compared to natural gas water heaters. In spite of low capital cost of this fossil fuel based systems, due to implicit environmental cost for remedy or separation of CO₂ fossil fuel burners it is worth the time, money or effort to search for less expensive, environmentally friendly alternatives such as solar energy, one of the most viable renewable based energy sources. A solar-assisted heat pump system (SAHP) is a particular technique to reduce or eliminate the primary energy (coal, natural gas, etc.) consumption through substitution of renewable based energy sources to achieve reduced CO₂ emission. The system is able to convert and transport low grade thermal energy from the sun to water or working medium or absorbers. On entire SAHP systems, energy sources and total energy load should be clarified for the assessment of those systems as these parameters may vary with components employed in the system, building loads and climate. For this reason, parameters like Free Energy Ratio (FER) or Seasonal Performance Factor (SPF) should also be considered on the entire system. Although the individual performance of the components is also significant, performance evaluations of solar collectors and heat pump do not merely picture the power need to meet the loads. Also, International Energy Agency Task 44 of the Solar Heating and Cooling (SHC) Programme is recently working on methods towards most effective use of solar heat pump systems for residential use.

In Chapter IIV, an indirect expansion solar assisted heat pump (IX-SAHP) application has been presented to illustrate a combination of solar thermal energy and heat pump for low temperature hot water applications. In this system, the solar collector loop enables to boost the heat source temperature of the heat pump, thereby improving the overall annual and seasonal performance. A low cost 'Sandwich' roof absorbs and emits heat from the ambient via convection, and solar radiation. Then, the absorbed low grade heat is transferred through the circulating water/glycol mixture across the heat exchanger and introduced to the evaporator. In the evaporator, glycol/water mixture exchanges heat with the refrigerant which becomes gas afterwards. At the end of this cycle, the low grade heat is upgraded to the high grade useful heat for hot water or space heating use.

8.2 GENERAL CONCLUSIONS

This project proposed a new kind of solar thermal collector mainly based on low cost and structurally unique polyethylene heat exchanger as a heat extraction component. The system meets the requirements and criterion set by IEA Task 41 Solar Energy and Architecture for aesthetic quality of building integrated solar thermal collectors.

The system also aims to overcome certain limitations of conventional solar thermal collectors such as being fragile, expensive to make and install and not aesthetically appealing, nor easily integrated into roofs or facades. In addition, it aims to provide an efficient renewable heat source for domestic heating and cooling applications.

A series of experiment (Chapter 5) was undertaken to investigate the performance characteristics of the 'invisible' collector with PV modules and to validate the thermal model developed by comparing the predicted results with the experimental data. The

comparative results indicate that the theoretical model makes a good compliance with the experimental results obtained. The results show that polyethylene heat exchanger with the unique structure has proven to be an efficient and cost-effective heat extraction component (temperature difference of up to 17°C and 26.6% thermal efficiency) for domestic water heating, solar assisted heating-cooling technologies and solar dryers etc. In addition to that the PV modules can yield better power energy performance due to achieved collector cooling. Hence the increased performance of the PV/T system will contribute to mitigate the energy supply of buildings and eventually reduce CO₂ emission towards zero-carbon homes and a sustainable environment. Other than the performance, removing waste heat away from the PV collectors can enhance the life cycle of modules since high operating temperatures may shorten the life-span.

The second set of experiments (Chapter 6) tested the 'invisible' solar collector coupled with a liquid desiccant enhanced indirect evaporative cooling system including a liquid desiccant based dehumidifier and a dew point evaporative cooler with a cross-flow core. The environmentally friendly, less corrosive, lower cost, lower density and viscosity potassium formate (HCOOK) solution was used as a liquid desiccant also considering its thermodynamic and physical benefits. Heat input to regenerate the dilute desiccant solution was partly harnessed from the roof loop and the remaining heat demand was met by employing a water immersion heater with rod thermostat. The combined experimental prototype was operated under various operational conditions to estimate the ability of such a combined small scale system for building applications and the results disclosed that the proposed system could meet the cooling needs and improve indoor air quality for occupants. In the broad picture, the system will help to mitigate

carbon emission by substituting the fossil fuel sources and bring along substantial amount of energy savings.

In the final set of experiment (Chapter 7), a novel solar thermal roof collector, also called 'Sandwich' roof, was investigated by primarily exploiting components and techniques widely available on the market and coupled with a commercial heat pump unit for water heating. A numerical model developed and validated by the experimental findings collected. As the comparison indicates, thermal model developed for this prototype has a good agreement with the experimental results obtained. The performance test results present that the flowing water/glycol mixture through tubes and risers of the heat exchanger layer can successfully convey the solar thermal energy and prove that proposed solar thermal collector can act as an efficient heat extraction component for solar source heat pump systems. The COPs of the heat pump and overall system are calculated in terms of experimental data from the outdoor test and encouraging results were obtained.

8.3 RECOMMENDATIONS

In addition to the further work detailed at the end of each chapter, the following elements also could lend themselves as possible areas for further research:

The applications of various solar thermal collectors are still limited due to product reliability and cost. Therefore, significant research is required mainly in thermal absorber design and fabrication, material and coating choice, energy conversion and effectiveness, cost reduction, performance testing and control of the system.

Solar assisted heat pump studies indicate that the effect of solar heat energy on the performance of both collector and heat pump individually, and on the entire SAHP

system to be majorly significant. Then again, the advanced configuration types of SAHP systems were found to be performing better than the conventional basic types with reference to reported COPs that might draw considerable interest for further investigations.

The future work is required for psychometric evaluation of various liquid desiccant cycles for air conditioning and new desiccant–augmented operative cooling cycles, new recirculation configuration, and combination of sorptive dehumidification with a conventional, electrically driven back up systems. This path seems to be worthwhile for future research and large scale demonstration projects.

Moreover, the advancement in zero water carry over dew point coolers utilizing hollow fibre membrane and combining dew point coolers with liquid desiccant dehumidification system for hot and humid climates are also intriguing research topics for future investigation in order to enhance the overall performance of liquid desiccant enhanced indirect evaporative dew point coolers. Also, further research on the development of liquid desiccant cooling systems employing innovative liquids like ionic solutions, and integrating thermal and thermo-chemical energy storage units with desiccant dehumidification based cooling systems would augment extend of the contribution that these system can potentially bring forward.

Lastly, the future investigation aiming to improve tri-generation systems (combined cooling, heating and power generation) is essential to serve residential and building applications. Harnessing the heat input from the tri-generation system for regeneration process of the liquid desiccant system is to be further researched using the new, efficient and environmentally friendly working fluids.

8.4 FUTURE WORK

Seasonal coefficient of performance (SCP) is the time and season of SAHP applications and is obtained by periodical computation of regular COP for a particular season or time frame. It is suggested to perform long term test of the systems assessed in this communication to obtain more reliable patterns regarding the system performance.

Economic analysis is an essential factor affecting the decision-making process on adoption of solar collector, solar assisted heating and cooling technology. Suggestions for future work include an economic model and a comparative evaluation study for pilot scale solar assisted heating and cooling systems, investigated in this project, applicable in international context including Middle East, Africa and South America region.

REFERENCES

- ABDALLA, S. A.; ABDALLA, KAMAL N. A radiant air-conditioning system using solar-driven liquid desiccant evaporative water cooler. *Journal of Engineering Science and Technology*, 2006, 1.2: 139-157.
- ABDEL-SALAM, Ahmed H.; GE, Gaoming; SIMONSON, Carey J. Thermo-economic performance of a solar membrane liquid desiccant air conditioning system. *Solar Energy*, 2014, 102: 56-73.
- ABU-ZOUR, A. M.; RIFFAT, S. B.; GILLOTT, M. New design of solar collector integrated into solar louvres for efficient heat transfer. *Applied thermal engineering*, 2006, 26.16: 1876-1882.
- ABU-ZOUR, Asaad; RIFFAT, Saffa. Environmental and economic impact of a new type of solar louvre thermal collector. *International Journal of Low-Carbon Technologies*, 2006, 1.3: 217-227.
- AGARWAL, Ram Kumar; GARG, H. P. Study of a photovoltaic-thermal system—thermosyphonic solar water heater combined with solar cells. *Energy conversion and management*, 1994, 35.7: 605-620.
- AGRAWAL, Basant; TIWARI, G. N. Life cycle cost assessment of building integrated photovoltaic thermal (BIPVT) systems. *Energy and Buildings*, 2010, 42.9: 1472-1481.
- AGRAWAL, Basant; TIWARI, G. N. Optimizing the energy and exergy of building integrated photovoltaic thermal (BIPVT) systems under cold climatic conditions. *Applied energy*, 2010, 87.2: 417-426.
- AGRAWAL, Sanjay; TIWARI, Arvind. Experimental validation of glazed hybrid micro-channel solar cell thermal tile. *Solar Energy*, 2011, 85.11: 3046-3056.
- AGRAWAL, Sanjay; TIWARI, G. N. Overall energy, exergy and carbon credit analysis by different type of hybrid photovoltaic thermal air collectors. *Energy Conversion and Management*, 2013, 65: 628-636.
- AHMAD, Aftab; REHMAN, Shafiqur; AL-HADHRAMI, Luai M. Performance evaluation of an indirect evaporative cooler under controlled environmental conditions. *Energy and Buildings*, 2013, 62: 278-285.
- AKYUZ, E., et al. A novel approach for estimation of photovoltaic exergy efficiency. *Energy*, 2012, 44.1: 1059-1066.
- AL-ALILI, A., et al. A high efficiency solar air conditioner using concentrating photovoltaic/thermal collectors. *Applied Energy*, 2012, 93: 138-147.

ALIZADEH, Shahab. A feasibility study of using solar liquid-desiccant air conditioner in Queensland, Australia. *Journal of Solar Energy Engineering*, 2008, 130.2: 021005.

ALIZADEH, Shahaboddin; SAMAN, Wasim Y. An experimental study of a forced flow solar collector/regenerator using liquid desiccant. *Solar Energy*, 2002, 73.5: 345-362.

ALKHAMIS, A. I.; SHERIF, S. A. Feasibility study of a solar-assisted heating/cooling system for an aquatic centre in hot and humid climates. *International journal of energy research*, 1997, 21.9: 823-839.

ALKILANI, Mahmud M., et al. Review of solar air collectors with thermal storage units. *Renewable and Sustainable Energy Reviews*, 2011, 15.3: 1476-1490.

ALOSAIMY, A. S.; HAMED, Ahmed M. Theoretical and experimental investigation on the application of solar water heater coupled with air humidifier for regeneration of liquid desiccant. *Energy*, 2011, 36.7: 3992-4001.

ALY, Ayman A.; ZEIDAN, El-Shafei B.; HAMED, Ahmed M. Solar-powered open absorption cycle modeling with two desiccant solutions. *Energy Conversion and Management*, 2011, 52.7: 2768-2776.

AMIN, Zakaria Mohd; HAWLADER, M. N. A. A review on solar assisted heat pump systems in Singapore. *Renewable and Sustainable Energy Reviews*, 2013, 26: 286-293.

ANDERSON, T. N.; MORRISON, G. L. Effect of load pattern on solar-boosted heat pump water heater performance. *Solar Energy*, 2007, 81.11: 1386-1395.

ANDERSON, Timothy N., et al. Performance of a building integrated photovoltaic/thermal (BIPVT) solar collector. *Solar Energy*, 2009, 83.4: 445-455.

ASHRAE, ANSI. Standard 55-2010:“Thermal Environmental Conditions for Human Occupancy”; ASHRAE. *Atlanta USA*, 2010.

ASHRAE, ASHRAE Handbook. HVAC Systems and Equipment, American Society of Heating. *Refrigeration and Air-conditioning Engineers, Atlanta, GA*, 2012.

ASTE, Niccolò; CHIESA, Giancarlo; VERRI, Francesco. Design, development and performance monitoring of a photovoltaic-thermal (PVT) air collector. *Renewable energy*, 2008, 33.5: 914-927.

ATHIENITIS, Andreas K., et al. A prototype photovoltaic/thermal system integrated with transpired collector. *Solar Energy*, 2011, 85.1: 139-153.

ATMACA, Ibrahim; KOCAK, Sezgi. Theoretical energy and exergy analyses of solar assisted heat pump space heating system. *Thermal Science*, 2013, 00: 24-24.

AUDAH, N.; GHADDAR, N.; GHALI, K. Optimized solar-powered liquid desiccant system to supply building fresh water and cooling needs. *Applied Energy*, 2011, 88.11: 3726-3736.

AXAOPOULOS, P.; PANAGAKIS, P.; KYRITSIS, S. Experimental comparison of a solar-assisted heat pump vs. a conventional thermosyphon solar system. *International journal of energy research*, 1998, 22.13: 1107-1120.

AYDIN, Devrim; CASEY, Sean P.; RIFFAT, Saffa. The latest advancements on thermochemical heat storage systems. *Renewable and Sustainable Energy Reviews*, 2015, 41: 356-367.

AYOMPE, L. M., et al. Comparative field performance study of flat plate and heat pipe evacuated tube collectors (ETCs) for domestic water heating systems in a temperate climate. *Energy*, 2011, 36.5: 3370-3378.

BADESCU, Viorel. Model of a thermal energy storage device integrated into a solar assisted heat pump system for space heating. *Energy conversion and management*, 2003, 44.10: 1589-1604.

BAI, Yu, et al. Analysis of a hybrid PV/thermal solar-assisted heat pump system for sports center water heating application. *International Journal of Photoenergy*, 2012, 2012.

BAKIRCI, Kadir; YUKSEL, Bedri. Experimental thermal performance of a solar source heat-pump system for residential heating in cold climate region. *Applied thermal engineering*, 2011, 31.8: 1508-1518.

BASSUONI, M. M. An experimental study of structured packing dehumidifier/regenerator operating with liquid desiccant. *Energy*, 2011, 36.5: 2628-2638.

BECCALI, Marco; FINOCCHIARO, Pietro; NOCKE, Bettina. Energy performance evaluation of a demo solar desiccant cooling system with heat recovery for the regeneration of the adsorption material. *Renewable Energy*, 2012, 44: 40-52.

BECKMAN, W.; DUFFIE, J. *Solar engineering of thermal process*. Wiley-Interscience Publication, 1980.

BERGENE, Trond; LØVVIK, Ole Martin. Model calculations on a flat-plate solar heat collector with integrated solar cells. *Solar energy*, 1995, 55.6: 453-462.

BERMEJO, Pablo; PINO, Francisco Javier; ROSA, Felipe. Solar absorption cooling plant in Seville. *Solar Energy*, 2010, 84.8: 1503-1512.

BERNARDO, Luís Ricardo, et al. Performance evaluation of low concentrating photovoltaic/thermal systems: A case study from Sweden. *Solar Energy*, 2011, 85.7: 1499-1510.

BERTO, Arnaldo Moreno. Ceramic tiles: Above and beyond traditional applications. *Journal of the European Ceramic Society*, 2007, 27.2: 1607-1613.

BERTRAM, Erik; PÄRISCH, Peter; TEPE, Rainer. Impact of solar heat pump system concepts on seasonal performance-Simulation studies. In: *Proceedings of the EuroSun 2012 Conference*. 2012.

BILGEN, E.; TAKAHASHI, H. Exergy analysis and experimental study of heat pump systems. *Exergy, an international journal*, 2002, 2.4: 259-265.

BILGILI, Mehmet. Hourly simulation and performance of solar electric-vapor compression refrigeration system. *Solar Energy*, 2011, 85.11: 2720-2731.

Bine, 2015. Available at www.bine.info ; accessed on 11th of January 2015.

BIROL, Fatih. World energy outlook 2010. *International Energy Agency*, 2010.

BONGS, Constanze; MORGENSTERN, Alexander; HENNING, Hans-Martin. Advanced performance of an open desiccant cycle with internal evaporative cooling. *Energy Procedia*, 2012, 30: 524-533.

BOURDOUKAN, P.; WURTZ, E.; JOUBERT, Patrice. Experimental investigation of a solar desiccant cooling installation. *Solar Energy*, 2009, 83.11: 2059-2073.

BRIDGEMAN, Andrew; HARRISON, Stephen. Preliminary experimental evaluations of indirect solar assisted heat pump systems. In: *3rd Canadian Solar Building Conference, Fredericton*. 2008.

British standard BS EN ISO 7730: Modern thermal environments.

BROGREN, Maria; KARLSSON, Bjorn. Low-concentrating water-cooled PV-thermal hybrid systems for high latitudes. In: *Photovoltaic Specialists Conference, 2002. Conference Record of the Twenty-Ninth IEEE*. IEEE, 2002. p. 1733-1736.

BRUNO, Frank. On-site experimental testing of a novel dew point evaporative cooler. *Energy and Buildings*, 2011, 43.12: 3475-3483.

BUDIARDJO, I.; MORRISON, G. L. Performance of water-in-glass evacuated tube solar water heaters. *Solar Energy*, 2009, 83.1: 49-56.

Building Services, 2015. Available at www.buildingservicesindex.co.uk ; accessed on 8th of January 2015.

Buker, M.S., Mempoouo, B., Riffat, S. (2013). Theoretical Investigation of the Thermal Performance of a Novel Building Integrated PV/Thermal Roof Collector. SET 2013 International Symposium on Sustainable Energy Technologies, August, 26-29, Hong-Kong, China.

BUKER, Mahmut Sami; MEMPOUO, Blaise; RIFFAT, Saffa B. Performance evaluation and techno-economic analysis of a novel building integrated PV/T roof collector: An experimental validation. *Energy and Buildings*, 2014, 76: 164-175.

ÇAĞLAR, Ahmet; YAMALI, Cemil. Performance analysis of a solar-assisted heat pump with an evacuated tubular collector for domestic heating. *Energy and Buildings*, 2012, 54: 22-28.

CALISKAN, Hakan; DINCER, Ibrahim; HEPBASLI, Arif. A comparative study on energetic, exergetic and environmental performance assessments of novel M-Cycle based air coolers for buildings. *Energy Conversion and Management*, 2012, 56: 69-79.

CERIT, Emine; ERBAY, L. Berrin. Investigation of the effect of rollbond evaporator design on the performance of direct expansion heat pump experimentally. *Energy Conversion and Management*, 2013, 72: 163-170.

CERVANTES, J. Gonzalo; TORRES-REYES, E. Experiments on a solar-assisted heat pump and an exergy analysis of the system. *Applied Thermal Engineering*, 2002, 22.12: 1289-1297.

CHANDRASHEKAR, M., et al. A comparative study of solar assisted heat pump systems for Canadian locations. *Solar Energy*, 1982, 28.3: 217-226.

CHATURVEDI, S. K.; CHEN, D. T.; KHEIREDDINE, A. Thermal performance of a variable capacity direct expansion solar-assisted heat pump. *Energy conversion and management*, 1998, 39.3: 181-191.

CHATURVEDI, S. K.; GAGRANI, V. D.; ABDEL-SALAM, T. M. Solar-assisted heat pump—a sustainable system for low-temperature water heating applications. *Energy Conversion and Management*, 2014, 77: 550-557.

CHATURVEDI, S. K.; MEI, V. C. Thermal performance of SAHP system with combined collector/evaporator. In: *AIAA terrestrial energy systems conference*, AIAA. 1979. p. 79-0976.

CHEMISANA, Daniel, et al. Building integration of concentrating systems for solar cooling applications. *Applied Thermal Engineering*, 2013, 50.2: 1472-1479.

CHEMISANA, Daniel. Building integrated concentrating photovoltaics: a review. *Renewable and Sustainable Energy Reviews*, 2011, 15.1: 603-611.

CHEMISANA, Daniel. Building integrated concentrating photovoltaics: a review. *Renewable and Sustainable Energy Reviews*, 2011, 15.1: 603-611.

CHEMISANA, Daniel; IBÁÑEZ, Manuel. Linear Fresnel concentrators for building integrated applications. *Energy Conversion and management*, 2010, 51.7: 1476-1480.

CHEN, Hongbing; RIFFAT, Saffa B.; FU, Yu. Experimental study on a hybrid photovoltaic/heat pump system. *Applied Thermal Engineering*, 2011, 31.17: 4132-4138.

CHEN, Qun, et al. A new approach to analysis and optimization of evaporative cooling system I: Theory. *Energy*, 2010, 35.6: 2448-2454.

CHEN, Xi; YANG, Hongxing. Performance analysis of a proposed solar assisted ground coupled heat pump system. *Applied Energy*, 2012, 97: 888-896.

CHENG, Qing; ZHANG, Xiaosong. Review of solar regeneration methods for liquid desiccant air-conditioning system. *Energy and Buildings*, 2013, 67: 426-433.

CHENG, Qing; ZHANG, Xiao-Song; LI, Xiu-Wei. Double-stage photovoltaic/thermal ED regeneration for liquid desiccant cooling system. *Energy and Buildings*, 2012, 51: 64-72.

CHOI, Jong Min; PARK, Yong-Jung; KANG, Shin-Hyung. Temperature distribution and performance of ground-coupled multi-heat pump systems for a greenhouse. *Renewable Energy*, 2014, 65: 49-55.

CHOI, Jongmin; KANG, Byun; CHO, Honghyun. Performance comparison between R22 and R744 solar-geothermal hybrid heat pumps according to heat source conditions. *Renewable Energy*, 2014, 71: 414-424.

CHONG, W. T., et al. Techno-economic analysis of a wind-solar hybrid renewable energy system with rainwater collection feature for urban high-rise application. *Applied Energy*, 2011, 88.11: 4067-4077.

CHOW, T. T. Performance analysis of photovoltaic-thermal collector by explicit dynamic model. *Solar Energy*, 2003, 75.2: 143-152.

CHOW, T. T., et al. Performance evaluation of a PV ventilated window applying to office building of Hong Kong. *Energy and Buildings*, 2007, 39.6: 643-650.

CHOW, T. T., et al. Potential application of a centralized solar water-heating system for a high-rise residential building in Hong Kong. *Applied Energy*, 2006, 83.1: 42-54.

CHOW, T. T.; QIU, Zhongzhu; LI, Chunying. Performance evaluation of PV ventilated glazing. In: Proceedings of the BS2009, 11th IBPSA conference, Glasgow, UK. 2009. p. 258-63.

CHOW, Tin Tai, et al. A comparative study of PV glazing performance in warm climate. *Indoor and Built Environment*, 2009, 18.1: 32-40.

CHOW, Tin Tai, et al. Analysis of a solar assisted heat pump system for indoor swimming pool water and space heating. *Applied Energy*, 2012, 100: 309-317.

CHOW, Tin Tai, et al. Annual performance of building-integrated photovoltaic/water-heating system for warm climate application. *Applied Energy*, 2009, 86.5: 689-696.

CHOW, Tin Tai, et al. Modelling and application of direct-expansion solar-assisted heat pump for water heating in subtropical Hong Kong. *Applied Energy*, 2010, 87.2: 643-649.

CHOW, Tin Tai. A review on photovoltaic/thermal hybrid solar technology. *Applied Energy*, 2010, 87.2: 365-379.

CHU, Jenny; CRUICKSHANK, Cynthia A. Solar-Assisted Heat Pump Systems: A Review of Existing Studies and Their Applicability to the Canadian Residential Sector. In: *ASME 2013 7th International Conference on Energy Sustainability collocated with the ASME 2013 Heat Transfer Summer Conference and the ASME 2013 11th International Conference on Fuel Cell Science, Engineering and Technology*. American Society of Mechanical Engineers, 2013. p. V001T01A009-V001T01A009.

CHUA, K. J., et al. Heat pump drying: Recent developments and future trends. *Drying Technology*, 2002, 20.8: 1579-1610.

CHYNG, J. P.; LEE, C. P.; HUANG, B. J. Performance analysis of a solar-assisted heat pump water heater. *Solar Energy*, 2003, 74.1: 33-44.

Citytrade, 2015. Available at www.citytrade.com.ph ; accessed on 13th of January 2015.

Code for Sustainable Homes, Source: <http://www.ukgbc.org>

CORBIN, Charles D.; ZHAI, Zhiqiang John. Experimental and numerical investigation on thermal and electrical performance of a building integrated photovoltaic–thermal collector system. *Energy and Buildings*, 2010, 42.1: 76-82.

CRISTOFARI, Christian, et al. Modelling and performance of a copolymer solar water heating collector. *Solar Energy*, 2002, 72.2: 99-112.

D'Antoni, M., and Sparber, W., 2011, IEA– SHC Task 44/Annex 38 Solar and Heat Pump Systems: Industry Newsletter First Issue. Available at www.task44.iea-shc.org/Data/Sites/1/publications/2011-10-Task33-Annex38-Newsletter.pdf

DAGDOUGUI, Hanane, et al. Thermal analysis and performance optimization of a solar water heater flat plate collector: application to Tétouan (Morocco). *Renewable and Sustainable Energy Reviews*, 2011, 15.1: 630-638.

DAGHIGH, R.; RUSLAN, M. H.; SOPIAN, K. Advances in liquid based photovoltaic/thermal (PV/T) collectors. *Renewable and Sustainable Energy Reviews*, 2011, 15.8: 4156-4170.

DAGHIGH, Ronak, et al. Review of solar assisted heat pump drying systems for agricultural and marine products. *Renewable and Sustainable Energy Reviews*, 2010, 14.9: 2564-2579.

DAOU, Kadoma; WANG, R. Z.; XIA, Z. Z. Desiccant cooling air conditioning: a review. *Renewable and Sustainable Energy Reviews*, 2006, 10.2: 55-77.

DAS, Rajat Subhra; SAHA, Pratik Kumar; JAIN, Sanjeev. Investigations on solar energy driven liquid desiccant cooling systems for tropical climates.

DELISLE, Veronique; COLLINS, Michael R. Model of a PV/thermal unglazed transpired solar collector. In: Proceedings of 32nd Solar and Sustainable Energy of Canada Inc. Conference, Calgary, Alberta, Canada. 2007. p. 10-13.

Department of Energy and Climate Change. Energy consumption in the UK (2013). Chapter 3, Domestic energy consumption in the UK between 1970 and 2013. Published on 31 July 2014.

DHARUMAN, Chinna; ARAKERI, J. H.; SRINIVASAN, Katepalli. Performance evaluation of an integrated solar water heater as an option for building energy conservation. *Energy and Buildings*, 2006, 38.3: 214-219.

DUBEY, Swapnil; SANDHU, G. S.; TIWARI, G. N. Analytical expression for electrical efficiency of PV/T hybrid air collector. *Applied Energy*, 2009, 86.5: 697-705.

DUBEY, Swapnil; SOLANKI, S. C.; TIWARI, Arvind. Energy and exergy analysis of PV/T air collectors connected in series. *Energy and Buildings*, 2009, 41.8: 863-870.

EICKER, Ursula; DALIBARD, Antoine. Photovoltaic–thermal collectors for night radiative cooling of buildings. *Solar Energy*, 2011, 85.7: 1322-1335.

ELSARRAG, Esam. Evaporation rate of a novel tilted solar liquid desiccant regeneration system. *Solar Energy*, 2008, 82.7: 663-668.

EL-SAWI, A. M., et al. Application of folded sheet metal in flat bed solar air collectors. *Applied Thermal Engineering*, 2010, 30.8: 864-871.

EL-SEBAIL, A. A., et al. Thermal performance investigation of double pass-finned plate solar air heater. *Applied Energy*, 2011, 88.5: 1727-1739.

Energy Saving Trust, 2010. Source: www.energysavingtrust.org.uk

ENTERIA, Napoleon; MIZUTANI, Kunio. The role of the thermally activated desiccant cooling technologies in the issue of energy and environment. *Renewable and Sustainable Energy Reviews*, 2011, 15.4: 2095-2122.

ESEN, Mehmet; ESEN, Hikmet. Experimental investigation of a two-phase closed thermosyphon solar water heater. *Solar Energy*, 2005, 79.5: 459-468.

Evap, 2015. Available at www.ecobuildingpulse.com ; accessed on 16th of January 2015.

FANINGER, Gerhard. The Potential of Solar Thermal Technologies in a Sustainable Energy Future. Results from, 2010, 32.

Feed-In-Tariffs Scheme (FITs). www.energysavingtrust.org.uk/Generating-energy/Getting-money-back/Feed-In-Tariffs-scheme-FITs ; accessed on January, 2014.

FERNÁNDEZ-SEARA, José, et al. Experimental analysis of a direct expansion solar assisted heat pump with integral storage tank for domestic water heating under zero solar radiation conditions. *Energy Conversion and Management*, 2012, 59: 1-8.

FONG, K. F., et al. Solar hybrid cooling system for high-tech offices in subtropical climate—Radiant cooling by absorption refrigeration and desiccant dehumidification. *Energy Conversion and Management*, 2011, 52.8: 2883-2894.

Fossil Fuel. Source: www.en.wikipedia.org/wiki/Fossil_fuel (accessed on May, 2014]

FRANK, Elimar, et al. Systematic classification of combined solar thermal and heat pump systems. In: *Proc. of the EuroSun 2010 Conference, Graz, Austria*. 2010.

FREEMAN, T. L.; MITCHELL, J. W.; AUDIT, T. E. Performance of combined solar-heat pump systems. *Solar Energy*, 1979, 22.2: 125-135.

FTHENAKIS, Vasilis; MASON, James E.; ZWEIBEL, Ken. The technical, geographical, and economic feasibility for solar energy to supply the energy needs of the US. *Energy Policy*, 2009, 37.2: 387-399.

FU, H. D., et al. Experimental study of a photovoltaic solar-assisted heat-pump/heat-pipe system. *Applied Thermal Engineering*, 2012, 40: 343-350.

FUMO, Nelson; GOSWAMI, D. Y. Study of an aqueous lithium chloride desiccant system: air dehumidification and desiccant regeneration. *Solar energy*, 2002, 72.4: 351-361.

GANDHIDASAN, P. Analysis of a solar space cooling system using liquid desiccants. *Journal of Energy Resources Technology*, 1990, 112.4: 246-250.

GANG, Pei, et al. Performance study and parametric analysis of a novel heat pipe PV/T system. *Energy*, 2012, 37.1: 384-395.

GAO, W. Z., et al. Experimental investigation on integrated liquid desiccant–Indirect evaporative air cooling system utilizing the Maisotesenko–Cycle. *Applied Thermal Engineering*, 2014.

GAO, W. Z., et al. Experimental study on partially internally cooled dehumidification in liquid desiccant air conditioning system. *Energy and Buildings*, 2013, 61: 202-209.

GARG, H. P.; AGARWAL, R. K.; JOSHI, J. C. Experimental study on a hybrid photovoltaic-thermal solar water heater and its performance predictions. *Energy Conversion and Management*, 1994, 35.7: 621-633.

GE, T. S., et al. Performance investigation on a novel two-stage solar driven rotary desiccant cooling system using composite desiccant materials. *Solar Energy*, 2010, 84.2: 157-159.

GEBREHIWOT, Betsegaw, et al. CFD Modeling of Indirect/Direct Evaporative Cooling Unit for Modular Data Center Applications. In: *ASME 2013 International Technical Conference and Exhibition on Packaging and Integration of Electronic and Photonic Microsystems*. American Society of Mechanical Engineers, 2013. p. V002T08A054-V002T08A054.

GEORGIEV, A. Testing solar collectors as an energy source for a heat pump. *Renewable Energy*, 2008, 33.4: 832-838.

GLO, 2015. Available at www.globalspec.com ; accessed on 2nd of January 2015.

GOLDSWORTHY, Mark; WHITE, Stephen. Optimisation of a desiccant cooling system design with indirect evaporative cooler. *International Journal of refrigeration*, 2011, 34.1: 148-158.

GOMMED, K.; GROSSMAN, G. A liquid desiccant system for solar cooling and dehumidification. *Journal of Solar Energy Engineering*, 2004, 126.3: 879-885.

GOROZABEL CHATA, Francis Benjamín; CHATURVEDI, S. K.; ALMOGBEL, A. Analysis of a direct expansion solar assisted heat pump using different refrigerants. *Energy Conversion and Management*, 2005, 46.15: 2614-2624.

HADORN, Jean-Christophe. IEA Solar and Heat Pump Systems Solar Heating and Cooling Task 44 & Heat Pump Programme Annex 38. *Energy Procedia*, 2012, 30: 125-133.

HALLER, Michel Y.; FRANK, Elimar. On the potential of using heat from solar thermal collectors for heat pump evaporators. In: *ISES Solar World Congress*. 2011.

HAMED, Ahamed M., et al. Application of solar energy for regeneration of liquid desiccant using rotating tilted wick. *International Journal of Mechanical & Mechatronics Engineering IJMME-IJENS*, 2012, 12.05: P21-29.

HAWLADER, M. N. A.; CHOU, S. K.; ULLAH, M. Z. The performance of a solar assisted heat pump water heating system. *Applied Thermal Engineering*, 2001, 21.10: 1049-1065.

HAWLADER, M. N. A.; RAHMAN, S. M. A.; JAHANGEER, K. A. Performance of evaporator-collector and air collector in solar assisted heat pump dryer. *Energy Conversion and Management*, 2008, 49.6: 1612-1619.

HE, Wei, et al. A study on incorporation of thermoelectric modules with evacuated-tube heat-pipe solar collectors. *Renewable Energy*, 2012, 37.1: 142-149.

HE, Wei; ZHANG, Yang; JI, Jie. Comparative experiment study on photovoltaic and thermal solar system under natural circulation of water. *Applied Thermal Engineering*, 2011, 31.16: 3369-3376.

HEGAZY, Adel A. Comparative study of the performances of four photovoltaic/thermal solar air collectors. *Energy Conversion and Management*, 2000, 41.8: 861-881.

HENNING, H. M., et al. The potential of solar energy use in desiccant cooling cycles. *International journal of refrigeration*, 2001, 24.3: 220-229.

HEPBASLI, Arif; KALINCI, Yildiz. A review of heat pump water heating systems. *Renewable and Sustainable Energy Reviews*, 2009, 13.6: 1211-1229.

HUANG, B. J., et al. Development of hybrid solar-assisted cooling/heating system. *Energy conversion and Management*, 2010, 51.8: 1643-1650.

HUANG, B. J., et al. System performance and economic analysis of solar-assisted cooling/heating system. *Solar Energy*, 2011, 85.11: 2802-2810.

HULIN, Huang; XINSHI, Ge; YUEHONG, Su. Theoretical thermal performance analysis of two solar-assisted heat-pump systems. *International journal of energy research*, 1999, 23.1: 1-6.

HVAC, 2015. Available at www.wescorhvac.com ; accessed on 16th of January 2015.

Hydro, 2015. Available at www.hydro.com ; accessed on 12th of January 2015.

IEA, I. E. A. Key World Energy Statistics, 2013.

IEA-SHC, 2015. Available at www.projects.iea-shc.org/task39 ; accessed on 12th of January 2015.

Insolation on Horizontal Surface. NASA Surface meteorology and Solar Energy: Daily Averaged Data. www.eosweb.larc.nasa.gov/cgi-bin/sse/daily.cgi?email=skip@larc.nasa.gov ; accessed on January 2014

ISETTI, Carlo; NANNEI, Enrico; MAGRINI, Anna. On the application of a membrane air—liquid contactor for air dehumidification. *Energy and Buildings*, 1997, 25.3: 185-193.

ITO, S.; MIURA, N.; WANG, K. Performance of a heat pump using direct expansion solar collectors. *Solar Energy*, 1999, 65.3: 189-196.

JAISANKAR, S., et al. A comprehensive review on solar water heaters. *Renewable and Sustainable Energy Reviews*, 2011, 15.6: 3045-3050.

Jl, Jie, et al. Effect of fluid flow and packing factor on energy performance of a wall-mounted hybrid photovoltaic/water-heating collector system. *Energy and buildings*, 2006, 38.12: 1380-1387.

Jl, Jie, et al. Experimental study of photovoltaic solar assisted heat pump system. *Solar Energy*, 2008, 82.1: 43-52.

Jl, Jie, et al. Thermal characteristics of a building-integrated dual-function solar collector in water heating mode with natural circulation. *Energy*, 2011, 36.1: 566-574.

JORDAN, R. C.; THRELKELD, J. L. Design and economics of solar energy heat pump system. *Heat., Piping Air Cond.:(United States)*, 1954, 26.

JRADI, M.; RIFFAT, S. Experimental investigation of a biomass-fuelled micro-scale tri-generation system with an organic Rankine cycle and liquid desiccant cooling unit. *Energy*, 2014.

KABEEL, A. E. Augmentation of the performance of solar regenerator of open absorption cooling system. *Renewable Energy*, 2005, 30.3: 327-338.

KALOGIROU, S. A.; TRIPANAGNOSTOPOULOS, Y. Hybrid PV/T solar systems for domestic hot water and electricity production. *Energy Conversion and Management*, 2006, 47.18: 3368-3382.

KALOGIROU, Soteris A. Building integration of solar renewable energy systems towards zero or nearly zero energy buildings. *International Journal of Low-Carbon Technologies*, 2013, ctt071.

KAMTHANIA, Deepali; NAYAK, Sujata; TIWARI, G. N. Performance evaluation of a hybrid photovoltaic thermal double pass facade for space heating. *Energy and Buildings*, 2011, 43.9: 2274-2281.

KANDILLI, Canan. Performance analysis of a novel concentrating photovoltaic combined system. *Energy Conversion and Management*, 2013, 67: 186-196.

KARA, Ozer; ULGEN, Koray; HEPBASLI, Arif. Exergetic assessment of direct-expansion solar-assisted heat pump systems: review and modeling. *Renewable and Sustainable Energy Reviews*, 2008, 12.5: 1383-1401.

KARACAVUS, Berrin; CAN, Ahmet. Experimental investigation of a solar energy heating system under the climatic conditions of Edirne. *Renewable Energy*, 2008, 33.9: 2084-2096.

KARAVA, Panagiota; JUBAYER, Chowdhury Mohammad; SAVORY, Eric. Numerical modelling of forced convective heat transfer from the inclined windward roof of an isolated low-rise building with application to photovoltaic/thermal systems. *Applied Thermal Engineering*, 2011, 31.11: 1950-1963.

KARIM, Md Azharul; HAWLADER, M. N. A. Performance investigation of flat plate, v-corrugated and finned air collectors. *Energy*, 2006, 31.4: 452-470.

KARSLI, Suleyman. Performance analysis of new-design solar air collectors for drying applications. *Renewable Energy*, 2007, 32.10: 1645-1660.

KATEJANEKARN, Thosapon; CHIRARATTANANON, Surapong; KUMAR, S. An experimental study of a solar-regenerated liquid desiccant ventilation pre-conditioning system. *Solar Energy*, 2009, 83.6: 920-933.

KATEJANEKARN, Thosapon; KUMAR, S. Performance of a solar-regenerated liquid desiccant ventilation pre-conditioning system. *Energy and Buildings*, 2008, 40.7: 1252-1267.

KAYGUSUZ, K.; AYHAN, T. Experimental and theoretical investigation of combined solar heat pump system for residential heating. *Energy Conversion and Management*, 1999, 40.13: 1377-1396.

KELIANG, Liu, et al. Performance study of a photovoltaic solar assisted heat pump with variable-frequency compressor—a case study in Tibet. *Renewable Energy*, 2009, 34.12: 2680-2687.

KHAN, Naghman; SU, Yuehong; RIFFAT, Saffa B. A review on wind driven ventilation techniques. *Energy and Buildings*, 2008, 40.8: 1586-1604.

KHANAL, Rakesh; LEI, Chengwang. Solar chimney—A passive strategy for natural ventilation. *Energy and Buildings*, 2011, 43.8: 1811-1819.

KIM, Jin-Hee, et al. Experimental Performance of Heating System with Building-integrated PVT (BIPVT) Collector. *Energy Procedia*, 2014, 48: 1374-1384.

KIM, Min-Hwi, et al. Annual operating energy savings of liquid desiccant and evaporative-cooling-assisted 100% outdoor air system. *Energy and Buildings*, 2014, 76: 538-550.

KIM, Min-Hwi; PARK, Jun-Seok; JEONG, Jae-Weon. Energy saving potential of liquid desiccant in evaporative-cooling-assisted 100% outdoor air system. *Energy*, 2013, 59: 726-736.

KOEHL, Michael, et al. Task 39 Exhibition–Assembly of Polymeric Components for a New Generation of Solar Thermal Energy Systems. *Energy Procedia*, 2014, 48.Complete: 130-136.

KÖHL, Michael, et al. (ed.). *Polymeric Materials for Solar Thermal Applications*. John Wiley & Sons, 2012.

KONG, X. Q., et al. Thermal performance analysis of a direct-expansion solar-assisted heat pump water heater. *Energy*, 2011, 36.12: 6830-6838.

KORONEOS, C.; TSAROUHIS, M. Exergy analysis and life cycle assessment of solar heating and cooling systems in the building environment. *Journal of Cleaner Production*, 2012, 32: 52-60.

KOZUBAL, Eric, et al. Desiccant enhanced evaporative air-conditioning (DEVap): Evaluation of a new concept in ultra efficient air conditioning. *Contract*, 2011, 303: 275-3000.

KRAKOW, K. I.; LIN, S. A computer model for the simulation of multiple source heat pump performance. *ASHRAE transactions*, 1983, 89: 590-616.

KRAUSE, Michael, et al. *Optimisation of a regenerator for open cycle liquid desiccant air conditioning systems*. 2006. PhD Thesis. Solar Energy Society.

KUANG, Y. H.; SUMATHY, K.; WANG, R. Z. Study on a direct-expansion solar-assisted heat pump water heating system. *International Journal of Energy Research*, 2003, 27.5: 531-548.

KUANG, Y. H.; WANG, R. Z. Performance of a multi-functional direct-expansion solar assisted heat pump system. *Solar Energy*, 2006, 80.7: 795-803.

KUMAR, Anil; BAREDAR, Prashant; QURESHI, Uzma. Historical and recent development of photovoltaic thermal (PVT) technologies. *Renewable and Sustainable Energy Reviews*, 2015, 42: 1428-1436.

KUMAR, Rakesh; ROSEN, Marc A. A critical review of photovoltaic–thermal solar collectors for air heating. *Applied Energy*, 2011, 88.11: 3603-3614.

LAZZARIN, Renato M. Technological innovations in heat pump systems. *International Journal of Low-Carbon Technologies*, 2007, 2.3: 262-288.

LI, Hong; YANG, Hongxing. Energy and exergy analysis of multi-functional solar-assisted heat pump system. *International Journal of Low-Carbon Technologies*, 2010, 5.3: 130-136.

LI, Hong; YANG, Hongxing. Study on performance of solar assisted air source heat pump systems for hot water production in Hong Kong. *Applied Energy*, 2010, 87.9: 2818-2825.

LI, Xiu-Wei; ZHANG, Xiao-Song. Photovoltaic–electrodialysis regeneration method for liquid desiccant cooling system. *Solar Energy*, 2009, 83.12: 2195-2204.

LI, Xiu-Wei; ZHANG, Xiao-Song; QUAN, Shuo. Single-stage and double-stage photovoltaic driven regeneration for liquid desiccant cooling system. *Applied Energy*, 2011, 88.12: 4908-4917.

LI, Y. W., et al. Experimental performance analysis and optimization of a direct expansion solar-assisted heat pump water heater. *Energy*, 2007, 32.8: 1361-1374.

LI, Yutong; LU, Lin; YANG, Hongxing. Energy and economic performance analysis of an open cycle solar desiccant dehumidification air-conditioning system for application in Hong Kong. *Solar Energy*, 2010, 84.12: 2085-2095.

LIN, Wenxian; GAO, Wenfeng; LIU, Tao. A parametric study on the thermal performance of cross-corrugated solar air collectors. *Applied Thermal Engineering*, 2006, 26.10: 1043-1053.

LIOR, Noam. Solar energy and the steam Rankine cycle for driving and assisting heat pumps in heating and cooling modes. *Energy Conversion*, 1977, 16.3: 111-123.

LIU, Liping; ZHANG, Hua. Energy-exergy analysis of a direct-expansion solar-assisted heat pump floor heating system. In: *Materials for Renewable Energy & Environment (ICMREE), 2011 International Conference on*. IEEE, 2011. p. 213-216.

LOF, George OG. Cooling with solar energy. In: *Congress on solar energy*. 1955. p. 171-189.

LOOSE, Anja, et al. Field test for performance monitoring of combined solar thermal and heat pump systems. In: *ISES Solar World Congress*. 2011.

LOWENSTEIN, Andrew. Review of liquid desiccant technology for HVAC applications. *HVAC&R Research*, 2008, 14.6: 819-839.

LOWENSTEIN, Andrew; SLAYZAK, Steve; KOZUBAL, Eric. A zero carryover liquid-desiccant air conditioner for solar applications. In: *ASME 2006 International Solar Energy Conference*. American Society of Mechanical Engineers, 2006. p. 397-407.

LUO, Yimo, et al. Investigation on feasibility of ionic liquids used in solar liquid desiccant air conditioning system. *Solar Energy*, 2012, 86.9: 2718-2724.

LYCHNOS, George; DAVIES, Philip A. Modelling and experimental verification of a solar-powered liquid desiccant cooling system for greenhouse food production in hot climates. *Energy*, 2012, 40.1: 116-130.

MA, Liangdong, et al. Thermal performance analysis of the glass evacuated tube solar collector with U-tube. *Building and Environment*, 2010, 45.9: 1959-1967.

MACARTHUR, J. W.; PALM, W. J.; LESSMANN, R. C. Performance analysis and cost optimization of a solar-assisted heat pump system. *Solar Energy*, 1978, 21.1: 1-9.

MARTINOPOULOS, G., et al. CFD modeling of a polymer solar collector. *Renewable Energy*, 2010, 35.7: 1499-1508.

MEI, L.; DAI, Y. J. A technical review on use of liquid-desiccant dehumidification for air-conditioning application. *Renewable and Sustainable Energy Reviews*, 2008, 12.3: 662-689.

MISHRA, R. K.; TIWARI, G. N. Energy and exergy analysis of hybrid photovoltaic thermal water collector for constant collection temperature mode. *Solar Energy*, 2013, 90: 58-67.

MITTELMAN, Gur; KRIBUS, Abraham; DAYAN, Abraham. Solar cooling with concentrating photovoltaic/thermal (CPVT) systems. *Energy Conversion and Management*, 2007, 48.9: 2481-2490.

MOHAMMAD, Abdulrahman Th, et al. Historical review of liquid desiccant evaporation cooling technology. *Energy and Buildings*, 2013, 67: 22-33.

MOHANRAJ, M.; JAYARAJ, S.; MURALEEDHARAN, C. A comparison of the performance of a direct expansion solar assisted heat pump working with R22 and a mixture of R407C–liquefied petroleum gas. *Proceedings of the Institution of Mechanical Engineers, Part A: Journal of Power and Energy*, 2009, 223.7: 821-833.

MOHANRAJ, M.; JAYARAJ, S.; MURALEEDHARAN, C. Exergy analysis of direct expansion solar-assisted heat pumps using artificial neural networks. *International Journal of Energy Research*, 2009, 33.11: 1005-1020.

MORADGHOLI, Meysam; NOWEE, Seyed Mostafa; ABRISHAMCHI, Iman. Application of heat pipe in an experimental investigation on a novel photovoltaic/thermal (PV/T) system. *Solar Energy*, 2014, 107: 82-88.

MORENO-RODRÍGUEZ, A., et al. Theoretical model and experimental validation of a direct-expansion solar assisted heat pump for domestic hot water applications. *Energy*, 2012, 45.1: 704-715.

MORGAN, R. G. Solar assisted heat pump. *Solar Energy*, 1982, 28.2: 129-135.

MUNARI PROBST, Maria Cristina, et al. Solar Energy Systems in Architecture-integration criteria and guidelines. Munari Probst, Maria Cristina and Roecker, Christian for International Energy Agency Solar Heating and Cooling Programme, 2013.

MUNARI PROBST, MariaCristina; ROECKER, Christian. Towards an improved architectural quality of building integrated solar thermal systems (BIST). *Solar Energy*, 2007, 81.9: 1104-1116.

NKWETTA, Dan Nchelatebe; SMYTH, Mervyn. Performance analysis and comparison of concentrated evacuated tube heat pipe solar collectors. *Applied Energy*, 2012, 98: 22-32.

NORTON, Brian. Anatomy of a solar collector: developments in materials, components and efficiency improvements in solar thermal collector systems. *Refocus*, 2006, 7.3: 32-35.

NOTTON, Gilles, et al. Performances and numerical optimization of a novel thermal solar collector for residential building. *Renewable and Sustainable Energy Reviews*, 2014, 33: 60-73.

OLIVARES, A., et al. A test procedure for extruded polymeric solar thermal absorbers. *Solar Energy Materials and Solar Cells*, 2008, 92.4: 445-452.

OLIVEIRA, Armando C., et al. Thermal performance of a novel air conditioning system using a liquid desiccant. *Applied Thermal Engineering*, 2000, 20.13: 1213-1223.

OMOJARO, Peter; BREITKOPF, Cornelia. Direct expansion solar assisted heat pumps: A review of applications and recent research. *Renewable and Sustainable Energy Reviews*, 2013, 22: 33-45.

OTANICAR, Todd; TAYLOR, Robert A.; PHELAN, Patrick E. Prospects for solar cooling—An economic and environmental assessment. *Solar Energy*, 2012, 86.5: 1287-1299.

OZGEN, Filiz; ESEN, Mehmet; ESEN, Hikmet. Experimental investigation of thermal performance of a double-flow solar air heater having aluminium cans. *Renewable Energy*, 2009, 34.11: 2391-2398.

OZGOREN, M., et al. Experimental Performance Investigation of Photovoltaic/Thermal (PV–T) System. In: *EPJ Web of Conferences*. EDP Sciences, 2013. p. 01106.

PALMERO-MARRERO, Ana I.; OLIVEIRA, Armando C. Effect of louver shading devices on building energy requirements. *Applied Energy*, 2010, 87.6: 2040-2049.

PALMERO-MARRERO, Ana I.; OLIVEIRA, Armando C. Evaluation of a solar thermal system using building louvre shading devices. *Solar energy*, 2006, 80.5: 545-554.

PALMERO-MARRERO, Ana I.; OLIVEIRA, Armando C. Evaluation of a solar cooling system with louvre thermal collectors. *International Journal of Low-Carbon Technologies*, 2007, 2.2: 99-108.

PANARAS, G.; MATHIOULAKIS, E.; BELESSIOTIS, V. A method for the dynamic testing and evaluation of the performance of combined solar thermal heat pump hot water systems. *Applied Energy*, 2014, 114: 124-134.

PANTIC, S.; CANDANEDO, L.; ATHIENTIS, A. K. Modelling of energy performance of a house with three configurations of building-integrated photovoltaic/thermal systems. *Energy and Buildings*, 2010, 42.10: 1779-1789.

PENG, Donggen; ZHANG, Xiaosong. Modelling and performance analysis of solar air pretreatment collector/regenerator using liquid desiccant. *Renewable Energy*, 2009, 34.3: 699-705.

PENG, Donggen; ZHANG, Xiaosong; YIN, Yonggao. Theoretical storage capacity for solar air pretreatment liquid collector/regenerator. *Applied Thermal Engineering*, 2008, 28.11: 1259-1266.

PETRAKIS, M.; BARAKOS, G.; KAPLANIS, S. Roof integrated mini-parabolic solar collectors. Comparison between simulation and experimental results. *Open Fuels & Energy Science Journal*, 2009, 2: 71-81.

PONS, Michel. Exergy analysis of solar collectors, from incident radiation to dissipation. *Renewable Energy*, 2012, 47: 194-202.

PV, 2015. Available at www.ecmweb.com ; accessed on 7th of June 2015.

Qian Jian-Feng, Zhang Ji-Lil MA, Lianf-dong. Analysis of a new photovoltaic thermal building integration system and correlative technology. *Build Energy Environ*, 2010, 29(2):12-6.

QIU, Guoquan; LIU, Hao; RIFFAT, Saffa B. Experimental investigation of a liquid desiccant cooling system driven by flue gas waste heat of a biomass boiler. *International Journal of Low-Carbon Technologies*, 2013, 8.3: 165-172.

QUAN, Z., et al. The experiment research for solar PV/T system based on flat-plate heat pipes. In: Proceeding the 17th Chinese national HVAC&R academic conference. 2010.

RIANGVILAIKUL, B.; KUMAR, S. An experimental study of a novel dew point evaporative cooling system. *Energy and Buildings*, 2010, 42.5: 637-644.

RIFFAT, S. B.; JAMES, S. E.; WONG, C. W. Experimental analysis of the absorption and desorption rates of HCOOK/H₂O and LiBr/H₂O. *International journal of energy research*, 1998, 22.12: 1099-1103.

ROSEN, Marc A.; DINCER, Ibrahim; KANOGLU, Mehmet. Role of exergy in increasing efficiency and sustainability and reducing environmental impact. *Energy Policy*, 2008, 36.1: 128-137.

RUSCHENBURG, Jörn, et al. A Review of Market-Available Solar Thermal Heat Pump Systems. 2013.

SAIDUR, R., et al. Exergy analysis of solar energy applications. *Renewable and Sustainable Energy Reviews*, 2012, 16.1: 350-356.

Salt Air Conditioner. Available at www.geeky-gadgets.com; accessed on 16th of January 2015.

SARBU, Ioan; SEBARCHIEVICI, Calin. Review of solar refrigeration and cooling systems. *Energy and Buildings*, 2013, 67: 286-297.

SARHADDI, F., et al. Exergetic performance assessment of a solar photovoltaic thermal (PV/T) air collector. *Energy and Buildings*, 2010, 42.11: 2184-2199.

SCHOEN, Tony JN. Building-integrated PV installations in the Netherlands: examples and operational experiences. *Solar energy*, 2001, 70.6: 467-477.

ŞEVIK, Seyfi, et al. Mushroom drying with solar assisted heat pump system. *Energy Conversion and Management*, 2013, 72: 171-178.

SHAN, Feng, et al. Performance evaluations and applications of photovoltaic–thermal collectors and systems. *Renewable and Sustainable Energy Reviews*, 2014, 33: 467-483.

SHARPLES, S.; CHARLESWORTH, P. S. Full-scale measurements of wind-induced convective heat transfer from a roof-mounted flat plate solar collector. *Solar Energy*, 1998, 62.2: 69-77.

SHE, Xiaohui; YIN, Yonggao; ZHANG, Xiaosong. Thermodynamic analysis of a novel energy-efficient refrigeration system subcooled by liquid desiccant dehumidification and evaporation. *Energy Conversion and Management*, 2014, 78: 286-296.

SHILIN, Qu; FEI, Ma. Experimental Performance Analysis on Solar-Water Compound Source Heat Pump for Radiant Floor Heating System. In: *Power and Energy Engineering Conference (APPEEC), 2010 Asia-Pacific*. IEEE, 2010. p. 1-4.

SHUKLA, Ashish, et al. A state of art review on the performance of transpired solar collector. *Renewable and Sustainable Energy Reviews*, 2012, 16.6: 3975-3985.

SOLANKI, S. C.; DUBEY, Swapnil; TIWARI, Arvind. Indoor simulation and testing of photovoltaic thermal (PV/T) air collectors. *Applied energy*, 2009, 86.11: 2421-2428.

SolarVenti, 2015. Available at www.solarventi.com ; accessed on 09th of January 2015.

SÖZEN, Adnan; ALTIPARMAK, Duran; USTA, Hüseyin. Development and testing of a prototype of absorption heat pump system operated by solar energy. *Applied Thermal Engineering*, 2002, 22.16: 1847-1859.

SPORN, Phillip; AMBROSE, E. R. The heat pump and solar energy. In: *Proc. of the World Symposium on Applied Solar Energy*. Phoenix, US. 1955.

STASINOPOULOS, Thanos N. Sunny walls vs sunnier roofs: a study on the advantages of roofs for solar collection. *Environmental Management and Health*, 2002, 13.4: 339-347.

STERLING, S. J.; COLLINS, M. R. Feasibility analysis of an indirect heat pump assisted solar domestic hot water system. *Applied Energy*, 2012, 93: 11-17.

SULTANA, Tanzeen, et al. Heat loss from cavity receiver for solar micro-concentrating collector. In: *AuSES Solar Conference*. Canberra, Australia. 2010.

SULTANA, Tanzeen; MORRISON, Graham L.; ROSENGARTEN, Gary. Thermal performance of a novel rooftop solar micro-concentrating collector. *Solar Energy*, 2012, 86.7: 1992-2000.

TANG, Xiao; QUAN, Zhen Hua; ZHAO, Yao Hua. Experimental Investigation of Solar Panel Cooling by a Novel Micro Heat Pipe Array. In: *Power and Energy Engineering Conference (APPEEC), 2010 Asia-Pacific*. IEEE, 2010. p. 1-4.

TIWARI, Arvind; SODHA, M. S. Performance evaluation of solar PV/T system: an experimental validation. *Solar Energy*, 2006, 80.7: 751-759.

TONUI, J. K.; TRIPANAGNOSTOPOULOS, Y. Improved PV/T solar collectors with heat extraction by forced or natural air circulation. *Renewable Energy*, 2007, 32.4: 623-637.

TORRES-REYES, E.; CERVANTES DE GORTARI, J. Optimal performance of an irreversible solar-assisted heat pump. *Exergy, An International Journal*, 2001, 1.2: 107-111.

TU, Min, et al. Simulation and analysis of a novel liquid desiccant air-conditioning system. *Applied Thermal Engineering*, 2009, 29.11: 2417-2425.

UCAR, A.; INALLI, M. Thermal and exergy analysis of solar air collectors with passive augmentation techniques. *International communications in heat and mass transfer*, 2006, 33.10: 1281-1290.

UK inflation rate. Trading Economics, <http://www.tradingeconomics.com/united-kingdom/interest-rate> ; accessed on January, 2014.

VALEH-E-SHEYDA, Peyvand, et al. Using a wind-driven ventilator to enhance a photovoltaic cell power generation. *Energy and Buildings*, 2014, 73: 115-119.

WALL, Maria, et al. Achieving solar energy in architecture-IEA SHC Task 41. *Energy Procedia*, 2012, 30: 1250-1260.

WANG, Qin, et al. Development and experimental validation of a novel indirect-expansion solar-assisted multifunctional heat pump. *Energy and buildings*, 2011, 43.2: 300-304.

WANG, R. Z., et al. Solar sorption cooling systems for residential applications: options and guidelines. *International journal of Refrigeration*, 2009, 32.4: 638-660.

WOREK, William M., et al. Integrated Desiccant–Indirect Evaporative Cooling System Utilizing the Maisotsenko Cycle. In: *ASME 2012 Heat Transfer Summer Conference collocated with the ASME 2012 Fluids Engineering Division Summer Meeting and the ASME 2012 10th International Conference on Nanochannels, Microchannels, and Minichannels*. American Society of Mechanical Engineers, 2012. p. 21-28.

XIONG, Z. Q.; DAI, Y. J.; WANG, R. Z. Development of a novel two-stage liquid desiccant dehumidification system assisted by CaCl_2 solution using exergy analysis method. *Applied Energy*, 2010, 87.5: 1495-1504.

XU, Guoying, et al. Simulation of a photovoltaic/thermal heat pump system having a modified collector/evaporator. *Solar Energy*, 2009, 83.11: 1967-1976.

XU, Guoying; ZHANG, Xiaosong; DENG, Shiming. Experimental study on the operating characteristics of a novel low-concentrating solar photovoltaic/thermal integrated heat pump water heating system. *Applied Thermal Engineering*, 2011, 31.17: 3689-3695.

YANG, Tingting; ATHIENITIS, Andreas K. A study of design options for a building integrated photovoltaic/thermal (BIPV/T) system with glazed air collector and multiple inlets. *Solar Energy*, 2014, 104: 82-92.

YANG, Yuguo, et al. A building integrated solar collector: All-ceramic solar collector. *Energy and Buildings*, 2013, 62: 15-17.

YANG, Yuguo, et al. All-ceramic solar collectors. *Ceramics International*, 2013, 39.5: 6009-6012.

YANG, Zhiyong; WANG, Yiping; ZHU, Li. Building space heating with a solar-assisted heat pump using roof-integrated solar collectors. *Energies*, 2011, 4.3: 504-516.

YIN, H. M., et al. Design and performance of a novel building integrated PV/thermal system for energy efficiency of buildings. *Solar Energy*, 2013, 87: 184-195.

YIN, Yonggao, et al. Experimental study on a new internally cooled/heated dehumidifier/regenerator of liquid desiccant systems. *International Journal of Refrigeration*, 2008, 31.5: 857-866.

YIN, Yonggao; ZHANG, Xiaosong. Comparative study on internally heated and adiabatic regenerators in liquid desiccant air conditioning system. *Building and Environment*, 2010, 45.8: 1799-1807.

YIN, Yonggao; ZHANG, Xiaosong; CHEN, Qingyan. Condensation Risk in a Room with a High Latent Load and Chilled Ceiling Panels and with Air Supplied from a Liquid Desiccant System. *HVAC&R Research*, 2009, 15.2: 315-327.

YONG, Li, et al. Experimental study on a hybrid desiccant dehumidification and air conditioning system. *Journal of solar energy engineering*, 2006, 128.1: 77-82.

YUTONG, Li; HONGXING, Yang. Investigation on solar desiccant dehumidification process for energy conservation of central air-conditioning systems. *Applied Thermal Engineering*, 2008, 28.10: 1118-1126.

ZEIDAN, El-Shafei B.; ALY, Ayman A.; HAMED, Ahmed M. Modeling and simulation of solar-powered liquid desiccant regenerator for open absorption cooling cycle. *Solar Energy*, 2011, 85.11: 2977-2986.

ZHAI, X. Q., et al. Experience on integration of solar thermal technologies with green buildings. *Renewable Energy*, 2008, 33.8: 1904-1910.

ZHAN, Changhong, et al. Comparative study of the performance of the M-cycle counter-flow and cross-flow heat exchangers for indirect evaporative cooling—paving the path toward sustainable cooling of buildings. *Energy*, 2011, 36.12: 6790-6805.

ZHANG, Xingxing, et al. Characterization of a solar photovoltaic/loop-heat-pipe heat pump water heating system. *Applied Energy*, 2013, 102: 1229-1245.

ZHANG, Xingxing, et al. Dynamic performance of a novel solar photovoltaic/loop-heat-pipe heat pump system. *Applied Energy*, 2014, 114: 335-352.

ZHANG, Xingxing, et al. Review of R&D progress and practical application of the solar photovoltaic/thermal (PV/T) technologies. *Renewable and Sustainable Energy Reviews*, 2012, 16.1: 599-617.

ZHAO, X.; LI, J. M.; RIFFAT, S. B. Numerical study of a novel counter-flow heat and mass exchanger for dew point evaporative cooling. *Applied Thermal Engineering*, 2008, 28.14: 1942-1951.

ZHAO, Xudong, et al. Theoretical study of the performance of a novel PV/e roof module for heat pump operation. *Energy Conversion and Management*, 2011, 52.1: 603-614.

ZHEN, Li, et al. District cooling and heating with seawater as heat source and sink in Dalian, China. *Renewable energy*, 2007, 32.15: 2603-2616.

ZONDAG, H. A., et al. The yield of different combined PV-thermal collector designs. *Solar energy*, 2003, 74.3: 253-269.

APPENDIX 1

Chapter 5 & 6 – Roof data belongs to testing period

08-Jul						
Time	T _{outside} (°C)	Radiation (W/m ²)	T _{PV w/o HE} (°C)	T _{PV with HE} (°C)	T _{water HE In} (°C)	T _{water HE Out} (°C)
8:00AM	22.801074	5100.91141	26.93785	20.365464	17.090956	17.295374
8:15AM	23.84355	5334.12752	30.383102	22.248536	17.222394	17.435718
8:30AM	26.24287	5870.88814	33.44326	23.914392	17.384392	17.658466
8:45AM	24.18512	5410.54139	35.038948	25.36625	17.52143	17.817124
9:00AM	29.536422	6607.70067	38.31014	26.981898	17.701572	18.006342
9:15AM	28.342554	6340.61611	40.707728	28.729604	17.896094	18.235556
9:30AM	26.748316	5983.96331	41.840508	30.104936	18.082938	18.426716
9:45AM	30.917432	6916.65145	44.660476	31.31556	18.244562	18.710134
10:00AM	30.241868	6765.51857	46.82618	32.775544	18.465802	18.905302
10:15AM	29.43042	6583.98658	48.1951	34.525228	18.681664	19.134182
10:30AM	31.195508	6978.86085	51.15732	35.904572	18.9024	19.407004
10:45AM	37.03164	8284.48322	53.5576	37.359416	19.166822	19.784524
11:00AM	34.398492	7695.41208	54.425336	38.50692	19.323496	19.932592
11:15AM	35.99616	8052.83221	55.823232	39.624144	19.537872	20.255668
11:30AM	33.853532	7573.49709	57.434716	40.452196	19.774674	20.518684
11:45AM	35.515988	7945.41119	57.607688	41.438176	20.03983	20.827266
12:00PM	38.261072	8559.52394	59.068716	42.169684	20.209304	21.074874
12:15PM	36.286324	8117.74586	60.576368	43.01536	20.49289	21.380054
12:30PM	36.279748	8116.27472	60.946168	43.794888	20.639158	21.552544
12:45PM	37.810832	8458.79911	61.892568	44.192152	20.997948	21.93683
1:00 PM	39.743172	8891.08993	62.189028	44.737248	21.191758	22.108922
1:15 PM	37.030968	8284.33289	61.721552	44.845252	21.28527	22.18969
1:30 PM	39.822296	8908.79105	63.032032	45.454356	21.544338	22.479234
1:45 PM	39.283904	8788.34541	62.063704	45.340404	21.643178	22.625872
2:00 PM	35.545172	7951.94004	61.246792	45.59022	21.888154	22.848914
2:15 PM	34.95716	7820.39374	61.649028	45.649096	22.109958	23.131454
2:30 PM	39.404296	8815.27875	61.527708	45.4513	22.188666	23.20159
2:45 PM	38.560624	8626.53781	60.287516	45.023928	22.365854	23.38753
3:00 PM	37.378456	8362.07069	60.576156	45.118852	22.604174	23.60827
3:15 PM	36.193996	8097.09083	58.117928	44.935888	22.618184	23.630964
3:30 PM	37.54154	8398.55481	57.348096	44.277568	22.781034	23.750214
3:45 PM	39.830664	8910.66309	56.50296	43.361232	22.871972	23.901756
4:00 PM	36.894852	8253.88188	55.226828	42.833032	22.985026	24.00622
4:15 PM	36.611856	8190.57181	53.120896	42.187992	23.083358	24.043622
4:30 PM	35.100508	7852.46264	51.680316	41.554444	23.14676	24.102628
4:45 PM	36.039604	8062.55123	50.598556	40.59518	23.095536	24.064672
5:00 PM	34.24082	7660.1387	48.251696	39.543624	23.126704	24.048

09-Jul						
Time	T _{outside} (°C)	Radiation (W/m ²)	T _{PV w/o HE} (°C)	T _{PV with HE} (°C)	T _{water HE In} (°C)	T _{water HE Out} (°C)
8:00AM	19.27164	4169.67159	23.060412	20.446392	18.12489	18.311876
8:15AM	18.638432	4114.15928	22.230126	20.238012	18.203778	18.39075
8:30AM	18.390292	4077.05817	21.228304	19.88116	18.27735	18.438122
8:45AM	18.22445	4110.60805	20.997466	19.619368	18.263556	18.324298
9:00AM	18.374418	4570.08814	22.14911	19.578034	18.291848	18.326586
9:15AM	20.428294	4717.88591	24.89499	20.671608	18.341586	18.389416
9:30 AM	21.08895	4255.70917	27.176262	22.104046	18.415968	18.524722
9:45 AM	19.02302	4285.52752	24.843408	22.297852	18.480126	18.614872
10:00AM	19.156308	4215.33468	24.147688	21.80261	18.570196	18.65275
10:15AM	18.842546	4463.97047	22.918964	21.445734	18.568906	18.612366
10:30AM	19.953948	4814.10738	25.141736	21.370712	18.537372	18.593928
10:45AM	21.51906	4967.00492	27.926456	22.71962	18.568378	18.668388
11:00AM	22.202512	4682.20984	28.677952	23.695692	18.653822	18.797282
11:15AM	20.929478	4793.71186	27.070892	23.988096	18.765196	18.917182
11:30AM	21.427892	4968.09262	26.846008	23.38209	18.69905	18.885956
11:45AM	22.207374	5520.62327	29.825612	23.562538	18.741054	18.906134
12:00PM	24.677186	5313.71544	32.389412	25.12576	18.88471	19.084492
12:15PM	23.752308	4626.39911	30.211998	25.577708	18.96188	19.170372
12:30PM	20.680004	5138.36063	27.863592	24.80382	18.933356	19.133316
12:45PM	22.968472	4993.07383	29.770022	24.710528	18.982896	19.19575
1:00 PM	22.31904	4984.73378	28.696732	24.866632	19.039708	19.291814
1:15 PM	22.28176	5081.59239	29.055438	24.890054	19.163206	19.393292
1:30 PM	22.714718	5061.66174	28.405764	24.635266	19.175754	19.371316
1:45 PM	22.625628	5274.96018	27.856772	24.10585	19.160028	19.359766
2:00 PM	23.579072	5315.69754	30.359582	24.366092	19.165182	19.395268
2:15 PM	23.761168	5310.48412	31.86398	25.72171	19.26064	19.49981
2:30 PM	23.737864	5003.49351	30.548394	25.918512	19.350112	19.610886
2:45 PM	22.365616	4696.55928	27.603074	25.217542	19.403744	19.664316
3:00 PM	20.99362	5303.91991	27.81956	24.38959	19.374472	19.656856
3:15 PM	23.708522	4791.90604	30.143032	24.681738	19.489854	19.741688
3:30 PM	21.41982	5094.4519	28.433992	24.956346	19.48774	19.774462
3:45 PM	22.7722	4840.55078	29.115868	24.655638	19.528322	19.802332
4:00 PM	21.637262	5268.50022	27.971538	24.947902	19.552846	19.817938
4:15 PM	23.550196	4618.84877	28.201096	24.368224	19.595778	19.85214
4:30 PM	20.646254	4616.14899	26.612076	24.376466	19.612776	19.882218
4:45 PM	20.634186	5116.86219	25.267678	23.663432	19.574528	19.843976
5:00 PM	22.872374	0	27.909772	23.548462	19.559144	19.815706

10-Jul						
Time	T _{outside} (°C)	Radiation (W/m ²)	T _{PV w/o HE} (°C)	T _{PV with HE} (°C)	T _{water HE In} (°C)	T _{water HE Out} (°C)
8:00 AM	15.65684	3502.64877	21.784044	17.867608	16.336448	16.54117
8:15 AM	16.40899	3670.91499	22.67348	18.758744	16.430852	16.609336
8:30 AM	17.129634	3832.13289	23.724982	19.039938	16.485792	16.694676
8:45 AM	18.099578	4049.1226	23.962982	19.757458	16.664668	16.825636
9:00 AM	17.153148	3837.39329	25.703652	20.65301	16.735494	16.866048
9:15 AM	23.113314	5170.76376	28.987156	21.634618	16.807398	16.95543
9:30 AM	19.842042	4438.93557	27.720742	22.300196	17.006556	17.136896
9:45 AM	27.988114	6261.32304	36.777172	24.35567	17.027808	17.19329
10:00AM	29.37111	6570.71812	42.709124	28.530032	17.270922	17.501526
10:15AM	25.845928	5782.0868	42.901892	30.549414	17.364738	17.691232
10:30AM	29.313902	6557.91991	47.598448	31.591422	17.595742	17.926548
10:45AM	31.745612	7101.92662	48.288504	33.247044	17.815204	18.198162
11:00AM	32.52517	7276.32438	50.430028	34.337744	17.988274	18.436284
11:15AM	31.26924	6995.3557	50.033832	35.451704	18.20727	18.720486
11:30AM	33.542198	7503.84743	52.737028	36.368048	18.426696	18.974926
11:45AM	35.426768	7925.45145	53.344152	37.019728	18.67188	19.211282
12:00PM	32.922394	7365.18881	54.371964	38.276048	18.945198	19.53266
12:15PM	31.44633	7034.97315	54.824452	39.028224	19.090518	19.68645
12:30PM	31.770878	7107.57897	55.855812	39.376456	19.273808	19.904542
12:45PM	31.933424	7143.94273	56.191884	40.24208	19.550002	20.206758
1:00 PM	30.625606	6851.366	57.41204	40.795672	19.753218	20.43584
1:15 PM	35.742844	7996.16197	57.936084	41.31978	19.949038	20.636294
1:30 PM	32.614158	7296.23221	54.968008	41.245964	20.056186	20.79568
1:45 PM	33.84614	7571.8434	57.372772	40.781444	20.2673	21.006676
2:00 PM	33.049984	7393.73244	57.087136	41.053408	20.44335	21.2046
2:15 PM	35.3126	7899.91051	57.501904	41.538748	20.5742	21.321926
2:30 PM	34.098976	7628.40626	57.591504	41.572816	20.71019	21.497416
2:45 PM	35.202892	7875.36734	56.39244	41.753252	20.888822	21.680296
3:00 PM	33.204396	7428.27651	55.04556	41.244732	21.13807	21.92485
3:15 PM	32.081204	7177.00313	53.758332	40.555556	21.077206	21.894502
3:30 PM	33.09233	7403.20582	52.845448	39.97738	21.248472	22.009444
3:45 PM	32.176582	7198.34049	52.216908	39.564104	21.346312	22.120098
4:00 PM	30.452712	6812.68725	50.775568	39.181172	21.492838	22.227364
4:15 PM	33.048168	7393.32617	49.39328	38.5269	21.593264	22.345332
4:30 PM	31.42341	7029.84564	48.67742	37.826592	21.644948	22.396986
4:45 PM	29.629952	6628.62461	47.205396	36.91358	21.558662	22.319644
5:00 PM	30.865468	6905.0264	44.50174	35.978612	21.639408	22.361174

11-Jul						
Time	T _{outside} (°C)	Radiation (W/m ²)	T _{PV w/o HE} (°C)	T _{PV with HE} (°C)	T _{water HE In} (°C)	T _{water HE Out} (°C)
8:00 AM	16.078666	3597.017	20.13651	17.161646	16.196168	16.40947
8:15 AM	16.079158	3597.12707	21.138626	17.941228	16.301224	16.510138
8:30 AM	16.573678	3707.75794	22.92724	18.792784	16.469326	16.625946
8:45 AM	17.515554	3918.46846	24.387698	19.782382	16.545962	16.720058
9:00 AM	17.613806	3940.44877	26.095662	20.609446	16.66158	16.844404
9:15 AM	19.373808	4334.18523	28.888104	22.032546	16.807194	17.03351
9:30 AM	22.103186	4944.78434	31.102124	23.269932	16.934174	17.138616
9:45 AM	22.499696	5033.48904	35.89472	25.43629	17.119466	17.367382
10:00AM	24.641364	5512.6094	39.429568	27.19802	17.219156	17.515296
10:15AM	26.44135	5915.29083	42.137916	29.909958	17.467784	17.815712
10:30AM	25.92728	5800.28635	43.713532	31.174366	17.627244	18.036072
10:45AM	26.991102	6038.27785	44.712188	31.84076	17.906434	18.324292
11:00AM	27.001628	6040.63266	46.83904	33.391586	18.126452	18.59624
11:15AM	31.111638	6960.09799	49.246352	35.102924	18.35904	18.850756
11:30AM	30.772498	6884.22774	51.443148	36.14312	18.581112	19.13383
11:45AM	31.248874	6990.79955	53.770556	37.69388	18.813592	19.431456
12:00PM	35.770052	8002.24877	54.846624	38.934844	19.101936	19.741474
12:15PM	36.294804	8119.64295	55.776212	39.81814	19.31596	19.981556
12:30PM	34.192528	7649.33512	56.929852	40.879748	19.67958	20.388584
12:45PM	37.038228	8285.95705	57.470644	41.570864	19.866856	20.584664
1:00 PM	35.45544	7931.86577	59.036308	42.088572	20.150686	20.937868
1:15 PM	39.013108	8727.76465	58.581752	42.5791	20.293878	21.120564
1:30 PM	38.08386	8519.87919	58.977156	42.844904	20.554634	21.354832
1:45 PM	37.11658	8303.48546	56.9664	42.980176	20.770878	21.641002
2:00 PM	34.227556	7657.17136	55.165288	41.813436	20.913984	21.77966
2:15 PM	39.137748	8755.64832	57.587708	42.514116	21.139164	22.01794
2:30 PM	35.757984	7999.54899	52.592504	42.011244	21.340966	22.249888
2:45 PM	35.19294	7873.14094	52.133628	40.497224	21.390172	22.286194
3:00 PM	39.536516	8844.85817	52.883116	40.140508	21.488394	22.40611
3:15 PM	36.640492	8196.97808	52.03	40.43444	21.717862	22.570332
3:30 PM	36.071928	8069.78255	50.246504	40.037812	21.85	22.732654
3:45 PM	35.0895	7850	49.532532	39.158548	21.866374	22.75356
4:00 PM	34.978336	7825.1311	51.29998	39.622076	21.96989	22.874408
4:15 PM	37.49144	8387.34676	48.62272	39.731236	22.106286	22.997656
4:30 PM	34.221412	7655.79687	44.291884	38.375632	22.238918	23.11715
4:45 PM	32.255062	7215.89754	43.595676	36.843124	22.27356	23.130208
5:00 PM	34.094664	7627.44161	43.136556	35.93538	22.309916	23.14895

12-Jul						
Time	T _{outside} (°C)	Radiation (W/m ²)	T _{PV} w/o HE (°C)	T _{PV} with HE (°C)	T _{water} HE In (°C)	T _{water} HE Out (°C)
8:00AM	26.292786	5882.05503	31.038084	23.589544	18.155868	18.412322
8:15 AM	29.941904	6698.41253	33.795744	25.586632	18.38029	18.645616
8:30 AM	33.44278	7481.60626	37.166092	27.356056	18.512322	18.812348
8:45 AM	35.610316	7966.51365	40.463228	29.378514	18.71909	19.066878
9:00 AM	37.98928	8498.72036	43.314604	31.270252	18.860406	19.30414
9:15 AM	35.533396	7949.30559	45.370348	32.83863	19.095224	19.577942
9:30 AM	37.456416	8379.51141	47.85778	34.717312	19.363062	19.858954
9:45 AM	41.079392	9190.02058	50.899824	36.334228	19.58785	20.153228
10:00AM	38.61862	8639.5123	49.12952	37.543032	19.860674	20.464974
10:15AM	37.878284	8473.88904	49.545668	37.610116	20.08697	20.717314
10:30AM	37.375488	8361.40671	50.982752	37.984612	20.296542	20.974902
10:45AM	37.013808	8280.49396	52.42396	39.129096	20.519192	21.223388
11:00AM	42.245532	9450.90201	55.931144	40.332492	20.734436	21.469386
11:15AM	40.27838	9010.82327	58.055336	42.188332	21.01408	21.80529
11:30AM	43.473972	9725.72081	59.607572	43.25464	21.145186	22.01033
11:45AM	38.536468	8621.13378	60.89848	44.484532	21.477416	22.373
12:00PM	45.496104	10178.0993	62.181208	45.222652	21.651246	22.59439
12:15PM	40.480984	9056.14855	63.738004	46.267856	22.000768	22.965602
12:30PM	38.412704	8593.44609	58.461084	46.987404	22.141884	23.124394
12:45PM	45.044556	10077.0819	64.492828	46.62668	22.41579	23.419652
1:00 PM	41.254928	9229.29038	63.796008	48.264664	22.616696	23.668234
1:15 PM	36.710576	8212.65682	53.829868	46.452872	22.816736	23.898736
1:30 PM	42.952148	9608.98166	62.960008	45.036248	23.011794	24.08494
1:45 PM	36.546484	8175.9472	50.341084	45.46052	23.123972	24.16679
2:00 PM	39.890748	8924.1047	62.035944	44.563412	23.158298	24.257778
2:15 PM	42.64436	9540.12528	65.81498	48.194956	23.396958	24.504738
2:30 PM	39.382608	8810.42685	50.326144	44.88272	23.624366	24.72327
2:45 PM	36.401876	8143.59642	48.233348	41.25888	23.597752	24.636036
3:00 PM	41.804736	9352.28993	54.977008	42.04258	23.655322	24.637078
3:15 PM	37.710596	8436.37494	50.954552	42.989404	23.737156	24.71904
3:30 PM	33.790928	7559.49172	40.997048	39.430308	23.744868	24.72221
3:45 PM	35.621596	7969.03714	44.80228	36.823996	23.791756	24.673484
4:00 PM	35.512604	7944.65414	49.619648	38.83556	23.73319	24.60211
4:15 PM	34.041636	7615.57852	44.553152	38.837128	23.764078	24.693804
4:30 PM	35.882424	8027.38792	41.708784	37.319376	23.825514	24.733284
4:45 PM	31.636402	7077.49485	37.2519	35.176616	23.788146	24.652496
5:00 PM	38.024908	8506.69083	44.625788	34.4569	23.73714	24.553916

13-Jul						
Time	T _{outside} (°C)	Radiation (W/m ²)	T _{PV w/o HE} (°C)	T _{PV with HE} (°C)	T _{water HE In} (°C)	T _{water HE Out} (°C)
8:00AM	17.686628	3956.74004	19.817222	18.61819	19.28338	19.40913
8:15 AM	17.570808	3930.82953	20.801122	19.137536	19.293842	19.450318
8:30 AM	17.76333	3973.89933	21.149638	19.698506	19.355628	19.455578
8:45 AM	18.932684	4235.49978	21.76082	19.819	19.423808	19.515032
9:00 AM	17.878152	3999.58658	22.236734	20.29884	19.48738	19.596044
9:15 AM	18.779766	4201.28993	22.345718	20.373492	19.470858	19.61859
9:30 AM	18.245326	4081.72841	22.441862	20.46523	19.506336	19.680042
9:45 AM	19.09114	4270.94855	22.76447	20.91071	19.612358	19.725376
10:00AM	18.74838	4194.26846	23.073072	20.793902	19.595756	19.72167
10:15AM	20.975804	4692.5736	25.406092	21.567096	19.625178	19.746728
10:30AM	20.190086	4516.79776	26.457962	22.222962	19.604054	19.769214
10:45AM	22.886638	5120.05324	28.155548	23.073138	19.66959	19.830192
11:00AM	22.945074	5133.12617	28.498196	23.99295	19.810652	19.958346
11:15AM	25.258754	5650.72796	32.436042	24.887482	19.80165	19.979868
11:30AM	27.514788	6155.43356	40.203524	27.46766	19.857078	20.082868
11:45AM	28.430274	6360.24027	44.818052	31.613274	19.961834	20.304936
12:00PM	29.760642	6657.86174	46.871872	32.753036	20.26559	20.621688
12:15PM	30.257952	6769.11678	51.18004	36.369084	20.318924	20.801006
12:30PM	36.67298	8204.24609	52.38232	37.179912	20.620904	21.146444
12:45PM	34.721004	7767.56242	57.0823	39.2706	20.811474	21.401892
1:00 PM	37.000248	8277.4604	56.589732	40.396248	21.05226	21.70789
1:15 PM	36.11244	8078.84564	58.913444	42.018836	21.335988	22.013248
1:30 PM	37.620532	8416.2264	60.263948	43.179996	21.634186	22.411212
1:45 PM	35.325816	7902.86711	57.69034	43.497932	21.851076	22.619456
2:00 PM	33.864408	7575.9302	57.5032	42.893392	22.139646	22.938504
2:15 PM	34.530124	7724.85996	54.001344	41.446276	22.213648	23.04291
2:30 PM	34.297484	7672.81521	54.057136	40.512504	22.43624	23.226218
2:45 PM	35.518016	7945.86488	49.85638	40.370344	22.59692	23.42613
3:00 PM	32.314926	7229.28993	52.290972	39.687092	22.63058	23.412118
3:15 PM	34.44852	7706.60403	51.791964	39.481936	22.746068	23.51903
3:30 PM	33.32742	7455.79866	49.046524	39.213928	22.899684	23.676906
3:45 PM	31.556064	7059.52215	47.022652	38.4138	23.022802	23.769516
4:00 PM	30.599004	6845.41477	46.390288	37.37652	23.075136	23.822008
4:15 PM	31.620594	7073.95839	45.611916	36.467584	23.12199	23.86014
4:30 PM	32.670506	7308.83803	47.66398	36.957728	23.15582	23.889416
4:45 PM	33.418144	7476.09485	42.765664	36.40658	23.106892	23.814806
5:00 PM	32.053242	7170.74765	44.718528	35.578456	23.085852	23.797936

14-Jul						
Time	T _{outside} (°C)	Radiation (W/m ²)	T _{PV} w/o HE (°C)	T _{PV} with HE (°C)	T _{water} HE In (°C)	T _{water} HE Out (°C)
8:00AM	24.420874	5463.28277	28.852154	21.463444	17.648234	17.843832
8:15 AM	24.846796	5558.56734	31.904058	23.621526	17.820024	18.067998
8:30 AM	26.721838	5978.03982	35.049548	25.23475	18.027804	18.267006
8:45 AM	28.383224	6349.71454	37.729084	27.449142	18.246928	18.560108
9:00 AM	29.39372	6575.77629	40.857256	29.152964	18.454498	18.850362
9:15 AM	32.263272	7217.73423	43.72072	31.100036	18.782504	19.18244
9:30 AM	29.887794	6686.30738	45.781636	32.436436	18.915904	19.376688
9:45 AM	36.01892	8057.92394	48.206396	34.169332	19.20416	19.651948
10:00AM	38.612276	8638.09306	50.355352	35.514128	19.420938	19.986008
10:15AM	38.306124	8569.60268	51.910864	36.966272	19.676384	20.28513
10:30AM	38.938456	8711.06398	53.601064	37.974212	19.910098	20.59264
10:45AM	37.816024	8459.96063	54.730828	39.150508	20.183658	20.85753
11:00AM	36.286964	8117.88904	56.501128	40.274772	20.57882	21.248326
11:15AM	42.00744	9397.63758	58.351848	41.263164	20.732252	21.38861
11:30AM	38.297968	8567.77808	57.791476	42.32424	21.045588	21.819362
11:45AM	39.072248	8740.99508	59.309708	42.621116	21.258178	22.079716
12:00PM	38.88458	8699.01119	60.164916	43.458348	21.529274	22.450746
12:15PM	36.226832	8104.43669	58.173572	43.300332	21.697468	22.631876
12:30PM	41.921556	9378.42416	58.955944	42.695812	21.968784	22.933266
12:45PM	39.459676	8827.66801	60.033676	43.656356	22.1282	23.044902
1:00 PM	37.794216	8455.08188	59.42374	43.94078	22.26336	23.193204
1:15 PM	37.552744	8401.0613	59.442644	43.918044	22.451998	23.486084
1:30 PM	43.01502	9623.04698	56.996628	43.1843	22.628824	23.684324
1:45 PM	36.855848	8245.15615	56.430964	43.549876	22.741678	23.801622
2:00 PM	34.026224	7612.13065	55.014288	42.451832	22.861646	23.908452
2:15 PM	37.200628	8322.28814	57.577608	43.084508	23.000386	23.973558
2:30 PM	35.409684	7921.62953	51.61022	42.313464	23.215424	24.053692
2:45 PM	36.571752	8181.6	52.734096	40.676976	23.273948	24.220652
3:00 PM	39.690692	8879.34944	56.159156	41.623148	23.278864	24.121438
3:15 PM	38.28674	8565.26622	58.812432	43.729216	23.354002	24.335794
3:30 PM	37.44234	8376.36242	56.232996	43.331632	23.560344	24.563712
3:45 PM	36.950748	8266.38658	54.175372	42.882528	23.618844	24.552832
4:00 PM	36.499112	8165.34944	52.76532	42.0271	23.740756	24.679
4:15 PM	34.910268	7809.90336	51.353964	41.127548	23.875042	24.843602
4:30 PM	35.174652	7869.04966	50.468688	40.468944	23.929442	24.90665
4:45 PM	34.320212	7677.89978	47.667952	40.385088	24.055446	24.91093
5:00 PM	35.352424	7908.81969	48.0101	38.579176	24.065674	24.921152

15-Jul						
Time	T _{outside} (°C)	Radiation (W/m ²)	T _{PV} w/o HE (°C)	T _{PV} with HE (°C)	T _{water} HE In (°C)	T _{water} HE Out (°C)
8:00AM	28.7697	6436.1745	27.641592	22.097696	19.292096	19.474556
8:05AM	27.416242	6133.38747	28.602364	22.774272	19.388156	19.574776
8:10AM	29.332892	6562.16823	29.453168	23.271512	19.404454	19.552002
8:15AM	29.498954	6599.31857	30.65742	24.052722	19.44168	19.702244
8:20AM	28.600716	6398.37047	31.514792	24.584644	19.537462	19.676274
8:25AM	31.962482	7150.4434	32.923736	25.239044	19.57877	19.930502
8:30AM	33.746492	7549.55078	33.831648	25.91099	19.655856	19.851346
8:35AM	33.504376	7495.38613	34.828716	26.561832	19.70809	19.964242
8:40AM	34.60642	7741.92841	35.518684	27.0935	19.762342	20.122748
8:45AM	32.101692	7181.58658	36.268368	27.823388	19.891466	20.121612
8:50AM	32.199292	7203.42103	36.957652	28.293036	19.91149	20.106942
8:55AM	33.77896	7556.81432	37.88824	28.8345	19.949192	20.3357
9:00AM	32.091126	7179.22282	38.736748	29.392932	20.017108	20.43411
9:05AM	34.755404	7775.25817	39.818432	29.948266	20.030766	20.44757
9:10AM	33.62954	7523.38702	40.363728	30.496624	20.137532	20.502382
9:15AM	32.734768	7323.21432	41.017376	30.987626	20.286386	20.5339
9:20AM	35.486788	7938.87875	42.437108	31.550992	20.274148	20.725742
9:25AM	37.293408	8343.0443	43.352448	32.004596	20.325202	20.811638
9:30AM	36.342564	8130.32752	44.073584	32.735336	20.479892	20.822858
9:35AM	38.64368	8645.11857	44.61282	33.166386	20.456658	20.955926
9:40AM	36.09276	8074.44295	45.50894	33.694472	20.628046	20.953546
9:45AM	36.263252	8112.58434	46.199388	34.185436	20.652784	21.134556
9:50AM	35.893248	8029.8094	46.50644	34.765148	20.738246	21.220176
9:55AM	38.948052	8713.21074	47.430072	35.186612	20.836552	21.374882
10:00AM	35.676232	7981.25996	48.114252	35.493404	20.861266	21.399584
10:05AM	34.555832	7730.61119	48.349828	36.021232	20.97344	21.372904
10:10AM	39.64234	8868.53244	49.815308	36.42688	21.02583	21.59892
10:15AM	35.888332	8028.70962	50.084944	36.904488	21.130344	21.655678
10:20AM	39.388108	8811.65727	50.806452	37.355	21.171236	21.696552
10:25AM	38.469544	8606.16197	51.627572	37.716104	21.225712	21.807616
10:30AM	38.750184	8668.94497	51.96282	38.09506	21.355006	21.888956
10:35AM	32.931874	7367.30962	52.741056	38.810652	21.43712	22.06663
10:40AM	40.862884	9141.58479	53.149208	39.021568	21.508104	22.007354
10:45AM	34.660448	7754.01521	53.570016	39.470812	21.583864	22.23507
10:50AM	40.165544	8985.58031	53.8446	39.970284	21.707114	22.319084
10:55AM	39.012916	8727.7217	54.235572	40.444128	21.821404	22.385634
11:00AM	38.879444	8697.86219	54.842464	40.66312	21.931506	22.448004
11:05AM	37.440804	8376.01879	55.021912	41.035788	21.90796	22.46364
11:10AM	41.292596	9237.71723	55.611324	41.381364	22.000314	22.538734

11:15AM	38.466096	8605.3906	56.49434	41.506964	22.036202	22.765502
11:20AM	39.90812	8927.99105	56.88134	42.095796	22.174118	22.83411
11:25AM	34.887672	7804.84832	56.500956	42.306436	22.297756	22.98795
11:30AM	36.507952	8167.32707	56.52664	42.732972	22.282496	22.972506
11:35AM	34.580412	7736.11007	56.91138	42.85376	22.387422	23.095158
11:40AM	40.19184	8991.46309	57.479088	42.992476	22.459098	23.214264
11:45AM	37.482764	8385.40582	58.170296	43.35492	22.60429	23.311532
11:50AM	37.58346	8407.93289	58.728524	43.484944	22.701606	23.46533
11:55AM	37.326868	8350.52975	58.41898	44.00746	22.84694	23.489198
12:00PM	39.63378	8866.61745	59.480384	43.976916	22.713736	23.529634
12:05PM	37.474044	8383.45503	59.110476	44.356672	22.877164	23.502202
12:10PM	38.214892	8549.19284	59.496524	44.61076	22.976636	23.640574
12:15PM	40.696096	9104.27204	60.579524	44.969048	23.053336	23.843128
12:20PM	40.715884	9108.69888	60.546312	44.89654	23.176476	23.853542
12:25PM	36.92554	8260.7472	60.310244	45.37564	23.152034	23.859548
12:30PM	41.568848	9299.51857	60.887708	45.381292	23.16478	23.998168
12:35PM	37.434612	8374.63356	61.881088	45.820772	23.291028	24.115454
12:40PM	42.86596	9589.70022	62.44652	46.081236	23.388754	24.25658
12:45PM	38.954596	8714.67472	61.930564	46.353188	23.520146	24.292462
12:50PM	37.575064	8406.05459	60.835652	46.491608	23.635138	24.385848
12:55PM	36.675484	8204.80626	61.08992	46.538408	23.569716	24.342002
1:00 PM	39.741856	8890.79553	61.287404	46.528524	23.65324	24.412632
1:05 PM	41.54704	9294.63982	61.705772	46.47016	23.695546	24.598116
1:10 PM	39.853484	8915.76823	62.108292	46.690256	23.830346	24.607014
1:15 PM	36.14218	8085.49888	62.49188	47.009168	23.901906	24.821522
1:20 PM	40.142984	8980.53333	63.0516	47.41498	23.98548	24.887662
1:25 PM	38.468712	8605.97584	61.542852	47.360832	23.958314	24.878082
1:30 PM	38.231072	8552.81253	61.726648	47.584768	24.062386	24.921456
1:35 PM	40.545844	9070.65861	62.461404	47.496008	24.12073	25.062288
1:40 PM	39.2571	8782.34899	61.608984	47.519404	24.204456	25.10668
1:45 PM	39.523568	8841.96152	62.497112	47.825156	24.310416	25.212756
1:50 PM	38.10282	8524.12081	61.84168	47.637648	24.41915	25.256082
1:55 PM	37.636288	8419.75123	62.81238	47.834156	24.49908	25.388262
2:00 PM	38.72826	8664.04027	62.397852	47.617084	24.399534	25.379976
2:05 PM	42.049796	9407.1132	62.233172	47.596308	24.51574	25.3528
2:10 PM	39.95188	8937.78076	56.900012	47.339308	24.552992	25.528792
2:15 PM	36.580328	8183.51857	59.873612	46.177788	24.643464	25.580118
2:20 PM	40.626792	9088.76779	60.171864	46.055956	24.69055	25.648878
2:25 PM	36.954828	8267.29933	61.030192	46.008728	24.72791	25.69074
2:30 PM	36.178348	8093.59016	60.455208	46.5082	24.837794	25.796204
2:35 PM	40.412444	9040.81521	60.832744	46.61886	24.864392	25.8443

2:40 PM	40.051632	8960.09664	61.439964	46.505352	24.915924	25.904472
2:45 PM	40.421896	9042.92975	60.925212	46.746184	24.851482	25.848762
2:50 PM	40.854728	9139.76018	60.384896	46.830804	24.916022	25.77019
2:55 PM	40.328216	9021.97226	61.22776	46.92778	24.9412	25.934258
3:00 PM	37.642992	8421.25101	60.504032	47.0268	25.042488	25.913936
3:05 PM	39.608996	8861.07293	60.683836	47.095688	25.047606	26.070778
3:10 PM	41.072572	9188.49485	61.227668	47.216	25.131848	26.115892
3:15 PM	40.564968	9074.93691	58.283272	46.98212	25.2195	26.117058
3:20 PM	39.03002	8731.5481	58.516548	46.6035	25.262734	26.151582
3:25 PM	39.914464	8929.41029	59.254324	46.484968	25.313672	26.219844
3:30 PM	40.77592	9122.12975	59.523244	46.324088	25.329502	26.356982
3:35 PM	38.886916	8699.53378	57.431656	46.252096	25.4153	26.377628
3:40 PM	36.105332	8077.25548	54.892808	45.767308	25.463038	26.386466
3:45 PM	39.056672	8737.51051	55.965132	45.263916	25.400688	26.25058
3:50 PM	39.501024	8836.91812	56.000324	44.96548	25.367254	26.373006
3:55 PM	36.756912	8223.02282	55.231984	44.762952	25.44107	26.334138
4:00 PM	38.85964	8693.43177	55.653828	44.535944	25.4423	26.43517
4:05 PM	37.165304	8314.38568	56.388544	44.431016	25.460226	26.435724
4:10 PM	36.87808	8250.12975	55.16806	44.637864	25.50289	26.430816
4:15 PM	38.566284	8627.80403	54.765192	44.27868	25.537854	26.431046
4:20 PM	34.345732	7683.60895	54.098184	44.278304	25.606564	26.447646
4:25 PM	35.658532	7977.30022	53.893616	43.845656	25.566924	26.537816
4:30 PM	35.984976	8050.3302	52.551104	43.59828	25.59977	26.566486
4:35 PM	36.526628	8171.50515	53.234452	43.218092	25.58863	26.563842
4:40 PM	35.027884	7836.21566	52.596764	43.249748	25.681314	26.55272
4:45 PM	36.920932	8259.71633	51.3557	42.968324	25.701666	26.51231
4:50 PM	37.065244	8292.00089	51.715172	42.69958	25.726434	26.571776
4:55 PM	34.978144	7825.08814	50.89304	42.398436	25.72183	26.528126
5:00 PM	37.777708	8451.38881	51.160312	42.172624	25.716016	26.634932

16-Jul

Time	T _{outside} (°C)	Radiation (W/m ²)	T _{PV w/o HE} (°C)	T _{PV with HE} (°C)	T _{water HE In} (°C)	T _{water HE Out} (°C)
8:00 AM	20.683444	4627.16868	24.556006	22.619258	20.869876	21.030524
8:05 AM	22.357524	5001.68322	25.992866	22.518178	20.873244	21.055294
8:10 AM	22.745722	5088.52841	26.77517	22.65018	20.931342	21.057316
8:15 AM	22.140746	4953.18702	26.64897	23.095834	20.999522	21.081922
8:20 AM	21.612784	4835.07472	26.711422	23.349266	20.992908	21.162064
8:25 AM	23.365106	5227.09306	27.747194	23.34336	21.02185	21.212784
8:30 AM	23.973726	5363.24966	28.350954	23.679224	21.04124	21.236338
8:35 AM	24.905982	5571.80805	29.163188	24.127224	21.05605	21.285802
8:40 AM	22.208496	4968.34362	28.553574	24.510906	21.123966	21.297458

8:45 AM	22.487606	5030.78434	28.03513	24.845252	21.11656	21.285512
8:50 AM	22.662664	5069.9472	28.77959	24.599914	21.095954	21.308656
8:55 AM	25.356328	5672.5566	30.471624	24.958642	21.178	21.26929
9:00 AM	24.3678	5451.4094	30.76992	25.25858	21.171236	21.40097
9:05 AM	25.18594	5634.43848	30.452932	25.579218	21.219782	21.380198
9:10 AM	23.778064	5319.4774	30.434554	25.76784	21.235742	21.469822
9:15 AM	22.825306	5106.33244	30.049642	25.929336	21.280948	21.519186
9:20 AM	23.467206	5249.93423	29.804312	25.83404	21.306528	21.549304
9:25 AM	23.10119	5168.05145	29.72537	25.888862	21.391842	21.560946
9:30 AM	22.942054	5132.45056	29.597716	25.695898	21.306362	21.553494
9:35 AM	22.442254	5020.63848	28.48242	25.561724	21.375528	21.47514
9:40 AM	21.56815	4825.08949	28.17088	25.360696	21.407756	21.52043
9:45 AM	22.915136	5126.42864	28.04395	25.025392	21.392476	21.557224
9:50 AM	22.717438	5082.20089	28.256456	24.78948	21.381288	21.628596
9:55 AM	23.167642	5182.91767	28.483268	24.671436	21.43225	21.57957
10:00AM	22.383194	5007.42595	28.777332	24.781638	21.49046	21.568474
10:05AM	21.44481	4797.49664	29.225618	25.081928	21.42739	21.644204
10:10AM	22.422986	5016.32796	29.018402	25.12807	21.452072	21.621168
10:15AM	22.730076	5085.02819	29.995386	25.38185	21.459462	21.598072
10:20AM	25.157052	5627.97584	31.862876	25.563176	21.441748	21.62391
10:25AM	25.218182	5641.65145	32.313434	26.056304	21.477108	21.615906
10:30AM	24.841736	5557.43535	32.026386	26.496232	21.51151	21.633076
10:35AM	24.194932	5412.73647	31.81081	26.684562	21.453648	21.735588
10:40AM	23.358812	5225.68501	30.923538	26.741502	21.549824	21.688614
10:45AM	23.67606	5296.65772	30.889872	26.772418	21.585216	21.741422
10:50AM	24.399528	5458.50738	30.743586	26.526258	21.524234	21.814868
10:55AM	23.996102	5368.25548	32.150612	26.68134	21.59319	21.831748
11:00AM	23.496888	5256.5745	30.919068	26.814722	21.65363	21.792408
11:05AM	23.188486	5187.58076	30.566722	26.896212	21.61407	21.85679
11:10AM	21.095164	4719.27606	30.465546	26.630844	21.590024	21.854518
11:15AM	23.645618	5289.84743	30.168478	26.578704	21.594114	21.875836
11:20AM	22.51266	5036.38926	29.772212	26.462088	21.615278	21.88412
11:25AM	23.120792	5172.43669	29.457692	26.307518	21.685656	21.837306
11:30AM	22.889232	5120.63356	29.276192	26.146528	21.67993	21.840288
11:35AM	22.2725	4982.66219	29.908416	25.885998	21.669976	21.938806
11:40AM	24.21002	5416.11186	30.681174	25.910602	21.685952	21.898368
11:45AM	24.96772	5585.61969	31.522694	26.333428	21.729074	21.954358
11:50AM	22.164658	4958.53647	30.678692	26.607346	21.765622	21.969318
11:55AM	24.138688	5400.15391	31.087744	26.52185	21.722972	22.013564
12:00PM	23.769666	5317.59866	31.456618	26.616466	21.813774	21.943828
12:05PM	24.814942	5551.44116	31.315802	26.733734	21.792898	21.988072

12:10PM	24.965248	5585.06667	31.567774	26.866282	21.82618	21.97365
12:15PM	24.268486	5429.1915	30.958948	26.785138	21.857558	22.022246
12:20PM	23.813172	5327.33154	30.688184	26.716084	21.800928	22.10456
12:25PM	23.720664	5306.63624	30.1664	26.615482	21.812596	22.090106
12:30PM	22.797294	5100.06577	29.332098	26.413498	21.804696	22.142964
12:35PM	22.117208	4947.92125	29.087734	26.107262	21.761514	22.065346
12:40PM	24.770874	5541.58255	30.382642	26.003562	21.78754	22.03477
12:45PM	22.854328	5112.82506	31.453522	25.999996	21.783962	22.022486
12:50PM	23.77434	5318.6443	31.023892	26.530964	21.844578	22.004916
12:55PM	23.81635	5328.04251	30.98822	26.607406	21.864884	22.05134
1:00 PM	26.053292	5828.47696	32.342926	26.705296	21.855034	22.084836
1:05 PM	24.538614	5489.62282	31.845544	26.89917	21.8113	22.110576
1:10 PM	24.75166	5537.28412	31.056222	27.197434	21.898908	22.076464
1:15 PM	23.78582	5321.21253	30.24459	27.068984	21.903972	22.116544
1:20 PM	23.775802	5318.97136	29.77727	26.82195	21.933126	22.132442
1:25 PM	24.034818	5376.91678	29.505778	26.471178	21.89722	22.191936
1:30 PM	23.431608	5241.97047	29.166604	26.28537	21.96198	22.113786
1:35 PM	22.94015	5132.02461	30.240784	26.2626	21.956554	22.168928
1:40 PM	24.415924	5462.17539	30.508486	26.246248	21.952832	22.187158
1:45 PM	24.359414	5449.53333	30.697646	26.41886	21.922526	22.217236
1:50 PM	24.226996	5419.90962	30.342632	26.485496	21.959294	22.17602
1:55 PM	24.219222	5418.17047	30.627334	26.4866	21.960212	22.211764
2:00 PM	23.67128	5295.58837	30.380974	26.511122	21.971946	22.218954
2:05 PM	23.684188	5298.47606	30.202154	26.575694	22.006452	22.223172
2:10 PM	24.462388	5472.57002	31.624698	26.400558	21.95168	22.151182
2:15 PM	23.73588	5310.04027	31.253132	26.717618	21.96243	22.105532
2:20 PM	25.353158	5671.84743	31.880834	26.986264	21.932992	22.180194
2:25 PM	28.743856	6430.39284	35.52396	27.206848	21.938082	22.198154
2:30 PM	27.322906	6112.50694	36.47724	27.908702	21.928728	22.258258
2:35 PM	27.054948	6052.56107	36.353836	28.67858	22.045484	22.214694
2:40 PM	27.475896	6146.73289	37.518104	29.231346	21.991684	22.316846
2:45 PM	26.87058	6011.31544	36.100012	29.719292	22.08529	22.284964
2:50 PM	26.221014	5865.99866	36.885368	29.915068	22.044306	22.347884
2:55 PM	29.095584	6509.07919	37.473184	30.095834	22.079484	22.326848
3:00 PM	26.652592	5962.54855	38.09476	30.46222	22.09176	22.395326
3:05 PM	27.511486	6154.69485	37.924816	30.686204	22.126604	22.41294
3:10 PM	27.383654	6126.09709	38.177752	31.147722	22.15402	22.49674
3:15 PM	28.025246	6269.62998	36.61566	31.116946	22.17489	22.535014
3:20 PM	28.630376	6405.00582	37.37094	30.835772	22.190476	22.606788
3:25 PM	29.064106	6502.03714	37.77052	30.822116	22.30675	22.618968
3:30 PM	27.514376	6155.34139	36.257212	30.904178	22.319898	22.588976

3:35 PM	27.17036	6078.38031	35.418948	30.690064	22.281708	22.589392
3:40 PM	26.700448	5973.25459	35.108504	30.350072	22.269428	22.624796
3:45 PM	27.736678	6205.07338	36.502728	30.097854	22.26586	22.634282
3:50 PM	26.984772	6036.86174	35.603056	30.20385	22.277112	22.706642
3:55 PM	26.713448	5976.16286	36.872716	30.277648	22.312754	22.720324
4:00 PM	27.864188	6233.59911	36.786404	30.336484	22.328616	22.718968
4:05 PM	28.035154	6271.84653	37.401668	30.519536	22.405318	22.717322
4:10 PM	27.926022	6247.43221	38.000272	31.009684	22.42534	22.759286
4:15 PM	24.819594	5552.48188	36.505344	31.23059	22.448846	22.838972
4:20 PM	25.602288	5727.58121	34.461296	30.975516	22.477804	22.78128
4:25 PM	25.453784	5694.35884	33.955608	30.470534	22.52404	22.862312
4:30 PM	25.05946	5606.14318	32.662224	29.76239	22.528514	22.857894
4:35 PM	25.301052	5660.1906	32.420834	29.103706	22.483746	22.887102
4:40 PM	24.212362	5416.63579	32.16344	28.832476	22.501052	22.87395
4:45 PM	25.211952	5640.25772	31.718728	28.713962	22.555292	22.8457
4:50 PM	26.037694	5824.98747	32.498856	28.45036	22.514874	22.892306
4:55 PM	24.670794	5519.19329	32.226428	28.357744	22.52572	22.903148
5:00 PM	24.222742	5418.95794	32.25114	28.201492	22.524504	22.906096

17-Jul						
Time	T _{outside} (°C)	Radiation (W/m ²)	T _{PV w/o HE} (°C)	T _{PV with HE} (°C)	T _{water HE In} (°C)	T _{water HE Out} (°C)
8:00AM	15.336904	3431.07472	17.6576	17.217874	18.823162	18.98804
8:05 AM	15.328094	3429.1038	17.74471	17.27443	18.78838	19.05742
8:10 AM	15.47779	3462.59284	17.789314	17.65885	18.806762	19.024008
8:15 AM	15.840284	3543.6877	18.037456	17.393294	18.7851	19.045606
8:20 AM	15.972558	3573.27919	18.342824	17.56416	18.812346	19.072846
8:25 AM	16.073954	3595.96286	18.304908	17.65214	18.8437	19.073842
8:30 AM	16.062944	3593.49978	18.337384	17.976304	18.811082	19.04559
8:35 AM	15.67524	3506.7651	17.92509	17.694562	18.877166	19.037866
8:40 AM	15.748492	3523.15257	17.480166	17.723834	18.845696	19.102014
8:45 AM	16.003964	3580.30515	17.582422	17.778412	18.89131	19.043282
8:50 AM	15.699192	3512.12349	17.3918	17.548692	18.918518	19.039942
8:55 AM	15.861968	3548.5387	17.45826	17.758716	18.867458	19.067238
9:00 AM	16.262376	3638.11544	17.431062	17.653094	18.844652	19.079156
9:05 AM	15.963428	3571.23669	17.685894	17.424552	18.85978	19.072652
9:10 AM	15.922084	3561.98747	17.727022	17.674798	18.848884	19.061758
9:15 AM	16.03555	3587.37136	17.792482	17.661828	18.857556	19.057338
9:20 AM	16.243964	3633.99642	17.651986	17.421216	18.93462	19.030242
9:25 AM	16.180728	3619.84966	17.723842	17.479982	18.91515	19.036574
9:30 AM	15.572372	3483.75213	17.761824	17.509422	18.922738	19.039988

9:35 AM	15.81368	3537.73602	17.784748	17.63681	18.880374	19.07579
9:40 AM	15.846438	3545.06443	17.804356	17.7565	18.83906	19.056108
9:45 AM	16.101898	3602.21432	18.028304	17.606174	18.85432	19.05828
9:50 AM	15.636762	3498.15705	18.004398	17.891236	18.87806	19.077838
9:55 AM	16.196932	3623.47472	18.153192	17.744396	18.93132	19.039842
10:00AM	16.065714	3594.11946	18.249034	17.883752	18.853124	19.066
10:05AM	16.1783	3619.30649	18.265384	18.039284	18.912728	19.090876
10:10AM	16.286306	3643.4689	18.420676	17.816008	18.90307	19.111386
10:15AM	16.833828	3765.95705	18.770554	17.953216	18.9269	19.048514
10:20AM	16.480392	3686.88859	18.696616	17.913982	18.909516	19.104928
10:25AM	16.472622	3685.15034	19.149344	18.171646	18.945212	19.079912
10:30AM	16.380878	3664.62595	19.097056	18.341232	18.936552	19.110144
10:35AM	16.29468	3645.34228	18.994148	18.216248	18.963604	19.063394
10:40AM	16.624128	3719.0443	19.122044	18.209442	18.991902	19.104782
10:45AM	16.379724	3664.36779	18.948302	18.25295	18.983022	19.09173
10:50AM	16.335946	3654.57405	18.826626	18.179052	18.956976	19.122028
10:55AM	16.785166	3755.07069	18.817976	18.074526	18.969956	19.139372
11:00AM	16.345572	3656.72752	18.827696	18.406012	18.962218	19.14036
11:05AM	15.99951	3579.30872	18.852522	18.231158	19.039406	19.10884
11:10AM	16.884154	3777.21566	18.999156	18.12102	19.0297	19.15984
11:15AM	16.729328	3742.57897	18.953488	18.223402	18.996932	19.175072
11:20AM	16.525436	3696.96555	19.006654	18.450466	19.011018	19.193326
11:25AM	16.93212	3787.94631	18.938334	18.64289	19.04268	19.185718
11:30AM	17.32637	3876.14541	19.157474	18.375494	19.07059	19.148938
11:35AM	16.600506	3713.75973	19.420174	18.321006	19.068494	19.194456
11:40AM	17.135626	3833.47338	19.792048	18.789398	19.07172	19.197492
11:45AM	16.724906	3741.58971	19.318232	18.862174	19.014526	19.170656
11:50AM	17.16648	3840.37584	19.375868	18.480902	19.011276	19.17177
11:55AM	17.282934	3866.42819	19.370368	18.488492	19.031764	19.1141
12:00PM	17.444066	3902.47562	19.504882	18.723298	19.044714	19.144688
12:05PM	17.329622	3876.87293	19.642468	18.73516	19.008766	19.186712
12:10PM	16.808578	3760.30828	19.605424	19.15857	19.032604	19.180196
12:15PM	17.089834	3823.22908	19.451466	18.7393	19.08253	19.17814
12:20PM	17.57537	3931.85011	19.549132	18.702294	19.08025	19.197484
12:25PM	17.41855	3896.76734	19.53156	18.780352	19.114846	19.175548
12:30PM	17.265068	3862.43132	20.12123	18.735762	19.092082	19.204954
12:35PM	17.41421	3895.79642	20.144002	19.1972	19.09742	19.201756
12:40PM	16.526602	3697.2264	19.915318	19.012748	19.143082	19.208146
12:45PM	17.30836	3872.11633	20.090502	19.174394	19.122418	19.23946
12:50PM	17.39206	3890.84116	19.826526	19.01914	19.140746	19.26651
12:55PM	17.131622	3832.57763	19.540968	18.994112	19.185146	19.271836

1:00 PM	17.462874	3906.68322	19.840522	19.0635	19.133122	19.2936
1:05 PM	17.753392	3971.67606	19.9563	19.392358	19.144822	19.2795
1:10 PM	17.652082	3949.01163	20.046642	19.056898	19.15251	19.287
1:15 PM	17.710798	3962.1472	20.231494	19.332558	19.163356	19.310744
1:20 PM	17.144228	3835.39776	20.052974	19.48452	19.193564	19.319324
1:25 PM	16.638244	3722.20224	19.514724	19.332272	19.17616	19.323736
1:30 PM	16.974178	3797.35526	19.180474	19.071964	19.2499	19.280248
1:35 PM	17.620112	3941.85951	19.936432	18.933894	19.198922	19.333406
1:40 PM	16.457024	3681.66085	19.837954	19.299756	19.191254	19.317206
1:45 PM	16.618258	3717.7311	19.698832	19.04789	19.243282	19.286718
1:50 PM	17.08814	3822.85011	19.628416	19.22482	19.259342	19.311504
1:55 PM	18.30982	4096.1566	20.064308	19.274708	19.226906	19.361578
2:00 PM	18.53375	4146.2528	21.075418	19.5328	19.215864	19.3549
2:05 PM	18.206438	4073.02864	21.460764	19.653142	19.284266	19.331874
2:10 PM	18.412744	4119.1821	21.280444	20.071556	19.242886	19.355746
2:15 PM	18.460626	4129.89396	22.152554	20.106296	19.242748	19.36433
2:20 PM	18.607806	4162.82013	21.917932	19.901836	19.233354	19.311696
2:25 PM	18.623014	4166.22237	22.548752	20.047082	19.218208	19.326704
2:30 PM	19.329978	4324.37987	22.824642	20.24162	19.260558	19.308168
2:35 PM	20.210014	4521.25593	24.345506	20.392726	19.233292	19.328894
2:40 PM	20.132536	4503.92304	24.933252	21.019562	19.225564	19.373132
2:45 PM	18.426642	4122.29128	23.599836	21.411538	19.248046	19.38708
2:50 PM	18.405872	4117.64474	22.566328	21.330022	19.275094	19.42721
2:55 PM	18.804652	4206.85727	23.348716	20.994254	19.330344	19.41285
3:00 PM	19.865162	4444.10783	24.313742	21.134094	19.38767	19.418206
3:05 PM	20.6785	4626.06264	25.720552	21.530128	19.358298	19.440612
3:10 PM	21.197682	4742.21074	26.7682	21.970608	19.36011	19.503492
3:15 PM	20.909666	4677.77763	26.625144	22.147122	19.3807	19.528252
3:20 PM	20.673432	4624.92886	26.322964	22.696102	19.466072	19.535674
3:25 PM	20.199158	4518.82729	25.60818	22.795698	19.479054	19.556998
3:30 PM	19.789734	4427.23356	25.197038	22.525402	19.43379	19.546632
3:35 PM	19.6693	4400.29083	25.538562	22.790628	19.404368	19.56064
3:40 PM	20.346796	4551.85593	25.039468	22.501104	19.427074	19.600604
3:45 PM	20.332372	4548.62908	25.141804	22.647344	19.44299	19.616704
3:50 PM	20.56929	4601.63087	25.415424	22.727208	19.479614	19.640242
3:55 PM	22.143822	4953.87517	26.390774	22.47784	19.50788	19.655416
4:00 PM	21.008014	4699.77942	26.711182	22.74416	19.54004	19.665954
4:05 PM	21.359698	4778.45593	26.405552	22.977732	19.526716	19.70914
4:10 PM	20.572416	4602.3302	26.190118	23.046988	19.583066	19.717704
4:15 PM	20.8125	4656.04027	26.087862	23.16464	19.627266	19.714116
4:20 PM	20.404878	4564.84966	25.998574	23.295668	19.615102	19.719396

4:25 PM	21.118638	4724.52752	25.870272	23.066864	19.603188	19.76797
4:30 PM	20.816296	4656.88949	25.712862	22.951866	19.61798	19.752614
4:35 PM	20.305714	4542.66532	25.227598	22.966924	19.650522	19.77188
4:40 PM	19.73592	4415.19463	25.101336	23.008982	19.688136	19.809868
4:45 PM	20.31285	4544.26174	24.989026	22.727182	19.714168	19.796462
4:50 PM	20.591336	4606.56286	25.22309	22.576292	19.6587	19.84528
4:55 PM	20.742144	4640.30067	25.312384	22.614114	19.73984	19.852656
5:00 PM	20.652746	4620.30112	25.456664	22.629096	19.707072	19.893834

18-Jul						
Time	T _{outside} (°C)	Radiation (W/m ²)	T _{PV w/o HE} (°C)	T _{PV with HE} (°C)	T _{water HE In} (°C)	T _{water HE Out} (°C)
8:00AM	15.673928	3506.47159	16.912116	16.772634	17.77776	17.960428
8:05AM	16.206188	3625.54541	17.14715	16.781374	17.790864	17.960428
8:10 AM	16.023054	3584.57584	17.03388	16.703042	17.817034	17.938748
8:15 AM	15.99454	3578.19687	16.975176	16.962064	17.810398	17.971228
8:20 AM	16.049022	3590.38523	16.711324	16.776698	17.855878	17.960122
8:25 AM	16.558982	3704.47025	17.168592	16.768046	17.834132	17.986224
8:30 AM	17.143446	3835.22282	18.039316	16.986696	17.861028	17.956726
8:35 AM	17.294588	3869.03535	18.968274	17.142226	17.846896	18.02082
8:40 AM	16.993156	3801.60089	19.336938	17.37597	17.863116	18.045582
8:45 AM	17.251832	3859.47025	19.42599	17.726108	17.899858	18.008656
8:50 AM	16.929622	3787.38747	19.878276	17.83912	17.904252	18.069436
8:55 AM	17.471382	3908.58658	20.366902	18.249532	17.923556	18.08437
9:00 AM	17.836452	3990.25772	21.048312	18.483814	17.975632	18.066766
9:05 AM	18.039498	4035.68188	21.610858	18.521652	17.943804	18.117718
9:10 AM	18.679952	4178.96018	22.31847	18.827396	17.976108	18.132552
9:15 AM	17.96835	4019.7651	21.964562	19.272112	18.06404	18.133526
9:20 AM	17.984702	4023.42327	21.621156	19.4582	18.062924	18.101842
9:25 AM	18.516814	4142.46398	22.381178	19.434514	17.99991	18.05649
9:30 AM	18.930536	4235.01924	23.164992	19.844538	17.957614	18.018562
9:35 AM	19.273416	4311.72617	23.33243	19.99553	17.969466	17.995478
9:40 AM	19.11431	4276.13199	23.528936	20.28882	17.936854	17.984702
9:45 AM	17.947688	4015.14273	23.466176	20.321432	17.947688	17.9737
9:50 AM	19.2895	4315.32438	23.543028	20.698068	17.902968	17.998664
9:55 AM	20.028182	4480.57763	23.990752	20.73624	17.919384	18.00198
10:00AM	20.54056	4595.20358	24.314154	20.56671	17.923618	17.988936
10:05AM	20.518692	4590.31141	24.7624	20.783592	17.910444	18.027784
10:10AM	20.254558	4531.22103	24.504786	20.958138	17.959112	18.050438
10:15AM	19.980704	4469.95615	24.83203	21.18797	17.99392	18.067776
10:20AM	20.066274	4489.09933	25.489436	21.373268	17.975194	18.075062
10:25AM	21.733732	4862.13244	26.384102	21.460692	18.041198	18.102142

10:30AM	21.656568	4844.8698	26.725424	21.73874	18.0766	18.17665
10:35AM	22.335454	4996.74586	27.869676	22.266192	18.105924	18.218882
10:40AM	21.95954	4912.64877	27.982522	22.617746	18.159054	18.224168
10:45AM	22.157552	4956.94676	28.088816	23.001604	18.24033	18.292534
10:50AM	21.765352	4869.20626	27.43281	23.085602	18.268444	18.35956
10:55AM	20.207762	4520.75213	27.438044	23.285644	18.321546	18.403926
11:00AM	22.394312	5009.9132	28.014586	23.078024	18.369224	18.429962
11:05AM	23.791934	5322.58031	29.450068	23.256106	18.370102	18.487402
11:10AM	24.615674	5506.86219	30.225478	23.791564	18.37391	18.486844
11:15AM	24.460274	5472.09709	30.332586	24.106538	18.408348	18.543104
11:20AM	25.119958	5619.6774	31.094392	24.662886	18.50372	18.6341
11:25AM	28.801912	6443.38076	34.001032	24.8741	18.555564	18.7034
11:30AM	28.99073	6485.62192	36.603128	25.657852	18.58551	18.772432
11:35AM	30.765562	6882.67606	38.465468	26.77861	18.62839	18.819478
11:40AM	31.27464	6996.56376	40.71272	27.967206	18.67546	18.901454
11:45AM	29.857286	6679.48233	41.022028	28.998826	18.71816	19.009414
11:50AM	33.940476	7592.94765	45.163248	29.984538	18.907594	19.133548
11:55AM	35.220736	7879.35928	47.904012	31.260822	18.867774	19.14154
12:00PM	33.31358	7452.70246	47.823	32.887158	18.926468	19.291462
12:05PM	35.396404	7918.65861	47.847352	33.844008	19.088156	19.418398
12:10PM	34.906004	7808.94944	47.514264	34.530348	19.121528	19.490834
12:15PM	36.37792	8138.23714	48.350576	34.702808	19.248428	19.65676
12:20PM	36.210872	8100.86622	51.004592	35.235208	19.307372	19.780722
12:25PM	39.647956	8869.78881	53.750184	36.061424	19.340536	19.879098
12:30PM	36.82202	8237.58837	55.499012	37.200552	19.45017	19.997406
12:35PM	37.120348	8304.32841	56.181544	38.19498	19.571222	20.135848
12:40PM	37.29628	8343.6868	55.919504	39.324628	19.632162	20.253248
12:45PM	35.065364	7844.60045	56.731096	40.164124	19.775342	20.422512
12:50PM	38.58302	8631.5481	56.772648	40.822404	19.924098	20.61459
12:55PM	39.810952	8906.25324	57.09694	41.311392	20.020326	20.676094
1:00 PM	32.117226	7185.06174	56.23252	41.447336	20.12288	20.800196
1:05 PM	36.51756	8169.47651	53.76816	41.433616	20.206748	20.9274
1:10 PM	37.597788	8411.13826	54.221468	41.133408	20.39083	21.085624
1:15 PM	40.568792	9075.79239	54.84624	40.805556	20.452512	21.129846
1:20 PM	40.319356	9019.99016	57.277872	40.738276	20.468502	21.236932
1:25 PM	39.5928	8857.44966	59.617052	41.610988	20.616344	21.358746
1:30 PM	41.361356	9253.09978	60.945036	42.728652	20.652772	21.421288
1:35 PM	43.647116	9764.45548	61.909884	43.782068	20.781666	21.576234
1:40 PM	31.330116	7008.9745	57.2105	44.300044	20.94772	21.737834
1:45 PM	38.163336	8537.65906	56.38624	43.685644	20.962588	21.813464
1:50 PM	40.3556	9028.09843	56.567108	43.039116	21.053622	21.939272

1:55 PM	33.27079	7443.12975	53.834984	42.934364	21.243336	22.016238
2:00 PM	35.296484	7896.30515	49.876676	42.32834	21.252424	22.046896
2:05 PM	37.037312	8285.75213	52.44662	40.908064	21.264226	22.115286
2:10 PM	36.483548	8161.86756	56.213668	40.708276	21.34	22.212776
2:15 PM	38.728496	8664.09306	57.472372	41.58772	21.523532	22.30081
2:20 PM	37.976892	8495.94899	57.737288	42.604768	21.510848	22.353236
2:25 PM	37.581728	8407.54541	56.134068	43.036332	21.653224	22.443292
2:30 PM	37.944452	8488.69172	55.759416	43.228064	21.74895	22.573966
2:35 PM	39.073804	8741.34318	58.027188	43.065424	21.796778	22.717118
2:40 PM	39.16606	8761.9821	58.527992	43.38996	21.96372	22.844972
2:45 PM	38.365436	8582.87159	56.498668	43.605432	21.923092	22.830478
2:50 PM	36.693696	8208.88054	54.101424	43.638784	22.003386	22.910718
2:55 PM	35.276792	7891.89978	52.32656	43.004924	22.127124	23.034368
3:00 PM	39.672916	8875.37271	54.055516	42.112248	22.216	23.101624
3:05 PM	39.405984	8815.65638	56.763244	42.337856	22.320396	23.227698
3:10 PM	41.347	9249.88814	58.514948	42.752508	22.389012	23.287566
3:15 PM	43.202748	9665.0443	58.663116	43.405328	22.311326	23.201424
3:20 PM	39.759608	8894.76689	57.244632	44.058772	22.38713	23.359624
3:25 PM	40.723984	9110.51096	57.750908	43.987296	22.463748	23.41047
3:30 PM	40.947212	9160.45011	59.964704	44.32772	22.58249	23.555028
3:35 PM	42.00574	9397.25727	59.511476	44.731348	22.678948	23.651602
3:40 PM	41.114116	9197.78881	59.293448	45.029632	22.67629	23.67504
3:45 PM	39.307456	8793.61432	59.8762	45.148	22.70989	23.804078
3:50 PM	42.270124	9456.40358	59.463792	45.500476	22.82435	23.866272
3:55 PM	40.877224	9144.79284	58.890592	45.487536	22.912768	24.05441
4:00 PM	41.291704	9237.51767	58.455984	45.431244	22.935682	24.068804
4:05 PM	39.7711	8897.33781	57.169776	45.209672	23.013826	24.14688
4:10 PM	40.759348	9118.42237	55.685672	45.102744	23.132392	24.204684
4:15 PM	40.85932	9140.78747	56.420552	44.738236	23.2292	24.301412
4:20 PM	41.851984	9362.85996	55.001076	44.408456	23.257774	24.377578
4:25 PM	39.272144	8785.71454	55.10814	44.216708	23.345966	24.470042
4:30 PM	39.588436	8856.47338	53.91734	43.80908	23.316948	24.358856
4:35 PM	41.63816	9315.02461	54.663628	43.42246	23.353276	24.395344
4:40 PM	39.294888	8790.80268	53.647408	43.500116	23.427798	24.443734
4:45 PM	39.376892	8809.1481	53.32862	43.285452	23.44558	24.526494
4:50 PM	37.273196	8338.5226	50.868224	42.882412	23.483356	24.546858
4:55 PM	39.34336	8801.64653	50.957936	42.196924	23.523004	24.586476
5:00 PM	36.16504	8090.61298	51.516056	41.91388	23.602104	24.626596

19-Jul						
Time	T _{outside} (°C)	Radiation (W/m ²)	T _{PV w/o HE} (°C)	T _{PV with HE} (°C)	T _{water HE In} (°C)	T _{water HE Out} (°C)

8:00AM	18.628832	4167.52394	20.670372	20.02825	20.01953	20.054222
8:05 AM	18.80703	4207.38926	20.271272	20.453406	19.984658	20.09764
8:10 AM	18.423974	4121.69441	19.428798	19.884854	19.975854	20.07576
8:15 AM	18.418426	4120.45324	19.071004	19.514476	20.044246	20.105096
8:20 AM	18.391226	4114.36823	19.439696	19.448228	19.973856	20.117172
8:25 AM	18.404324	4117.29843	19.374262	19.40916	20.05632	20.112622
8:30 AM	18.561094	4152.37002	19.960774	19.239592	19.986936	20.134422
8:35 AM	18.463076	4130.44206	20.06723	19.650302	19.967324	20.09756
8:40 AM	18.332356	4101.19821	19.641448	19.94558	20.002076	20.114868
8:45 AM	18.225764	4077.35213	19.056968	19.821864	20.03894	20.103962
8:50 AM	18.173368	4065.63043	18.643708	19.413394	20.086522	20.121212
8:55 AM	18.266976	4086.57181	18.536882	19.054714	20.014884	20.114788
9:00 AM	18.174424	4065.86667	18.56202	18.95804	20.074496	20.113736
9:05 AM	18.247534	4082.22237	18.508904	18.844034	20.051962	20.117172
9:10 AM	18.208496	4073.48904	18.600256	18.756814	20.08672	20.125768
9:15 AM	18.344712	4103.96242	18.68425	18.871346	20.035838	20.109578
9:20 AM	18.279418	4089.35526	18.640798	18.954074	19.99243	20.083804
9:25 AM	18.341588	4103.26353	18.80295	19.28995	20.032714	20.067408
9:30 AM	18.339562	4102.81029	19.005458	19.109802	20.043772	20.056854
9:35 AM	18.439774	4125.22908	19.192504	19.175052	20.009076	20.052678
9:40 AM	18.669516	4176.6255	19.67377	19.530598	19.986426	20.07325
9:45 AM	18.606454	4162.51767	19.814978	19.337088	20.001536	20.032056
9:50 AM	19.049222	4261.57092	20.09167	19.740172	19.952714	20.04826
9:55 AM	19.083938	4269.33736	21.151102	19.535938	19.965794	20.044088
10:00AM	19.312174	4320.39687	21.301142	19.907246	19.998246	20.024408
10:05AM	19.713706	4410.22506	21.211792	20.07848	19.956962	20.05251
10:10AM	19.969948	4467.54989	21.702726	20.265092	19.948334	20.065304
10:15AM	19.951406	4463.40179	22.253042	20.736434	19.96866	20.081458
10:20AM	20.246296	4529.37271	22.400202	20.60638	20.011812	20.090106
10:25AM	20.16681	4511.5906	22.94085	21.047942	19.94558	20.114868
10:30AM	19.730258	4413.92796	22.86506	21.45862	19.990956	20.12991
10:35AM	20.143782	4506.43893	21.832982	21.26378	20.03535	20.165392
10:40AM	19.67992	4402.66667	21.13429	21.238656	20.044896	20.162044
10:45AM	19.380102	4335.59329	20.422288	20.604404	20.044718	20.170588
10:50AM	19.172408	4289.12931	20.115054	20.39728	20.050032	20.1977
10:55AM	19.19312	4293.76286	20.03168	20.625858	20.083622	20.205128
11:00AM	19.464754	4354.5311	19.95549	20.107528	20.037956	20.207236
11:05AM	19.306172	4319.05414	20.01405	20.01405	20.04457	20.205128
11:10AM	19.213846	4298.39955	20.00879	19.9176	20.043484	20.19987
11:15AM	19.02116	4255.29306	19.981736	20.107422	20.05965	20.207316
11:20AM	19.135492	4280.87069	20.021864	20.000062	20.117404	20.182424

11:25AM	19.142186	4282.36823	20.076134	19.967698	20.110824	20.16731
11:30AM	19.01397	4253.68456	19.739824	19.787418	20.069716	20.173974
11:35AM	18.65383	4173.11633	19.454232	19.888474	20.053412	20.17492
11:40AM	18.41027	4118.62864	19.215184	19.888604	20.023208	20.157798
11:45AM	18.378704	4111.56689	18.9575	19.488062	20.078696	20.134994
11:50AM	18.317968	4097.97942	18.866434	19.423016	20.018038	20.152442
11:55AM	18.303998	4094.85414	18.769738	19.24821	20.081996	20.116876
12:00PM	18.317088	4097.78255	18.904638	19.35708	20.07365	20.13431
12:05PM	18.457722	4129.2443	19.119198	19.245156	20.001028	20.113822
12:10PM	18.745258	4193.57002	19.836298	19.423472	20.040104	20.100956
12:15PM	19.698212	4406.75884	21.391772	19.433284	20.041194	20.071714
12:20PM	20.088964	4494.17539	23.55647	19.837388	19.99361	20.088964
12:25PM	21.277406	4760.04609	25.671946	20.78167	20.01847	20.066054
12:30PM	21.646516	4842.62103	28.686592	21.663934	19.926934	20.078784
12:35PM	21.820656	4881.57852	31.841118	22.63219	20.009738	20.1358
12:40PM	22.420184	5015.70112	35.395864	23.750552	20.027658	20.175328
12:45PM	24.32408	5441.62864	39.934976	25.037004	20.1127	20.216764
12:50PM	24.859068	5561.31275	46.930596	27.285222	20.116086	20.289712
12:55PM	24.250622	5425.19508	46.84916	29.620002	20.099478	20.31234
1:00 PM	24.457966	5471.58076	48.085228	31.06663	20.164372	20.411906
1:05 PM	24.298996	5436.017	47.196696	32.446736	20.278032	20.54298
1:10 PM	24.716338	5529.3821	48.246168	32.71429	20.267036	20.58846
1:15 PM	27.434362	6137.44116	51.5682	33.416958	20.32916	20.689598
1:20 PM	26.622604	5955.83982	55.716076	34.498072	20.408584	20.80784
1:25 PM	27.607674	6176.21342	57.748484	36.637044	20.537148	20.884644
1:30 PM	24.260446	5427.39284	57.73556	38.060208	20.564392	21.028766
1:35 PM	25.927482	5800.33154	58.018732	39.460844	20.714572	21.222458
1:40 PM	26.624158	5956.18747	58.090044	40.146344	20.794244	21.336946
1:45 PM	26.467384	5921.11499	57.880592	40.578	20.922676	21.486722
1:50 PM	25.119882	5619.6604	57.071916	41.11298	21.04404	21.67336
1:55 PM	27.097364	6062.05011	56.868872	41.313216	21.130344	21.72914
2:00 PM	29.925792	6694.80805	56.79498	41.48512	21.187708	21.851794
2:05 PM	34.210572	7653.37181	56.662972	41.81352	21.409946	22.026028
2:10 PM	33.36271	7463.69351	57.242812	42.002924	21.468292	22.175388
2:15 PM	31.403432	7025.37629	56.876796	42.08766	21.471062	22.165286
2:20 PM	31.63863	7077.99329	53.692444	41.965692	21.617174	22.26363
2:25 PM	31.214652	6983.14362	51.67716	41.346708	21.709182	22.429394
2:30 PM	31.419144	7028.89128	47.737104	40.587872	21.84607	22.522876
2:35 PM	30.265206	6770.7396	45.491548	39.412236	21.909762	22.621348
2:40 PM	27.734786	6204.65011	42.114564	37.819496	21.977022	22.697278
2:45 PM	26.99472	6039.08725	38.431264	36.354696	21.98313	22.607836

2:50 PM	26.35185	5895.26846	36.34284	34.919036	22.00521	22.634448
2:55 PM	26.42692	5912.06264	34.06222	33.493084	22.041918	22.662244
3:00 PM	26.331832	5890.79016	33.214802	31.915288	22.015602	22.640484
3:05 PM	26.422448	5911.06219	33.48019	30.913682	22.0026	22.60989
3:10 PM	26.264784	5875.7906	32.87838	30.5232	22.091434	22.616574
3:15 PM	28.755462	6432.98926	34.485272	30.152196	22.097962	22.596988
3:20 PM	30.836148	6898.46711	40.072292	29.999776	22.013124	22.55116
3:25 PM	34.24448	7660.95749	46.22426	31.182984	22.104734	22.53867
3:30 PM	33.608668	7518.71767	49.026676	33.377326	22.079974	22.565952
3:35 PM	33.51913	7498.6868	52.091136	35.625744	22.127816	22.648588
3:40 PM	31.196414	6979.06353	49.852408	37.183756	22.143808	22.716602
3:45 PM	31.002648	6935.71544	48.234108	38.048052	22.240182	22.821636
3:50 PM	32.733406	7322.90962	47.620192	38.034	22.311688	22.914864
3:55 PM	30.944042	6922.60447	48.467648	37.527676	22.223578	22.848548
4:00 PM	32.22311	7208.74944	46.599992	37.491004	22.315734	22.931962
4:05 PM	32.77927	7333.17002	47.650124	37.391848	22.356782	22.994742
4:10 PM	33.164054	7419.25145	48.736848	37.41672	22.429248	23.080034
4:15 PM	32.40673	7249.82774	50.297128	38.027112	22.448348	23.120872
4:20 PM	30.621498	6850.44698	46.09002	38.246372	22.554646	23.196668
4:25 PM	28.088384	6283.75481	41.963876	37.904108	22.586122	23.258576
4:30 PM	29.73526	6652.18345	41.58886	36.825372	22.691762	23.338066
4:35 PM	31.155086	6969.8179	43.067928	35.839208	22.746332	23.371244
4:40 PM	30.274606	6772.84251	43.152168	35.685128	22.754346	23.374716
4:45 PM	29.221684	6537.28949	39.66966	35.485528	22.68519	23.297082
4:50 PM	28.029046	6270.48009	37.62548	34.854124	22.669002	23.30246
4:55 PM	25.97882	5811.81655	34.472348	33.96716	22.646	23.305566
5:00 PM	25.490318	5702.53199	30.945976	32.454532	22.70804	23.302524

20-Jul						
Time	T _{outside} (°C)	Radiation (W/m ²)	T _{PV w/o HE} (°C)	T _{PV with HE} (°C)	T _{water HE In} (°C)	T _{water HE Out} (°C)
8:00AM	18.187602	4068.81477	20.485874	20.003868	19.200764	19.413582
8:05 AM	18.091576	4047.33244	20.951068	20.302832	19.252582	19.447944
8:10 AM	18.601612	4161.43445	22.28936	20.182472	19.257894	19.42291
8:15 AM	19.11199	4275.61298	23.26152	20.17979	19.246676	19.416054
8:20 AM	20.048182	4485.0519	26.074842	20.925986	19.318892	19.46228
8:25 AM	22.207534	4968.12841	28.578042	21.843156	19.336924	19.497566
8:30 AM	21.097374	4719.77047	28.979656	22.408454	19.40799	19.555538
8:35 AM	22.526428	5039.46935	30.32884	23.17206	19.360852	19.560556
8:40 AM	23.638758	5288.31275	32.570812	23.993562	19.381742	19.581636
8:45 AM	22.689436	5075.93647	33.905752	24.964754	19.441752	19.667614
8:50 AM	23.499608	5257.183	34.835308	25.73709	19.476576	19.715518

8:55 AM	23.722498	5307.04653	37.087772	26.321328	19.569872	19.761014
9:00 AM	24.691876	5523.90962	38.6263	27.492188	19.579114	19.796232
9:05 AM	24.203378	5414.62595	39.859404	28.518624	19.626618	19.891696
9:10 AM	24.512326	5483.74183	40.631944	29.17901	19.676124	19.975888
9:15 AM	24.370372	5451.98479	39.98724	29.949432	19.628656	20.03289
9:20 AM	22.810654	5103.05459	38.942172	30.280366	19.702266	20.110456
9:25 AM	22.728434	5084.66085	38.205532	30.306774	19.793738	20.219524
9:30 AM	24.015762	5372.65369	39.546692	30.234532	19.82842	20.223874
9:35 AM	25.625382	5732.74765	41.193996	30.433856	19.8862	20.290354
9:40 AM	24.324748	5441.77808	42.267128	31.035226	19.977634	20.438048
9:45 AM	24.670686	5519.16913	41.386704	31.241436	19.968542	20.476716
9:50 AM	24.458764	5471.75928	41.054776	31.580694	20.059774	20.529064
9:55 AM	27.65203	6186.13647	41.786492	31.894078	20.146586	20.628922
10:00AM	31.813204	7117.04787	43.528788	31.920282	20.16393	20.728682
10:05AM	32.69579	7314.49441	44.710836	32.503334	20.27243	20.841494
10:10AM	31.270202	6995.57092	45.992396	33.436588	20.329088	20.820072
10:15AM	33.06749	7397.64877	46.39092	34.062804	20.348078	20.917298
10:20AM	32.37447	7242.61074	45.441892	34.575384	20.473654	21.003606
10:25AM	31.783088	7110.31051	46.380736	34.784872	20.577422	21.137828
10:30AM	32.229962	7210.28233	46.92448	35.33564	20.577604	21.190098
10:35AM	29.334356	6562.49575	42.129976	35.294904	20.61296	21.277712
10:40AM	28.261326	6322.4443	38.0677	34.39238	20.766018	21.369712
10:45AM	27.604118	6175.4179	36.413188	33.038918	20.74087	21.414078
10:50AM	28.157778	6299.27919	35.271132	32.052044	20.89094	21.503288
10:55AM	27.559606	6165.45996	35.616732	31.142538	20.921582	21.520852
11:00AM	26.898448	6017.54989	34.720136	30.375808	20.893766	21.462752
11:05AM	25.99121	5814.58837	33.98116	29.947648	20.927846	21.457804
11:10AM	26.735752	5981.15257	33.936048	29.5761	20.959948	21.515838
11:15AM	26.652218	5962.46488	34.38764	29.265746	20.936858	21.53612
11:20AM	27.59658	6173.73154	35.035944	29.042194	21.02334	21.531484
11:25AM	28.004118	6264.90336	35.678308	29.14396	21.017384	21.55166
11:30AM	27.445056	6139.83356	36.91276	29.475362	21.039844	21.565402
11:35AM	28.482218	6371.86085	40.186412	29.861186	21.060918	21.590824
11:40AM	27.735732	6204.86174	38.694916	30.669234	21.119814	21.636632
11:45AM	29.573476	6615.99016	40.716412	30.962944	21.16852	21.668088
11:50AM	30.854558	6902.58568	46.527568	31.572372	21.176376	21.714942
11:55AM	31.814802	7117.40537	48.381468	33.362316	21.2431	21.794894
12:00PM	32.639884	7301.98747	50.57868	34.564972	21.187438	21.75213
12:05PM	33.309436	7451.77539	52.127832	35.991052	21.205446	21.791902
12:10PM	34.38978	7693.46309	53.720396	37.401972	21.263498	21.945526
12:15PM	32.760342	7328.93557	49.489572	38.446472	21.368426	22.07652

12:20PM	32.460372	7261.82819	46.491232	38.012468	21.48988	22.206616
12:25PM	31.28842	6999.64653	45.966004	37.056816	21.433768	22.176462
12:30PM	33.482646	7490.52483	50.764572	36.65026	21.482536	22.207982
12:35PM	37.172948	8316.09575	53.895216	37.164532	21.559448	22.276146
12:40PM	30.563898	6837.56107	49.644312	38.62574	21.669734	22.395076
12:45PM	33.27293	7443.6085	49.55256	38.723052	21.759428	22.5237
12:50PM	34.341468	7682.65503	52.550596	38.38428	21.843738	22.586202
12:55PM	35.639096	7972.95213	54.888848	39.043736	21.933278	22.662824
1:00 PM	30.228548	6762.5387	45.943728	39.681736	21.888394	22.66148
1:05 PM	33.285546	7446.43087	48.714304	38.510424	21.908842	22.694784
1:10 PM	35.031988	7837.13378	47.934576	38.124752	21.98679	22.807494
1:15 PM	31.34461	7012.217	48.603756	37.790632	22.070084	22.869172
1:20 PM	31.068524	6950.4528	43.41362	37.516856	22.111186	22.923488
1:25 PM	29.908364	6690.90917	40.657764	36.60976	22.123496	22.983266
1:30 PM	30.142248	6743.23221	42.633692	35.417312	22.246742	22.984818
1:35 PM	35.827816	8015.17136	50.013064	35.020536	22.194972	23.007036
1:40 PM	35.070292	7845.70291	50.935732	36.33368	22.205858	23.030964
1:45 PM	33.048066	7393.30336	46.556132	37.359292	22.2436	22.960304
1:50 PM	35.420072	7923.95347	53.303192	37.342888	22.248018	22.999522
1:55 PM	36.05964	8067.03356	54.903508	38.519496	22.250972	23.032738
2:00 PM	37.243392	8331.85503	55.743316	39.615836	22.331694	23.139322
2:05 PM	35.528912	7948.30246	57.043132	40.550824	22.365718	23.225334
2:10 PM	32.472686	7264.583	47.939952	40.779364	22.51159	23.327994
2:15 PM	37.39686	8366.18792	54.69758	39.619832	22.568674	23.393552
2:20 PM	38.349824	8579.37897	57.568084	40.300544	22.655012	23.462438
2:25 PM	35.04186	7839.34228	55.41572	41.329008	22.567728	23.4274
2:30 PM	33.808436	7563.4085	46.646824	41.651304	22.645396	23.526758
2:35 PM	37.515012	8392.62013	49.985728	39.674284	22.691018	23.554956
2:40 PM	33.434258	7479.69978	49.945428	39.458484	22.704712	23.59927
2:45 PM	34.1611	7642.30425	48.173408	39.193588	22.741374	23.661996
2:50 PM	38.510072	8615.22864	50.296492	39.032532	22.819474	23.692214
2:55 PM	32.347878	7236.66174	44.8284	39.269776	22.870362	23.75592
3:00 PM	33.86184	7575.3557	43.340204	37.86072	22.906594	23.78797
3:05 PM	37.575372	8406.12349	50.883852	37.247272	22.949564	23.813522
3:10 PM	38.637284	8643.6877	54.325956	37.990892	22.96053	23.854912
3:15 PM	34.819952	7789.69843	51.8281	39.801136	23.060522	23.911364
3:20 PM	36.535228	8173.42908	48.65976	40.09188	23.00442	23.894424
3:25 PM	33.908836	7585.86935	50.158176	39.46796	23.013568	23.890528
3:30 PM	31.040484	6944.17987	43.52734	38.987824	23.06475	23.9636
3:35 PM	32.660592	7306.62013	42.862132	37.557548	23.05902	23.970726
3:40 PM	36.666248	8202.74004	49.754692	36.824208	23.12395	23.97059

3:45 PM	35.516676	7945.5651	53.376648	37.424764	23.1275	24.000226
3:50 PM	35.402608	7920.04653	54.501644	39.166212	23.193904	24.066394
3:55 PM	37.09	8297.53915	54.569284	40.300444	23.241474	24.126972
4:00 PM	38.110844	8525.91588	54.251308	41.115072	23.312978	24.194084
4:05 PM	35.089584	7850.01879	52.1302	41.14188	23.343944	24.28153
4:10 PM	31.473064	7040.95391	45.849404	40.92126	23.448178	24.324844
4:15 PM	34.287844	7670.65861	46.711668	39.455616	23.473476	24.358818
4:20 PM	30.218346	6760.25638	41.050036	38.46702	23.518398	24.373292
4:25 PM	29.543912	6609.37629	39.561148	37.370068	23.541934	24.41854
4:30 PM	28.785888	6439.79597	37.601532	35.72312	23.525952	24.39822
4:35 PM	30.881256	6908.55839	41.954584	34.649636	23.561902	24.395224
4:40 PM	32.2254	7209.26174	38.628904	34.242616	23.536212	24.326092
4:45 PM	35.646588	7974.62819	44.640548	34.052864	23.47876	24.307602
4:50 PM	33.424962	7477.62013	45.94818	35.031272	23.562112	24.313056
4:55 PM	32.273476	7220.017	44.528536	35.832552	23.454342	24.21857
5:00 PM	29.434468	6584.89217	38.6924	36.083452	23.453356	24.191318

21-Jul						
Time	T _{outside} (°C)	Radiation (W/m ²)	T _{PV w/o HE} (°C)	T _{PV with HE} (°C)	T _{water HE In} (°C)	T _{water HE Out} (°C)
8:00AM	18.84759	4216.46309	21.045456	18.973764	19.525558	19.738326
8:05AM	19.329934	4324.37002	21.788284	19.6165	19.577434	19.73388
8:10AM	19.286236	4314.59418	21.974682	19.729256	19.59462	19.7467
8:15AM	19.6888	4404.65324	22.845078	20.101354	19.623758	19.780194
8:20AM	19.327122	4323.74094	23.116868	20.351536	19.626774	19.78321
8:25AM	19.318296	4321.76644	22.29304	20.537918	19.652842	19.839422
8:30AM	18.586486	4158.05056	22.170376	20.597394	19.59953	19.807924
8:35AM	18.63649	4169.23714	22.675518	20.960502	19.623134	19.80555
8:40AM	19.489378	4360.03982	22.693622	20.782924	19.676172	19.810798
8:45AM	19.138376	4281.51588	22.408572	21.131774	19.663936	19.850706
8:50AM	19.153352	4284.86622	22.596832	20.715932	19.705074	19.874396
8:55AM	19.338872	4326.36957	22.23995	20.77998	19.738452	19.899238
9:00AM	18.488384	4136.1038	21.829672	20.99074	19.753524	19.896862
9:05AM	18.448018	4127.07338	21.77634	20.94173	19.743722	19.926116
9:10AM	19.029828	4257.23221	21.944456	20.99251	19.777292	19.942242
9:15AM	18.80148	4206.14765	22.007206	20.70766	19.822698	19.931148
9:20AM	19.181694	4291.20671	22.44724	20.909638	19.815884	19.976658
9:25AM	20.733356	4638.33468	23.870122	21.033448	19.796462	19.978662
9:30AM	22.971448	5139.0264	26.865748	21.113626	19.837278	19.99786
9:35AM	22.266332	4981.28233	28.913	22.240216	19.812856	19.977612
9:40AM	22.934652	5130.79463	31.338626	22.86977	19.74825	19.982784

9:45AM	22.29662	4988.05817	31.830518	23.968884	19.860452	20.034114
9:50AM	22.347894	4999.52886	29.910186	24.893166	19.881678	20.115996
9:55AM	21.433052	4794.86622	27.660136	24.985594	19.935404	20.165354
10:00AM	20.811312	4655.7745	26.511562	24.963612	19.986896	20.229916
10:05AM	20.832478	4660.50962	25.951126	24.23283	20.025516	20.229672
10:10AM	22.13967	4952.94631	26.597158	23.856174	20.04695	20.320282
10:15AM	22.933688	5130.57897	28.091442	24.02504	20.08134	20.294206
10:20AM	22.580866	5051.64787	28.740546	23.9587	20.045324	20.30577
10:25AM	22.458762	5024.33154	29.333926	24.55955	20.070856	20.348734
10:30AM	23.146814	5178.25817	30.234706	24.9944	20.134198	20.381736
10:35AM	23.176346	5184.86488	30.46175	25.291656	20.172704	20.398444
10:40AM	22.9091	5125.0783	30.995386	25.612612	20.187116	20.443366
10:45AM	23.52786	5263.50336	30.947048	25.857402	20.177618	20.455282
10:50AM	22.667994	5071.1396	30.37101	25.955468	20.189106	20.466958
10:55AM	24.988332	5590.23087	32.311908	26.269874	20.24961	20.514374
11:00AM	25.60114	5727.32438	32.662582	26.351476	20.314344	20.56166
11:05AM	23.087472	5164.98255	31.80707	26.993116	20.335724	20.622074
11:10AM	24.50434	5481.95526	31.109576	26.727094	20.33637	20.675018
11:15AM	24.399162	5458.4255	31.121476	26.587952	20.312932	20.647224
11:20AM	24.208544	5415.78166	31.207038	26.8462	20.386508	20.673032
11:25AM	24.766118	5540.51857	31.734008	26.665176	20.416486	20.694478
11:30AM	26.516192	5932.034	33.425392	26.81779	20.431302	20.73506
11:35AM	25.039908	5601.76913	33.779496	27.24384	20.474214	20.791226
11:40AM	25.230176	5644.33468	33.72896	27.89781	20.53061	20.847606
11:45AM	25.9616	5807.96421	34.962856	27.8267	20.532434	20.910056
11:50AM	24.81765	5552.04698	33.356086	28.403226	20.528456	20.875956
11:55AM	25.75048	5760.73378	32.830262	28.299882	20.545394	20.914488
12:00PM	24.647018	5513.87427	33.4915	27.984926	20.578614	20.95622
12:05PM	25.68488	5746.05817	33.889432	28.071818	20.613886	20.991488
12:10PM	25.305574	5661.20224	33.057446	28.339118	20.662364	21.044306
12:15PM	25.409838	5684.52752	32.099904	28.215202	20.754112	21.07958
12:20PM	26.158448	5852.00179	33.564572	28.092412	20.803422	21.159184
12:25PM	25.951978	5805.81163	35.40752	27.921114	20.747504	21.177154
12:30PM	26.46524	5920.63535	35.36072	28.449608	20.725192	21.128896
12:35PM	25.820448	5776.38658	35.512632	28.920772	20.83202	21.174896
12:40PM	27.773806	6213.37942	37.008236	29.161804	20.828086	21.236116
12:45PM	28.119622	6290.74318	42.076964	29.634096	20.868672	21.289568
12:50PM	28.459538	6366.78702	43.759288	30.81696	20.833698	21.289646
12:55PM	30.16613	6748.57494	45.798076	32.235202	20.914276	21.344058
1:00 PM	33.399746	7471.97897	46.748888	33.386798	20.931404	21.421972
1:05 PM	34.422796	7700.84922	51.664304	34.717316	21.063494	21.51917

1:10 PM	33.17138	7420.89038	53.582972	36.523028	21.171422	21.631606
1:15 PM	32.282634	7222.06577	48.718332	37.547484	21.185832	21.798042
1:20 PM	34.926988	7813.64385	54.330336	37.992712	21.34337	21.912158
1:25 PM	34.638052	7749.00492	54.673508	38.797848	21.300096	21.912068
1:30 PM	37.139372	8308.58434	56.728928	39.827396	21.426804	22.060482
1:35 PM	35.956924	8044.05459	57.045012	40.806664	21.472818	22.16742
1:40 PM	39.13812	8755.73154	57.892708	41.58854	21.639114	22.359744
1:45 PM	35.040504	7839.03893	58.273064	42.072824	21.639666	22.360294
1:50 PM	34.61062	7742.86801	58.371224	42.607336	21.726472	22.490386
1:55 PM	36.559732	8178.91096	58.833476	43.055872	21.838368	22.619622
2:00 PM	34.420256	7700.28098	53.925456	43.302908	21.921776	22.694278
2:05 PM	35.322428	7902.10917	55.487328	42.346316	22.004206	22.807116
2:10 PM	35.787404	8006.13065	56.42654	42.198932	22.128772	22.944848
2:15 PM	33.654476	7528.96555	58.220264	42.368576	22.210034	23.043458
2:20 PM	38.50284	8613.61074	58.623376	42.7036	22.226918	23.03404
2:25 PM	35.936028	8039.37987	54.611784	43.095864	22.241878	23.140344
2:30 PM	33.46733	7487.09843	53.19472	42.587968	22.361152	23.263888
2:35 PM	38.9355	8710.40268	56.417488	42.018128	22.495692	23.350682
2:40 PM	35.703684	7987.40134	57.250688	42.220376	22.527896	23.460958
2:45 PM	35.725116	7992.19597	57.310616	42.546716	22.539892	23.451392
2:50 PM	36.483052	8161.7566	56.601808	42.871364	22.632936	23.522626
2:55 PM	37.696384	8433.19553	57.14608	42.858468	22.704974	23.63394
3:00 PM	37.47044	8382.64877	57.65664	42.89236	22.807878	23.71938
3:05 PM	31.814694	7117.38121	48.253208	43.153228	22.92681	23.833882
3:10 PM	34.724652	7768.37852	51.187944	41.392324	23.01807	23.890302
3:15 PM	35.008588	7831.89888	52.287688	40.935912	22.919318	23.804656
3:20 PM	34.975164	7824.42148	53.047616	40.73306	23.006448	23.852602
3:25 PM	35.911404	8033.87114	52.39844	40.890224	23.027524	23.926022
3:30 PM	34.857408	7798.07785	53.247464	40.569928	23.05103	23.971436
3:35 PM	34.778212	7780.36063	53.35894	40.767796	23.100674	24.016508
3:40 PM	32.988118	7379.89217	47.918148	41.068036	23.220478	24.092762
3:45 PM	33.04919	7393.55481	53.214644	41.553356	26.986078	26.986078
3:50 PM	31.500174	7047.01879	47.280236	39.667472	26.661312	26.830116
3:55 PM	32.697368	7314.84743	46.81106	38.249556	25.701236	26.393414
4:00 PM	35.630832	7971.10336	51.243264	37.892016	26.445214	26.42786

22-Jul						
Time	T _{outside} (°C)	Radiation	T _{PV w/o HE} (°C)	T _{PV with HE} (°C)	T _{water HE In} (°C)	T _{water HE Out} (°C)

	(W/m ²)					
8:00AM	20.053586	4486.26085	24.065028	20.423574	18.725166	18.968608
8:05AM	19.835368	4437.44251	25.25457	20.635054	18.7671	19.023434
8:10AM	20.780046	4648.77987	25.55386	20.988632	18.877384	19.068628
8:15AM	20.62327	4613.70694	25.816532	21.444636	18.85966	19.059442
8:20AM	21.899014	4899.10828	25.991828	21.61673	18.866836	19.075346
8:25AM	21.658408	4845.28143	26.799302	21.98403	18.978236	19.15201
8:30AM	23.400158	5234.93468	29.451344	22.178646	18.990792	19.19928
8:35AM	23.779292	5319.75213	31.57574	22.675248	19.03658	19.262512
8:40AM	26.949546	6028.98121	33.809552	23.37794	19.037558	19.28094
8:45AM	28.579878	6393.70872	35.610936	24.50782	19.173364	19.360202
8:50AM	27.426496	6135.68143	37.065364	25.494186	19.166876	19.432046
8:55AM	27.39319	6128.23043	37.207244	26.63666	19.241104	19.519346
9:00AM	27.190732	6082.93781	37.232708	27.43581	19.353032	19.604892
9:05AM	31.79079	7112.03356	38.670452	28.041962	19.380974	19.706782
9:10AM	28.650274	6409.45727	39.358388	28.404666	19.385574	19.724654
9:15AM	29.59438	6620.66667	40.283496	28.966602	19.478482	19.813178
9:20AM	31.629954	7076.05235	40.869756	29.63952	19.580294	19.919322
9:25AM	31.115776	6961.02371	41.34316	30.068908	19.596618	19.970336
9:30AM	35.424776	7925.00582	42.473996	30.533246	19.618556	20.066206
9:35AM	32.445976	7258.60761	43.241492	30.929698	19.663208	20.128092
9:40AM	34.070948	7622.13602	44.11302	31.484754	19.799174	20.207714
9:45AM	30.713368	6870.99955	44.826684	31.990976	19.838296	20.329272
9:50AM	31.617636	7073.29664	45.832192	32.503846	19.875612	20.392918
9:55AM	30.040684	6720.51096	45.928368	33.178078	19.969006	20.455762
10:00AM	31.731968	7098.87427	45.942472	33.588808	20.107752	20.598818
10:05AM	33.089538	7402.58121	45.767676	33.704628	20.098722	20.672408
10:10AM	31.981444	7154.68546	46.42046	33.940152	20.193988	20.745846
10:15AM	31.83603	7122.15436	48.128488	34.290836	20.332344	20.888688
10:20AM	34.529404	7724.69888	48.121696	34.542148	20.378472	20.89122
10:25AM	33.906868	7585.42908	49.344272	34.994676	20.482178	21.00796
10:30AM	35.870152	8024.64251	50.516192	35.46574	20.47479	21.091876
10:35AM	37.881984	8474.71678	51.044032	35.932264	20.575918	21.19315
10:40AM	35.03596	7838.02237	52.375516	36.457948	20.625112	21.27679
10:45AM	35.560372	7955.34049	52.084664	37.087676	20.711108	21.336796
10:50AM	35.074288	7846.59687	53.482468	37.794876	20.83553	21.522132
10:55AM	38.968904	8717.87562	53.567072	38.271456	20.99486	21.61625
11:00AM	38.249916	8557.02819	54.911212	38.585984	20.966966	21.61431
11:05AM	35.117256	7856.2094	51.177724	39.084592	21.05382	21.753186
11:10AM	36.638908	8196.62371	50.128276	39.323124	21.157424	21.891566
11:15AM	31.010834	6937.54676	45.89432	39.052888	21.23628	21.970758

11:20AM	40.412484	9040.82416	51.501096	38.419504	21.379546	22.070032
11:25AM	38.535676	8620.9566	55.371944	38.10126	21.405978	22.153232
11:30AM	41.107992	9196.41879	53.957968	38.742792	21.36418	22.12452
11:35AM	34.28358	7669.7047	49.00728	39.254888	21.477616	22.216312
11:40AM	33.160072	7418.36063	44.070008	39.142616	21.570776	22.309422
11:45AM	32.666058	7307.84295	45.972652	37.81042	21.604342	22.36908
11:50AM	31.124928	6963.07114	41.347944	37.056472	21.728238	22.423462
11:55AM	31.608828	7071.32617	39.299416	36.036092	21.777236	22.494004
12:00PM	34.04832	7617.07383	46.890064	34.890692	21.805834	22.53129
12:05PM	34.008968	7608.27025	47.285144	34.826064	21.861336	22.5563
12:10PM	35.592036	7962.42416	48.765264	35.626128	21.922826	22.591838
12:15PM	38.856392	8692.70515	48.690264	36.022528	21.886762	22.53403
12:20PM	36.372516	8137.02819	48.653416	36.402464	21.89552	22.612222
12:25PM	33.34341	7459.37584	45.173192	36.770408	21.935408	22.665332
12:30PM	36.50044	8165.64653	45.533764	36.696412	22.011624	22.732804
12:35PM	35.578612	7959.42103	45.399044	36.167432	22.071672	22.736256
12:40PM	36.137992	8084.56197	47.369592	36.159336	22.136746	22.8274
12:45PM	34.165104	7643.2	47.295456	36.083988	22.17244	22.854376
12:50PM	33.898396	7583.53378	47.543212	36.590772	22.197032	22.922462
12:55PM	33.399276	7471.87383	46.046676	36.71664	22.242362	22.99822
1:00 PM	34.69504	7761.75391	46.183976	36.748832	22.214538	22.887942
1:05 PM	33.614268	7519.97047	46.616732	36.436036	22.212432	22.946556
1:10 PM	32.571708	7286.73557	44.762	36.692316	22.281926	22.994448
1:15 PM	31.230628	6986.71767	42.642664	36.393432	22.307142	23.03705
1:20 PM	30.219868	6760.59687	40.283948	36.042092	22.374984	23.109016
1:25 PM	30.843588	6900.13154	38.10432	35.141748	22.440956	23.105352
1:30 PM	28.40439	6354.44966	37.471612	34.17982	22.407198	23.132514
1:35 PM	32.120212	7185.72975	37.575768	33.225856	22.461478	23.091062
1:40 PM	30.427016	6806.9387	39.647036	32.47971	22.410432	23.140092
1:45 PM	31.384386	7021.11544	40.386904	32.380996	22.44512	23.070552
1:50 PM	30.74574	6878.24161	41.2327	32.566632	22.42877	23.084472
1:55 PM	30.05832	6724.45638	40.256	32.622586	22.420064	23.093172
2:00 PM	31.049454	6946.18658	40.713832	32.776054	22.479568	23.087584
2:05 PM	31.174724	6974.21119	42.414548	32.918614	22.471702	23.127574
2:10 PM	31.443454	7034.32975	42.886956	33.110226	22.48321	23.134726
2:15 PM	32.015358	7162.27248	43.243948	33.660944	22.567206	23.144922
2:20 PM	32.544422	7280.63132	44.168328	33.896384	22.52749	23.196192
2:25 PM	32.445942	7258.6	43.780784	34.321068	22.545188	23.20972
2:30 PM	31.942388	7145.9481	43.687884	34.633212	22.579414	23.25679
2:35 PM	32.717788	7319.41566	44.288784	34.784476	22.602488	23.301598
2:40 PM	35.345236	7907.21163	45.855936	35.003264	22.663664	23.336646

2:45 PM	32.015622	7162.33154	46.212032	35.177088	22.709554	23.321816
2:50 PM	34.76238	7776.81879	47.824096	35.626204	22.713948	23.395788
2:55 PM	32.77499	7332.21253	48.448932	36.320516	22.764002	23.432582
3:00 PM	34.354536	7685.57852	48.311872	36.641164	22.67734	23.37641
3:05 PM	33.524384	7499.86219	47.3083	36.928444	22.687182	23.429736
3:10 PM	33.414952	7475.38076	46.267668	37.34002	22.763002	23.470912
3:15 PM	35.720236	7991.10425	48.225532	37.239124	22.824994	23.523984
3:20 PM	35.266208	7889.53199	52.419464	37.302252	22.871422	23.579084
3:25 PM	35.584812	7960.80805	53.530264	37.862528	22.899342	23.680908
3:30 PM	35.760384	8000.08591	54.192652	38.853824	22.938368	23.724452
3:35 PM	36.510332	8167.85951	54.858728	39.63764	22.96205	23.800102
3:40 PM	35.703364	7987.32975	54.68868	40.1864	23.070502	23.895444
3:45 PM	36.100948	8076.27472	49.77384	40.696972	23.14425	23.960262
3:50 PM	35.557336	7954.6613	52.036916	40.394392	23.221312	23.972068
3:55 PM	36.611892	8190.57987	53.04592	40.112708	23.3111	24.092424
4:00 PM	36.83764	8241.08277	53.641868	40.116848	23.244756	24.004574
4:05 PM	37.5543	8401.4094	53.034968	40.64062	23.287974	24.074036
4:10 PM	34.291956	7671.57852	49.73658	40.737624	23.351686	24.15075
4:15 PM	34.040236	7615.26532	49.054244	40.675448	23.422546	24.190766
4:20 PM	32.67501	7309.84564	44.911192	40.085068	23.461408	24.264562
4:25 PM	35.097516	7851.79329	49.708496	39.005132	23.485634	24.327508
4:30 PM	36.99362	8275.97763	51.72946	38.621084	23.531324	24.312706
4:35 PM	32.972886	7376.48456	49.58708	38.99684	23.57575	24.3743
4:40 PM	32.562858	7284.7557	44.308096	39.512552	23.607306	24.392988
4:45 PM	33.83908	7570.26398	47.304496	38.608788	23.630434	24.433484
4:50 PM	35.596028	7963.31723	48.14464	38.037892	23.659898	24.480126
4:55 PM	33.698504	7538.81521	47.9296	38.127024	23.689724	24.514466
5:00 PM	34.104392	7629.6179	48.28406	37.948832	23.724684	24.514638

23-Jul						
Time	T _{outside} (°C)	Radiation (W/m ²)	T _{PV w/o HE} (°C)	T _{PV with HE} (°C)	T _{water HE In} (°C)	T _{water HE Out} (°C)
8:00AM	26.789958	5993.27919	27.720934	21.932064	18.43503	18.704712
8:05AM	25.659784	5740.44385	28.119686	22.177586	18.498824	18.772666
8:10AM	26.176042	5855.93781	28.450578	22.64073	18.567812	18.82855
8:15AM	25.009404	5594.94497	28.950176	22.948492	18.57234	18.86799
8:20AM	24.878556	5565.67248	28.015598	23.280452	18.627414	18.927226
8:25AM	28.346456	6341.48904	30.000274	23.673578	18.718158	18.983228
8:30AM	28.504362	6376.81477	31.489318	23.922588	18.803226	19.063916
8:35AM	29.10332	6510.80984	32.601834	24.351908	18.843782	19.0872
8:40AM	28.748226	6431.37047	33.107388	25.018	18.906036	19.162344

8:45AM	28.631772	6405.31812	33.6997	25.534914	18.92266	19.265842
8:50AM	29.593866	6620.55168	34.590368	26.09026	19.065024	19.33894
8:55AM	30.5944	6844.38479	34.856088	26.62013	19.082586	19.369394
9:00AM	30.576938	6840.4783	35.239728	27.114254	19.125292	19.442438
9:05AM	29.71165	6646.90157	36.187712	27.25777	19.200262	19.487048
9:10AM	28.545014	6385.90917	37.568612	27.76541	19.241634	19.558942
9:15AM	31.192504	6978.18881	37.724564	28.05652	19.265702	19.634964
9:20AM	27.567644	6167.25817	39.572564	28.632722	19.347036	19.703382
9:25AM	34.753352	7774.79911	41.293512	29.235774	19.403516	19.738232
9:30AM	32.978844	7377.81745	41.861752	29.942758	19.457696	19.844348
9:35AM	30.702694	6868.61163	41.993784	30.942984	19.583496	19.96575
9:40AM	31.083536	6953.81119	39.455372	31.2294	19.625534	20.0819
9:45AM	28.56414	6390.18792	37.702436	31.373624	19.649688	20.053916
9:50AM	29.563312	6613.71633	39.053492	30.933048	19.70679	20.080474
9:55AM	30.188386	6753.55391	41.179432	30.986468	19.782094	20.207886
10:00AM	30.490632	6821.17047	41.734356	31.026878	19.796498	20.235174
10:05AM	33.946608	7594.31946	46.068512	31.775626	19.885634	20.324472
10:10AM	37.40666	8368.38031	49.12246	32.469696	19.955074	20.43293
10:15AM	35.602504	7964.766	50.335864	33.693972	19.990704	20.438224
10:20AM	37.569572	8404.82595	51.493	34.954592	20.105592	20.54019
10:25AM	35.728064	7992.85548	51.129664	36.162164	20.216156	20.71135
10:30AM	34.763744	7777.12394	50.06046	36.875812	20.273108	20.881386
10:35AM	33.000138	7382.58121	46.550864	37.127056	20.29788	20.893076
10:40AM	33.41845	7476.16331	45.681384	36.977548	20.391884	21.000104
10:45AM	34.101292	7628.92438	45.235284	36.418324	20.516408	21.102982
10:50AM	32.99931	7382.39597	46.611708	35.94284	20.65503	21.17203
10:55AM	34.41126	7698.26846	47.181436	35.796292	20.66933	21.195038
11:00AM	34.985532	7826.74094	48.00658	35.824488	20.666786	21.296664
11:05AM	35.491756	7939.99016	47.524476	36.160192	20.79973	21.38201
11:10AM	33.124814	7410.47293	44.532556	36.269152	20.857886	21.487672
11:15AM	30.347884	6789.23579	42.21916	36.12852	20.89178	21.486708
11:20AM	31.739398	7100.53647	42.349848	35.404112	20.925182	21.541872
11:25AM	37.323704	8349.82192	47.784784	34.649744	20.981192	21.584978
11:30AM	37.316352	8348.17718	51.776244	35.068964	21.077362	21.68546
11:35AM	37.401368	8367.19642	53.14572	36.062068	21.185038	21.736854
11:40AM	33.361844	7463.49978	56.157064	37.710548	21.233916	21.8639
11:45AM	39.424152	8819.72081	56.153572	39.105304	21.336196	22.00929
11:50AM	41.108224	9196.47069	56.507028	40.120784	21.257226	21.982604
11:55AM	37.190508	8320.02416	53.792712	40.527412	21.320622	22.072088
12:00PM	38.347204	8578.79284	54.089108	41.23898	21.483926	22.230946
12:05PM	33.646704	7527.22685	52.820564	41.10098	21.627658	22.348484

12:10PM	35.652544	7975.96063	49.758044	40.802528	21.637146	22.336392
12:15PM	31.538694	7055.63624	50.980228	40.456348	21.689912	22.463118
12:20PM	36.43964	8152.04474	51.737428	39.617164	21.747014	22.515832
12:25PM	35.288652	7894.55302	57.707024	39.549436	21.82034	22.615036
12:30PM	38.435308	8598.50291	57.196956	40.272804	21.946536	22.680428
12:35PM	36.043828	8063.4962	60.665052	41.324092	22.05727	22.812856
12:40PM	40.512832	9063.27338	57.818344	41.979456	21.967578	22.81875
12:45PM	37.74546	8444.1745	55.565052	42.893192	22.101212	22.882878
12:50PM	39.26726	8784.62192	60.800664	43.269452	22.147654	23.029164
12:55PM	34.901296	7807.8962	53.50166	43.459872	22.259464	23.136548
1:00 PM	32.567368	7285.76465	50.758204	42.972112	22.364982	23.241996
1:05 PM	36.23874	8107.10067	49.447924	42.027872	22.375782	23.179222
1:10 PM	33.483242	7490.65817	46.716388	40.946292	22.418074	23.221488
1:15 PM	33.663464	7530.97629	44.427748	39.582232	22.456788	23.286274
1:20 PM	34.28516	7670.05817	43.453624	38.469276	22.539418	23.294914
1:25 PM	34.622636	7745.55615	44.870552	37.226876	22.525408	23.324408
1:30 PM	34.796432	7784.43669	46.232256	36.939892	22.59299	23.33125
1:35 PM	37.417452	8370.79463	46.136324	36.735824	22.584392	23.37485
1:40 PM	33.776628	7556.29262	44.962332	36.739532	22.657202	23.404124
1:45 PM	35.662416	7978.16913	48.33038	36.707948	22.711544	23.467134
1:50 PM	33.832772	7568.8528	52.650688	36.859736	22.726692	23.495318
1:55 PM	36.374668	8137.50962	51.851712	37.904192	22.666806	23.426768
2:00 PM	36.432416	8150.42864	53.698752	38.943504	22.68165	23.459
2:05 PM	33.619524	7521.14631	54.614812	39.927248	22.739798	23.564948
2:10 PM	38.173516	8539.93647	54.90794	40.676724	22.831486	23.599862
2:15 PM	36.148492	8086.91096	53.042728	41.202492	22.873386	23.720004
2:20 PM	36.420932	8147.85951	51.742056	41.31218	22.92411	23.749142
2:25 PM	36.103068	8076.74899	51.172672	41.182984	23.008516	23.88113
2:30 PM	37.119212	8304.07427	51.662548	41.018076	23.086606	23.915698
2:35 PM	37.108956	8301.77987	50.59114	40.748544	23.149622	23.918
2:40 PM	36.089312	8073.67159	48.2381	40.302652	23.057988	23.930944
2:45 PM	34.874992	7802.01163	46.439024	39.877808	23.097526	23.905062
2:50 PM	32.29145	7224.03803	45.003492	39.164712	23.16194	23.943538
2:55 PM	33.558844	7507.57136	43.826976	38.268648	23.158124	23.961462
3:00 PM	36.49232	8163.82998	45.241472	37.511552	23.184806	24.009678
3:05 PM	34.18362	7647.34228	44.741588	36.916564	23.177762	24.028718
3:10 PM	33.89678	7583.17226	43.7714	36.840512	23.252002	24.029204
3:15 PM	33.505996	7495.74855	43.653	36.814852	23.269386	24.055272
3:20 PM	34.368068	7688.60582	43.796732	36.400664	23.225542	24.063426
3:25 PM	33.927332	7590.00716	43.6623	36.401564	23.32214	24.073028
3:30 PM	33.458118	7485.03758	42.573604	36.225176	23.29904	24.071866

3:35 PM	32.969346	7375.69262	43.23194	36.086164	23.292342	24.08256
3:40 PM	36.110748	8078.46711	43.086748	35.772912	23.31717	24.068252
3:45 PM	33.785076	7558.18255	44.515232	35.712956	23.303914	24.102628
3:50 PM	34.354532	7685.57763	45.235368	35.869972	23.307004	24.071132
3:55 PM	32.584484	7289.59374	48.212328	36.214972	23.32296	24.087078
4:00 PM	33.338916	7458.37047	45.786788	36.86474	23.358368	24.105082
4:05 PM	32.42432	7253.76286	44.190916	37.246216	23.321076	24.141702
4:10 PM	30.32254	6783.566	42.560944	37.112728	23.345758	24.174874
4:15 PM	33.397216	7471.41298	44.52522	36.581508	23.365306	24.172676
4:20 PM	32.148406	7192.03714	44.337316	36.335896	23.440932	24.161706
4:25 PM	35.812048	8011.64385	48.876048	36.452984	23.421162	24.23719
4:30 PM	34.763048	7776.96823	48.9473	36.930876	23.472848	24.219306
4:35 PM	36.429852	8149.85503	51.581808	37.671328	23.449224	24.286966
4:40 PM	36.15466	8088.29083	52.011096	38.589296	23.48631	24.337064
4:45 PM	36.649572	8199.0094	51.584736	39.434624	23.554886	24.38387
4:50 PM	36.770668	8226.10022	53.176792	40.123596	23.629756	24.406544
4:55 PM	36.182588	8094.5387	52.01058	40.587452	23.652526	24.51621
5:00 PM	33.363166	7463.79553	47.565872	40.649296	23.553734	24.461128

24-Jul						
Time	T _{outside} (°C)	Radiation (W/m ²)	T _{PV} w/o HE (°C)	T _{PV} with HE (°C)	T _{water} HE In (°C)	T _{water} HE Out (°C)
8:00AM	16.467296	3683.95884	20.518264	18.993966	19.41091	19.576096
8:05AM	17.390762	3890.55078	22.297234	19.448628	19.422454	19.600726
8:10AM	17.049864	3814.28725	22.17111	19.456894	19.435084	19.643692
8:15AM	17.467992	3907.82819	22.396318	20.085834	19.491222	19.66057
8:20AM	18.393478	4114.87204	25.31713	20.031462	19.393582	19.5802
8:25AM	18.096918	4048.52752	25.88566	20.308732	19.423316	19.62301
8:30AM	17.91661	4008.19016	24.974598	21.128652	19.478188	19.65645
8:35AM	18.213562	4074.62237	25.285822	21.272618	19.51367	19.722076
8:40AM	19.171906	4289.017	27.126076	21.473954	19.563002	19.741062
8:45AM	19.791282	4427.57987	29.127488	21.81512	19.595782	19.7435
8:50AM	19.772048	4423.27696	29.216262	22.529326	19.637418	19.780772
8:55AM	20.07623	4491.32662	31.284674	23.032426	19.650772	19.846076
9:00AM	19.855232	4441.88635	30.989804	23.673518	19.7117	19.928986
9:05AM	20.290314	4539.22013	32.065822	24.224126	19.765006	19.921424
9:10AM	19.999814	4474.23132	31.848192	24.725648	19.81724	19.995454
9:15AM	20.566206	4600.94094	33.30809	25.08229	19.845732	20.071526
9:20AM	21.537436	4818.21834	34.849916	25.42674	19.922936	20.113838
9:25AM	21.716444	4858.26488	36.888944	25.91533	19.923584	20.132114
9:30AM	21.65125	4843.68009	36.766116	26.867612	19.962576	20.197072

9:35AM	21.845314	4887.09485	35.555612	27.628158	20.035566	20.296012
9:40AM	22.880178	5118.60805	35.843424	27.853668	20.062976	20.36701
9:45AM	22.663834	5070.20895	38.054388	28.1426	20.098314	20.402338
9:50AM	23.137074	5176.07919	35.914628	28.379926	20.17694	20.50255
9:55AM	24.38005	5454.14989	32.892064	28.444408	20.18098	20.545818
10:00AM	23.559888	5270.66846	33.023396	28.142366	20.244416	20.617948
10:05AM	25.488268	5702.07338	35.622636	27.78907	20.325544	20.651308
10:10AM	24.343046	5445.87159	34.879224	27.643658	20.378128	20.72112
10:15AM	24.795606	5547.11544	36.663136	27.865762	20.328378	20.736566
10:20AM	24.576464	5498.09038	34.897484	28.202828	20.408156	20.772928
10:25AM	24.101918	5391.92796	34.038336	28.316342	20.444456	20.848252
10:30AM	21.294512	4763.87293	29.616424	27.86489	20.556624	20.869256
10:35AM	25.545438	5714.86309	37.097076	27.162842	20.586472	20.8991
10:40AM	27.44989	6140.91499	39.522016	27.320756	20.567446	20.958132
10:45AM	27.535206	6160.00134	40.817332	28.67885	20.59201	20.987232
10:50AM	26.98533	6036.98658	42.259452	29.33507	20.65423	21.005866
10:55AM	26.511538	5930.99284	39.312632	30.561558	20.715038	21.114582
11:00AM	28.393532	6352.02058	43.512376	30.819512	20.736802	21.201306
11:05AM	29.333338	6562.26801	46.856008	31.38532	20.817898	21.278206
11:10AM	28.012628	6266.80716	44.895624	32.13443	20.776622	21.284862
11:15AM	28.398904	6353.22237	43.937792	33.182506	20.897184	21.357464
11:20AM	29.676572	6639.05414	45.728208	33.043854	20.998762	21.445944
11:25AM	25.908412	5796.06532	38.957416	33.32534	21.014658	21.548748
11:30AM	28.137902	6294.83266	41.49236	33.077694	21.04069	21.57477
11:35AM	28.578182	6393.32931	42.389724	32.411094	21.141514	21.61042
11:40AM	27.03856	6048.89485	41.294036	32.31498	21.165228	21.690734
11:45AM	25.782014	5767.78837	40.363556	32.576634	21.221748	21.764274
11:50AM	23.903204	5347.47293	33.635348	32.470906	21.318324	21.843582
11:55AM	23.92641	5352.66443	30.380912	31.33112	21.359	21.879886
12:00PM	24.74569	5535.94855	31.820406	29.537456	21.371664	21.888194
12:05PM	23.247844	5200.85996	29.106966	28.42753	21.383406	21.88687
12:10PM	23.255344	5202.53781	28.63258	27.474568	21.321604	21.803316
12:15PM	22.592742	5054.3047	27.341118	26.87954	21.360816	21.773228
12:20PM	22.641878	5065.29709	24.974506	26.159832	21.32743	21.752916
12:25PM	27.20241	6085.55034	34.701768	25.093778	21.316744	21.733524
12:30PM	23.361278	5226.23669	31.205708	25.619762	21.301564	21.722702
12:35PM	22.673572	5072.38747	27.257456	26.42897	21.263516	21.702084
12:40PM	24.771566	5541.73736	29.639832	26.18635	21.340982	21.666684
12:45PM	26.951492	6029.41655	36.51134	25.794066	21.316038	21.66352
12:50PM	29.893902	6687.67383	45.464832	26.316766	21.307126	21.645898
12:55PM	32.20335	7204.32886	48.36394	28.84236	21.26838	21.728718

1:00 PM	27.651376	6185.99016	43.104084	31.35021	21.338844	21.777388
1:05 PM	27.66113	6188.17226	42.587148	32.929954	21.387466	21.869346
1:10 PM	30.758424	6881.07919	46.50114	33.426948	21.508882	21.93885
1:15 PM	30.322324	6783.51767	48.43274	33.72676	21.500178	22.042776
1:20 PM	31.293622	7000.81029	49.879308	34.6477	21.588788	22.092364
1:25 PM	32.8582	7350.82774	51.059908	35.6745	21.64722	22.198654
1:30 PM	29.937372	6697.39866	48.441016	36.34398	21.729598	22.315628
1:35 PM	30.104504	6734.78837	47.279488	36.761092	21.737426	22.280118
1:40 PM	31.176928	6974.70425	47.697628	36.507684	21.768878	22.398228
1:45 PM	31.311466	7004.80224	51.588948	36.364624	21.8741	22.438496
1:50 PM	31.098362	6957.12796	50.718912	36.701416	21.899698	22.546392
1:55 PM	32.343514	7235.68546	49.044996	37.026316	21.961252	22.625326
2:00 PM	29.600936	6622.13333	46.483632	37.446764	22.063918	22.740988
2:05 PM	29.664204	6636.28725	43.29082	36.769676	22.06225	22.717758
2:10 PM	28.24654	6319.13647	43.29374	35.600888	22.060298	22.737564
2:15 PM	30.538882	6831.96465	46.617676	34.973564	22.129742	22.802618
2:20 PM	29.527692	6605.74765	44.427364	34.771144	22.149246	22.85692
2:25 PM	31.186396	6976.82237	47.064244	34.802444	22.21132	22.914422
2:30 PM	29.66895	6637.34899	48.512124	35.292052	22.330662	22.93383
2:35 PM	31.528682	7053.39642	47.783652	35.929256	22.339874	23.030234
2:40 PM	28.125408	6292.03758	40.8259	36.64686	22.4409	23.061608
2:45 PM	30.153392	6745.72528	42.92656	35.935836	22.489014	23.096648
2:50 PM	31.84818	7124.87248	49.47362	34.8858	22.493612	23.166302
2:55 PM	27.252468	6096.74899	41.84788	35.153728	22.430728	23.11234
3:00 PM	31.687862	7089.00716	45.45932	35.14474	22.443224	23.120292
3:05 PM	29.710258	6646.59016	46.639624	34.620456	22.461714	23.13896
3:10 PM	30.200774	6756.32528	47.51998	35.526744	22.535542	23.199702
3:15 PM	30.826846	6896.38613	45.806492	35.7993	22.590806	23.22014
3:20 PM	31.800678	7114.24564	47.957424	36.341496	22.673392	23.27659
3:25 PM	29.427	6583.22148	44.00704	36.377092	22.661306	23.355658
3:30 PM	28.24755	6319.36242	38.676284	36.284688	22.723256	23.404716
3:35 PM	30.89062	6910.65324	44.47342	35.200988	22.72801	23.439724
3:40 PM	28.838062	6451.46801	43.781604	34.798272	22.80938	23.447308
3:45 PM	27.362036	6121.26085	37.065376	34.70452	22.839812	23.49947
3:50 PM	29.967236	6704.07964	42.329196	33.960364	22.81906	23.517864
3:55 PM	30.136824	6742.01879	44.038364	33.280736	22.760122	23.376518
4:00 PM	27.641318	6183.74004	38.875052	33.44772	22.751206	23.406558
4:05 PM	26.20819	5863.12975	34.145424	33.442356	22.797824	23.401156
4:10 PM	26.195632	5860.32036	31.715606	32.244586	22.798098	23.371176
4:15 PM	25.910232	5796.47248	31.643192	30.8237	22.785914	23.34141
4:20 PM	26.050604	5827.87562	33.461846	29.86255	22.761476	23.299772

4:25 PM	27.705884	6198.18434	34.693876	29.310068	22.712156	23.302288
4:30 PM	26.879636	6013.34139	35.829968	29.442832	22.681004	23.284578
4:35 PM	25.50474	5705.75839	33.015754	29.733646	22.744438	23.2349
4:40 PM	23.778802	5319.64251	28.930406	29.576268	22.789592	23.340736
4:45 PM	18.929162	4234.71186	24.641346	28.551774	22.777564	23.254962
4:50 PM	19.716368	4410.82058	24.38597	27.416558	22.72124	23.246506
4:55 PM	20.31489	4544.71812	27.736448	25.481808	22.673596	23.18148
5:00 PM	21.823348	4882.18076	28.190822	24.283658	22.64472	23.061454

25-Jul						
Time	T _{outside} (°C)	Radiation (W/m ²)	T _{PV} w/o HE (°C)	T _{PV} with HE (°C)	T _{water} HE In (°C)	T _{water} HE Out (°C)
8:00AM	18.579874	4156.57136	23.88233	21.225816	19.275242	19.492408
8:05AM	19.309538	4319.80716	25.384138	21.525194	19.335714	19.444202
8:10AM	19.550254	4373.65861	25.997826	21.722148	19.367994	19.511186
8:15AM	19.617174	4388.62953	25.112058	21.888726	19.395854	19.534682
8:20AM	20.633504	4615.99642	26.362258	22.27533	19.435402	19.569864
8:25AM	21.155738	4732.82729	26.547998	22.154506	19.42717	19.631416
8:30AM	19.804492	4430.53512	25.669376	22.552998	19.483072	19.613358
8:35AM	19.647698	4395.45817	24.253674	22.63513	19.517604	19.643524
8:40AM	19.77876	4424.77852	24.289046	22.462418	19.514038	19.687744
8:45AM	19.625396	4390.4689	24.261686	22.174426	19.590504	19.712244
8:50AM	20.049304	4485.30291	24.713946	21.912792	19.545706	19.754298
8:55AM	19.797328	4428.93244	24.528048	21.903696	19.60638	19.780076
9:00AM	20.19218	4517.26622	25.14961	22.038056	19.658108	19.81018
9:05AM	22.865258	5115.27025	29.961634	21.958652	19.648348	19.748088
9:10AM	26.162088	5852.81611	36.228116	22.5187	19.644214	19.778844
9:15AM	24.727236	5531.82013	36.617104	24.234688	19.710754	19.849548
9:20AM	23.881204	5342.55123	34.683756	26.02727	19.672574	19.941814
9:25AM	24.536184	5489.07919	34.447924	26.98085	19.748234	19.974236
9:30AM	24.38832	5456	35.274564	27.195126	19.777698	20.025116
9:35AM	25.642596	5736.59866	38.048088	27.640276	19.853434	20.118276
9:40AM	25.594182	5725.76779	37.410476	27.996172	19.912874	20.164818
9:45AM	26.364726	5898.14899	36.26912	28.512932	19.928816	20.184926
9:50AM	25.59374	5725.6689	36.534308	28.660326	19.946558	20.24626
9:55AM	25.795906	5770.8962	37.211192	28.633778	20.011024	20.341038
10:00AM	26.152406	5850.65011	37.856496	28.817404	20.065636	20.439034
10:05AM	28.397984	6353.01655	42.291212	29.170058	20.055974	20.459886
10:10AM	25.33994	5668.89038	36.9851	29.767542	20.111612	20.541472
10:15AM	24.717434	5529.62729	38.422456	30.12873	20.254492	20.597706
10:20AM	26.660486	5964.31454	37.939552	30.18495	20.302606	20.723684

10:25AM	25.486066	5701.58076	36.97742	30.063868	20.301346	20.727164
10:30AM	26.813412	5998.52617	38.201076	29.830282	20.325884	20.821038
10:35AM	28.565754	6390.54899	40.416444	29.745938	20.383832	20.86589
10:40AM	30.054774	6723.66309	42.569976	30.067752	20.504448	20.908222
10:45AM	31.336358	7010.37092	45.425568	30.567826	20.4663	20.94397
10:50AM	31.08131	6953.3132	46.303596	31.741886	20.511608	20.993808
10:55AM	29.629416	6628.5047	45.519748	32.843834	20.66426	21.124434
11:00AM	28.43885	6362.15884	45.14728	33.268662	20.747334	21.194786
11:05AM	28.699048	6420.36868	42.44074	33.87814	20.80143	21.378976
11:10AM	29.55282	6611.36913	45.053304	33.172298	20.917758	21.390912
11:15AM	27.193502	6083.55749	38.271296	33.07135	20.875348	21.348512
11:20AM	29.780416	6662.28546	41.103068	32.590652	20.91292	21.451218
11:25AM	30.689152	6865.5821	44.797524	31.775722	20.92923	21.432866
11:30AM	30.081372	6729.61342	47.819704	32.336136	21.035976	21.53124
11:35AM	29.616012	6625.50604	47.988668	33.475322	21.088022	21.661088
11:40AM	29.76936	6659.81208	45.172616	34.115344	21.120962	21.73737
11:45AM	27.953518	6253.58345	43.676468	34.173784	21.187756	21.708712
11:50AM	27.941744	6250.94944	43.109812	34.213448	21.201682	21.831302
11:55AM	29.759804	6657.67427	44.031868	33.815664	21.322526	21.84778
12:00PM	31.921262	7141.22192	48.836252	33.528316	21.321074	21.88552
12:05PM	29.301084	6555.05235	47.791592	34.068988	21.404836	21.938958
12:10PM	31.44034	7033.63311	47.02176	35.228452	21.420008	21.975892
12:15PM	28.85714	6455.73602	43.162076	34.96476	21.429072	22.045712
12:20PM	31.819572	7118.47248	47.019956	34.794844	21.455852	22.154816
12:25PM	29.567622	6614.68054	43.328764	34.620648	21.551616	22.124858
12:30PM	26.044962	5826.61342	37.53662	34.807248	21.602068	22.240392
12:35PM	25.574614	5721.39016	34.150476	33.500324	21.651288	22.224298
12:40PM	26.206396	5862.72841	32.476516	31.678222	21.599322	22.220048
12:45PM	23.357298	5225.34631	28.739386	30.230006	21.583718	22.19139
12:50PM	23.159878	5181.18076	27.410136	28.930334	21.624622	22.110958
12:55PM	20.908736	4677.56957	24.882442	27.34626	21.504222	22.012184
1:00 PM	20.53771	4594.566	22.829998	26.252544	21.511574	21.850106
1:05 PM	19.331276	4324.67025	22.540064	25.028496	21.49425	21.837142
1:10 PM	18.84346	4215.53915	22.31046	23.971174	21.447026	21.720448
1:15 PM	19.567198	4377.44922	22.110474	22.747604	21.377018	21.60293
1:20 PM	18.909406	4230.29217	21.776974	22.214992	21.268922	21.485954
1:25 PM	20.511218	4588.63937	22.906644	22.43896	21.306706	21.488886
1:30 PM	20.803816	4654.09754	24.876814	21.711406	21.199164	21.381548
1:35 PM	21.978324	4916.85101	28.357672	22.507294	21.179832	21.36222
1:40 PM	21.85887	4890.12752	33.178398	23.20229	21.14687	21.368274
1:45 PM	21.707578	4856.28143	30.846114	24.049612	21.12582	21.412376

1:50 PM	21.406082	4788.83266	28.680808	24.983628	21.167068	21.445096
1:55 PM	21.543664	4819.61163	26.44337	25.45806	21.148418	21.409026
2:00 PM	21.200202	4742.7745	25.384124	24.79984	21.182778	21.36081
2:05 PM	19.972306	4468.0774	22.967514	24.221932	21.142074	21.33299
2:10 PM	19.631262	4391.78121	21.413916	23.587088	21.110122	21.288164
2:15 PM	20.031784	4481.38345	21.587454	22.289942	21.062094	21.235784
2:20 PM	20.76386	4645.15884	22.971774	21.775422	21.063564	21.26756
2:25 PM	21.237318	4751.07785	25.416402	21.723228	20.972322	21.085412
2:30 PM	25.14228	5624.67114	32.745312	21.808462	20.91439	21.031652
2:35 PM	27.74781	6207.56376	42.056996	23.138604	20.943474	21.165104
2:40 PM	26.507724	5930.1396	41.2141	25.536054	20.949168	21.21398
2:45 PM	25.937044	5802.47069	37.581536	28.531662	21.0523	21.321636
2:50 PM	25.237092	5645.88188	35.066112	29.271304	21.061412	21.42203
2:55 PM	24.05742	5381.97315	32.869294	29.733226	21.142548	21.463946
3:00 PM	25.97811	5811.65772	33.620924	28.882244	21.097876	21.523436
3:05 PM	26.74758	5983.79866	38.147032	28.715322	21.18985	21.52411
3:10 PM	25.634518	5734.7915	35.17294	28.837346	21.190794	21.594738
3:15 PM	25.151064	5626.63624	32.576436	29.388648	21.283288	21.63949
3:20 PM	24.388498	5456.03982	31.59011	28.808588	21.287444	21.743424
3:25 PM	23.392	5233.10962	29.338192	28.147462	21.210362	21.657658
3:30 PM	22.393246	5009.67472	27.060132	27.624938	21.243526	21.61697
3:35 PM	18.210938	4074.03535	23.280978	26.645572	21.264696	21.6902
3:40 PM	16.988058	3800.4604	19.207986	25.342154	21.296928	21.683418
3:45 PM	16.46339	3683.08501	19.183004	23.370886	21.354556	21.667188
3:50 PM	16.271842	3640.23311	18.852394	21.338148	21.290234	21.650598
3:55 PM	16.369574	3662.09709	19.054284	20.539476	21.243472	21.616914
4:00 PM	16.110984	3604.24698	18.495616	20.32169	21.226016	21.555912
4:05 PM	15.889238	3554.63937	17.968804	19.456924	21.222958	21.453058
4:10 PM	15.975978	3574.0443	17.797366	19.159348	21.182638	21.495124
4:15 PM	15.797082	3534.02282	17.44398	19.085604	21.16091	21.35201
4:20 PM	16.951922	3792.37629	18.48598	19.066058	21.115444	21.345376
4:25 PM	19.308144	4319.4953	25.171462	18.950554	21.02626	21.2564
4:30 PM	19.440464	4349.09709	24.939298	19.483896	20.99323	21.171098
4:35 PM	18.443512	4126.06532	22.798716	20.781506	20.968306	21.133296
4:40 PM	17.791136	3980.11991	22.466992	21.457098	20.949304	21.14896
4:45 PM	17.665916	3952.10649	22.238696	21.059104	20.954726	21.11555
4:50 PM	16.426052	3674.73199	20.175226	21.36546	20.927156	21.100678
4:55 PM	16.479278	3686.63937	17.992426	20.688624	20.871078	21.083818
5:00 PM	16.248138	3634.9302	17.718064	20.458976	20.880384	21.0541

26-Jul

Time	T _{outside} (°C)	Radiation (W/m ²)	T _{PV} w/o HE (°C)	T _{PV} with HE (°C)	T _{water} HE In (°C)	T _{water} HE Out (°C)
8:00AM	17.864188	3996.46264	21.149662	18.658996	17.49462	17.69024
8:05AM	20.355856	4553.88277	23.356998	18.702904	17.477788	17.71709
8:10AM	22.621892	5060.82595	26.211788	19.416148	17.52937	17.755372
8:15AM	21.902646	4899.92081	28.328704	19.806516	17.624058	17.784908
8:20AM	22.13346	4951.55705	30.66199	20.880456	17.655466	17.886192
8:25AM	23.020948	5150.10022	32.111064	22.285544	17.686336	17.86902
8:30AM	22.293788	4987.42461	30.706202	23.106924	17.75538	17.964066
8:35AM	20.416356	4567.41745	27.846388	23.863908	17.873606	18.021328
8:40AM	21.715842	4858.1302	29.686244	23.896262	17.918642	18.153498
8:45AM	22.076304	4938.77047	26.764308	24.117228	17.988536	18.167
8:50AM	21.42991	4794.16331	27.496604	23.75864	18.040526	18.210248
8:55AM	21.18652	4739.71365	27.388946	23.534022	18.101256	18.288056
9:00AM	21.275128	4759.53647	27.270146	23.42357	18.18988	18.372494
9:05AM	21.794948	4875.82729	28.508796	23.076776	18.180614	18.3805
9:10AM	25.442748	5691.88993	31.3815	23.073508	18.150754	18.402846
9:15AM	22.823912	5106.02058	30.339632	23.611196	18.260758	18.478094
9:20AM	20.890528	4673.4962	28.49532	24.303204	18.291934	18.561458
9:25AM	20.989932	4695.73423	27.496614	24.45393	18.413362	18.63485
9:30AM	22.156114	4956.62506	29.284942	24.254362	18.420732	18.64677
9:35AM	21.188264	4740.1038	28.408252	23.839562	18.411664	18.703174
9:40AM	21.2129	4745.61521	27.890536	24.00685	18.48418	18.727666
9:45AM	23.020578	5150.01745	29.111736	23.924372	18.535924	18.757576
9:50AM	22.895832	5122.11007	30.502544	24.193028	18.562588	18.836608
9:55AM	21.988296	4919.08188	29.549464	24.1917	18.604716	18.887264
10:00AM	21.553622	4821.83937	27.604854	24.484398	18.594856	18.82523
10:05AM	24.57699	5498.20805	32.73463	24.408464	18.596774	18.896782
10:10AM	25.374632	5676.65145	34.9605	24.58104	18.644108	18.92646
10:15AM	23.388724	5232.37673	32.07814	25.750408	18.722784	18.97059
10:20AM	24.501454	5481.30962	29.690486	26.156756	18.763612	19.024312
10:25AM	23.80529	5325.56823	29.308082	25.84655	18.784714	19.03687
10:30AM	24.661458	5517.1047	31.131692	25.364758	18.785426	19.11138
10:35AM	25.479754	5700.16868	37.168752	25.609066	18.822822	19.114242
10:40AM	29.355532	6567.23311	40.869772	26.298692	18.86651	19.153366
10:45AM	31.226982	6985.90201	45.426884	27.525724	18.937208	19.215324
10:50AM	27.053622	6052.26443	41.40068	29.38724	19.002256	19.341432
10:55AM	25.700378	5749.52528	35.831036	30.574958	18.965642	19.387338
11:00AM	24.79052	5545.97763	33.72202	30.41255	19.109336	19.435402
11:05AM	24.806026	5549.44653	32.794982	29.449454	19.098922	19.533658
11:10AM	23.08574	5164.59508	30.622902	28.573286	19.22629	19.56086
11:15AM	23.861354	5338.11051	30.14764	27.573768	19.21796	19.62668

11:20AM	22.897904	5122.5736	29.364068	26.849752	19.216032	19.61584
11:25AM	22.635402	5063.84832	27.982208	26.05091	19.204926	19.622182
11:30AM	22.768454	5093.61387	27.405354	25.614028	19.307786	19.651246
11:35AM	24.495706	5480.02371	28.69361	24.923376	19.329262	19.624932
11:40AM	26.11169	5841.54139	34.091528	24.730832	19.300736	19.67454
11:45AM	26.412868	5908.91902	36.277576	25.071794	19.317668	19.7
11:50AM	24.959018	5583.67293	35.053272	26.26172	19.35178	19.738464
11:55AM	24.262376	5427.82461	32.464988	27.083404	19.437772	19.724694
12:00PM	24.329062	5442.74318	31.298722	27.201418	19.430928	19.75255
12:05PM	26.62882	5957.23043	38.561688	27.011854	19.421568	19.81278
12:10PM	26.850122	6006.7387	38.04172	27.482314	19.523098	19.818724
12:15PM	28.68378	6416.95302	43.14	28.494124	19.509596	19.896424
12:20PM	29.222352	6537.43893	44.068976	29.420186	19.496586	19.940102
12:25PM	26.771384	5989.12394	39.848136	30.85782	19.599242	19.964428
12:30PM	28.03147	6271.02237	39.751116	31.492088	19.650898	20.085454
12:35PM	26.083526	5835.24072	36.568208	31.369828	19.748064	20.12193
12:40PM	27.19899	6084.78523	39.300348	30.850606	19.738734	20.229934
12:45PM	31.601734	7069.73915	40.199068	30.679558	19.725894	20.204024
12:50PM	27.944882	6251.65145	40.965972	30.603584	19.761728	20.248372
12:55PM	26.670818	5966.62595	37.375072	31.371328	19.861064	20.295742
1:00 PM	25.768068	5764.66846	33.060798	31.172752	19.942112	20.372216
1:05 PM	28.349206	6342.10425	35.7144	30.256038	19.948306	20.426354
1:10 PM	27.48817	6149.47875	37.31984	29.403224	19.985956	20.394438
1:15 PM	26.30554	5884.90828	33.679128	29.629052	19.996364	20.404844
1:20 PM	25.386818	5679.37763	31.721006	29.444654	20.014418	20.470838
1:25 PM	25.381358	5678.15615	30.398382	28.757692	20.082678	20.495678
1:30 PM	24.743522	5535.46353	30.116524	27.883336	20.0587	20.506198
1:35 PM	24.31725	5440.10067	29.69727	27.283146	20.13902	20.499698
1:40 PM	25.51611	5708.30201	30.75996	26.715654	20.11391	20.474598
1:45 PM	27.500372	6152.2085	35.07522	26.457944	20.110646	20.4755
1:50 PM	29.78846	6664.08501	38.164752	26.95235	20.152782	20.496024
1:55 PM	28.466474	6368.3387	37.612	27.812898	20.152194	20.51723
2:00 PM	27.948754	6252.51767	34.194176	28.777966	20.171708	20.541096
2:05 PM	27.08794	6059.94183	33.113984	29.026742	20.11526	20.575812
2:10 PM	26.517684	5932.36779	32.689434	28.673552	20.139966	20.613586
2:15 PM	26.786046	5992.40403	32.377884	28.292276	20.175558	20.627564
2:20 PM	25.22217	5642.54362	32.346886	28.101988	20.243972	20.591548
2:25 PM	28.225698	6314.47383	33.684164	27.92461	20.199172	20.642454
2:30 PM	26.39112	5904.05369	33.179752	27.833924	20.277216	20.628954
2:35 PM	25.202192	5638.07427	31.950428	28.017802	20.24553	20.636688
2:40 PM	26.387394	5903.22013	32.680298	27.813432	20.273474	20.59944

2:45 PM	27.578744	6169.74139	34.65122	27.660546	20.218842	20.662118
2:50 PM	27.247972	6095.74318	35.052568	27.915024	20.2498	20.675822
2:55 PM	28.074976	6280.75526	33.83386	28.208176	20.30702	20.693802
3:00 PM	26.079834	5834.41477	32.332912	28.569076	20.328426	20.75859
3:05 PM	25.392832	5680.72304	30.315964	28.427114	20.358616	20.81056
3:10 PM	24.686798	5522.7736	28.628166	27.845592	20.405512	20.774834
3:15 PM	23.572032	5273.38523	27.194582	27.276408	20.426028	20.825658
3:20 PM	21.348012	4775.84161	23.265264	26.221466	20.40132	20.800958
3:25 PM	19.875472	4446.41432	21.591144	25.409682	20.384248	20.792606
3:30 PM	21.011184	4700.48859	21.91352	23.87021	20.38136	20.741972
3:35 PM	21.116776	4724.11096	22.300292	22.560858	20.343726	20.713064
3:40 PM	20.355272	4553.75213	22.246528	22.363862	20.311682	20.65488
3:45 PM	20.398042	4563.32036	21.977508	21.600382	20.280724	20.62829
3:50 PM	20.251922	4530.63132	21.95291	21.333004	20.26917	20.568988
3:55 PM	19.740372	4416.1906	22.314348	21.247712	20.236122	20.566268
4:00 PM	19.821216	4434.27651	21.783668	21.102882	20.221406	20.464762
4:05 PM	19.341926	4327.0528	21.175922	21.275548	20.17281	20.477008
4:10 PM	19.717706	4411.11991	20.969164	21.051566	20.13101	20.435216
4:15 PM	19.635848	4392.80716	20.718002	20.78716	20.118368	20.405144
4:20 PM	18.07187	4042.92394	19.092136	20.917766	20.131898	20.348924
4:25 PM	16.707306	3737.65235	17.590178	20.290608	20.06485	20.325482
4:30 PM	16.936892	3789.01387	16.626364	19.435924	20.001366	20.283806
4:35 PM	16.96864	3796.11633	17.230832	18.71409	19.967638	20.228286
4:40 PM	18.177114	4066.46846	18.652198	18.098518	20.096898	20.301042
4:45 PM	18.888328	4225.57673	20.015078	18.121374	20.006358	20.201798
4:50 PM	19.424148	4345.44698	21.67729	18.710454	19.985048	20.124192
4:55 PM	20.3275	4547.53915	23.066402	19.092886	19.914826	20.11464
5:00 PM	22.743322	5087.9915	26.367408	20.017208	19.882412	20.060428

27-Jul						
Time	T _{outside} (°C)	Radiation (W/m ²)	T _{PV w/o HE} (°C)	T _{PV with HE} (°C)	T _{water HE In} (°C)	T _{water HE Out} (°C)
8:00AM	15.824138	3540.07562	16.874262	17.104932	17.370328	17.561788
8:05AM	15.730088	3519.03535	17.159172	17.115854	17.389984	17.581252
8:10AM	15.805128	3535.82282	18.16886	16.859828	17.403768	17.586488
8:15AM	15.573634	3484.03445	18.646388	17.033858	17.442874	17.577728
8:20AM	15.576096	3484.58523	18.19692	17.384358	17.401642	17.549418
8:25AM	15.37946	3440.59508	17.17507	17.253342	17.379668	17.562392
8:30AM	14.416788	3225.23221	16.738712	17.400288	17.426312	17.543694
8:35AM	14.672534	3282.44609	16.579536	16.94537	17.40228	17.584812
8:40AM	14.764168	3302.94586	16.601286	17.041026	17.41091	17.563052

8:45AM	14.862278	3324.89441	17.00825	16.973476	17.439116	17.565234
8:50AM	15.00093	3355.91275	17.394398	16.67181	17.459548	17.581488
8:55AM	14.76263	3302.60179	17.09193	16.73488	17.413932	17.592284
9:00AM	14.694682	3287.40089	16.615148	16.580174	17.46826	17.607288
9:05AM	14.937216	3341.65906	16.625854	16.665008	17.417988	17.63128
9:10AM	15.085542	3374.84161	17.483224	16.808578	17.426622	17.622254
9:15AM	15.743936	3522.13333	17.999366	16.646266	17.48644	17.59945
9:20AM	15.877858	3552.09351	18.39768	16.993496	17.48097	17.61563
9:25AM	16.679806	3731.50022	18.875776	16.867186	17.450442	17.632966
9:30AM	16.600242	3713.70067	18.583234	17.479764	17.483944	17.65355
9:35AM	16.028816	3585.86488	18.344128	17.309604	17.514182	17.69233
9:40AM	16.39169	3667.04474	18.271354	17.576028	17.549818	17.702132
9:45AM	16.560522	3704.81477	18.773768	17.822566	17.518138	17.727048
9:50AM	15.810272	3536.9736	19.143722	17.848566	17.539964	17.731212
9:55AM	16.391198	3666.93468	18.679118	17.96255	17.562432	17.753866
10:00AM	16.667792	3728.81253	18.546496	17.925366	17.560184	17.75162
10:05AM	16.368764	3661.91588	18.3354	17.613898	17.570406	17.69651
10:10AM	16.238918	3632.86756	18.375262	17.545336	17.554074	17.680178
10:15AM	16.654864	3725.92036	19.068682	17.851688	17.577652	17.72123
10:20AM	16.655812	3726.13244	19.81366	17.522194	17.58316	17.691794
10:25AM	16.989768	3800.84295	20.12957	17.92524	17.607918	17.699078
10:30AM	17.398874	3892.36555	20.133626	18.259644	17.642368	17.755554
10:35AM	17.698762	3959.45459	20.033524	18.11175	17.672744	17.768458
10:40AM	15.453228	3457.09799	20.557914	18.214778	17.684466	17.793282
10:45AM	16.448802	3679.82148	20.545878	18.333132	17.711524	17.8116
10:50AM	16.881202	3776.55526	20.225228	18.65087	17.690654	17.855868
10:55AM	17.500192	3915.03177	20.738636	18.933818	17.704548	17.86558
11:00AM	18.430356	4123.12215	21.124712	18.729832	17.717452	17.873926
11:05AM	18.369124	4109.42371	21.237106	18.694802	17.78684	17.882356
11:10AM	18.081928	4045.17405	21.410226	18.82879	17.755718	17.890542
11:15AM	18.325992	4099.7745	20.825434	18.9771	17.76534	17.873958
11:20AM	18.166218	4064.03087	20.153122	19.043564	17.757618	17.909718
11:25AM	18.28432	4090.4519	20.006044	19.296834	17.788784	17.919238
11:30AM	18.470994	4132.21342	20.309992	19.187664	17.823434	17.949516
11:35AM	18.508874	4140.6877	20.70844	18.79543	17.822028	17.965766
11:40AM	17.627446	3943.50022	21.299544	18.696634	17.849252	17.966786
11:45AM	18.412066	4119.03043	22.095044	18.907176	17.903666	17.981894
11:50AM	18.244788	4081.60805	21.928044	19.160968	17.896972	18.036148
11:55AM	17.097312	3824.90201	21.469642	19.706028	17.924102	18.045806
12:00PM	17.299756	3870.1915	21.415406	19.477438	17.965226	18.048008
12:05PM	17.918682	4008.65369	22.28735	19.71787	17.95324	18.088042

12:10PM	19.231324	4302.30962	22.898584	19.653504	18.010684	18.084728
12:15PM	17.396032	3891.72975	22.48623	19.647894	17.944118	18.066012
12:20PM	18.117876	4053.21611	21.979624	20.100114	17.931054	18.065856
12:25PM	17.478382	3910.15257	21.806288	19.969758	17.974604	18.057004
12:30PM	17.824266	3987.53154	22.003212	19.823632	17.976552	18.102616
12:35PM	18.403414	4117.09485	21.97379	20.168202	18.020896	18.13386
12:40PM	18.480566	4134.35481	21.94227	19.910474	17.993648	18.158824
12:45PM	18.593334	4159.58255	22.509698	19.979898	18.058996	18.150124
12:50PM	18.82681	4211.81432	22.690268	19.83948	18.027166	18.192338
12:55PM	19.247574	4305.94497	23.37777	20.087428	18.070618	18.196674
1:00 PM	18.14228	4058.67562	24.623194	20.21111	18.081338	18.181388
1:05 PM	19.540744	4371.5311	25.489116	20.436886	18.12904	18.229086
1:10 PM	17.654858	3949.63266	23.712506	20.632214	18.146266	18.259408
1:15 PM	18.491802	4136.86846	22.48643	20.886356	18.087476	18.243906
1:20 PM	17.23123	3854.8613	21.464694	21.10466	18.079958	18.249486
1:25 PM	16.555636	3703.7217	21.113316	20.435592	18.101734	18.266894
1:30 PM	17.335664	3878.22461	20.913476	20.183334	18.16667	18.257982
1:35 PM	16.801818	3758.79597	21.058824	20.246316	18.155902	18.299226
1:40 PM	16.091946	3599.98792	20.286604	19.812486	18.13095	18.304646
1:45 PM	16.695126	3734.92752	20.66582	19.55669	18.131902	18.31889
1:50 PM	17.245196	3857.98568	20.388748	19.305564	18.198142	18.311088
1:55 PM	19.595674	4383.81969	23.326596	19.174236	18.166564	18.301342
2:00 PM	18.047884	4037.55794	25.090438	19.433314	18.199952	18.29145
2:05 PM	19.068852	4265.96242	24.452478	19.959818	18.186778	18.304282
2:10 PM	18.870142	4221.50828	23.520812	20.782476	18.192214	18.352998
2:15 PM	18.751586	4194.98568	23.563012	20.69441	18.186558	18.364994
2:20 PM	17.940858	4013.61477	22.769238	20.765624	18.253922	18.388692
2:25 PM	18.560176	4152.16465	21.79659	20.902512	18.25155	18.425614
2:30 PM	18.300478	4094.06667	20.64725	20.838428	18.270108	18.439612
2:35 PM	18.130866	4056.12215	19.872886	20.708172	18.25255	18.435344
2:40 PM	18.209268	4073.66174	19.820746	20.281972	18.287478	18.443886
2:45 PM	18.64618	4171.40492	20.4277	19.883864	18.263542	18.446144
2:50 PM	19.170378	4288.67517	21.416944	19.726076	18.28856	18.444968
2:55 PM	19.187806	4292.57405	21.499486	19.756576	18.30581	18.440766
3:00 PM	19.161696	4286.73289	21.165096	19.61272	18.340616	18.44482
3:05 PM	19.270084	4310.98076	20.71752	19.74326	18.279568	18.457802
3:10 PM	18.731628	4190.52081	20.495978	20.004496	18.31447	18.483968
3:15 PM	18.520808	4143.35749	20.158822	19.954466	18.31221	18.460074
3:20 PM	18.968508	4243.51409	20.019552	19.75431	18.307908	18.486138
3:25 PM	18.574118	4155.28367	19.707394	19.624526	18.308964	18.487194
3:30 PM	18.460134	4129.78389	19.467584	19.237512	18.299176	18.477408

3:35 PM	18.671958	4177.17181	19.371072	19.305826	18.376456	18.48066
3:40 PM	18.57523	4155.53244	19.743394	19.270222	18.318808	18.497036
3:45 PM	19.061714	4264.36555	20.269822	19.139874	18.301316	18.47537
3:50 PM	19.029132	4257.07651	20.624072	19.450238	18.360018	18.477508
3:55 PM	18.192544	4069.92036	20.9607	19.547858	18.349338	18.462276
4:00 PM	18.571828	4154.77136	20.896714	19.357868	18.315406	18.489272
4:05 PM	19.111566	4275.51812	20.989076	19.380542	18.338292	18.481596
4:10 PM	19.41214	4342.76063	21.641066	19.850756	18.360992	18.46975
4:15 PM	19.56922	4377.90157	22.201446	19.865022	18.327252	18.479476
4:20 PM	19.273064	4311.64743	21.988038	19.83763	18.32621	18.500072
4:25 PM	19.291452	4315.76107	21.602952	20.08237	18.344422	18.51847
4:30 PM	18.759566	4196.77092	21.40553	19.93648	18.36842	18.507546
4:35 PM	19.47788	4357.46756	21.00844	19.917044	18.318402	18.4879
4:40 PM	19.640702	4393.89306	20.862868	20.08038	18.285672	18.472636
4:45 PM	18.939636	4237.05503	21.164626	19.838652	18.292118	18.496542
4:50 PM	19.548454	4373.25593	21.621518	19.77885	18.319374	18.475968
4:55 PM	19.827754	4435.73915	21.35772	19.979998	18.389784	18.481266
5:00 PM	19.623108	4389.95705	21.309944	20.34105	18.333356	18.494312

28-Jul						
Time	T _{outside} (°C)	Radiation (W/m ²)	T _{PV} w/o HE (°C)	T _{PV} with HE (°C)	T _{water} HE In (°C)	T _{water} HE Out (°C)
8:00 AM	19.409184	4342.099329	24.666746	20.952136	17.653064	17.853032
8:05 AM	19.209608	4297.451454	24.40921	20.809446	17.771344	17.888696
8:10 AM	19.51186	4365.069351	24.68722	20.980814	17.8081	17.921082
8:15 AM	19.782436	4425.600895	25.162204	20.955786	17.809026	17.961312
8:20 AM	20.44618	4574.089485	26.359708	21.40553	17.829244	18.007728
8:25 AM	20.448138	4574.527517	27.28426	21.580938	17.93127	18.070442
8:30 AM	20.458772	4576.906488	27.402672	22.090218	17.859138	18.033252
8:35 AM	21.54578	4820.085011	30.957502	22.274028	17.878544	18.0481
8:40 AM	22.281106	4984.587472	33.171402	22.683766	17.916026	18.094308
8:45 AM	22.377024	5006.045638	33.394314	23.74808	17.951504	18.181798
8:50 AM	21.579878	4827.713199	33.11842	24.603168	18.003876	18.182148
8:55 AM	23.178724	5185.396868	32.979336	25.203208	18.017352	18.286928
9:00 AM	20.924368	4681.066667	33.644008	25.7456	18.077728	18.342928
9:05 AM	21.977046	4916.565101	33.668748	25.933746	18.206416	18.402122
9:10 AM	21.728448	4860.950336	32.53397	26.074304	18.174492	18.439864
9:15 AM	22.943444	5132.761521	33.090644	26.218338	18.180438	18.515462
9:20 AM	21.999488	4921.585682	32.746456	26.21483	18.250564	18.57665
9:25 AM	21.910854	4901.757047	33.116578	26.669432	18.361758	18.631452
9:30 AM	22.4945	5032.326622	33.537254	26.728432	18.38184	18.734082

9:35 AM	22.944936	5133.095302	35.61498	26.548096	18.390176	18.72932
9:40 AM	23.476728	5252.06443	35.38062	26.921724	18.424148	18.776378
9:45 AM	23.458828	5248.059955	34.651104	27.435564	18.506014	18.845318
9:50 AM	23.77264	5318.263982	36.05664	27.88618	18.543002	18.886662
9:55 AM	22.608414	5057.810738	35.030436	27.835104	18.56937	18.921752
10:00AM	22.35402	5000.899329	36.136128	28.413618	18.666452	19.005716
10:05AM	25.002034	5593.296197	35.587404	28.444334	18.688476	19.05828
10:10AM	26.02759	5822.727069	40.508412	28.36606	18.730882	19.144116
10:15AM	25.736492	5757.604474	41.102164	29.318982	18.771602	19.145556
10:20AM	27.638588	6183.129306	42.6474	30.208382	18.810804	19.19347
10:25AM	26.862114	6009.421477	42.793164	30.959918	18.915822	19.320272
10:30AM	24.846836	5558.576286	47.126688	31.31822	18.913196	19.339272
10:35AM	27.43217	6136.950783	46.10996	32.640342	18.96466	19.464686
10:40AM	28.04442	6273.919463	41.998852	33.705708	19.088102	19.575184
10:45AM	31.074402	6951.767785	43.883508	33.797612	19.124132	19.624284
10:50AM	30.722394	6873.018792	44.99982	33.575992	19.154044	19.693246
10:55AM	31.09327	6955.988814	46.435036	34.13698	19.28582	19.777192
11:00AM	35.29636	7896.277405	49.231588	34.3215	19.272924	19.825164
11:05AM	34.480224	7713.696644	52.22174	34.991212	19.368436	19.890302
11:10AM	35.742632	7996.114541	52.633536	36.267532	19.474014	20.052334
11:15AM	35.401556	7919.811186	51.7387	37.2505	19.540622	20.08422
11:20AM	34.645504	7750.672036	53.016428	37.707592	19.610734	20.236948
11:25AM	38.651596	8646.889485	54.842224	38.256852	19.727468	20.371062
11:30AM	37.665224	8426.224609	55.792384	38.85936	19.751334	20.407992
11:35AM	35.260936	7888.352573	56.346144	39.794436	19.881844	20.564588
11:40AM	35.75306	7998.447427	55.990976	40.27176	19.948002	20.691726
11:45AM	35.093368	7850.865324	50.272272	41.008924	20.142844	20.851408
11:50AM	35.188536	7872.155705	50.727136	40.299504	20.112864	20.869378
11:55AM	36.865108	8247.22774	55.75756	39.316144	20.2073	20.97702
12:00PM	37.446924	8377.387919	56.692816	39.865852	20.30827	21.051792
12:05PM	37.78224	8452.402685	58.401988	40.763356	20.45361	21.210118
12:10PM	38.464016	8604.92528	57.66362	41.28112	20.518374	21.33147
12:15PM	36.17614	8093.096197	58.689652	41.824456	20.487872	21.326936
12:20PM	36.27476	8115.158837	58.82846	42.210224	20.574046	21.45244
12:25PM	40.325548	9021.375391	59.779704	42.897372	20.714502	21.575384
12:30PM	38.724664	8663.235794	59.736636	43.290628	20.883058	21.726602
12:35PM	41.992088	9394.203132	60.070272	43.7986	20.996094	21.84392
12:40PM	36.499184	8165.365548	60.09934	43.987176	20.966962	21.86706
12:45PM	39.022108	8729.778076	60.773976	44.28304	21.083092	22.004684
12:50PM	37.750108	8445.214318	60.119704	44.637572	21.242536	22.142444
12:55PM	41.115808	9198.167338	60.233096	44.90766	21.31947	22.271368

1:00 PM	38.491468	8611.066667	60.6958	44.843172	21.32425	22.245866
1:05 PM	40.813732	9130.588814	60.735536	45.08462	21.37565	22.379928
1:10 PM	39.582788	8855.209843	61.641428	45.15362	21.501224	22.513922
1:15 PM	37.333976	8352.119911	57.29348	45.2812	21.604652	22.630512
1:20 PM	40.008036	8950.343624	56.834956	45.00368	21.633126	22.633048
1:25 PM	38.020044	8505.602685	59.356408	44.601788	21.74238	22.75943
1:30 PM	36.428288	8149.505145	57.64794	44.227824	21.802552	22.841502
1:35 PM	41.618932	9310.723043	58.129004	44.523216	21.918368	22.961574
1:40 PM	40.385104	9034.698881	58.314024	44.14136	22.018602	23.07913
1:45 PM	40.688108	9102.485011	60.493792	44.248308	21.983546	23.044102
1:50 PM	38.80674	8681.597315	57.669676	44.73532	22.088412	23.127322
1:55 PM	39.063964	8739.141834	59.277656	45.003436	22.172016	23.245658
2:00 PM	41.204468	9218.00179	58.567692	44.952364	22.2915	23.352
2:05 PM	37.93226	8485.964206	58.38714	44.775788	22.386032	23.468196
2:10 PM	41.779616	9346.670246	58.228532	44.752724	22.339284	23.412982
2:15 PM	42.729124	9559.088143	58.209264	44.879796	22.421088	23.490366
2:20 PM	38.66184	8649.181208	57.1618	45.00248	22.546112	23.641192
2:25 PM	39.309904	8794.161969	56.895056	44.760484	22.573308	23.712034
2:30 PM	42.777136	9569.829083	57.894716	44.612112	22.684422	23.796964
2:35 PM	42.446808	9495.930201	57.497816	44.565956	22.726964	23.874252
2:40 PM	44.584532	9974.168233	58.53628	44.538216	22.731858	23.831318
2:45 PM	40.952024	9161.526622	58.431668	44.498468	22.754996	23.902258
2:50 PM	38.120716	8528.124385	57.395464	44.725564	22.866026	23.96991
2:55 PM	41.44578	9271.986577	57.52278	44.681384	22.897518	24.044846
3:00 PM	38.136544	8531.665324	56.901852	44.708016	23.006502	24.162426
3:05 PM	40.407108	9039.621477	56.35078	44.607924	23.097836	24.258028
3:10 PM	42.478276	9502.970022	55.351084	44.20986	23.161242	24.28661
3:15 PM	40.106344	8972.336465	55.80364	44.14386	23.148248	24.282506
3:20 PM	40.288	9012.975391	55.932184	43.77114	23.138274	24.281044
3:25 PM	38.377448	8585.558837	54.763656	43.917248	23.252694	24.35644
3:30 PM	40.345508	9025.840716	54.117712	43.735428	23.226234	24.381968
3:35 PM	38.444552	8600.570917	53.942488	43.361972	23.324554	24.432586
3:40 PM	36.891948	8253.232215	54.013976	43.031852	23.30682	24.480052
3:45 PM	37.437368	8375.250112	52.3953	43.005448	23.413888	24.526
3:50 PM	36.855816	8245.148993	50.679104	42.678316	23.469044	24.590178
3:55 PM	37.60126	8411.914989	47.304668	42.03984	23.480112	24.605392
4:00 PM	36.481324	8161.370022	45.872916	41.181004	23.518236	24.608724
4:05 PM	36.541028	8174.726622	45.282408	40.392	23.52673	24.608522
4:10 PM	39.2703	8785.302013	47.54366	39.338292	23.556628	24.612516
4:15 PM	36.302364	8121.334228	47.56982	38.854068	23.540176	24.626492
4:20 PM	34.280668	7669.053244	44.140988	39.167736	23.590834	24.611932

4:25 PM	36.010232	8055.980313	43.645908	38.614468	23.530308	24.525382
4:30 PM	37.528592	8395.658166	46.450844	37.746104	23.479634	24.50951
4:35 PM	34.972492	7823.823714	46.713932	37.616236	23.464434	24.472596
4:40 PM	35.89404	8029.986577	50.113744	39.026768	26.522422	26.945844
4:45 PM	35.846472	8019.344966	46.743264	38.868892	26.469796	26.902102

29-Jul						
Time	T _{outside} (°C)	Radiation (W/m ²)	T _{PV w/o HE} (°C)	T _{PV with HE} (°C)	T _{water HE In} (°C)	T _{water HE Out} (°C)
8:00 AM	17.687322	3956.895302	19.744728	19.96618	19.718752	19.766532
8:05 AM	17.732748	3967.057718	19.034278	20.185168	19.690346	19.82061
8:10 AM	17.823092	3987.268904	18.428512	19.545984	19.69352	19.823972
8:15 AM	17.587662	3934.6	18.432746	19.319968	19.697938	19.82801
8:20 AM	17.491796	3913.153468	18.189064	19.346	19.741218	19.823698
8:25 AM	17.479964	3910.506488	18.042066	18.8343	19.77283	19.798994
8:30 AM	17.235678	3855.856376	18.564646	18.808116	19.690346	19.81189
8:35 AM	17.179114	3843.202237	18.277328	18.673436	19.70348	19.812126
8:40 AM	17.414566	3895.876063	18.320882	18.964782	19.738262	19.807848
8:45 AM	17.460502	3906.152573	18.871402	18.958302	19.705806	19.827348
8:50 AM	17.823348	3987.326174	19.724114	19.050798	19.693774	19.802424
8:55 AM	18.302524	4094.524385	21.509274	18.802992	19.719734	19.789322
9:00 AM	18.617804	4165.056823	21.006824	19.265732	19.726204	19.782518
9:05 AM	18.577452	4156.02953	21.64021	19.616482	19.746564	19.785624
9:10 AM	18.171048	4065.111409	21.760608	20.365872	19.719242	19.810444
9:15 AM	18.52701	4144.744966	21.998248	20.099998	19.74831	19.809176
9:20 AM	19.246566	4305.719463	23.00628	20.175702	19.746106	19.81133
9:25 AM	19.598174	4384.378971	24.420868	20.453152	19.728636	19.850174
9:30 AM	20.953422	4687.566443	27.749414	21.249106	19.759782	19.859704
9:35 AM	21.111536	4722.938702	28.991286	22.310386	19.778684	19.904582
9:40 AM	22.636304	5064.050112	27.711176	23.104488	19.86181	19.92267
9:45 AM	21.817798	4880.93915	27.2705	23.742686	19.86374	19.967826
9:50 AM	22.01375	4924.776286	27.013344	23.674082	19.851248	20.02491
9:55 AM	21.46373	4801.729306	26.838886	23.86631	19.90526	20.074366
10:00AM	23.57399	5273.823266	28.878176	23.764364	19.894016	20.06767
10:05AM	22.151576	4955.609843	27.790608	23.954258	19.928256	20.071578
10:10AM	23.04582	5155.66443	29.751194	24.236104	19.93761	20.13723
10:15AM	23.36242	5226.49217	30.730274	24.517652	20.024836	20.159426
10:20AM	23.382432	5230.969128	30.484468	24.922242	20.075232	20.222896
10:25AM	23.188926	5187.679195	30.786412	25.169962	20.046364	20.259044
10:30AM	23.540736	5266.383893	31.21606	25.442706	19.977454	20.233742
10:35AM	23.860266	5337.867114	32.102028	26.089022	20.063754	20.28515

10:40AM	28.962594	6479.327517	37.228804	26.176572	20.138818	20.316612
10:45AM	25.7278	5755.659955	36.0193	27.03313	20.103188	20.402854
10:50AM	26.673422	5967.208501	35.142736	28.066926	20.196002	20.417378
10:55AM	24.13919	5400.266219	35.011016	28.593274	20.195646	20.473496
11:00AM	25.946656	5804.621029	34.53676	28.528072	20.236174	20.5576
11:05AM	23.953052	5358.624609	32.55967	28.445438	20.321332	20.634022
11:10AM	23.843188	5334.046532	30.824088	28.096502	20.341376	20.615026
11:15AM	24.69118	5523.753915	31.582808	27.399878	20.328034	20.657964
11:20AM	26.399468	5905.921253	35.62362	27.394248	20.378664	20.695508
11:25AM	26.943504	6027.62953	38.884884	28.100664	20.44904	20.752984
11:30AM	25.693604	5748.009843	35.643568	28.608352	20.466688	20.831256
11:35AM	25.281764	5655.875615	34.488716	29.01707	20.534436	20.864504
11:40AM	26.692302	5971.432215	36.187588	28.962928	20.59023	20.941692
11:45AM	25.210572	5639.948993	34.956584	29.017632	20.545042	20.927394
11:50AM	28.19707	6308.069351	39.079688	29.025934	20.570454	20.956968
11:55AM	31.463414	7038.795078	43.21458	29.615944	20.65562	21.0029
12:00PM	30.091412	6731.859508	45.015076	30.94652	20.713978	21.091738
12:05PM	28.845332	6453.094407	43.053748	32.58696	20.68146	21.094082
12:10PM	29.845992	6676.955705	43.9835	33.311356	20.799914	21.20795
12:15PM	29.49518	6598.474273	46.49386	33.341712	20.821282	21.285756
12:20PM	27.977678	6258.988367	40.74846	34.144384	20.958596	21.384198
12:25PM	28.430526	6360.296644	44.138564	33.838428	20.976728	21.428268
12:30PM	30.663334	6859.806264	45.19782	33.808976	21.019914	21.488862
12:35PM	30.817778	6894.357494	46.154092	34.146648	21.101822	21.57093
12:40PM	33.612736	7519.62774	50.787032	35.153788	21.188108	21.674226
12:45PM	29.084242	6506.541834	44.302	36.01482	21.187816	21.717484
12:50PM	31.68852	7089.154362	47.638488	35.937432	21.316374	21.815696
12:55PM	30.365384	6793.150783	44.480456	35.713152	21.31249	21.907228
1:00 PM	28.969684	6480.913647	43.3756	35.62124	21.37902	21.926214
1:05 PM	31.03382	6942.689038	42.882964	35.174136	21.422122	21.977814
1:10 PM	31.786072	7110.978076	43.828396	34.560652	21.487604	22.060684
1:15 PM	33.538548	7503.030872	50.29894	34.73952	21.582316	22.12488
1:20 PM	32.312642	7228.778971	50.962996	35.890524	21.62438	22.193046
1:25 PM	31.161656	6971.287696	44.3692	36.742724	21.711084	22.310182
1:30 PM	30.433156	6808.312304	44.562932	36.457356	21.822672	22.387092
1:35 PM	29.261266	6546.144519	41.699892	36.05346	21.77037	22.369442
1:40 PM	29.506662	6601.042953	42.97254	35.141716	21.848702	22.41292
1:45 PM	30.337148	6786.834004	41.73658	34.520008	21.854392	22.436204
1:50 PM	30.701112	6868.257718	47.576464	34.429708	21.857676	22.4656
1:55 PM	31.60742	7071.011186	48.133728	35.627904	21.946578	22.523998
2:00 PM	30.202056	6756.612081	42.6702	35.781832	21.998598	22.593402

2:05 PM	29.123674	6515.363311	41.57164	35.53936	22.046396	22.667288
2:10 PM	30.996726	6934.390604	42.726808	34.68154	22.06842	22.68041
2:15 PM	31.506356	7048.40179	47.756968	34.683316	22.169392	22.755416
2:20 PM	32.274738	7220.299329	48.281428	35.34452	22.054912	22.680154
2:25 PM	29.029032	6494.190604	39.728048	36.141736	22.132194	22.683618
2:30 PM	32.977276	7377.466667	42.702484	35.279464	22.187934	22.773952
2:35 PM	32.78136	7333.637584	45.76772	34.742792	22.223956	22.805796
2:40 PM	29.506782	6601.069799	41.693248	35.088424	22.235906	22.830796
2:45 PM	30.669492	6861.183893	39.417032	34.997084	22.299232	22.8765
2:50 PM	32.896518	7359.4	46.917984	34.426056	22.330966	22.912946
2:55 PM	35.078192	7847.470246	50.343568	34.95432	22.315656	22.949664
3:00 PM	30.360152	6791.980313	42.3953	36.491024	22.445912	23.036166
3:05 PM	33.532836	7501.75302	47.909548	35.99996	22.423056	23.087272
3:10 PM	30.714054	6871.15302	45.518256	36.173108	22.49452	23.1326
3:15 PM	32.96157	7373.95302	44.94382	36.49872	22.521622	23.19884
3:20 PM	33.386692	7469.058613	45.040932	35.705384	22.456194	23.103182
3:25 PM	33.728952	7545.626846	48.842264	35.670776	22.477048	23.10228
3:30 PM	33.45134	7483.521253	50.811796	36.4442	22.512682	23.150754
3:35 PM	32.982784	7378.698881	47.120824	37.448744	22.528818	23.218892
3:40 PM	30.3531	6790.402685	43.346628	37.5543	22.600974	23.304432
3:45 PM	29.631866	6629.052796	42.397148	37.023836	22.623948	23.327394
3:50 PM	32.08918	7178.787472	46.4371	36.292212	22.655568	23.367508
3:55 PM	32.229854	7210.258166	48.452232	36.4665	22.710992	23.396808
4:00 PM	32.863292	7351.96689	48.524292	37.05932	22.81515	23.487866
4:05 PM	31.96571	7151.165548	47.96716	37.720608	22.859632	23.536674
4:10 PM	33.011554	7385.135123	47.7376	37.951868	22.91708	23.59844
4:15 PM	31.900134	7136.495302	47.247516	37.864212	22.844484	23.543464
4:20 PM	31.827758	7120.303803	47.37034	37.775336	22.87508	23.569506
4:25 PM	32.574578	7287.377629	46.645236	37.67274	22.947596	23.624782
4:30 PM	32.727092	7321.497092	45.929556	37.368664	22.971294	23.665672
4:35 PM	32.375564	7242.855481	46.033208	37.251708	23.021006	23.70685
4:40 PM	33.343578	7459.413423	46.071796	37.107408	23.038736	23.759162
4:45 PM	32.895192	7359.103356	45.670776	37.26324	23.08865	23.783154
4:50 PM	32.119618	7185.596868	44.266188	36.916268	23.11694	23.785342
4:55 PM	32.110618	7183.583445	44.219508	36.805128	23.137952	23.840934
5:00 PM	32.775264	7332.273826	44.267036	36.430488	23.173216	23.872022
30-Jul						
Time	T _{outside} (°C)	Radiation (W/m ²)	T _{PV w/o HE} (°C)	T _{PV with HE} (°C)	T _{water HE In} (°C)	T _{water HE Out} (°C)
8:00 AM	18.267064	4086.591499	22.514056	19.244312	18.566956	18.688414
8:05 AM	17.76723	3974.771812	23.64818	19.68761	18.580698	18.728528
8:10 AM	18.395366	4115.294407	24.85464	20.294174	18.634504	18.769238

8:15 AM	17.976282	4021.539597	25.181056	20.52736	18.672158	18.806696
8:20 AM	18.698778	4183.171812	25.995854	20.871126	18.720412	18.842232
8:25 AM	18.065732	4041.550783	26.372446	21.368698	18.735566	18.8312
8:30 AM	18.523282	4143.910962	26.519664	21.43865	18.736208	18.879658
8:35 AM	18.407544	4118.018792	25.665272	21.75282	18.80323	18.937756
8:40 AM	18.402484	4116.886801	26.44394	21.977788	18.841628	19.006694
8:45 AM	18.964486	4242.614318	27.833454	22.421134	18.894854	19.007932
8:50 AM	19.108286	4274.78434	27.493636	22.417348	18.877964	19.056116
8:55 AM	20.773156	4647.238479	28.033864	22.639972	18.92304	19.123004
9:00 AM	20.633306	4615.952125	28.60162	23.02927	19.026616	19.148408
9:05 AM	21.130362	4727.150336	29.643398	23.186564	18.988796	19.162762
9:10 AM	21.88664	4896.340045	29.206138	23.801782	19.072052	19.228366
9:15 AM	21.977106	4916.578523	28.013952	23.693068	19.08019	19.301754
9:20 AM	22.695488	5077.29038	29.930134	23.643932	19.134846	19.348054
9:25 AM	23.044088	5155.276957	31.171266	24.039534	19.17579	19.366992
9:30 AM	20.617502	4612.416555	27.543412	24.320964	19.189496	19.411042
9:35 AM	22.97156	5139.051454	29.903678	24.39509	19.246458	19.455098
9:40 AM	23.571548	5273.276957	32.95858	24.38465	19.266326	19.501134
9:45 AM	23.623882	5284.984787	32.81419	25.084852	19.366632	19.540356
9:50 AM	24.609086	5505.388367	32.826602	25.679226	19.36988	19.547968
9:55 AM	24.982056	5588.826846	35.493028	25.844674	19.375484	19.62753
10:00AM	24.560982	5494.626846	36.326936	26.652556	19.44733	19.673382
10:05AM	24.458266	5471.647875	35.9791	27.479828	19.543924	19.774318
10:10AM	27.347944	6118.108277	40.35674	27.52853	19.492414	19.792408
10:15AM	25.260008	5651.008501	38.105584	28.538342	19.563032	19.858462
10:20AM	24.993292	5591.340492	38.30236	29.21087	19.663846	19.963798
10:25AM	26.33584	5891.686801	38.528784	29.409532	19.738252	20.04672
10:30AM	28.160522	6299.893065	43.53288	29.423332	19.734326	20.064408
10:35AM	26.124828	5844.480537	40.94766	30.17943	19.785582	20.146168
10:40AM	28.249238	6319.740045	40.909152	30.564354	19.896608	20.20523
10:45AM	28.344442	6341.038479	42.672752	30.689664	20.005504	20.32263
10:50AM	25.454002	5694.407606	39.667304	31.075244	19.973632	20.347434
10:55AM	27.642832	6184.078747	39.955316	31.07065	20.068524	20.416148
11:00AM	26.849386	6006.574049	39.602892	30.65693	20.088142	20.492236
11:05AM	26.202392	5861.832662	38.839684	30.82412	20.109596	20.518042
11:10AM	27.228738	6091.440268	40.928576	30.369542	20.175118	20.566296
11:15AM	26.893246	6016.38613	41.791384	30.241028	20.27951	20.644508
11:20AM	28.497422	6375.262192	44.772204	30.489794	20.30901	20.691242
11:25AM	27.042492	6049.774497	44.186188	31.54493	20.364316	20.798636
11:30AM	27.877624	6236.604922	44.516108	32.526458	20.372342	20.780892
11:35AM	27.893094	6240.065772	42.572032	32.755912	20.422392	20.856884

11:40AM	28.426776	6359.457718	43.891824	32.49506	20.457206	20.9004
11:45AM	26.997452	6039.698434	42.28764	32.76073	20.508372	20.973334
11:50AM	25.393654	5680.906935	35.521452	32.960494	20.623614	21.049512
11:55AM	27.695102	6195.77226	41.469448	31.462218	20.681512	21.085612
12:00PM	24.15492	5403.785235	34.793276	31.03547	20.72765	21.140256
12:05PM	24.632422	5510.608949	33.31657	30.443216	20.754212	21.210566
12:10PM	25.352602	5671.723043	32.697976	29.256946	20.790838	21.238278
12:15PM	27.639152	6183.255481	39.076744	28.51697	20.815686	21.23262
12:20PM	25.971468	5810.171812	36.96388	28.643426	20.812922	21.247474
12:25PM	24.90395	5571.353468	35.90538	29.069478	20.817964	21.21331
12:30PM	30.18378	6752.52349	39.665308	29.07347	20.813266	21.18702
12:35PM	30.882204	6908.77047	47.883392	29.903636	20.797706	21.205934
12:40PM	31.177968	6974.936913	46.952132	31.778932	20.822586	21.261492
12:45PM	29.08129	6505.881432	43.751408	32.959832	20.898432	21.311174
12:50PM	29.55931	6612.821029	45.417972	33.286496	20.94286	21.38608
12:55PM	25.512354	5707.461745	37.88562	33.431312	21.02446	21.43281
1:00 PM	27.239252	6093.792394	40.688056	32.480304	21.09768	21.545202
1:05 PM	25.448382	5693.150336	35.29886	31.705802	21.064456	21.57694
1:10 PM	27.919456	6245.963311	38.306156	30.977194	21.144428	21.591936
1:15 PM	26.158906	5852.104251	37.812256	30.731902	21.17025	21.613206
1:20 PM	26.868904	6010.940492	35.383412	30.755178	21.219456	21.610516
1:25 PM	27.94419	6251.496644	38.726528	30.234454	21.160386	21.538394
1:30 PM	26.395386	5905.008054	37.406476	30.532836	21.133768	21.58128
1:35 PM	25.569908	5720.33736	36.569264	30.563266	21.17313	21.624794
1:40 PM	25.089074	5612.768233	33.50209	30.23025	21.220548	21.66803
1:45 PM	26.549356	5939.453244	37.201292	29.632704	21.210514	21.63187
1:50 PM	25.289698	5657.650559	34.64076	29.79857	21.226506	21.678148
1:55 PM	25.957002	5806.93557	35.243312	29.649354	21.279544	21.696334
2:00 PM	27.79976	6219.185682	37.498716	29.391408	21.309742	21.691876
2:05 PM	30.338626	6787.164653	43.047392	29.70801	21.273238	21.707638
2:10 PM	30.025818	6717.185235	46.720244	31.08024	21.338406	21.746846
2:15 PM	31.840032	7123.049664	49.081792	32.792362	21.333312	21.793818
2:20 PM	28.329048	6337.594631	42.430036	34.492584	21.460514	21.881788
2:25 PM	26.550802	5939.776734	36.894928	34.478452	21.532776	21.95403
2:30 PM	25.84577	5782.051454	34.994948	33.242226	21.554256	22.044782
2:35 PM	23.76869	5317.380313	31.10888	31.594514	21.4752	21.970298
2:40 PM	18.487284	4135.857718	26.16221	29.897258	21.437388	21.92796
2:45 PM	17.921556	4009.296644	21.626732	27.671408	21.479034	21.913366
2:50 PM	18.914628	4231.460403	20.03093	24.637076	21.449312	21.809822
2:55 PM	20.266338	4533.856376	21.71855	22.360792	21.349302	21.744676
3:00 PM	19.404516	4341.055034	20.850476	22.036124	21.380658	21.741186

3:05 PM	17.521688	3919.840716	19.007278	21.26719	21.306206	21.632104
3:10 PM	15.098064	3377.642953	15.728126	20.37906	21.253042	21.548278
3:15 PM	14.58087	3261.939597	15.583474	18.38177	21.260898	21.534548
3:20 PM	16.358644	3659.651902	18.026108	17.78572	21.158524	21.37557
3:25 PM	20.407512	4565.438926	22.556044	18.092966	21.129192	21.3114
3:30 PM	18.899002	4227.964653	23.916684	18.850996	21.049236	21.20986
3:35 PM	21.749136	4865.578523	31.260148	20.128644	21.063218	21.171944
3:40 PM	22.042124	4931.123937	37.603108	22.085468	21.065814	21.117902
3:45 PM	23.015174	5148.808501	39.233268	24.260474	21.111194	21.067818
3:50 PM	23.257076	5202.92528	43.033892	25.804168	21.114236	21.057788
3:55 PM	22.782862	5096.837136	41.282404	28.312748	21.109088	21.091852
4:00 PM	20.939166	4684.377181	37.062188	29.335048	21.217048	21.152082
4:05 PM	22.968156	5138.289933	39.98236	29.386356	21.199164	21.19045
4:10 PM	23.631014	5286.580313	42.033156	29.135858	21.275732	21.26702
4:15 PM	24.957592	5583.353915	44.05222	29.569806	21.219374	21.340964
4:20 PM	21.95719	4912.123043	38.63254	30.70237	21.362664	21.445232
4:25 PM	21.74825	4865.380313	33.80558	31.165848	21.361968	21.557394
4:30 PM	22.030832	4928.597763	36.866248	29.892264	21.371194	21.6274
4:35 PM	21.615312	4835.640268	32.875	29.730472	21.376528	21.610958
4:40 PM	19.957952	4464.866219	29.570596	28.79744	21.37547	21.614256
4:45 PM	20.350636	4552.714989	27.66664	27.907862	21.363458	21.615312
4:50 PM	20.164714	4511.1217	24.890334	26.883322	21.373328	21.620824
4:55 PM	20.235738	4527.010738	22.606696	25.558344	21.37043	21.609218
5:00 PM	18.392128	4114.570022	21.540338	24.641174	21.336196	21.609642

31-Jul						
Time	T _{outside} (°C)	Radiation (W/m ²)	T _{PV} w/o HE (°C)	T _{PV} with HE (°C)	T _{water} HE In (°C)	T _{water} HE Out (°C)
8:00 AM	18.51735	4142.583893	23.04803	18.130688	17.665484	17.913296
8:05 AM	19.574392	4379.058613	24.633334	19.065302	17.718418	17.940208
8:10 AM	19.368178	4332.925727	25.020106	19.5859	17.786532	17.99521
8:15 AM	19.376352	4334.754362	25.231246	20.437686	17.85586	18.055796
8:20 AM	21.484712	4806.423266	26.006516	20.885808	17.899718	18.060536
8:25 AM	21.539472	4818.673826	27.106092	21.313928	17.941716	18.119994
8:30 AM	21.233318	4750.182998	27.461346	21.666974	17.995518	18.152148
8:35 AM	20.95796	4688.581655	27.739604	22.289808	18.037538	18.219982
8:40 AM	21.16692	4735.328859	27.387346	22.532804	18.111986	18.307516
8:45 AM	21.72858	4860.979866	27.406378	22.655968	18.122226	18.278842
8:50 AM	22.188658	4963.905593	29.77539	22.795106	18.12725	18.331702
8:55 AM	24.208288	5415.724385	30.58938	23.370118	18.248414	18.405012
9:00 AM	21.523082	4815.007159	29.714088	24.051432	18.285806	18.48169

9:05 AM	20.674236	4625.108725	26.716886	24.266056	18.336434	18.571406
9:10 AM	20.690834	4628.821924	26.785276	23.963036	18.365966	18.57911
9:15 AM	24.595208	5502.283669	31.248286	23.618902	18.341576	18.593626
9:20 AM	25.24161	5646.892617	35.101516	24.067926	18.418918	18.671144
9:25 AM	27.880008	6237.138255	37.447804	25.312226	18.506984	18.75502
9:30 AM	27.382984	6125.947204	38.837968	26.525152	18.522348	18.818008
9:35 AM	27.632	6181.655481	38.190008	27.843076	18.625416	18.916878
9:40 AM	25.836278	5779.927964	39.850688	28.622838	18.677612	19.01251
9:45 AM	27.057796	6053.19821	37.516668	29.194322	18.737404	19.054834
9:50 AM	25.271306	5653.536018	34.685672	29.486856	18.819972	19.124482
9:55 AM	24.872432	5564.302461	34.407432	28.767106	18.891664	19.222336
10:00AM	25.33136	5666.970917	35.240808	28.381044	18.92756	19.280036
10:05AM	24.805224	5549.267114	32.555184	27.903434	18.941216	19.315122
10:10AM	23.077212	5162.687248	30.636234	27.37562	18.978326	19.343494
10:15AM	23.100152	5167.819239	29.8696	26.921278	19.070774	19.4014
10:20AM	23.773138	5318.375391	29.308444	26.43695	19.116154	19.455302
10:25AM	22.204546	4967.459955	29.760514	25.890516	19.142722	19.521122
10:30AM	22.896892	5122.347204	29.621474	25.56985	19.210658	19.536698
10:35AM	22.85366	5112.675615	30.064292	25.470634	19.18855	19.536592
10:40AM	24.142702	5401.051902	31.028202	25.382968	19.195692	19.51301
10:45AM	23.448624	5245.777181	30.679674	25.68355	19.18113	19.56369
10:50AM	22.156552	4956.723043	28.91412	25.571982	19.229492	19.555526
10:55AM	23.178966	5185.451007	29.024648	25.251034	19.249608	19.58
11:00AM	22.448864	5022.117226	30.0038	25.077032	19.256922	19.630928
11:05AM	22.97141	5139.017897	29.244842	25.182794	19.311182	19.641558
11:10AM	22.580828	5051.639374	29.292162	25.200048	19.33705	19.67614
11:15AM	22.748842	5089.226398	29.914336	24.995916	19.309744	19.67065
11:20AM	23.3839	5231.297539	30.010974	25.192062	19.381186	19.720266
11:25AM	24.08738	5388.675615	30.528302	25.341102	19.400594	19.748392
11:30AM	23.922832	5351.863982	31.377368	25.478998	19.46136	19.787336
11:35AM	22.763662	5092.541834	30.843892	25.563378	19.420006	19.724376
11:40AM	23.063694	5159.663087	29.470508	25.771418	19.434066	19.725162
11:45AM	22.403	5011.856823	28.819448	25.731534	19.4543	19.780658
11:50AM	22.055058	4934.01745	28.309516	25.33425	19.419504	19.797634
11:55AM	22.344918	4998.863087	28.24406	24.931368	19.496606	19.80077
12:00PM	22.339426	4997.634452	28.78255	24.61025	19.473464	19.834326
12:05PM	22.929588	5129.661745	28.610094	24.61011	19.508218	19.829824
12:10PM	22.596422	5055.127964	28.615348	24.624074	19.478806	19.887444
12:15PM	22.74275	5087.863535	28.509018	24.653246	19.560248	19.873306
12:20PM	21.707592	4856.284564	28.258754	24.708108	19.506656	19.893864
12:25PM	21.261008	4756.377629	27.571464	24.734114	19.554574	19.906882

12:30PM	21.664052	4846.544072	27.166796	24.478962	19.584992	19.889134
12:35PM	22.06917	4937.174497	28.032298	24.177006	19.577208	19.920598
12:40PM	21.917074	4903.148546	28.21703	24.064466	19.568578	19.920504
12:45PM	22.373404	5005.235794	27.830202	24.211684	19.624902	19.916334
12:50PM	22.67491	5072.686801	29.27508	24.166038	19.574736	19.93557
12:55PM	23.016444	5149.092617	29.678124	24.528346	19.61711	19.934516
1:00 PM	22.125144	4949.696644	29.190894	24.886182	19.62893	19.959224
1:05 PM	22.756912	5091.031767	28.59676	24.991886	19.661484	19.9658
1:10 PM	21.994946	4920.569575	28.169814	24.912084	19.64659	19.968162
1:15 PM	20.794214	4651.949441	27.018294	24.822478	19.647648	19.97358
1:20 PM	20.868062	4668.470246	26.268672	24.281738	19.595268	19.960646
1:25 PM	21.163942	4734.66264	26.468074	23.919062	19.644182	19.961584
1:30 PM	21.042758	4707.552125	26.114552	23.624588	19.670396	19.944188
1:35 PM	20.980864	4693.705593	26.647934	23.588906	19.669306	19.960538
1:40 PM	21.32351	4770.360179	27.315102	23.376574	19.62152	19.97798
1:45 PM	21.50223	4810.342282	27.54428	23.516254	19.639866	19.961628
1:50 PM	20.62614	4614.348993	26.920414	23.67242	19.678928	19.948548
1:55 PM	20.560014	4599.555705	26.165126	23.801164	19.638734	19.951776
2:00 PM	21.040468	4707.039821	24.726116	23.32753	19.624676	19.972416
2:05 PM	21.465278	4802.075615	25.892406	23.054434	19.672456	19.9853
2:10 PM	22.00019	4921.742729	28.8819	22.85588	19.656016	19.960522
2:15 PM	22.962956	5137.126622	30.510602	23.474888	19.676504	19.963564
2:20 PM	22.2661	4981.230425	30.078716	24.356048	19.678756	19.991598
2:25 PM	22.703582	5079.101119	28.847246	24.696496	19.716496	20.01644
2:30 PM	20.787304	4650.403579	27.811828	24.746268	19.657798	20.01008
2:35 PM	20.40961	4565.908277	25.610324	24.482316	19.705548	20.048906
2:40 PM	19.018076	4254.603132	22.05407	23.993162	19.757584	20.057706
2:45 PM	18.929936	4234.885011	21.224262	22.795736	19.743634	20.02196
2:50 PM	19.232774	4302.634004	22.876198	22.263922	19.728528	20.041736
2:55 PM	18.924792	4233.734228	23.731426	21.539938	19.72541	20.0299
3:00 PM	18.553606	4150.694855	22.971814	21.82525	19.707192	20.020026
3:05 PM	17.35065	3881.577181	21.305932	21.661366	19.725658	20.025598
3:10 PM	17.424032	3897.993736	20.289708	21.187992	19.681154	19.998546
3:15 PM	17.631734	3944.459508	20.56575	20.296448	19.679366	19.974956
3:20 PM	18.462972	4130.418792	21.921694	20.116414	19.638442	19.955656
3:25 PM	18.009832	4029.04519	21.57862	20.286046	19.63843	19.92986
3:30 PM	18.33921	4102.731544	21.156308	20.37968	19.619282	19.884362
3:35 PM	18.904784	4229.258166	22.114802	20.370054	19.605292	19.874924
3:40 PM	19.097468	4272.364206	22.563422	20.562148	19.59346	19.854184
3:45 PM	17.96401	4018.794183	21.398284	20.287876	19.579578	19.857748
3:50 PM	19.206896	4296.844743	21.507936	20.336784	19.572	19.824386

3:55 PM	18.079762	4044.689485	20.858766	20.689574	19.577622	19.834178
4:00 PM	17.635248	3945.245638	19.538752	20.25579	19.538752	19.812568
4:05 PM	17.2821	3866.241611	18.520684	19.89993	19.534726	19.79546
4:10 PM	16.75929	3749.281879	18.230166	19.753642	19.514326	19.753642
4:15 PM	17.500162	3915.025056	19.112504	19.260276	19.482188	19.695342
4:20 PM	18.210386	4073.911857	21.130804	18.76345	19.446584	19.646468
4:25 PM	17.573942	3931.530649	20.96206	19.447	19.442448	19.6338
4:30 PM	18.786944	4202.895749	20.755104	19.635242	19.395908	19.617608
4:35 PM	18.251592	4083.130201	21.628316	19.848608	19.518286	19.713796
4:40 PM	18.702662	4184.040716	21.183018	20.25497	19.525036	19.72927
4:45 PM	18.082102	4045.212975	20.61289	20.343976	19.501254	19.688234
4:50 PM	18.379874	4111.828635	20.557864	20.0501	19.50706	19.706934
4:55 PM	18.35833	4107.008949	22.234324	19.928674	19.420292	19.685412
5:00 PM	19.453102	4351.924385	24.744682	19.94403	19.47055	19.652984

01-Aug						
Time	T _{outside} (°C)	Radiation (W/m ²)	T _{PV w/o HE} (°C)	T _{PV with HE} (°C)	T _{water HE In} (°C)	T _{water HE Out} (°C)
8:00 AM	15.681444	3508.15302	16.875918	16.592938	17.515772	17.720128
8:05 AM	15.65957	3503.259508	17.0893	16.753914	17.520142	17.711392
8:10 AM	15.64857	3500.798658	17.22612	16.49888	17.569742	17.730792
8:15 AM	15.594816	3488.773154	17.18155	17.016066	17.586154	17.751378
8:20 AM	15.706096	3513.668009	17.427378	16.674022	17.575148	17.722902
8:25 AM	15.902382	3557.579866	18.018574	16.978858	17.601	17.74894
8:30 AM	15.97851	3574.610738	18.850352	17.042002	17.564026	17.73362
8:35 AM	16.35323	3658.440716	19.47254	17.446242	17.598568	17.772338
8:40 AM	16.506656	3692.764206	19.051082	17.71254	17.608086	17.786412
8:45 AM	16.17402	3618.348993	19.089072	17.606802	17.676502	17.793864
8:50 AM	16.385204	3665.593736	18.982042	17.691476	17.617598	17.795922
8:55 AM	16.437332	3677.255481	19.121144	17.678224	17.682592	17.84344
9:00 AM	16.518794	3695.479642	19.428916	17.985762	17.650794	17.820566
9:05 AM	16.385412	3665.640268	19.55699	18.282932	17.68314	17.852718
9:10 AM	16.413552	3671.93557	19.576336	18.054746	17.776386	17.880826
9:15 AM	16.485346	3687.996868	19.860898	18.191378	17.71309	17.878488
9:20 AM	16.65263	3725.420582	20.053916	17.962628	17.74103	17.86256
9:25 AM	16.668836	3729.046085	19.96581	18.491548	17.700628	17.86584
9:30 AM	16.578048	3708.73557	19.636146	18.079692	17.753674	17.875394
9:35 AM	16.682544	3732.112752	19.888294	18.55743	17.757812	17.914472
9:40 AM	16.743544	3745.759284	20.127156	18.418496	17.80984	17.918644
9:45 AM	16.918496	3784.898434	20.558076	18.66667	17.771604	17.91516
9:50 AM	17.116756	3829.251902	20.96419	18.343156	17.82163	17.943344

9:55 AM	17.624716	3942.889485	22.4236	18.546262	17.78139	17.937856
10:00 AM	18.166112	4064.007159	24.111054	19.103978	17.870306	17.95727
10:05 AM	18.16481	4063.715884	25.669476	19.720786	17.89084	17.986536
10:10 AM	18.291848	4092.136018	25.670646	20.69548	17.9093	18.039738
10:15 AM	18.532796	4146.039374	25.935158	21.179404	17.937484	18.0721
10:20 AM	19.337086	4325.970022	27.657084	21.492478	17.955544	18.10781
10:25 AM	19.147994	4283.667562	28.356536	22.015044	17.92728	18.123028
10:30 AM	18.984084	4246.998658	28.31886	22.488178	17.98044	18.149982
10:35 AM	18.471188	4132.256823	27.634896	22.955306	18.010468	18.201836
10:40 AM	18.251626	4083.137808	25.929056	23.203692	18.103738	18.268898
10:45 AM	18.273896	4088.119911	24.89639	22.624548	18.065448	18.27845
10:50 AM	18.481438	4134.549888	25.351952	22.190342	18.07711	18.31175
10:55 AM	19.110822	4275.351678	27.36495	22.27227	18.180936	18.367916
11:00 AM	19.137562	4281.333781	28.660724	22.385808	18.199154	18.38613
11:05 AM	20.09238	4494.939597	30.019764	22.830448	18.19347	18.441376
11:10 AM	20.506784	4587.647427	31.421048	23.376926	18.177228	18.425134
11:15 AM	20.258198	4532.035347	31.78452	24.041864	18.211466	18.472466
11:20 AM	21.111604	4722.953915	33.787036	24.889604	18.321744	18.547802
11:25 AM	21.070632	4713.787919	34.434924	25.426974	18.333076	18.615876
11:30 AM	20.525428	4591.818345	33.814624	26.144464	18.361622	18.674776
11:35 AM	20.579016	4603.806711	32.200936	26.602298	18.502414	18.763166
11:40 AM	20.960278	4689.100224	30.399522	26.36485	18.409654	18.75335
11:45 AM	21.203138	4743.43132	30.15502	25.999006	18.46586	18.791894
11:50 AM	23.681902	5297.964653	34.144652	25.654076	18.552108	18.830308
11:55 AM	24.00643	5370.565996	38.09496	26.029448	18.58302	18.869936
12:00 PM	26.61409	5953.935123	41.691624	27.394382	18.620934	18.981838
12:05 PM	28.212694	6311.564653	45.379572	29.047198	18.685126	19.002378
12:10 PM	27.251926	6096.62774	46.418124	30.846986	18.703362	19.081508
12:15 PM	26.631954	5957.931544	45.915848	32.553272	18.810456	19.21494
12:20 PM	24.615978	5506.930201	40.403472	33.233994	18.864216	19.26413
12:25 PM	25.02742	5598.975391	38.666764	32.723492	18.925746	19.356368
12:30 PM	25.832562	5779.096644	37.927944	31.512496	18.95432	19.419642
12:35 PM	26.074076	5833.126622	39.598816	30.848934	19.049892	19.475924
12:40 PM	26.705348	5974.350783	42.091804	30.6583	19.125612	19.551808
12:45 PM	24.17307	5407.845638	37.674188	31.259722	19.230536	19.669592
12:50 PM	24.236386	5422.010291	35.497312	30.812704	19.167758	19.68951
12:55 PM	26.099276	5838.764206	36.471512	30.14079	19.234578	19.730328
1:00 PM	26.217778	5865.27472	37.027184	29.67005	19.275552	19.792904
1:05 PM	26.932346	6025.133333	36.5206	29.596878	19.370614	19.827256
1:10 PM	27.679628	6192.310515	41.141956	29.60833	19.360346	19.886574
1:15 PM	25.58686	5724.129754	37.614396	30.240862	19.4087	19.93472

1:20 PM	27.605298	6175.681879	40.859472	30.39786	19.397448	19.919112
1:25 PM	26.077206	5833.826846	38.523228	30.810692	19.502018	19.971694
1:30 PM	28.771528	6436.583445	43.135888	31.094924	19.55074	20.046374
1:35 PM	30.477602	6818.255481	44.09936	31.670326	19.659538	20.13352
1:40 PM	27.515762	6155.651454	41.023068	32.285156	19.652898	20.12707
1:45 PM	26.15731	5851.747204	38.722916	32.514984	19.698958	20.216332
1:50 PM	25.113926	5618.327964	34.962804	31.758914	19.748372	20.265726
1:55 PM	25.781908	5767.764653	35.00856	30.672164	19.789924	20.298734
2:00 PM	25.647684	5737.736913	36.490276	29.94988	19.81133	20.333022
2:05 PM	27.116694	6066.374497	36.18186	29.771816	19.892222	20.3574
2:10 PM	24.70044	5525.825503	36.32866	29.463574	19.793072	20.345284
2:15 PM	28.683348	6416.856376	42.485016	29.64383	19.848964	20.348844
2:20 PM	29.591512	6620.025056	45.473016	30.816828	19.93049	20.426168
2:25 PM	30.770848	6883.858613	49.4988	32.41764	19.957306	20.496374
2:30 PM	31.22815	6986.163311	48.809072	34.181528	20.050498	20.628562
2:35 PM	32.322784	7231.047875	50.408592	35.470392	20.067814	20.66785
2:40 PM	31.693382	7090.242058	46.840664	36.31002	20.198286	20.798452
2:45 PM	31.25791	6992.821029	47.921908	36.061876	20.291292	20.92154
2:50 PM	32.371662	7241.98255	47.578332	35.83982	20.398048	20.967624
2:55 PM	28.840138	6451.932438	43.893472	36.07466	20.497922	21.145496
3:00 PM	30.376812	6795.707383	47.518476	35.339568	20.424858	21.085728
3:05 PM	29.195796	6531.497987	43.447844	35.405812	20.513466	21.148152
3:10 PM	29.852976	6678.518121	40.059548	34.660096	20.582982	21.23487
3:15 PM	28.814052	6446.096644	40.827212	33.639652	20.600526	21.287256
3:20 PM	26.647442	5961.396421	36.75276	33.57602	20.700728	21.331158
3:25 PM	27.152036	6074.280984	36.67616	32.381046	20.674338	21.348148
3:30 PM	24.665778	5518.071141	34.498724	31.587226	20.700318	21.365216
3:35 PM	23.462976	5248.987919	31.225226	30.61892	20.708038	21.346984
3:40 PM	25.812526	5774.614318	32.032516	29.139556	20.621714	21.27396
3:45 PM	26.12461	5844.431767	33.065728	28.439546	20.631506	21.187722
3:50 PM	27.93105	6248.557047	39.710432	28.116266	20.635094	21.117816
3:55 PM	25.14332	5624.903803	35.981312	29.299614	20.636348	21.092934
4:00 PM	24.88839	5567.872483	32.561248	29.660628	20.637134	21.11531
4:05 PM	25.918992	5798.432215	33.768328	28.789366	20.60335	21.0249
4:10 PM	24.581674	5499.255928	31.5793	28.160926	20.550778	21.033342
4:15 PM	22.72863	5084.704698	29.33794	27.579054	20.506852	21.006672
4:20 PM	22.94688	5133.530201	28.34252	26.783164	20.617278	21.021394
4:25 PM	22.43756	5019.588367	27.220432	26.098532	20.558324	20.971364
4:30 PM	21.712556	4857.395078	26.136212	25.513938	20.531166	20.909168
4:35 PM	20.261586	4532.793289	24.141438	24.821594	20.448646	20.86589
4:40 PM	20.184252	4515.492617	22.038466	24.046944	20.458314	20.797308

4:45 PM	17.950944	4015.871141	20.99962	23.407776	20.38704	20.760912
4:50 PM	17.62239	3942.369128	19.720288	22.555062	20.416192	20.729238
4:55 PM	17.79607	3981.223714	19.605854	21.760428	20.288742	20.614704
5:00 PM	17.562574	3928.987472	19.002584	20.68188	20.303812	20.573302

02-Aug						
Time	T _{outside} (°C)	Radiation (W/m ²)	T _{PV w/o HE} (°C)	T _{PV with HE} (°C)	T _{water HE In} (°C)	T _{water HE Out} (°C)
8:00 AM	14.529878	3250.531991	18.90158	15.942378	15.541652	15.785678
8:05 AM	14.063376	3146.169128	18.772142	16.1131	15.594878	15.852018
8:10 AM	14.43331	3228.928412	18.77516	16.372972	15.680644	15.898402
8:15 AM	14.891488	3331.429083	19.353044	16.511948	15.71547	15.959274
8:20 AM	14.996488	3354.919016	19.688104	16.912718	15.724742	15.942494
8:25 AM	14.752038	3300.232215	20.000478	16.625666	15.763832	15.968456
8:30 AM	14.800912	3311.165996	20.105462	16.909168	15.81248	16.038964
8:35 AM	15.001266	3355.987919	20.400156	17.552384	15.899346	16.10414
8:40 AM	14.763042	3302.69396	20.701316	17.658784	15.96671	16.145254
8:45 AM	14.93313	3340.744966	20.102758	17.397574	16.053556	16.210224
8:50 AM	14.96555	3347.997763	20.239112	17.734574	16.03803	16.234056
8:55 AM	15.143644	3387.839821	20.78904	17.716136	16.11122	16.259136
9:00 AM	15.737302	3520.649217	22.486058	17.882428	16.125042	16.273148
9:05 AM	15.721718	3517.162864	22.492504	18.272022	16.183614	16.318596
9:10 AM	15.861002	3548.322595	22.760104	18.698372	16.218288	16.3968
9:15 AM	16.022064	3584.354362	23.498078	18.576154	16.24414	16.427022
9:20 AM	15.987412	3576.602237	23.718474	19.29443	16.270522	16.41842
9:25 AM	16.576136	3708.30783	24.01254	19.038668	16.293094	16.471594
9:30 AM	17.013092	3806.06085	25.214654	19.579686	16.36482	16.504156
9:35 AM	16.910634	3783.139597	26.742276	19.989768	16.379608	16.558098
9:40 AM	17.340642	3879.338255	27.107986	20.223748	16.470718	16.579444
9:45 AM	17.307704	3871.969575	27.148644	20.698592	16.49859	16.651026
9:50 AM	17.908342	4006.340492	27.609478	21.483846	16.53842	16.703776
9:55 AM	17.782338	3978.151678	28.987568	21.59205	16.538502	16.695304
10:00 AM	18.881816	4224.119911	30.351758	21.807186	16.576	16.728428
10:05 AM	17.908592	4006.396421	29.922024	22.635114	16.612606	16.804176
10:10 AM	18.780278	4201.404474	30.809072	22.956576	16.662264	16.86238
10:15 AM	19.299742	4317.61566	32.356304	23.411998	16.702958	16.92055
10:20 AM	19.26416	4309.655481	33.368568	23.756738	16.780574	17.007084
10:25 AM	19.232218	4302.50962	33.28687	24.242774	16.77917	17.009858
10:30 AM	19.788294	4426.911409	34.723744	24.789558	16.856732	17.100706
10:35 AM	20.550958	4597.529754	35.586376	25.18418	16.911552	17.137658
10:40 AM	21.096626	4719.603132	38.067912	25.874766	16.98017	17.223932

10:45 AM	20.741396	4640.133333	35.144968	26.587014	16.984902	17.24158
10:50 AM	24.007842	5370.881879	37.70088	26.396712	17.01458	17.30203
10:55 AM	21.121838	4725.2434	38.720644	26.904474	17.070252	17.370794
11:00 AM	20.909352	4677.707383	37.342	27.632634	17.153336	17.462218
11:05 AM	21.051876	4709.591946	34.9626	27.516028	17.204888	17.539778
11:10 AM	21.18764	4739.964206	33.450164	27.362536	17.205978	17.51067
11:15 AM	22.2386	4975.0783	38.472324	26.584842	17.173092	17.512548
11:20 AM	26.294942	5882.53736	41.167124	26.928724	17.206586	17.58535
11:25 AM	31.740956	7100.885011	49.123424	28.09072	17.30187	17.602172
11:30 AM	27.706594	6198.343177	46.8876	30.192174	17.38271	17.783262
11:35 AM	26.570502	5944.183893	41.107008	32.151996	17.466198	17.875268
11:40 AM	26.074196	5833.153468	38.472396	31.499976	17.49306	17.915034
11:45 AM	25.307118	5661.547651	36.129888	30.71202	17.60477	17.970322
11:50 AM	23.720582	5306.617897	33.757084	29.680716	17.64037	18.053754
11:55 AM	23.951592	5358.297987	32.85091	28.321734	17.703062	18.094782
12:00 PM	22.850254	5111.913647	32.643188	27.51382	17.678096	18.091468
12:05 PM	25.765482	5764.089933	33.61724	26.701142	17.6929	18.04988
12:10 PM	25.05355	5604.821029	38.075608	26.768508	17.752368	18.156986
12:15 PM	24.027702	5375.324832	34.099912	27.485008	17.83992	18.149024
12:20 PM	22.817956	5104.688143	30.69836	27.464482	17.828166	18.22403
12:25 PM	20.918454	4679.743624	28.054388	26.531846	17.788888	18.202224
12:30 PM	20.679498	4626.285906	26.536144	25.473502	17.86727	18.167634
12:35 PM	20.580668	4604.176286	26.511512	24.530614	17.838108	18.155564
12:40 PM	20.636278	4616.617002	26.635152	23.696146	17.780472	18.145974
12:45 PM	21.750322	4865.843848	26.499864	23.287698	17.83075	18.113464
12:50 PM	20.518082	4590.174944	26.774212	23.04231	17.771024	18.123428
12:55 PM	20.725626	4636.605369	26.284754	22.989404	17.852734	18.100512
1:00 PM	21.20364	4743.543624	27.303426	22.855158	17.843866	18.091834
1:05 PM	23.64863	5290.521253	30.50984	22.852856	17.824272	18.133188
1:10 PM	24.21457	5417.129754	33.934456	23.441072	17.828298	18.167778
1:15 PM	23.454854	5247.170917	33.329772	24.526314	17.898724	18.181426
1:20 PM	24.620914	5508.034452	33.133988	25.246068	17.876652	18.246492
1:25 PM	23.836992	5332.660403	32.931572	25.721924	17.973976	18.278682
1:30 PM	24.372236	5452.40179	33.396102	25.691566	17.908312	18.265236
1:35 PM	25.867754	5786.969575	34.103972	26.147426	18.00334	18.312402
1:40 PM	23.303722	5213.360626	33.703096	26.27644	18.08949	18.385438
1:45 PM	23.091118	5165.79821	32.931804	26.409414	18.053954	18.441396
1:50 PM	22.895698	5122.080089	31.599474	26.396364	18.062084	18.453702
1:55 PM	22.454446	5023.365996	30.920164	26.345564	18.13228	18.489142
2:00 PM	22.691228	5076.33736	30.33618	25.99997	18.187226	18.557168
2:05 PM	23.138108	5176.310515	30.491428	25.53989	18.200982	18.58819

2:10 PM	24.169454	5407.036689	30.677668	25.364948	18.267872	18.603064
2:15 PM	22.798446	5100.32349	30.729926	25.413078	18.268424	18.590522
2:20 PM	24.10482	5392.577181	31.538962	25.447452	18.263502	18.646516
2:25 PM	24.864878	5562.612528	32.88895	25.326412	18.263294	18.637392
2:30 PM	26.110382	5841.24877	35.25958	25.718398	18.3019	18.689084
2:35 PM	26.512516	5931.211633	36.211712	26.443658	18.333874	18.70795
2:40 PM	30.541302	6832.50604	40.70774	27.392434	18.410198	18.784444
2:45 PM	25.980312	5812.150336	37.468052	28.198298	18.413466	18.813704
2:50 PM	25.462144	5696.229083	35.087656	28.800044	18.434112	18.808352
2:55 PM	24.93266	5577.776286	33.24723	28.603428	18.40051	18.800754
3:00 PM	23.860248	5337.863087	30.835418	27.853106	18.38233	18.75658
3:05 PM	23.191976	5188.361521	30.310278	27.109186	18.332688	18.772234
3:10 PM	24.8913	5568.52349	30.370526	26.30086	18.324584	18.729218
3:15 PM	25.458838	5695.489485	31.37534	25.665548	18.31823	18.723052
3:20 PM	25.916796	5797.94094	32.048004	25.67124	18.371788	18.719858
3:25 PM	24.533394	5488.455034	33.094898	25.689484	18.359764	18.716564
3:30 PM	24.289128	5433.809396	34.319756	26.049246	18.370808	18.723052
3:35 PM	23.091928	5165.979418	34.05688	26.639796	18.397606	18.789124
3:40 PM	23.950558	5358.066667	33.671468	26.628914	18.438848	18.751986
3:45 PM	24.24229	5423.331096	33.652268	26.734284	18.44505	18.754012
3:50 PM	25.018548	5596.990604	34.17504	26.810502	18.421914	18.809248
3:55 PM	24.032392	5376.374049	35.044172	26.796392	18.451184	18.834144
4:00 PM	23.888458	5344.174049	34.313364	27.233772	18.497774	18.863266
4:05 PM	24.382226	5454.636689	33.748048	27.062714	18.463756	18.881626
4:10 PM	25.140822	5624.344966	34.317644	26.932606	18.501718	18.897758
4:15 PM	25.950132	5805.398658	34.69168	27.20226	18.543868	18.870072
4:20 PM	24.053668	5381.133781	33.480392	27.235112	18.559286	18.929314
4:25 PM	24.766998	5540.715436	31.400788	27.356028	18.62483	18.964106
4:30 PM	23.186748	5187.191946	29.941448	26.92484	18.622956	19.036224
4:35 PM	23.044072	5155.273378	28.773234	26.240984	18.64945	19.045444
4:40 PM	21.805952	4878.289038	28.17747	25.757128	18.726312	19.091742
4:45 PM	24.377594	5453.600447	27.44647	25.05593	18.732386	19.115078
4:50 PM	23.05548	5157.825503	27.560374	24.829342	18.734716	19.10887
4:55 PM	22.72381	5083.626398	27.43382	24.382112	18.69328	19.097798
5:00 PM	22.672624	5072.175391	27.572076	24.21875	18.69849	19.111732

03-Aug						
Time	T _{outside} (°C)	Radiation (W/m ²)	T _{PV w/o HE} (°C)	T _{PV with HE} (°C)	T _{water HE In} (°C)	T _{water HE Out} (°C)
8:00 AM	14.253254	3188.647427	16.675058	14.763626	14.611162	14.90313

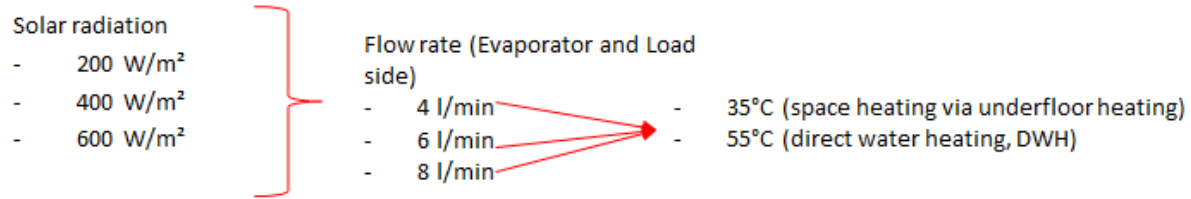
8:05 AM	15.2131	3403.378076	16.775968	14.943276	14.64675	14.925578
8:10 AM	14.57769	3261.228188	17.421604	15.227026	14.656114	15.000594
8:15 AM	14.48145	3239.697987	17.974132	15.544622	14.725674	15.043876
8:20 AM	14.19842	3176.380313	18.301124	15.449586	14.795982	15.066216
8:25 AM	14.69871	3288.302013	18.690948	15.761706	14.855728	15.108636
8:30 AM	15.130008	3384.789262	19.341936	15.957264	14.920878	15.143136
8:35 AM	15.304998	3423.936913	19.898078	16.22759	14.952034	15.187418
8:40 AM	16.51949	3695.635347	20.730604	16.82871	14.917688	15.19665
8:45 AM	16.712806	3738.882774	21.100234	16.839372	14.9807	15.190012
8:50 AM	17.478398	3910.156152	21.756132	17.417426	15.014104	15.275542
8:55 AM	16.679586	3731.451007	21.975102	17.437686	15.030026	15.322092
9:00 AM	17.354136	3882.357047	22.561812	17.876798	15.090376	15.343046
9:05 AM	17.113154	3828.446085	23.474712	18.01493	15.171908	15.411628
9:10 AM	18.404948	4117.438031	24.636364	18.526798	15.209678	15.4492
9:15 AM	19.281626	4313.562864	25.760338	19.077512	15.29117	15.539618
9:20 AM	20.452798	4575.570022	26.891614	19.572406	15.338954	15.535084
9:25 AM	20.947584	4686.260403	27.446936	20.15908	15.37497	15.596964
9:30 AM	21.246224	4753.070246	28.454968	20.48841	15.479332	15.657754
9:35 AM	20.87997	4671.134228	29.159146	20.992498	15.48076	15.672494
9:40 AM	22.218346	4970.547204	29.118682	21.79926	15.54811	15.722528
9:45 AM	21.847998	4887.695302	30.355628	21.99925	15.610014	15.788608
9:50 AM	24.528806	5487.428635	32.043564	22.80259	15.675112	15.866818
9:55 AM	24.024454	5374.59821	32.857388	23.218694	15.728924	15.890198
10:00 AM	24.62237	5508.360179	35.98596	24.146036	15.751428	15.97355
10:05 AM	27.926534	6247.546756	36.701044	24.995532	15.861844	16.058086
10:10 AM	25.876054	5788.826398	38.842056	25.914932	15.949496	16.193448
10:15 AM	27.914094	6244.763758	40.55526	26.654728	15.952358	16.191748
10:20 AM	28.455718	6365.932438	41.889852	27.816272	16.044182	16.32728
10:25 AM	27.2556	6097.449664	43.012348	28.64227	16.123942	16.420138
10:30 AM	29.734662	6652.049664	44.344352	29.709068	16.19273	16.545366
10:35 AM	30.91156	6915.337808	44.577288	30.548474	16.353786	16.702198
10:40 AM	31.384068	7021.044295	45.259912	30.995548	16.381688	16.730092
10:45 AM	31.46109	7038.275168	45.980636	31.58906	16.441538	16.82489
10:50 AM	27.127132	6068.70962	46.273632	32.09124	16.604824	16.99668
10:55 AM	33.755356	7551.533781	46.9456	32.158356	16.629402	17.016882
11:00 AM	30.718856	6872.227293	46.005624	32.76752	16.68378	17.140968
11:05 AM	26.29725	5883.053691	41.254264	32.973378	16.822816	17.271222
11:10 AM	26.997928	6039.804922	41.41814	32.310752	16.907902	17.382492
11:15 AM	26.650436	5962.066219	37.47252	31.344062	16.891458	17.374792
11:20 AM	26.546698	5938.858613	34.058272	30.210862	17.013074	17.435204
11:25 AM	28.0586	6277.091723	34.067956	28.921636	17.070194	17.470652

11:30 AM	28.705064	6421.714541	37.306888	27.991882	17.080818	17.537872
11:35 AM	29.778602	6661.879642	38.570292	28.285206	17.160018	17.56045
11:40 AM	28.086388	6283.308277	43.646344	28.486136	17.210688	17.624206
11:45 AM	33.498622	7494.098881	45.833456	29.644836	17.227496	17.671584
11:50 AM	30.581888	6841.585682	46.791992	30.697532	17.208148	17.65661
11:55 AM	30.44934	6811.932886	46.521824	31.74074	17.312098	17.703936
12:00 PM	30.399128	6800.699776	45.04946	32.89833	17.39948	17.79984
12:05 PM	30.433554	6808.401342	44.945708	33.213852	17.437858	17.91226
12:10 PM	29.288444	6552.224609	41.404248	33.060898	17.502634	18.003022
12:15 PM	32.229858	7210.25906	46.627836	32.51567	17.537338	18.02044
12:20 PM	33.502426	7494.949888	48.946364	32.389882	17.612762	18.065454
12:25 PM	29.70914	6646.340045	46.131432	33.513386	17.6664	18.16274
12:30 PM	29.497512	6598.995973	43.611464	33.47839	17.756128	18.217696
12:35 PM	30.97051	6928.525727	43.357504	33.30217	17.706156	18.285058
12:40 PM	28.808454	6444.844295	42.008204	32.820546	17.736152	18.297766
12:45 PM	28.069412	6279.510515	40.700672	32.365124	17.8065	18.294054
12:50 PM	28.56384	6390.120805	41.569952	31.60879	17.840802	18.389086
12:55 PM	31.226922	6985.888591	43.910196	31.517848	17.908786	18.435406
1:00 PM	36.26844	8113.744966	47.432824	31.837468	17.920384	18.451362
1:05 PM	33.487018	7491.502908	48.070532	32.595658	17.978664	18.487792
1:10 PM	34.74128	7772.098434	48.677164	33.641432	18.026522	18.535822
1:15 PM	29.937116	6697.341387	49.709496	34.466288	18.063374	18.61612
1:20 PM	32.323658	7231.2434	51.093404	35.112828	18.125706	18.6566
1:25 PM	31.560274	7060.463982	45.607268	35.788256	18.209672	18.770896
1:30 PM	27.864686	6233.710515	40.874276	35.304204	18.302504	18.863876
1:35 PM	27.135814	6070.651902	37.899632	33.952828	18.345638	18.902818
1:40 PM	27.93244	6248.868009	37.202036	32.245132	18.362022	18.931908
1:45 PM	28.202282	6309.235347	36.311596	30.904264	18.334342	18.852062
1:50 PM	27.46256	6143.749441	35.560564	30.011066	18.302392	18.868128
1:55 PM	27.24545	6095.178971	34.385548	29.368868	18.347816	18.856992
2:00 PM	26.39173	5904.190157	34.395912	28.86362	18.384884	18.872226
2:05 PM	26.175544	5855.826398	34.079972	28.428046	18.396876	18.884212
2:10 PM	27.3035	6108.165548	33.983096	27.998222	18.37172	18.885062
2:15 PM	26.123662	5844.219687	33.95226	27.954048	18.392138	18.901488
2:20 PM	25.744438	5759.382103	32.996948	27.663188	18.414074	18.866496
2:25 PM	26.50919	5930.467562	33.639068	27.532348	18.416324	18.825482
2:30 PM	26.328272	5889.993736	33.89888	27.43791	18.372856	18.894926
2:35 PM	25.508712	5706.64698	34.302544	27.398212	18.363252	18.872426
2:40 PM	26.787858	5992.809396	35.513664	27.445528	18.398178	18.863698
2:45 PM	29.83486	6674.465324	36.833664	27.544078	18.445596	18.832924
2:50 PM	28.682548	6416.677405	37.730244	28.161722	18.454058	18.854284

2:55 PM	28.938174	6473.86443	39.40244	28.64987	18.41619	18.873352
3:00 PM	31.218838	6984.080089	41.255	29.214782	18.499934	18.882884
3:05 PM	30.330942	6785.445638	42.748476	30.137762	18.490014	18.977504
3:10 PM	28.80264	6443.543624	40.869448	31.018836	18.530488	19.017968
3:15 PM	27.108422	6064.523937	38.990556	31.38137	18.563282	19.089828
3:20 PM	34.738932	7771.573154	45.678592	31.16876	18.616378	19.090734
3:25 PM	30.970734	6928.575839	45.628148	31.955828	18.667158	19.206752
3:30 PM	34.502888	7718.76689	46.919808	32.86082	18.664368	19.225968
3:35 PM	35.387256	7916.612081	51.731796	33.65814	18.775886	19.267636
3:40 PM	35.922384	8036.327517	53.320128	35.031768	18.776428	19.381416
3:45 PM	28.256816	6321.435347	44.837804	36.410528	18.877954	19.44819
3:50 PM	29.891962	6687.239821	42.4257	35.90632	18.971902	19.581162
3:55 PM	27.115826	6066.180313	38.472432	34.483884	19.040936	19.610908
4:00 PM	26.326164	5889.522148	35.49164	33.044754	19.039464	19.600718
4:05 PM	29.497676	6599.032662	40.085116	31.481754	19.007332	19.647104
4:10 PM	30.487296	6820.424161	41.06738	30.972224	19.051558	19.660778
4:15 PM	29.827112	6672.731991	41.77886	31.257094	19.126964	19.679646
4:20 PM	28.142716	6295.90962	38.748516	31.671812	19.147236	19.773858
4:25 PM	26.461694	5919.842058	36.46644	31.50238	19.179542	19.740922
4:30 PM	29.484458	6596.075615	36.974576	31.035698	19.245368	19.77638
4:35 PM	31.052944	6946.967338	41.372384	30.430572	19.14952	19.784864
4:40 PM	30.432328	6808.127069	44.815252	30.917648	19.20782	19.790992
4:45 PM	29.855934	6679.179866	44.05678	31.980724	19.285388	19.82947
4:50 PM	30.814818	6893.695302	43.331784	33.076934	19.316328	19.895092
4:55 PM	31.651528	7080.878747	51.402396	34.809576	22.868652	23.168066
5:00 PM	28.023202	6269.172707	43.302228	33.944196	22.390476	22.242676

APPENDIX 2

This appendix presents more results of section 7.



Performance evaluation of SAHP at 200 W/m², 6 l/min and 2 bar

Evaporator side:

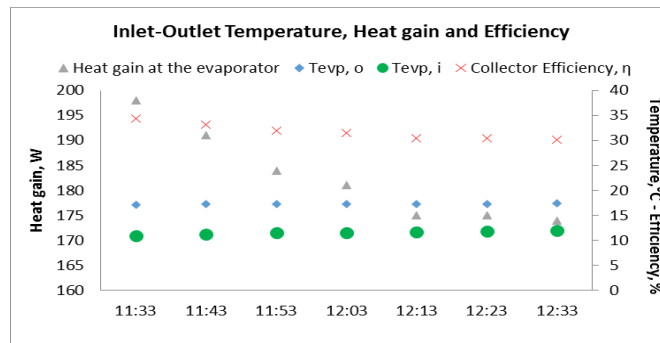


Figure 8.4.1 Evaporator performance at 200 W/m², 6 l/min and 2 bar (When HP is at space heating mode)

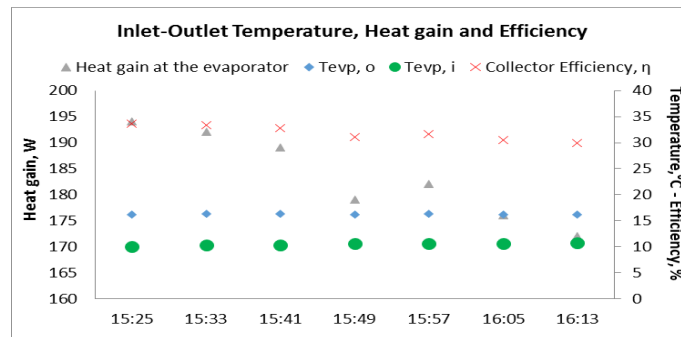


Figure 8.4.2 Evaporator performance at 200 W/m², 6 l/min and 2 bar (When HP is at DHW mode)

Load side:

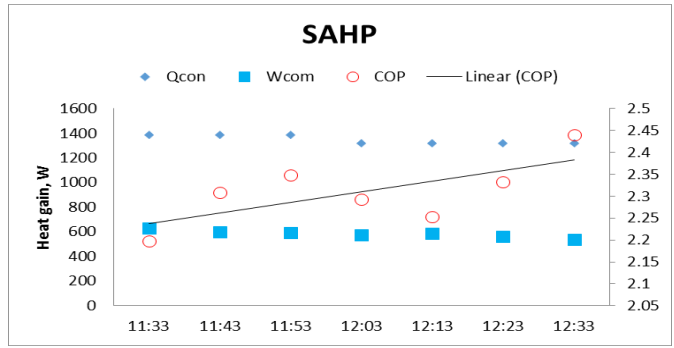


Figure 8.4.3 HP performance at 200 W/m², 6 l/min and 2 bar (When HP is at space heating mode)

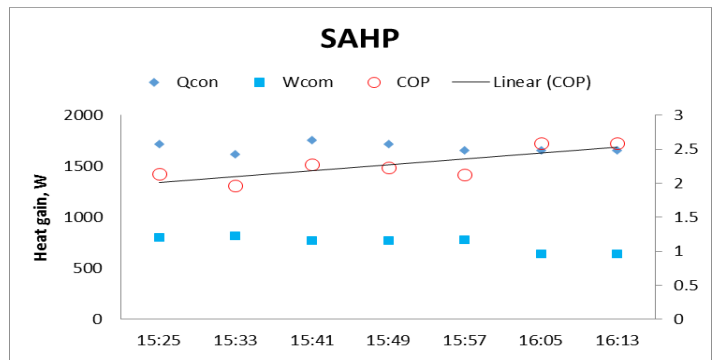


Figure 8.4.4 HP performance at 200 W/m², 6 l/min and 2 bar (When HP is at DHW mode)

Performance evaluation of SHP at 400 W/m², 6 l/min and 2 bar

Evaporator side:

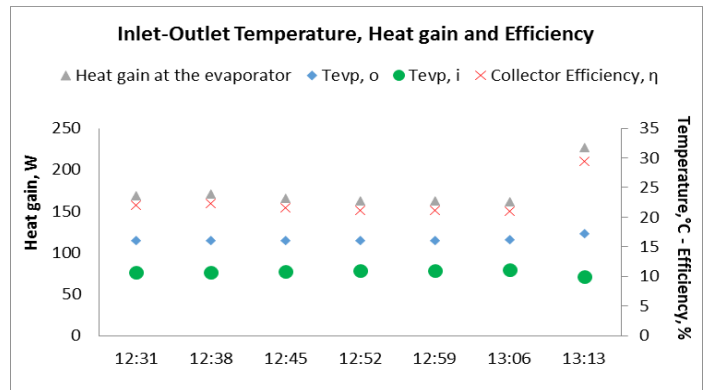


Figure 8.4.5 Evaporator performance at 400 W/m², 6 l/min and 2 bar (When HP is at space heating mode)

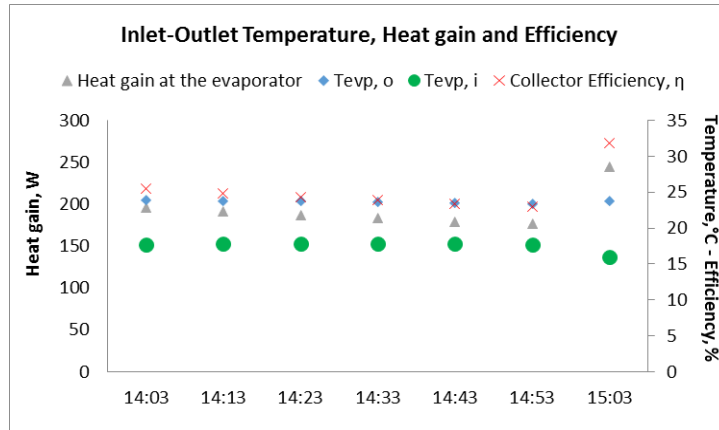


Figure 8.4.6 Evaporator performance at 400 W/m², 6 l/min and 2 bar (When HP is at DHW mode)

Load side:

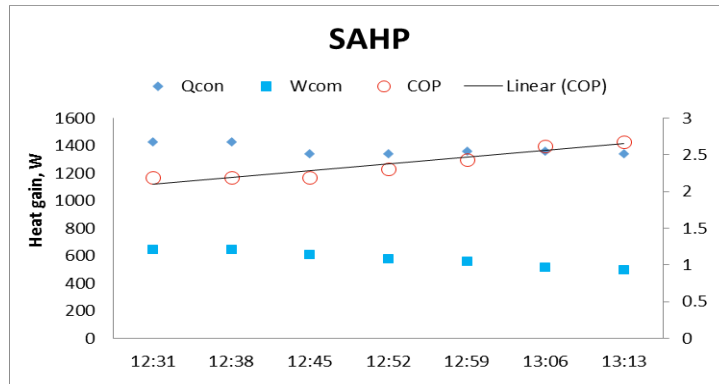


Figure 8.4.7 HP performance at 400 W/m², 6 l/min and 2 bar (When HP is at space heating mode)

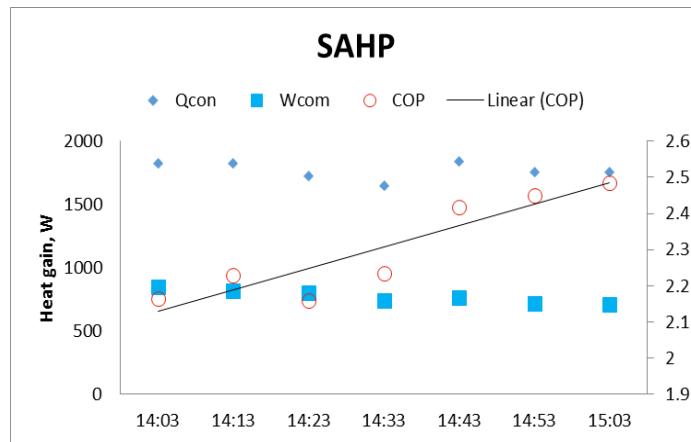


Figure 8.4.8 HP performance at 400 W/m², 6 l/min and 2 bar (When HP is at DHW mode)

Performance evaluation of SHP at 600 W/m², 6 l/min and 2 bar

Evaporator side:

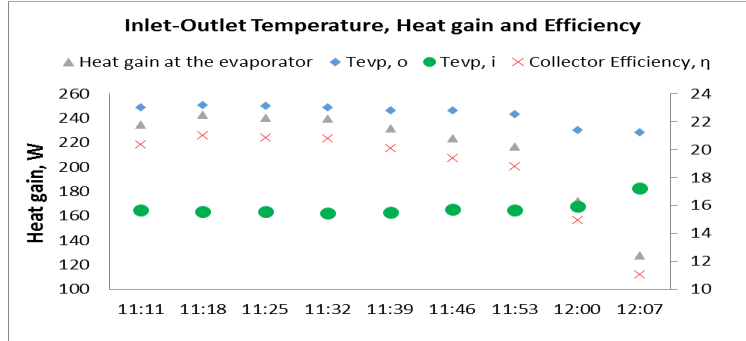


Figure 8.4.9 Evaporator performance at 600 W/m², 6 l/min and 2 bar (When HP is at space heating mode)

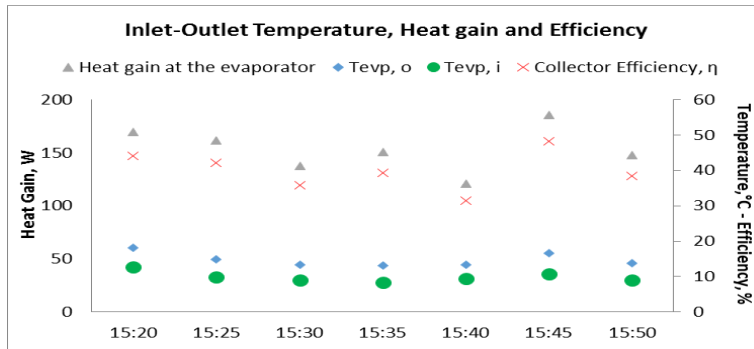


Figure 8.4.10 Evaporator performance at 600 W/m², 6 l/min and 2 bar (When HP is at DHW mode)

Load side:

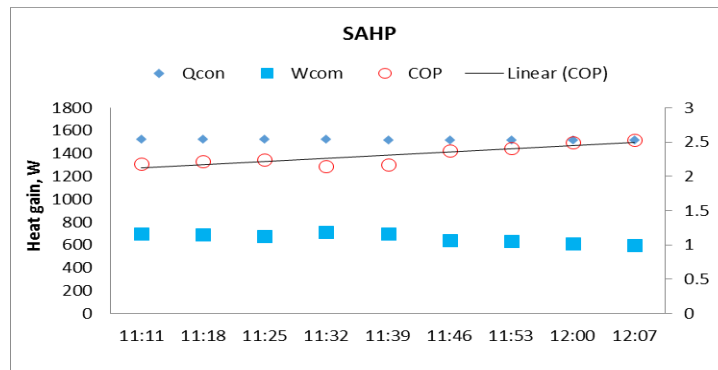


Figure 8.4.11 HP performance at 600 W/m², 6 l/min and 2 bar (When HP is at space heating mode)

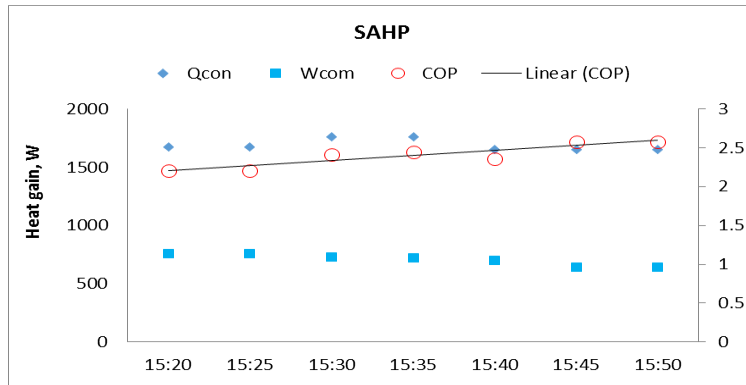


Figure 8.4.12 HP performance at 600 W/m², 6 l/min and 2 bar (When HP is at DHW mode)

Performance evaluation of SHP at 200 W/m², 8 l/min and 2 bar

Evaporator side:

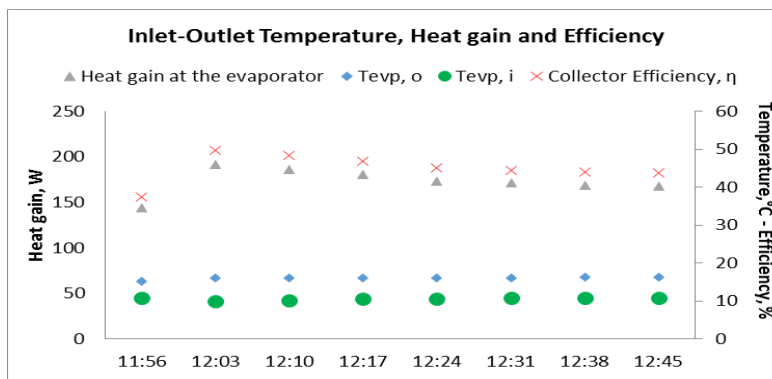


Figure 8.4.13 Evaporator performance at 200 W/m², 8 l/min and 2 bar (When HP is at space heating mode)

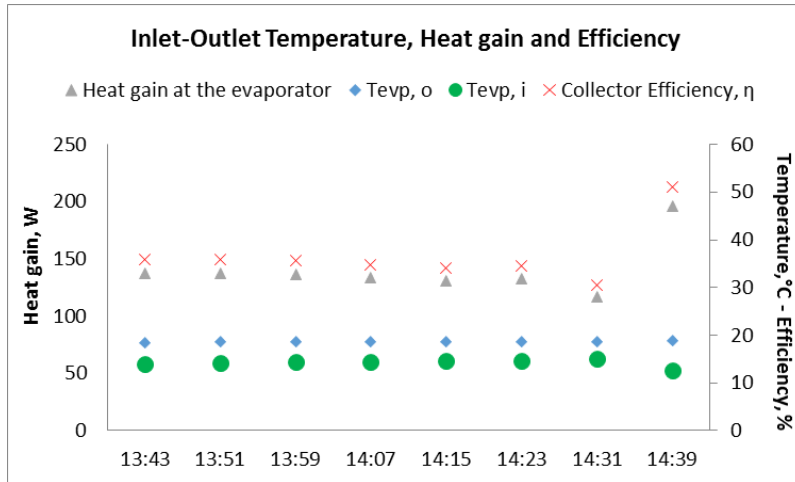


Figure 8.4.14 Evaporator performance at 200 W/m², 8 l/min and 2 bar (When HP is at DHW mode)

Load side:

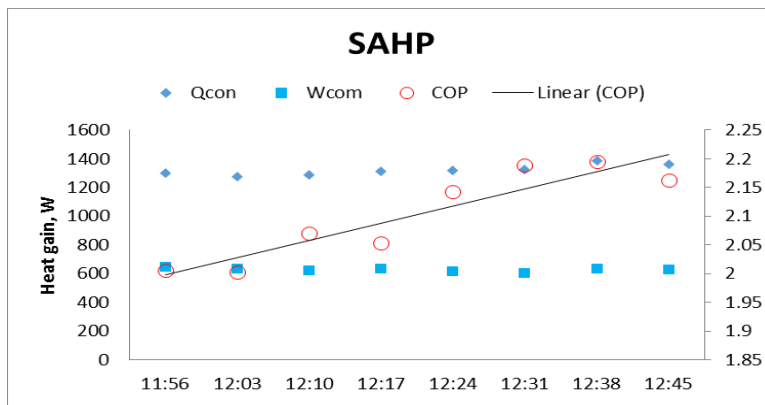


Figure 8.4.15 HP performance at 200 W/m², 8 l/min and 2 bar (When HP is at space heating mode)

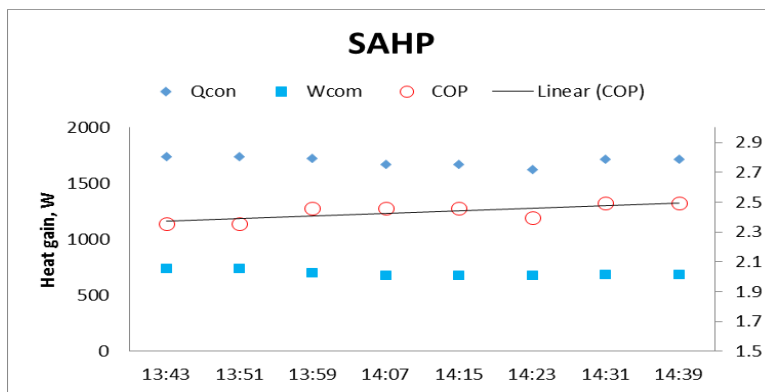


Figure 8.4.16 HP performance at 200 W/m², 8 l/min and 2 bar (When HP is at DHW mode)

Performance evaluation of SHP at 400 W/m², 8 l/min and 2 bar

Evaporator side:

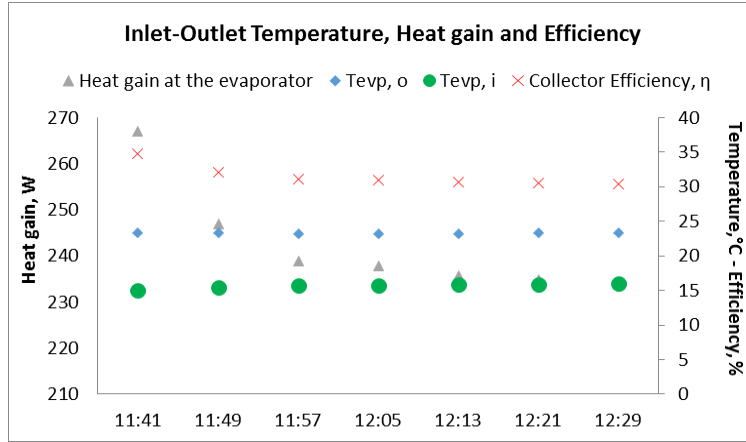


Figure 8.4.17 Evaporator performance at 400 W/m², 8 l/min and 2 bar (When HP is at space heating mode)

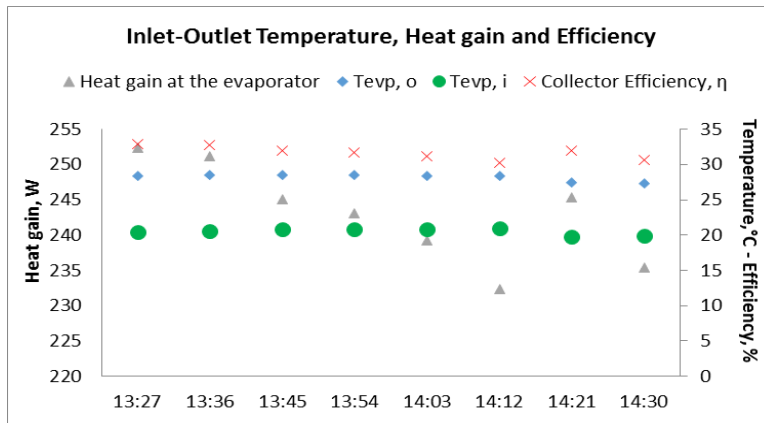


Figure 8.4.18 Evaporator performance at 400 W/m², 8 l/min and 2 bar (When HP is at DHW mode)

Load side:

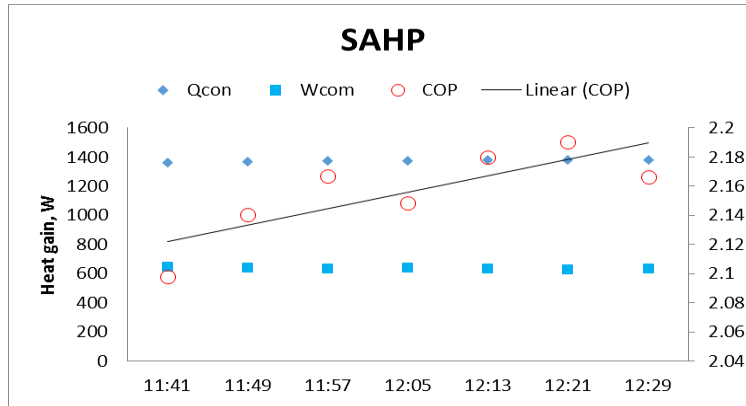


Figure 8.4.19 HP performance at 400 W/m², 8 l/min and 2 bar (When HP is at space heating mode)

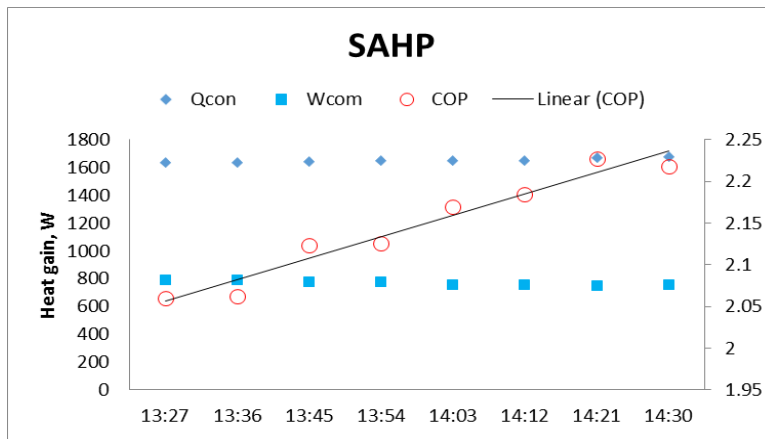


Figure 8.4.20 HP performance at 400 W/m², 8 l/min and 2 bar (When HP is at DHW mode)

Performance evaluation of SHP at 600 W/m², 8 l/min and 2 bar

Evaporator side:

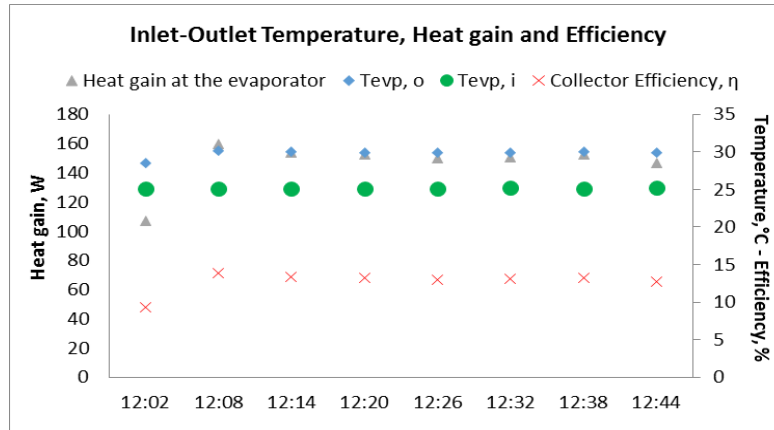


Figure 8.4.21 Evaporator performance at 600 W/m², 8 l/min and 2 bar (When HP is at space heating mode)

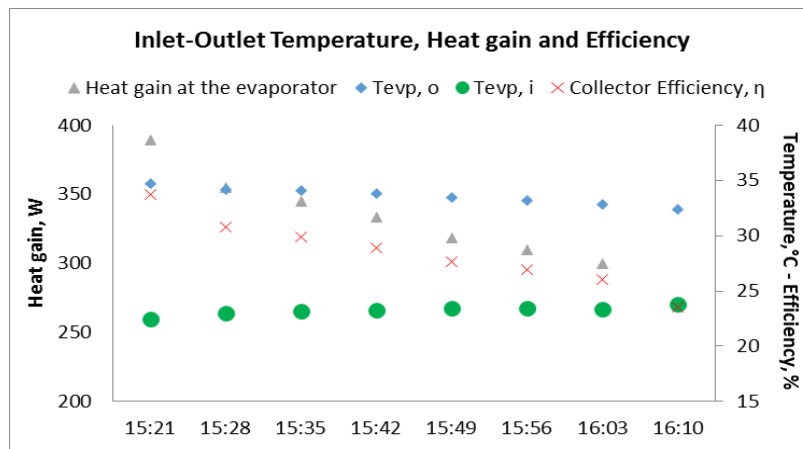


Figure 8.4.22 Evaporator performance at 600 W/m², 8 l/min and 2 bar (When HP is at DHW mode)

Load side:

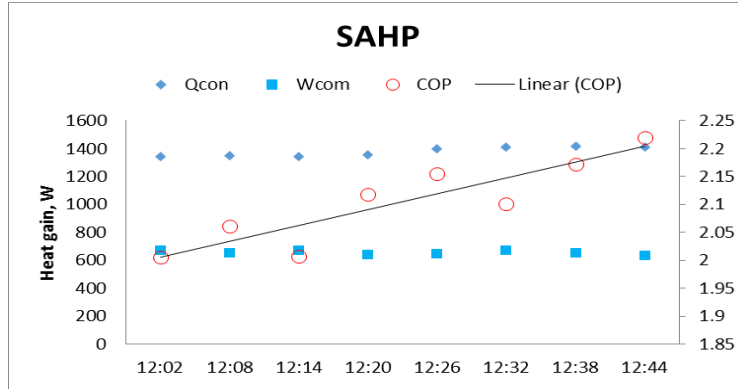


Figure 8.4.23 HP performance at 600 W/m², 8 l/min and 2 bar (When HP is at space heating mode)

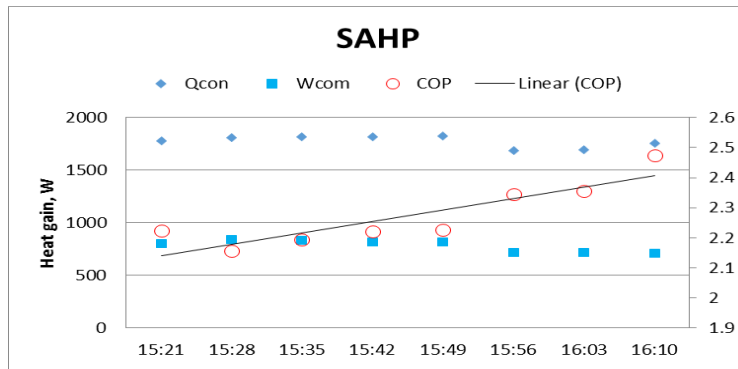


Figure 8.4.24 HP performance at 600 W/m², 8 l/min and 2 bar (When HP is at DHW mode)

Performance evaluation of SHP at 200 W/m², 4 l/min and 2 bar

Evaporator side:

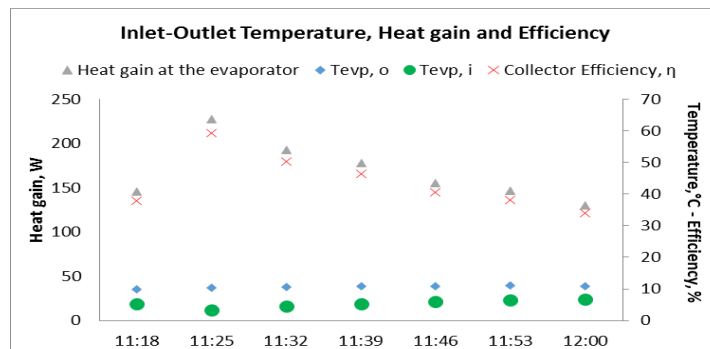


Figure 8.4.25 Evaporator performance at 200 W/m², 4 l/min and 2 bar (When HP is at space heating mode)

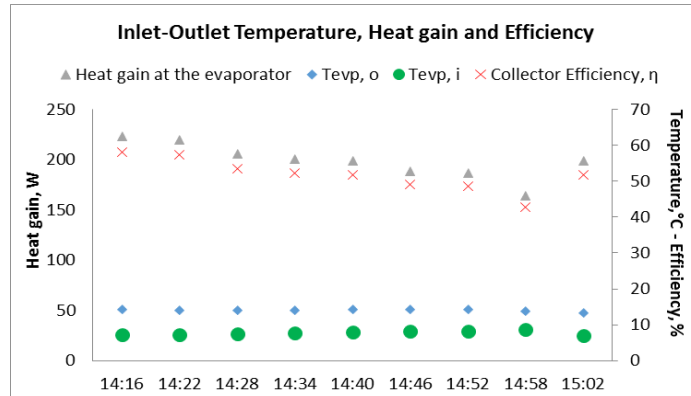


Figure 8.4.26 Evaporator performance at 200 W/m², 4 l/min and 2 bar (When HP is at DHW mode)

Load side:

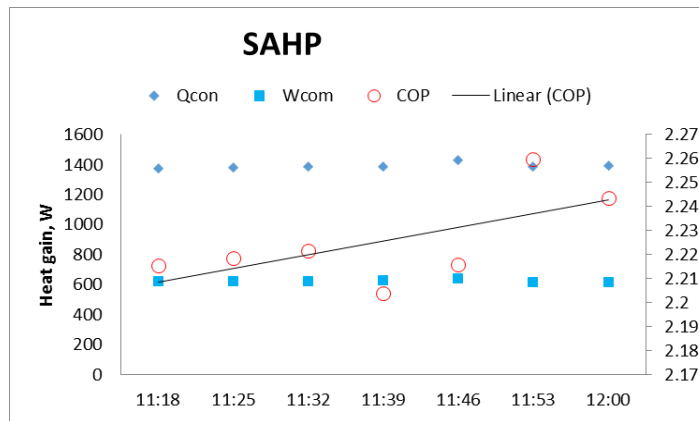


Figure 8.4.27 HP performance at 200 W/m², 4 l/min and 2 bar (When HP is at space heating mode)

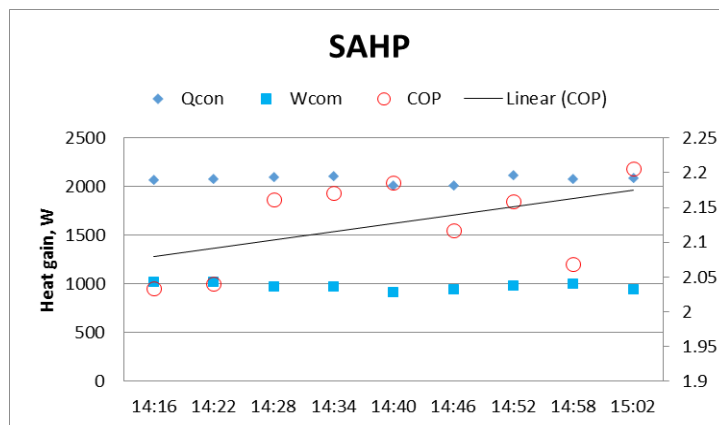


Figure 8.4.28 HP performance at 200 W/m², 4 l/min and 2 bar (When HP is at DHW mode)

Performance evaluation of SHP at 400 W/m², 4 l/min and 2 bar

Evaporator side:

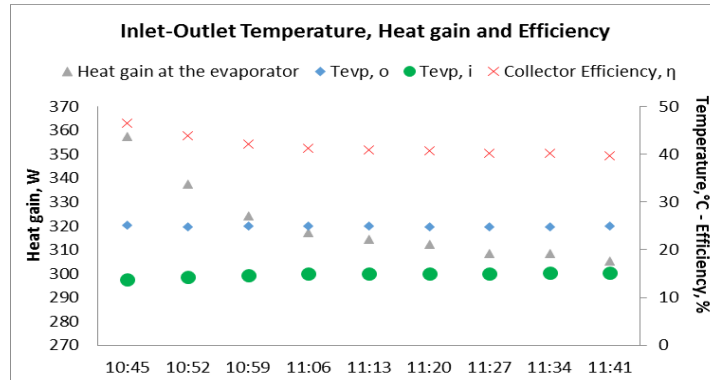


Figure 8.4.29 Evaporator performance at 400 W/m², 4 l/min and 2 bar (When HP is at space heating mode)

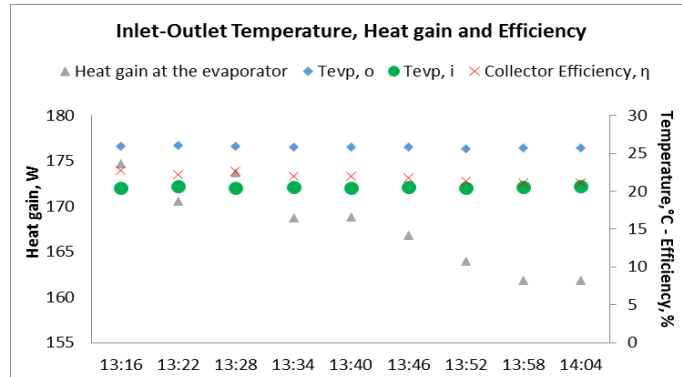


Figure 8.4.30 Evaporator performance at 400 W/m², 4 l/min and 2 bar (When HP is at DHW mode)

Load side:

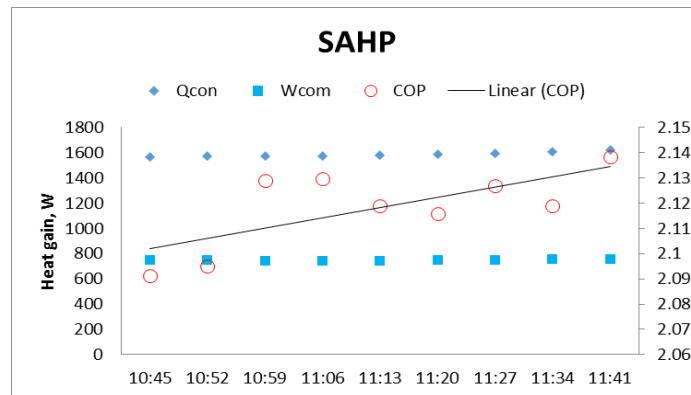


Figure 8.4.31 HP performance at 400 W/m², 4 l/min and 2 bar (When HP is at space heating mode)

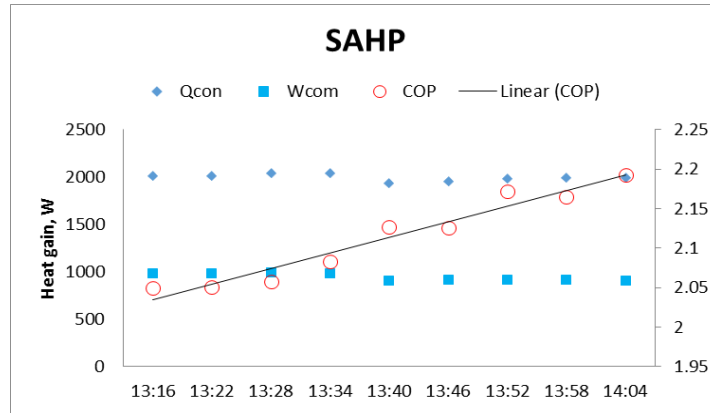


Figure 8.4.32 HP performance at 400 W/m², 4 l/min and 2 bar (When HP is at DHW mode)

Performance evaluation of SHP at 600 W/m², 4 l/min and 2 bar

Evaporator side:

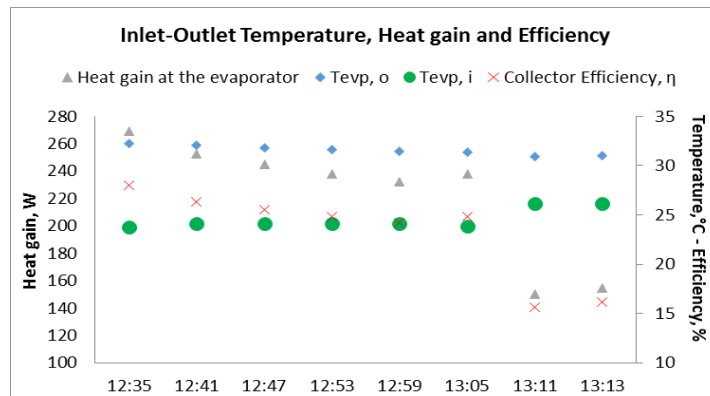


Figure 8.4.33 Evaporator performance at 600 W/m², 4 l/min and 2 bar (When HP is at space heating mode)

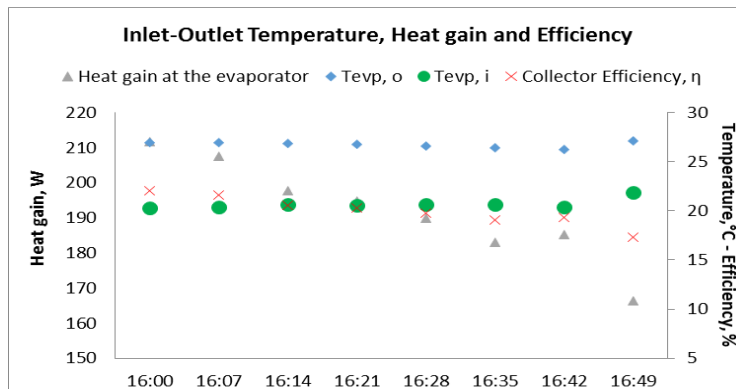


Figure 8.4.34 Evaporator performance at 600 W/m², 4 l/min and 2 bar (When HP is at DHW mode)

Load side:

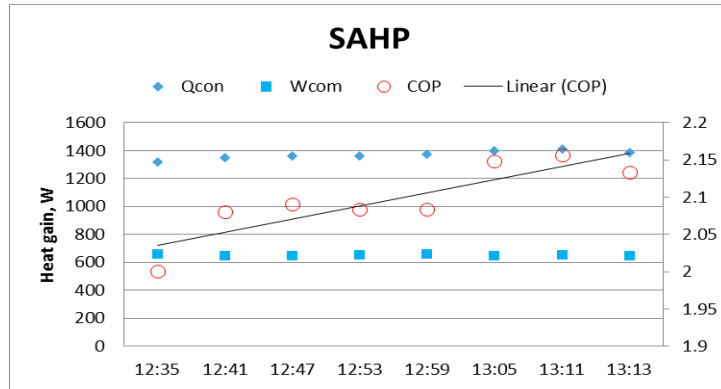


Figure 8.4.35 HP performance at 600 W/m², 4 l/min and 2 bar (When HP is at space heating mode)

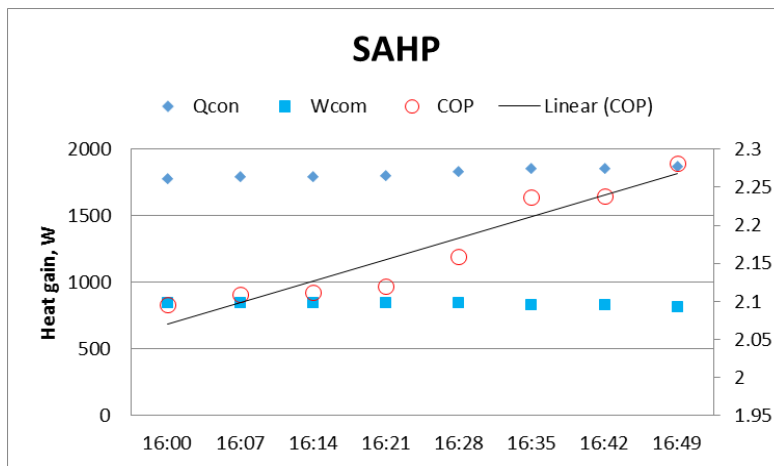


Figure 8.4.36 HP performance at 600 W/m², 4 l/min and 2 bar (When HP is at DHW mode)